# *IN VITRO* AND *IN VIVO* CULTURE SYSTEMS FOR DEVELOPMENT OF PORCINE TESTIS CELLS AND TISSUE

A Thesis Submitted to the College of
Graduate and Postdoctoral Studies
In Partial Fulfillment of the Requirements
For the Degree of Doctor of Philosophy
In the Department of Veterinary Biomedical Sciences
University of Saskatchewan
Saskatoon

By

Awang Hazmi Awang Junaidi

## PERMISSION TO USE

In presenting this thesis in partial fulfilment of the requirements for the degree of Doctor of Philosophy from the University of Saskatchewan, I agree that the Libraries of this University may make it freely available for inspection. I further agree that permission for copying of this thesis in any manner, in whole or in part, for scholarly purposes may be granted by the professor or professors who supervised my thesis work, or, in their absence, by the Head of the Department or the Dean of the College in which my thesis work was done. It is understood that any copying or publication or use of this thesis or parts thereof for financial gain shall not be allowed without my written permission. It is also understood that due recognition shall be given to me and to the University of Saskatchewan in any scholarly use which may be made of any material in my thesis.

Requests for permission to copy or to make other use of material in this thesis in whole or part should be addressed to:

Head of the Department of Veterinary Biomedical Sciences (VBMS)
Western College of Veterinary Medicine
52 Campus Drive
University of Saskatchewan
Saskatoon, Saskatchewan S7N 5B4 Canada

OR

Dean
College of Graduate and Postdoctoral Studies
University of Saskatchewan
116 Thorvaldson Building, 110 Science Place
Saskatoon, Saskatchewan S7N 5C9 Canada

## ABSTRACT

The studies presented in this thesis were designed to identify, examine, and manipulate potential factors associated with the development of porcine testis cells and tissue using *in vitro* and *in vivo* culture systems. The objective of the first *in vitro* study was to examine several conditions for short-term culture of testis cells to optimize the maintenance and propagation of neonatal porcine gonocytes. We found that culturing testis cells at $3.0 \times 10^4$ cells/cm$^2$ containing ~40% gonocytes in DMEM+10% FBS, at 37 °C, and without changing the medium for 7 days, improves *in vitro* maintenance, proliferation, and formation of gonocyte colonies. The goal of the second *in vitro* study was to apply these optimized conditions for prolonged culture to study the behavior, colony formation, and ultrastructure of gonocytes. We observed that gonocytes extensively migrate after developing various cytoplasmic projections, rapidly propagate, and form pluripotent embryoid body-like colonies (EBLC). The first *in vivo* study was designed to establish an efficient method for implantation of neonatal porcine testis cell aggregates under the back skin of recipient mice, and to explore the use of ultrasound biomicroscopy (UBM) for the non-invasive *in vivo* evaluation of implants. We showed that the subcutaneous injection approach, as compared with the conventional surgical approach, offers a less invasive route for implantation of cell aggregates, and results in a more consistent *de novo* formation of testis tissue in the implants. UBM proved to be a unique means for the non-invasive monitoring of implants and the prediction of the outcomes. The second *in vivo* study was aimed at utilizing this improved cell implantation model to examine the effects of pre-implantation exposure of testis cells to various growth factors (*i.e.*, EGF, GDNF, FGF2, FGF9, VEGF, LIF, SCF, and RA) on *de novo* morphogenesis of porcine testis tissue. We observed that each growth factor had a distinct effect on development of the testis tissue, ranging from enhanced development to improved gonocyte survival, and promotion of certain types of seminiferous cords. In summary, we discovered several critical elements for the *in vitro* and *in vivo* culture systems for the development of testis cells and tissue.

## ACKNOWLEDGEMENTS

I would like to express my sincere gratitude to my supervisor, Dr. Ali Honaramooz, for his continuous support and encouragement throughout my PhD program. I have been very fortunate to have the opportunity to work under a very patient, enthusiastic, and a visionary person like him. He has been a great mentor, and I thank him for his endless contribution during the preparation of the manuscripts and thesis.

I am indebted to my advisory committee, Drs. Karen Machin, Muhammad Anzar, Daniel MacPhee, and Patrick Krone for their constant guidance and insightful comments. I would also like to thank the external examiner for spending valuable time on my thesis.

I would like to acknowledge Universiti Putra Malaysia and Ministry of Higher Education Malaysia as well as the University of Saskatchewan for financial assistance, and the Natural Sciences and Engineering Research Council of Canada (NSERC) for support of our research.

I also sincerely thank the staff at the Prairie Swine Centre and Lab Animal Service Unit for their assistance with animal studies, Dr. Jaswant Singh for his support in the UBM study, and Eiko Kawamura and LaRhonda Sobchisin of WCVM Imaging Centre for their technical support in imaging.

Many special thanks to the rest of personnel in the VBMS including the researchers, academicians, staff, and graduate students for all the knowledge, supports, and good memories.

Finally, I am grateful to my family, colleagues and friends in Malaysia for their faith in me.
Thank you for always being there, through thick and thin.

## DEDICATION

This thesis is dedicated to my beloved parents Awang Junaidi and Dayang Rajanah, whom without their continuous love, encouragement, and prayers none of this would have happened. Not to forget my sister, Dayang Saftuyah, and brothers, Awang Ramzi and Awang Rosdi who always believe in me and are there whenever I need a shoulder to lean on.

## TABLE OF CONTENTS

## LIST OF TABLES

## LIST OF FIGURES

## LIST OF ABBREVIATIONS

| | |
|---|---|
| 2D | two-dimensional |
| 3D | three-dimensional |
| AMH | Anti Müllerian Hormone |
| ANOVA | Analysis of Variance |
| ART | Assisted Reproductive Technology |
| BCL6B | B-Cell Leukemia/lymphoma 6 |
| BW | body weight |
| cDNA | complementary DNA |
| c-kit | Tyrosine-protein kinase KIT |
| d | day(s) |
| DAPI | 4',6-Diamidino-2-Phenylindole |
| DAZL | Deleted In Azoospermia Like |
| DBA | *Dolichos Biflorus* Agglutinin |
| DIC | Differential Interference Contrast |
| DMEM | Dulbecco's Modified Eagle's Medium |
| DNA | Deoxyribonucleic Acid |
| DPBS | Dulbecco's Phosphate Buffered Saline |
| dpc | days post-coitum |
| dpp | days post-partum |
| EBLC | Embryoid Body-Like Colony |
| ECM | Extracellular Matrix |
| EDTA | Ethylenediaminetetraacetic Acid |
| EGF | Epidermal Growth Factor |
| ETV5 | ETS variant 5 |
| FBS | Fetal Bovine Serum |
| FFC | Fluid-Filled Cavities |
| FGF | Fibroblast Growth Factor |
| FITC | Fluorescein Isothiocyanate |
| FSH | Follicle-Stimulating Hormone |

| | |
|---|---|
| *g* | g-force |
| GCT | Germ Cell Transplantation |
| GDNF | Glial Cell-Derived Neurotrophic Factor |
| h | hour(s) |
| H&E | Hematoxylin and Eosin |
| HSCID | Hairless Severe Combined Immune Deficient |
| ICSI | Intra-Cytoplasmic Spermatozoa Injection |
| iPSC | induced Pluripotent Stem Cells |
| IVF | *In Vitro* Fertilization |
| KITL | KIT Ligand |
| KSR | Knockout Serum Replacement |
| LH | Luteinizing Hormone |
| LIF | Leukemia Inhibitory Factor |
| MEF | Mouse Embryonic Fibroblasts |
| MGSC | Male Germline Stem Cells |
| min | minute(s) |
| mo | month(s) |
| N.A | Numerical Aperture |
| N.S | Not Significant |
| NANOG | NANOG homeobox |
| OCT4 | Octamer-binding Transcription Factor 4 |
| PGC | Primordial germ cells |
| PGD2 | Prostaglandin D2 |
| PGP9.5 | Protein Gene Product 9.5 |
| POU5F1 | POU Class 5 Homeobox 1 |
| PSC | Pluripotent Stem Cells |
| RA | Retinoic Acid |
| ROSI | Round Spermatid Injection |
| RT | rete testis |
| RT-PCR | Reverse Transcription-Polymerase Chain Reaction |
| SBB | Sudan black B |

| | |
|---|---|
| SC | Seminiferous Cords |
| SCF | Stem Cell Factor |
| SCID | Severe Combined Immune Deficient |
| sec | seconds |
| SEM[1,2] | [1] Standard Error of Mean |
| | [2] Scanning Electron Microscopy |
| SHO | SCID Hairless Outbred |
| SOX9 | SRY (Sex determining region Y)-Box 9 |
| SRY | Sex Determining Region Y |
| SSC | Spermatogonial Stem Cells |
| SSEA-1 | Stage Specific Embryonic Antigen-1 |
| STO | SIM Embryo-Derived Thioguanine and Aoubain Resistant |
| TCI | Testis Cell Implantation |
| TEM | Transmission Electron Microscopy |
| TTX | Testis Tissue Xenografting |
| UBM | Ultrasound Biomicroscopy |
| UCHL1 | Ubiquitin C-terminal Hydrolase L1 |
| v/v | volume/volume |
| VAD | Vitamin A-Deficient |
| VEGF | Vascular Endothelial Growth Factor |
| VG | vesicular glands |
| *vs.* | versus |
| w/v | weight/volume |
| wk | week(s) |

# CHAPTER 1

# INTRODUCTION

Male germline stem cells (MGSC) are progenitors of all male germ cells, and form the foundation of spermatogenesis and male fertility. As putative multipotent stem cells, MGSC may also give rise to non-reproductive cells and tissues. However, our understanding of their biology and potential is limited, and due to the complexity of the testis architecture and cellular interactions, the study and manipulation of MGSC require proper *in vitro* and *in vivo* models.

Gonocytes are a transient population of MGSC after the mitotic arrest of primordial germ cells (PGC) and prior to differentiation into spermatogonial stem cells (SSC). In the neonatal testis, gonocytes are easily identified, because they are the only germ cells present in the neonatal testis, and have a distinct morphology (McGuinness and Orth, 1992). The presence of gonocytes in the postnatal testis continues for several days or up to several years, depending on the species (Hughes and Varley, 1980; McLean *et al.,* 2003; Li *et al.,* 2012). Based on the aforementioned characteristics, gonocytes are considered as the precursors of all germline lineages in the postnatal testis.

The study and manipulation of MGSC necessitates the development of high fidelity *in vitro* and *in vivo* models. This stems from the complex structure of the testis tissue, interactions of various somatic and germ cells, and involvement of for instance numerous known and unknown growth factors. As with other MGSC, gonocytes possess self-renewal and proliferation capacities, which can be manipulated *in vitro*. Gonocytes have been successfully maintained and propagated for long-term (~6 months) in culture (Han *et al.,* 2009; Lee *et al.,* 2013; Sahare *et al.,* 2016). Under certain conditions such as in the presence of retinoic acid (RA), differentiation of gonocytes to SSC can initiate (Wang and Culty, 2007; Zhou *et al.,* 2008). In addition, gonocytes form germ cell colonies that express pluripotency markers in culture (Han *et al.*, 2009; Fujihara *et al.*, 2011). Pluripotent stem cells are capable of giving rise to specialized cells and tissues of the three germinal layers

(*i.e.*, mesoderm, endoderm, and ectoderm) (Evans and Kaufman, 1981; Thomson *et al.,* 1998). Therefore, as a first step, we conducted a systemic study to examine and optimize a number of factors that can affect the maintenance and proliferation of porcine gonocytes in culture, as an *in vitro* system for their study and manipulation (Chapter 3). We then used these optimized culture conditions to examine porcine gonocytes further in terms of their *in vitro* behavior, ultrastructure, colony formation, and expression of pluripotency markers (Chapter 4).

An example of relevant *in vivo* models is the ectopic xenografting of testis tissue from diverse donor species into recipient mice, which is capable of promoting development of the grafted tissue, resulting in ultimate production of functional spermatozoa in the grafts (Honaramooz *et al.*, 2002a; Schlatt *et al.*, 2002a; Gassei *et al.*, 2006; Abbasi and Honaramooz, 2012). Therefore, ectopic testis tissue xenografting has provided an *in vivo* culture system for the study of testis function, development, and spermatogenesis. In addition, this system could be used as a potential tool for the preservation of genetic material. Dissociated cells, at least initially lack the structural framework that could maintain and support their transformation into a functioning tissue. However, rather surprisingly, *de novo* (*i.e.,* 'to restart from the beginning') formation of functional testis tissue was observed after ectopic implantation of dissociated porcine testis cells under the back skin of mouse hosts (Arregui *et al.*, 2008; Honaramooz *et al.*, 2007). The heterogeneous populations of implanted testis cells were fully capable of organizing themselves, and undergoing extensive rearrangement to once again form seminiferous cords, indistinguishable from those in the intact testis. This phenomenon opened an opportunity for the introduction of a new *in vivo* model, which is unique in that testis cells could be manipulated before implantation to study the potential factors involved in testis tissue morphogenesis. In this thesis, we set out to investigate several factors that could potentially improve the testis cell implantation model, and lead to more consistent results (Chapter 5), before utilizing it to examine the effects of various growth factors on *de novo* formation of testis tissue after implantation of cell aggregates (Chapter 6).

The laboratory mouse has long been used as an accessible and convenient model for biomedical research, and has contributed in a significant way to the understanding of human biology (Morse, 2007). The mouse also offers low maintenance costs, ease of management, and pronounced genetic similarities to humans (Waterston *et al.*, 2002). Most of our understanding of the biology of MGSC has been deciphered from the mouse model. The availability of transgenic, knockout/knockin,

mutant, and immunodeficient mice has also contributed significantly to the advancement of MGSC research and technologies. However, rodents are not an ideal animal model for the recapitulation of most human diseases and disorders (Seok *et al.*, 2013), and might respond differently to experimental interventions due to their marked pathophysiological differences with humans (Perlman, 2016). For this reason, the pig is considered a superior model for human biology and diseases (Kuzmuk and Schook, 2011).

Being omnivore and of comparable size to humans, pigs are also more closely related to humans in terms of anatomy, physiology, metabolic regulation, and predisposition to different disorders (Panepinto, 1996; Tumbleson and Schook, 1996; Spurney *et al.*, 2006; Kuzmuk and Schook, 2011; Swindle *et al.*, 2012; Dalgaard, 2015; Huppertz *et al.*, 2015). More specifically for the purpose of this thesis, the pig offered great advantages as a donor of testis cells and tissue for the study and manipulation of MGSC. Fresh neonatal pig testes could be obtained in large quantities at the time of routine castration of piglets at the University of Saskatchewan Prairie Swine Center. The collected testes can be processed to obtain large numbers of MGSC, particularly gonocytes. Compared with rodents (1-4 dpp), gonocytes in pigs are present for much longer periods of time (2 months) (Hughes and Varley, 1980; Russell, 1980; McLean *et al.*, 2003). This unique temporal pattern coupled with the availability of specific surface markers for pig gonocytes, such as *Dolichos biflorus* agglutinin (DBA) (Goel *et al.*, 2007), provide unequivocal means for identification of gonocytes. Improved methods for isolation and enrichment of pig gonocytes have also been introduced in recent years, allowing the isolation of high proportions of gonocytes (~40%), which could be further enriched (to ~90%) using density gradient centrifugation and differential plating (Yang *et al.*, 2010; Yang and Honaramooz, 2011). Pigs have also served as a donor species for the development of testis tissue xenografting model, as well as the ectopic cell implantation model (Honaramooz *et al.*, 2002a, 2007), and therefore were suited for the studies outlined in this thesis.

Gonocytes possess many potential applications in the fields of assisted reproductive technologies and regenerative medicine. For instance, gonocytes could be preserved (cryopreserved or 'biobanked') as a source of genetic material for fertility preservation, restoration, and conservation, as well as for the generation of induced pluripotent stem cells (iPSC) for cell-based therapy. On the other hand, gonocytes that fail to migrate to proper stem cell niches in the seminiferous tubules have been associated with cases of testicular *carcinoma in situ* (Skakkebaek *et al.*, 1987; Hoei-

Hansen *et al.*, 2005). Taken together, extensive research is required to understand further the biology, feasibility of manipulation, and safety of using gonocytes prior to their applications. Ironically, gonocytes are the least studied cells among MGSC, and hence are the subject of this thesis. Therefore, the overall objective of the present work was to study *in vitro* and *in vivo* culture systems for the development of porcine testis cells and tissue.

# CHAPTER 2

# LITERATURE REVIEW AND OBJECTIVES

## 2.1 Anatomy and Physiology of the Testis

### *2.1.1 Origin and Development of the Testis*

Embryonic development of the mammalian testis is unique because, in addition to complex folding of the germinal layers (*i.e.*, mesoderm and ectoderm) and migration of individual cells, it involves the formation and assembly of both germ cells and somatic cells (Svingen and Koopman, 2013). Based on the mouse model, development of the indifferent gonad begins with the formation of a paired thickening of the epithelial layer overlying the mesonephros (at 9.5 days post-coitum, dpc). The thickenings are due to the proliferation of the coelomic epithelium, which lead to the formation of the gonadal/genital ridges at 10-10.5 dpc (Svingen and Koopman, 2013; Tanaka and Nishinakamura, 2014). This coelomic epithelium also gives rise to the somatic cell lineages of the gonad. Formation of the genital ridge is known to be triggered by several genes including the steroidogenic factor 1 (*Sf1*) and Wilm's tumour-associated gene 1 (*Wt1*) (Hammes *et al.*, 2001; Wilhelm and Englert, 2002; Ozisik *et al.*, 2003; Buaas *et al.*, 2009). Primordial germ cells (PGC) that form the germ cell component of the gonad are derived from the epiblast cells, and can be found at the posterior primitive streak at 6.25 dpc (Tanaka and Nishinakamura, 2014). These cells are passively translocated from the mesoderm to the endoderm at 7.5 dpc, where they gain motility prior to their migration towards the genital ridges. PGC begin migrating toward the genital ridges at 8.5 dpc, via the hindgut, and reach the genital ridges at 10.5 dpc (Anderson *et al.*, 2000; Molyneaux *et al.*, 2001; Hara *et al.*, 2009).

Migration and proliferation of PGC occur through signals from chemo-attractants released by the developing genital ridges (Martineau *et al.*, 1997) and specific proteins expressed along the migratory route (Patni *et al.*, 2017). During this migration, PGC undergo extensive proliferation, increasing from an initial 50-80 cells to ~30,000 by the time they reach the genital ridge (Bendel–

Stenzel *et al.*, 1998; Wylie, 1999). Once arrived at the genital ridges, PGC become immotile and transform morphologically (lose cytoplasmic processes) to convert to gonocytes (Baillie, 1964; Donovan *et al.*, 1986). Development of the porcine testis follows the general mammalian pattern; the genital ridges are formed at ~18 dpc, and the indifferent gonads are completely formed by ~25 dpc (Hurst *et al.*, 1991). At this point, regardless of the genetic make-up (XX or XY), the primitive gonad is bipotential, equally capable of developing into a testis or an ovary depending on the molecular cues (Koopman *et al.*, 1991; Vidal *et al.*, 2001; Barrionuevo *et al.*, 2006). Differentiation of the indifferent gonad is initiated by the sex-determining region Y (SRY) protein, a testis-determining factor (TDF) encoded by the *Sry* found on the Y chromosome, and expressed by the pre-Sertoli cells (derived from the coelomic epithelium) (Gubbay *et al.*, 1990; Sinclair *et al.*, 1990; Koopman *et al.*, 1991). Expression of SRY activates the testicular genes, leading to deactivation of the ovarian genes (Li *et al.*, 2014). The duration of SRY expression is very short, lasting only ~6 h in mice (at ~11 dpc) (Hiramatsu *et al.*, 2009). Transient expression of SRY upregulates the expression of Sry-box 9 (SOX9) by the pre-Sertoli cells and leads to their differentiation into Sertoli cells (Sekido *et al.*, 2004; Wilhelm *et al.*, 2005). The expression of SOX9 also upregulates the expression of fibroblast growth factor 9 (FGF9) and anti Müllerian hormone (AMH) by Sertoli cells. While SOX9 and FGF9 drive the formation of the testis cords and proliferation of Sertoli cells, AMH prevents the formation of the Müllerian ducts (Josso, 1992; Kim *et al.*, 2006a). The persistent expression of SOX9 during testis development is crucial and is achieved via feedforward loops with FGF9 and prostaglandin-D2 (PGD2) (Kim *et al.*, 2006a; Moniot *et al.*, 2009).

Activation of *Sox9* and its upstream genes (*e.g.*, *Fgf9*) initiates the aggregation of Sertoli cells around germ cell clusters at 11.5 dpc (Combes *et al.*, 2009; Svingen and Koopman, 2013). Concurrently, FGF9 expression attracts the migration of endothelial and peritubular myoid cells from the mesonephros into the gonad (Martineau *et al.*, 1997). By 12.5 dpc (27 dpc in the pig), germ cells are completely surrounded by Sertoli cells, which in turn are enclosed by peritubular myoid cells to form testis cords (Hurst *et al.*, 1991; Combes *et al.*, 2009). At this point, germ cells begin undergoing mitotic arrest (Escalante-Alcalde and Merchant-Larios, 1992). Formation of testis cords results in the establishment of the interstitial compartment, which later hosts Leydig cells, mesenchymal cells, and blood vessels (Combes *et al.*, 2009). Growth of the early testis is rapid compared with the early ovary, because by 13.5 dpc the testis is twice the size of the same-age ovary (Schmahl *et al.*, 2000; Park and Jameson, 2005).

The origin of Leydig cells remains poorly understood; however, they are presumed to be derived from precursor cells of the coelomic epithelium and mesonephros mesenchyme (Merchant-Larios and Moreno-Mendoza, 1998; O'Shaughnessy *et al.*, 2006; Söder, 2007), regulated by AMH and other Sertoli cell signals (Patni *et al.*, 2017). Under the influence of SF1 and GATA4, Leydig cells express several genes for encoding enzymes such as steroidogenic acute regulatory protein (StAR), Cyp11a1 and Cyp17 (cytochrome P450 hydroxylases), and hydroxysteroid dehydrogenase (3ßHSD), required for testosterone biosynthesis (Park and Jameson, 2005; Patni *et al.*, 2017). Testosterone acts on the cranial and caudal portions of the mesonephric duct to form the epididymis and ductus deferens, respectively. The mesenchyme between the testicular cords then forms septa, which give rise to the lobulated structure of the testis parenchyma (Patni *et al.*, 2017). Later, the testis descends into the scrotum through two phases; the transabdominal phase, which in the mouse occurs between 15.5 and 17.5 dpc, and the inguinoscrotal phase, which occurs after birth at ~6 dpp. In the pig, these processes take place at 55 dpc and 85-90 dpc, respectively (Klonisch *et al.*, 2004).

### *2.1.2 Testis Structure and Function*

The mature testis is responsible for the production of male gametes and sex hormones, via the inter-related processes of spermatogenesis and steroidogenesis, respectively. These processes occur in distinct compartments of the testis parenchyma; spermatogenesis takes place in the seminiferous tubules and steroidogenesis happens in the interstitial compartment by Leydig cells. The activities in these compartments are regulated by a feedback system known as the hypothalamic-pituitary-gonadal (HPG) axis (Weinbauer *et al.,* 2010).

The testes are paired oval-shaped organs enclosed within the scrotum that are attached to the body via the spermatic cord. The cremaster muscles covering the spermatic cord is responsible for raising and lowering the testes for thermoregulation (Kayalioglu *et al.,* 2008). In most species (*i.e.*, mammals, amphibians, and birds), the testes are asymmetrical where the left testis is larger than the right testis (Birkhead *et al.,* 1997; Yu, 1998; Liu *et al.,* 2012). Surface of the testis is covered by a complex multi-layered tissue. These layers include the tunica vaginalis, which extends from the peritoneum and forms a lining that covers both the scrotal cavity (parietal tunica vaginalis) and the tunica albuginea (visceral tunica vaginalis). The fluid-filled space (*i.e.*, tunica vaginalis cavity) created by these two sub-layers allows the testes to move freely in the scrotum. The tunica

albuginea is a tough fibrous connective tissue that forms the outer surface of the testis and encapsulates it. Branching of the tunica albuginea (*i.e.*, septa) divide the testis parenchyma into several lobes and lobules that contain seminiferous tubules and interstitial tissue (Miller *et al.,* 1983; Sprengel *et al.,* 1990). In addition to acting as a protective physical barrier for the testis, the tunica albuginea plays a significant role in spermatozoa transport, testis vascularization, and maintenance of testis structure. The inner surface of the tunica albuginea is covered by the tunica vasculosa, an area enriched with blood vessels that facilitates the blood supply to the testis (Leeson and Cookson, 1974; Setchell *et al.,* 1994).

The testis parenchyma can be divided into two main compartments, namely the seminiferous tubules and the interstitial tissue. Seminiferous tubules are structures with a lumen and a seminiferous epithelium lining, made up of sustentacular Sertoli cells and germ cells in various stages of development (Siu and Cheng, 2004a; Jiang *et al.,* 2013). Germ cells form close contacts with Sertoli cells via N-cadherin and galactosyltransferase (GalTase) expressed on the surface of both cells (Newton *et al.*, 1993; Pratt *et al.*, 1993). During spermatogenesis, Sertoli cells nourish and facilitate the development of germ cells, establish dynamic interactions, regulate the environmental milieu within the seminiferous tubules (Griswold, 1998), and eliminate the residues produced during germ cell differentiation via phagocytosis (Yefimova *et al.*, 2013). Sertoli cells are joined together by tight junctions formed by basal cytoplasmic processes, creating a physical impediment commonly known as the blood-testis barrier. This structure provides an anatomical, physiological, and immunological barrier that divides the seminiferous tubule epithelium into a basal compartment and an adluminal compartment. The basal compartment consists of a specialized microenvironment, known as the stem cell niche, where Sertoli cells support and regulate the self-renewal and differentiation of spermatogonial stem cells (SSC) (De Rooij, 2009), while the adluminal compartment houses more advanced stages of germ cells. Thus, the blood-testis barrier provides an immunoprivileged environment to protect the haploid germ cells, while ensuring that nutrients reach these cells. In addition, the blood-testis barrier may have a role in preventing harmful substances from entering the adluminal compartment (Pelletier and Byers, 1992).

Fully developed seminiferous tubules have a constant number of Sertoli cells per unit length; although, the diameter and luminal volume of tubules change depending on the stage of the

spermatogenic cycle (Wing and Christensen, 1982). Seminiferous tubules are circumferentially enclosed by contractile cells known as the peritubular myoid cells, which contain an abundance of actin filaments and cytoskeleton proteins (Maekawa *et al.*, 1996). The contractile action of peritubular myoid cells assist the propulsion of spermatozoa and testicular fluid along the lumen of seminiferous tubules toward the rete testis, efferent ductules, and epididymis. The epididymis acts as temporary storage, where the maturation of spermatozoa continues (King, 1993; Hafez, 2000; Almeida *et al.*, 2006).

The interstitial compartment of the testis is mainly populated with the androgen-producing Leydig cells, along with other cells such as fibroblasts, mast cells, and macrophages (Schulze, 1984). Leydig cells are polygonal in shape and, being a steroid-producing cell, rich in smooth endoplasmic reticulum and mitochondria (Weinbauer *et al.*, 2010). Unlike adult germ cells and Sertoli cells, where the development continues from their preexisting predecessors of the embryogenic stage, adult Leydig cells are believed to be derived from stem Leydig cells, which are morphologically and functionally distinct from fetal Leydig cells. For instance, stem Leydig cells are originally spindle-shaped and lack LH receptors and steroidogenic-cell markers, but under the influence of growth factors and hormones they undergo transitional steps to ultimately differentiate into immature, and at puberty into adult Leydig cells. Most fetal Leydig cells regress shortly after birth and are not involved in the production of testosterone (Ge and Hardy, 1997; Faria *et al.*, 2003). The production of testosterone by Leydig cells is LH- and FSH-dependent, where testosterone has a significant influence on Sertoli cells and spermatogenesis (O'Shaughnessy *et al.*, 2009).

### *2.1.3 Spermatogenesis*

Spermatogenesis is a complex cyclical process where MGSC undergo a series of mitotic and meiotic divisions, eventually resulting in the production of mature spermatozoa (Russell *et al.*, 1993). Molecular cues for the initiation of spermatogenesis are poorly understood, but they also extend beyond the testis and involve the hypothalamus and pituitary gland. Regulation of spermatogenesis involves a systematic interplay between the hormonal/endocrine and paracrine/autocrine systems (de Kretser *et al.*, 1998); for instance, in mice, this process is triggered by the bone morphogenetic protein 8B (BMP8B) released by spermatogonia during the onset of puberty (Zhao *et al.*, 1996).

During spermatogenesis, germ cells develop into successively advanced stages, spanning from the basal compartment (during mitotic divisions) at the periphery of the seminiferous epithelium toward the adluminal compartments (for meiotic divisions). Prior to puberty, gonocytes and later spermatogonial stem cells (SSC) are the only germ cells in the testis.

Spermatogenesis begins at the basement membrane with mitosis of SSC. Spermatogonia type $A_{single}$ ($A_s$) comprise a rare and relatively quiescent population of cells that represent 'true' SSC, because they uniquely manage to retain their pluripotency and capability to undergo both self-renewal and differentiation (De Rooij and Russell, 2000). These cells can undergo division to form either two new $A_s$ (for self-renewal) or a pair of spermatogonia that remain connected $A_{pair}$ ($A_{pr}$, destined for differentiation). In rodents, differentiation of type $A_s$ to $A_{pr}$ is followed by a series of divisions that lead to the formation of type $A_{aligned}$ ($A_{al}$) spermatogonia which remain interconnected and can have chains of 4, 8, or 16 cells. While all are considered 'undifferentiated' spermatogonia, $A_{pr}$ and $A_{al}$ cells are on their way toward differentiation and hence are sometimes referred to as 'transient amplifying progenitor' cells. The next steps involve transition without cell division of $A_{al}$ into A1 differentiating spermatogonia, followed by five synchronized cell divisions to form A2, A3, A4, intermediate (In), and type B spermatogonia. Undifferentiated spermatogonia (types $A_s$, $A_{pr}$, and $A_{al}$) have similar cellular morphology; however, transition from $A_{al}$ to A1, which marks the beginning of differentiated spermatogonia is accompanied by significant morphological and mitotic behavior changes (de Rooij, 1998). Further differentiation of type B spermatogonia gives rise to spermatocytes and subsequently to haploid spermatids, which eventually develop into spermatozoa (Russell *et al.*, 1993; De Rooij and Russell, 2000).

Prior to further development, the resultant B-spermatogonia must leave the basal compartment by physically passing through the blood-testis barrier. Once in the adluminal compartment, B-spermatogonia undergo another mitotic division to produce primary spermatocytes that immediately enter the first phase of meiosis. During the long prophase of the first meiosis, the DNA undergoes complete replication to form tetrads, followed by crossing-over of homologous chromosomes to ensure genetic heterogeneity of the resultant germ cells. At the end of the first meiosis, each primary spermatocytes has produced two secondary spermatocytes (haploid, *N*), which are relatively short-lived and immediately undergoes the second meiotic division. Meiosis II leads to subdivision of each secondary spermatocyte into two haploid round (spherical)

spermatids, after which time, no further cell division will occur, instead they undergo extensive morphological differentiation to transform into spermatozoa via a process known as spermiogenesis. During the differentiation process, dramatic changes need to take place to transform round spermatids into elongating/elongated spermatids and spermatozoa, before they are released into the lumen of seminiferous tubules to be transported out of the testis (King, 1993; Dym, 1994; Gilbert, 2000; Hafez, 2000; Almeida *et al.*, 2006).

### *2.1.4 Regulation of Spermatogenesis*

At the onset of puberty, the release of gonadotropin-releasing hormone (GnRH) by the hypothalamus drives the release of gonadotropins, FSH and LH, from the pituitary gland. These gonadotropins initiate the first wave of spermatogenesis, which begins shortly after birth in mice and ~5-8 months of age in pigs (Vergouwen *et al.*, 1993; Almeida *et al.*, 2006; Gartner and Hiatt, 2006). FSH exerts its effect on Sertoli cells to promote their function in nourishing germ cells and facilitating spermatogenesis, while LH acts on Leydig cells to stimulate the production of testosterone. In turn, testosterone and inhibin-B (produced by Sertoli cells) act through a negative feedback mechanism to temporarily inhibit further release of GnRH, FSH, and LH (Boepple *et al.*, 2008).

During the first wave of spermatogenesis, the testis experiences sudden changes at the structural and hormonal levels. One of the most significant events occurring at this period is a massive Bax-dependent germ cell apoptosis, which is believed to establish a proper germ-Sertoli cell ratio (Rodriguez *et al.*, 1997; Print and Loveland, 2000). FSH and testosterone play a significant role in altering the rate of apoptosis during this process to bring about a balance (Rodriguez *et al.*, 1997; Ruwanpura *et al.*, 2007; Walczak-Jedrzejowska *et al.*, 2011). Reduced FSH levels during this period may result in significant increases in germ cell death (Billig *et al.*, 1995; Meachem *et al.*, 2005; Ruwanpura *et al.*, 2007), while supplementation of testosterone can have the opposite results (Rodriguez *et al.*, 1997).

During the subsequent spermatogenic cycles and throughout adulthood, FSH and testosterone seem to work in an independent, synergistic and/or overlapping manner to ensure completion of spermatogenesis (Saito *et al.*, 2000; Haywood *et al.*, 2003; Matthiesson *et al.*, 2005). FSH is important in ensuring the optimum spermiation output by maintaining or increasing (via

proliferation) the number of spermatogonia and thereby the population of more advanced germ cells (Zirkin *et al.*, 1994; Griswold, 1998; Simorangkir *et al.*, 2009; Walczak-Jedrzejowska *et al.*, 2011). Using transgenic mouse models lacking FSH or its receptor, it has been shown that although the mice can remain fertile, the number of germ cells and their survival rate are reduced (Dierich *et al.*, 1998; Meachem *et al.*, 1999; Abel *et al.*, 2000; Wreford *et al.*, 2001; Matthiesson *et al.*, 2005). Similarly, an increase in the number of spermatogonia and spermatocytes can be observed after FSH treatment of hypophysectomized and/or GnRH-immunoneutralized rats (Russell *et al.*, 1993; McLachlan *et al.*, 1995). Within seminiferous tubules, FSH receptors are only found on Sertoli cells, suggesting that any FSH effects on germ cells is likely achieved by modulating the Sertoli cell function (McLachlan *et al.*, 1995; Asatiani *et al.*, 2002). FSH, however, has no or limited direct effect on completion of meiosis and spermatogenesis (Russell *et al.*, 1993; McLachlan *et al.*, 1995).

Testosterone also plays a role in maintaining the population of spermatogonia; however, its most crucial function in spermatogenesis seems to be related to the transition of spermatocytes to spermatids (Welsh *et al.*, 2009; O'Shaughnessy *et al.*, 2012). Studies have shown that both testosterone withdrawal and lack of androgen receptors can result in male infertility, due to the failure to generate post-meiotic germ cells (Haywood *et al.*, 2003; Welsh *et al.*, 2009; O'Shaughnessy *et al.*, 2012). Using a hypophysectomized rat model, it was shown that while FSH supports the development of germ cells up to the step 7-8 spermatids, spermiogenesis was not observed in the absence of testosterone (Bartlett *et al.*, 1989; Kerr *et al.*, 1992). Furthermore, treatment with testosterone successfully recovers spermatogenesis of mice that have a mutation of the gonadotropin-releasing hormone gene, suggesting that this recovery is LH- and FSH-dependent (Cattanach *et al.*, 1977; Singh *et al.*, 1995). Similar to FSH, any effect of testosterone on germ cells is indirect and mediated through somatic cell populations, because androgen receptors are absent in germ cells but found abundantly in Sertoli, peritubular myoid, and Leydig cells (Skinner *et al.*, 1989; De Gendt *et al.*, 2004; Abel *et al.*, 2008).

A potential role has also been suggested for estrogen in the regulation of spermatogenesis; however, the mechanism by which estrogen acts to regulate this process is poorly understood. Androgens are converted to estrogens via aromatase activity in the testis (Dorrington *et al.*, 1978), where estrogen receptors-α and ß (ERα and ERß) as well as aromatase are found in abundance

(Couse *et al.*, 1997; Rosenfeld *et al.*, 1998), and the lack of ERα or aromatase leads to spermatogenesis impairment in mice (Lubahn *et al.*, 1993; Korach, 1994; Eddy *et al.*, 1996; Honda *et al.*, 1998; Robertson *et al.*, 1999; Toda *et al.*, 2001). Activin and inhibin are peptide growth factors mainly produced by Sertoli cells which participate in the regulation of spermatogenesis. As their names suggest, these structurally-related proteins have opposing biological effects; while activin has a stimulatory effect (Mather *et al.*, 1990; Nagano *et al.*, 2003), inhibin exerts inhibitory effects on proliferation of spermatogonia (Meachem *et al.*, 2001).

## 2.2 Origin and Development of Male Germline Stem Cells

### *2.2.1. Primordial Germ Cells*

Primordial germ cells (PGC) are the progenitors of both male and female germline, which arise from a small population of epiblast cells distributed throughout the primitive streak (Anderson *et al.,* 2000; Yabuta *et al.,* 2006). This event occurs during gastrulation (~6.0-6.5 dpc in mice), under the influence of bone morphogenetic proteins (BMP4 and BMP8b), produced by the cells of extraembryonic ectoderm and visceral endoderm (Ginsburg *et al.,* 1990; Saga, 2008; Ying *et al.,* 2000). These BMP induce the expression of PR-domain-containing protein 1 (PRDM1), also known as B-lymphocyte-induced maturation protein 1 (BLIMP1), which allows the specification of the epiblast cells to become PGC. This is achieved by promoting the expression of germ cell-specific genes (*e.g., Stella* and *Fragilis*) and repressing the expression of somatic genes (*e.g., Hox*) (Ohinata *et al.,* 2005; Saitou, 2009). Later, PGC develop cytoplasmic extensions and migrate to the base of the allantois (through the mesoderm and endoderm), where they are present as a cluster of alkaline phosphatase positive cells, at 7.0-7.5 dpc in mice (Chiquoine, 1954; Ginsburg *et al.,* 1990) or 22 days of gestation in humans (Falin, 1969). At this point, PGC are known as the pre-migratory PGC since they are about to begin their journey to the genital ridges.

Migration of PGC to the genital ridges occurs between ~8.5 and 13.5 dpc in mice (by 4.5 wk of gestation in humans). This migration is driven by chemotaxis and PGC undergo extensive multiplication while traveling along the hindgut, via the mesenchyme or dorsal mesentery (Tam and Snow, 1981; Francavilla *et al.*, 1990; Rabinovici and Jaffe, 1990; Anderson *et al.*, 2000). Migratory PGC maintain the expression of STELLA and also express the pluripotency markers OCT4, NANOG, SOX2, and stage-specific embryonic antigen-1 (SSEA-1) (Chuma *et al.*, 2005;

Hayashi *et al.*, 2007; Tilgner *et al.*, 2008; Saitou and Yamaji, 2012). Once in the gonadal ridges, the deleted in azoospermia-like protein (DAZL) ensures the population of PGC remain constant and healthy by preventing apoptosis and terminating abnormal PGC (Lin and Page, 2005; Chen *et al.*, 2014). Once residing in the gonadal ridges, PGC are subjected to sex determination.

Uniquely, the fate of PGC is not determined by their chromosomal sex, but largely by the surrounding somatic cells; therefore, PGC have an equal capacity to become gonocytes or oocytes (Adams and McLaren, 2002; Chiquoine, 1954; McLaren *et al.,* 1995; Molyneaux *et al.,* 2001; Tilgner *et al.,* 2008). Several studies have shown that PGC will enter meiosis if not co-cultured with embryonic testis tissue or if the testis architecture is disrupted in culture (Dolci and De Felici, 1990; McLaren and Southee, 1997; Yao *et al.,* 2003). Molecular cues involved in the sexual determination of PGC are poorly understood. During this phase, the sex determination genes are upregulated and the pluripotency genes are suppressed (Hu *et al.*, 2015). The DAZL is believed to be one of the important factors that promote this process, because its absence results in maintenance of pluripotency and inhibition of differentiation into advanced germ cells (Gill *et al.*, 2011). The presence of Sertoli cells also influences the sexual determination of PGC (Bowles *et al.*, 2006). Gender-specific behavior of PGC can be seen at ~12.5 dpc in mice; in male (XY) embryos, PGC are arranged in rows, while they are arranged in random arrays in female (XX) embryos (Jost *et al.*, 1973; Hilscher *et al.*, 1974; McLaren and Southee, 1997; McLaren, 2001). The male PGC undergo several rounds of mitotic divisions before entering a mitotic arrest in the $G_0/G_1$ phase of the cell cycle, where they become known as gonocytes and remain quiescent until after birth (McLaren, 2001). In the female, after several rounds of proliferation, PGC undergo arrest at the diplotene stage of prophase I of meiosis (Tam and Snow, 1981).

### *2.2.2 Gonocytes*

As the only type of germ cells present at birth, gonocytes are crucial for the development of more advanced stages of germ cells, ensuring the continuity of male germline throughout life (Culty, 2009; 2013). Gonocytes are a transitional population of MGSC found between the stages of PGC and SSC (de Rooij, 1998; Jiang and Short, 1998). They appear at ~13.5 dpc in rodents, and 7 wk of gestation in human embryos (McLaren, 2003; Culty, 2009) and their development is hormone-independent (Baker and O'Shaughnessy, 2001; O'Shaughnessy *et al.*, 2012). Concurrent with the

establishment of testis cords and upon activation of the germ cell nuclear antigen 1 (GCNA1), PGC are committed to adopting male germ cell fate and becoming gonocytes. This transition is marked by the complete suppression of the alkaline phosphatase activity at ~14.5 dpc in mice (Enders and May, 1994; Richards *et al.*, 1999). Gonocytes undergo several rounds of proliferation between 13.5 and 18 dpc in rodents, and at 18 wk of gestation in human embryos, before they undergo mitotic arrest and enter the quiescent stage (Ginsburg *et al.*, 1990; Vergouwen *et al.*, 1991; McLaren, 2003; Oatley and Brinster, 2008; Western *et al.*, 2008; Culty, 2009).

Gonocytes have heterogeneous subpopulations that can genetically and behaviorally overlap with both the preceding and subsequent stages (Nagano *et al.*, 2000). Based on mitotic activity and temporospatial distribution, gonocyte subpopulations can be more accurately categorized into: 1) Multiplying (M)-prospermatogonia; the population of gonocytes immediately following the PGC stage and prior to their mitotic arrest in the embryonic gonad. 2) Primary transitional (T1)-prospermatogonia; quiescent gonocytes in the first state of transition between M-prospermatogonia and A-spermatogonia that reside at the center of testis cords. 3) Secondary transitional (T2)-prospermatogonia; mitotically active gonocytes in the second state of transition to A-spermatogonia that have migrated to the basement membrane of cords (McLaren, 2003).

The proliferative activity of gonocytes (M-prospermatogonia) prior to their mitotic arrest has been suggested to occur under the influence of retinoic acid (RA). An increase in the number of rat gonocytes was observed after RA treatment in 12.5-14.5 dpc gonadal tissue cultures, but the opposite happened when RA was added to 16.5 dpc gonadal tissues (Livera *et al.*, 2000a; Trautmann *et al.*, 2008). The mechanisms involved in the mitotic arrest of gonocytes remain unknown; however, gonocytes enter the *G1-S* phase, and dephosphorylation of retinoblastoma protein (RB) occurs at 13.5 dpc in rodents (Western *et al.*, 2008; Spiller *et al.*, 2010). The quiescent stage of gonocytes (T1-prospermatogonia) has been observed in all examined mammalian species except in sheep (Hochereau-de Reviers *et al.,* 1995). This quiescent state lasts for days, weeks, months, or years after birth, depending on the species (Russell, 1990; Olaso and Habert, 2000; Shinohara *et al.*, 2001; McLaren, 2003; Oatley and Brinster, 2008; Culty, 2009). Gonocytes resume their proliferative activity at 1-4 dpp in rodents or ~8 wk after birth in the male infant (Culty, 2009). Throughout the quiescent stage, gonocytes reside at the center of seminiferous cords, where they

can be identified as distinctively large round cells, with one or two nucleoli in a prominent nucleus (McGuinness and Orth 1992).

Prior to birth or shortly after, gonocytes (T1-prospermatogonia) migrate to the basement membrane, resume mitotic divisions and differentiation into T2-prospermatogonia (Coucouvanis *et al.*, 1993; de Rooij, 1998; Jiang and Short, 1998). Prior to their migration, gonocytes undergo physical changes through the development of cytoplasmic extensions or pseudopods. These features are believed to aid in the amoeboid movement that directs the migration of gonocytes (McGuinness and Orth, 1992; Nagano *et al.*, 2000). The population of gonocytes that fail to develop these cytoplasmic extensions will remain in the center of the seminiferous cords, degenerate, and undergo apoptosis (Roosen-Runge and Leik, 1968; Orwig *et al.*, 2002a). In rats, gonocytes with pseudopods were able to drive full donor-derived spermatogenesis after transplantation into recipient testes, while most round, smooth gonocytes that lacked the cytoplasmic projections underwent apoptosis (Orwig *et al.*, 2002a). Migration of gonocytes requires the expression of molecular cues that allow the interaction of gonocytes and somatic cells. Gonocytes with pseudopods were shown to express c-kit, blocking of which reduced gonocyte numbers *in vitro* and disrupted their migration to the basement membrane *in vivo* (Orth *et al.*, 1997; Basciani *et al.*, 2008). Suppression of PDGF receptors (PDGFRα and ß) also exerted the same effects (Thuillier *et al.*, 2003; Basciani *et al.*, 2008). A role has also been suggested for A-Disintegrin and A-Metalloprotease domain (ADAM)-Integrin-Tetraspanin complexes (Kierszenbaum, 2005; Culty, 2009), due to their timely expression during the relocation and interaction with the extracellular matrix components of the basement membrane (Rosselot *et al.*, 2003; Siu and Cheng, 2004b).

In rats, approximately 20% of the neonatal gonocytes undergo mitosis between 4 and 5 dpp (McGuinness and Orth, 1992). This event has been known to be driven by several molecular cues including 17ß-estradiol (E2) and platelet-derived growth factor (PDGF) (Thuillier *et al.*, 2003; Wang *et al.*, 2004; Basciani *et al.*, 2008). Administration of E2 to mouse pups for three consecutive days after birth doubled the number of gonocytes (Vigueras-Villaseñor *et al.*, 2006), while in the absence of estrogen receptors, the number of gonocytes was reduced two fold (Delbès *et al.*, 2004). Other factors that have been identified to affect the proliferative activity of gonocytes include RA (Livera *et al.*, 2000b; Boulogne *et al.*, 2003; Zhou *et al.*, 2008), leukemia inhibitory factor (LIH)

(De Miguel *et al.*, 1996), and glial-derived neurotrophic factor (GDNF) (Braydich-Stolle *et al.,* 2007). Once settled at the basement membrane, gonocytes are confined in a special microenvironment, bounded by the basal lamina at the periphery, embedded between neighboring Sertoli cells, and isolated from the adluminal compartment via the blood-testis barrier. This microenvironment supports the differentiation of gonocytes to T2-prospermatogonia and future SSC, and hence is referred to as the 'stem cell niche'.

### *2.2.3 Spermatogonial Stem Cells*

Gonocytes that successfully migrate to the basement membrane (T2-prospermatogonia) resume proliferative activity, and a subset of this population (potentially NANOS3-positive) will differentiate and give rise to spermatogonial stem cells (SSC) (Yoshida, 2006; Nakagawa *et al.*, 2007; Suzuki *et al.*, 2009). In mice, SSC appear at 3-8 dpp (Vergouwen *et al.*, 1991; Drumond *et al.*, 2011) and immediately initiate the first wave of spermatogenesis (Yoshida, 2006). In pigs and infant boys, SSC can be first detected at 1-2 mo and 3-12 mo, respectively (Hughes and Varley, 1980; Goel *et al.*, 2007; Chen and Liu, 2015). As precursors to all subsequent generations of germ cells, SSC undergo continuous self-renewal and differentiation (spermatogenesis) to produce tens of millions of spermatozoa per day throughout the adult life (De Rooij and Russell, 2000; Kubota and Brinster, 2006). However, SSC are a rare population among testis cells; in adult rodents, they comprise ~0.02-0.2% of testis cells, other estimates put their numbers at ~0.03% of all germ cells or 30,000 per testis in mice (Huckins, 1971; Tegelenbosch and de Rooij, 1993; de Rooij, 1998; Kanatsu-Shinohara *et al.*, 2005). SSC reside in the stem cell niche, which ensures their survival, and regulates their differentiation and self-renewal (Oatley *et al.*, 2009; Oatley and Brinster, 2012).

Differentiation of gonocytes (T2-prospermatogonia) to SSC in rodents is induced by the RA and PDGF signaling pathways (Wang and Culty, 2007; Zhou *et al.*, 2008; Manku *et al.*, 2015). The involvement of microRNA (miRNA) in coordinating the differentiation of gonocytes to SSC has also been suggested (Tong *et al.*, 2011; McIver *et al.*, 2012). The differentiation to SSC is morphologically evident by proliferations to form spermatogonial clusters connected by intercellular bridges (Aponte *et al.*, 2005; Kanatsu-Shinohara and Shinohara, 2013).

Spermatogenesis begins at the basement membrane with mitosis of SSC to produce two daughter cells; one maintains its SSC characteristics to preserves the SSC pool to ensure continuity of the

process, while the other may continue mitotic divisions to form more advanced stages of spermatogonia. More detailed involvement of SSC in spermatogenesis was discussed in Chapter 2.1.3. This self-renewal capability is essential in ensuring the maintenance of SSC pool (De Rooij and Russell, 2000; De Rooij, 2001a). Self-renewal and differentiation of spermatogonia must be kept in balance, or it may lead to either germ cell tumor or depletion of SSC (Meng *et al.*, 2000). This balance is regulated by both extrinsic and intrinsic factors, including GDNF, as one of the most important regulators of SSC self-renewal, produced by Sertoli cells under the influence of FSH. GDNF signaling induces expression of specific genes such as Ets variant gene 5 (*Etv5*) and B-cell leukemia/lymphoma 6 (*Bcl6b*) that are involved in SSC self-renewal (Simon *et al.*, 2007), while RA and DAZL are crucial regulators for spermatogonial differentiation (van Pelt and de Rooij, 1990; de Rooij *et al.*, 1999).

## 2.3 *In Vitro* Culture and Manipulation of Gonocytes

### *2.3.1 Identification, Isolation, and Enrichment of Gonocytes*

Gonocytes have unique attributes that make them a suitable model for MGSC research and use in preserving or restoring fertility. However, gonocytes are present at very low numbers in the neonatal testis, comprising ~1-2% of total testis cells in rat pups, and ~7% of cells within seminiferous cords in piglets (Orwig *et al.*, 2002a; Honaramooz *et al.*, 2005a). The low number of gonocytes limits their use in downstream applications and necessitates their efficient identification, isolation, enrichment, and propagation in culture.

Being the only germ cells present in the testis at birth, gonocytes can be identified by their size, distribution, and distinct morphology (Orwig *et al.*, 2002a; Goel *et al.*, 2007). In the neonatal testis, gonocytes reside at the center of seminiferous cords, and are characterized as large round cells with one or more nucleoli in their prominent nucleus (McGuinness and Orth, 1992; Orth *et al.*, 2000). Upon digestion of the neonatal testis tissue, freshly isolated gonocytes are comparatively larger in size than Sertoli cells (Goel *et al.*, 2007). In culture, gonocytes develop pseudopodia or cytoplasmic extensions, an attribute that is believed to be crucial for their migration (McGuinness and Orth, 1992; van Dissel-Emiliani *et al.*, 1993). Transplanting donor rat gonocytes with or without pseudopods into infertile mice showed that only gonocytes with pseudopods are able to produce donor-derived spermatogenesis (Orwig *et al.*, 2002a). Although the morphological attributes of

gonocytes provide a valuable means for their identification, availability of molecular markers exclusively expressed by gonocytes remain crucial for their efficient identification, isolation, and enrichment.

Currently, no biomarker is known to be uniquely expressed by gonocytes; hence, identification of gonocytes commonly relies on using other germline- and stem cell-specific markers. Germline-specific markers such as DAZL and VASA, which are uniquely expressed in the germ cell lineage can be used to distinguish gonocytes from somatic cells (Castrillon *et al.*, 2000; Reijo *et al.*, 2000; Wu *et al.*, 2009; Fujihara *et al.*, 2011). Gonocytes have also been shown to express specific stem cell markers such as Oct3/Oct4, ZBTB16 (also known as PLZF), KIT, SSEA, NANOG and SALL4 (Ohbo *et al.*, 2003; Hoei-Hansen *et al.*, 2005; Yamaguchi *et al.*, 2005; Rajpert-De Meyts, 2006; Goel *et al.*, 2007; Basciani *et al.*, 2008; Fujihara *et al.*, 2011). Gonocytes also have alkaline phosphatase activity and express surface markers such as CD9, THY1 (CD90), ubiquitin carboxyl-terminal hydrolase-L1 (UCHL1, otherwise known as protein gene product 9.5 –PGP9.5) (Richards *et al.*, 1999; Han *et al.*, 2009) (Kubota *et al.*, 2003; Kanatsu-Shinohara *et al.*, 2004a; Luo *et al.*, 2006; Goel *et al.*, 2007; Lee *et al.*, 2013; Zheng *et al.*, 2014a). THY1 has been suggested as a reliable surface marker for undifferentiated male germ cells including gonocytes in farm animals (*i.e.,* cattle, pig, goat) (Reding *et al.*, 2010; Abbasi *et al.*, 2013; Zheng *et al.*, 2014a). Lectin *Dolichos biflorus* agglutinin (DBA) is also an alternative surface marker for identification and purification of gonocytes, especially in pigs (Goel *et al.*, 2007; Yang and Honaramooz, 2010; Abbasi *et al.*, 2013). In contrast to the germline-specific markers for which the expression is conserved in all cells of the germ cell lineage, the expression of stem cell markers and surface markers in gonocytes are stage-dependent and may show different patterns in different populations of gonocytes (*e.g.*, mitotic fetal, quiescent, and mitotic postnatal/migratory).

Ideally, the isolation of gonocytes from testes should be performed using neonatal donors (immediately or shortly after birth) to obtain a higher proportion of gonocytes and to exclude SSC. This is especially critical in studies involving rodents because the window of gonocyte presence in these species is shorter (few days) (Hamra *et al.*, 2008). The protocols for isolating gonocytes vary among laboratories, but a commonly used method has been a two-step enzymatic digestion. In the first step of this method, the parenchyma of neonatal testis tissue is minced and exposed to enzymes, such as collagenase and hyaluronidase, to dissociate the extracellular matrices/interstitial

tissue. In the second step, the tissue digestion is followed by treatment with trypsin either alone or in combination with other enzymes such as DNase to digest the seminiferous cords and prevent aggregation of cells (van Dissel-Emiliani *et al.*, 1993; Orwig *et al.*, 2002a; Goel *et al.*, 2007). The main drawback of the two-step method is that it has not been specifically designed for isolation of neonatal testis cells, thus results in low gonocyte yields (~10%) in the freshly isolated cells from various species (van Dissel-Emiliani *et al.*, 1989; van Dissel-Emiliani *et al.*, 1993; Li *et al.*, 1997; Orwig *et al.*, 2002a; Lo *et al.*, 2005; Herrid *et al.*, 2009). In more recent years, the technique for isolation of gonocytes from fresh neonatal testis tissue has been improved by the introduction of a three-step isolation method, where gentle enzymatic digestion is combined with mechanical agitation (by including two rounds of vortexing). This procedure results in obtaining ~40% gonocytes among the isolated neonatal pig testis cells (Yang *et al.*, 2010).

Several strategies have been applied to enrich gonocytes in the populations of isolated testis cells. Methods such as velocity sedimentation (STA-PUT) or density gradient centrifugation (*e.g.,* using BSA, Percoll, or Nycodenz) have allowed separation of gonocytes from other testis cells based on their cell size/density differences (van Dissel-Emiliani *et al.*, 1989; Luo *et al.*, 2006; Goel *et al.*, 2007; Yang and Honaramooz, 2011; Bryant *et al.*, 2013). For instance, gonocytes were purified to 70-75% among freshly isolated rat testis cells, using the two-step enzymatic digestion, followed by BSA separation (van Dissel-Emiliani *et al.*, 1989). The gonocyte proportion also has been increased from an initial 40% in the freshly isolated pig testis cell to ~80% after Nycodenz centrifugation (Yang and Honaramooz, 2011). Another commonly used approach to gonocyte enrichment is utilizing the differences in adhesion of somatic cells and gonocytes toward extracellular matrices (*e.g.,* fibronectin, laminin, or collagen). This strategy is referred to as differential plating and can be applied to either freshly isolated testis cells or gonocytes enriched using other methods for further purification. Using differential plating can lead to purification of gonocytes up to ~90% for testis cells of farm animals (Han *et al.*, 2009; Kuijk *et al.*, 2009; Kim *et al.*, 2010a; Yang and Honaramooz, 2011; Zheng *et al.*, 2014a). Alternatively, gonocytes can be enriched using cell sorting technologies targeted toward gonocyte surface markers (*i.e.,* fluorescent-activated cell sorting –FACS– and magnetic-activated cell sorting –MACS) (Valli *et al.*, 2014). Freshly isolated testis cells or cells enriched using other methods can be labelled with either single or double markers that can positively or negatively select gonocytes. Although this technology can yield highly enriched populations of gonocytes (Kubota *et al.*, 2004a; Abbasi *et al.*,

2013; Wu *et al.*, 2013; Kim *et al.*, 2014; McMillan *et al.*, 2014; Zheng *et al.*, 2014a), it also leads to a significant gonocyte loss that limits its use for most applications.

### *2.3.2 Maintenance and Propagation of Gonocytes in Culture*

The use of gonocytes for certain applications, such as transplantation into recipient testes, requires very high numbers that necessitates *in vitro* propagation of gonocytes. This requires the identification of ideal culture conditions that support self-renewal of gonocyte while maintaining their pluripotency. For mouse SSC, long-term culture systems (5 mo to 2 yr) have been successfully established (Kanatsu-Shinohara *et al.*, 2003; Ryu *et al.*, 2005). Application of either the same or modified culture systems for gonocytes using farm animal donors (*e.g.*, goats, cattle, pigs), however, has been less successful in maintaining them beyond 2 mo (Luo *et al.*, 2006; Goel *et al.*, 2007; Kuijk *et al.*, 2009; Bahadorani *et al.*, 2012; Heidari *et al.*, 2012; Zheng *et al.*, 2013; Sahare *et al.*, 2015). The reasons are not clear but likely involve a reduction in self-renewal capacity of gonocytes in culture, differentiation into SSC, or apoptosis over time (Zheng *et al.*, 2014b). However, a few studies have reported successful maintenance of bovine and porcine gonocytes in culture for various periods, with the longest being up to 6 mo (Han *et al.*, 2009; Lee *et al.*, 2013; Sahare *et al.*, 2016). These two groups each used a different culture system, and to date there is no standardized system for maintenance and propagation of gonocytes from farm animal species. Variations in culture conditions (*i.e.,* media, temperature, additives, feeder layer), protocols, and sources of cells make it difficult to replicate the reported systems for maintenance and propagation of gonocytes in different species/laboratory settings.

Once cultured, gonocytes are believed to require the presence of supporting cells or a feeder layer; therefore, at least initially, gonocytes are commonly co-cultured with Sertoli cells (Orth and Boehm, 1990; Orth and McGuinness, 1991; van Dissel-Emiliani *et al.*, 1993). Sertoli cells promote *in vitro* survival of gonocytes via the establishment of specific Sertoli-gonocyte contacts, even in the presence of other testis somatic cells (van Dissel-Emiliani *et al.*, 1993). However, it has also been suggested that various metabolic products or molecular signals released from Sertoli cells may potentially inhibit the proliferation of gonocytes, while promoting their differentiation (Griswold, 1998; Hasthorpe *et al.*, 2000). Alternative cells for co-culturing with MGSC have included mitotically-inactivated cells such as SIM embryo-derived thioguanine and aoubain

resistant (STO) or mouse embryonic fibroblasts (MEFs), obtained through mitomycin-C treatment or irradiation. The STO cells have been found to be the most effective feeder cells for maintenance of MGSC, notably SSC, and have also been used to co-culture with gonocytes of various donor species (*e.g.,* rodent, bovine, porcine, human) (van Dissel-Emiliani *et al.*, 1993; Olie *et al.*, 1995; Nagano *et al.*, 1998; Hasthorpe *et al.*, 1999; Oatley *et al.*, 2002; Kent Hamra *et al.*, 2004; Kubota *et al.*, 2004a; Childs *et al.*, 2008; Wu *et al.*, 2009; Han *et al.*, 2009; Nasiri *et al.*, 2012). The use of feeder cells, however, is not without its limitations. Different types of feeder cells have different effects on proliferation and self-renewal capability of MGSC, and there is considerable variation in the source, treatments applied, and batches among these cells. In addition, some of the same concerns remain over the potential adverse effects of their released metabolites/factors on MGSC (He *et al.*, 2015).

Since the establishment of *in vitro* culture systems for MGSC, the choice of culture media has always been an essential component of the culture system. Different types of media have been used for culturing gonocytes, ranging from very basic (*e.g.,* DMEM) to enriched/specialized (*e.g.,* DMEM/F12, StemPro) (van Dissel-Emiliani *et al.*, 1993; Goel *et al.*, 2007; Aponte *et al.*, 2008; Fujihara *et al.*, 2008; Kuijk *et al.*, 2009). The serum has been commonly added as a main component to these media to support optimal growth of cells; although its effect on cultured MGSC remains poorly understood. The use of serum may in fact have inadvertent influences on the rate of proliferation and differentiation of SSC, since higher serum concentrations were found to negatively affect the expansion of SSC (Kanatsu-Shinohara *et al.*, 2005; Bahadorani *et al.*, 2012). Effects of serum on gonocytes are even less studied, but have been suggested to be similar to SSC. Fetal bovine serum (FBS) used at 5% was shown to promote the survival of porcine gonocytes up to 9 days when cultured either alone or in the presence of Sertoli cells (Marret and Durand, 2000). However, FBS exerted deleterious effects when added at 2-8% to cultured rat gonocytes, where a reduction in gonocyte numbers was observed at 5 days onward (van Dissel-Emiliani *et al.*, 1993). Using neonatal pig testis cells, a negative correlation was observed between the colony formation potential of gonocytes and serum concentrations (*i.e.,* more colonies in 1% than 10% FBS) (Zheng *et al.*, 2013). High concentrations of serum in the media may also enhance the growth of somatic cells and exert detrimental effects on SSC proliferation (Izadyar *et al.*, 2003a; Bahadorani *et al.*, 2012; Zheng *et al.*, 2013). These findings collectively suggest that serum should be used cautiously

as an additive to the culture of gonocytes. Similar to feeder cells, variations in the sources, composition, batches, and manufactures of serum may influence the cell culture outcomes.

Given the limitations and uncertainty over the effects of feeder cells and serum on MGSC, alternative serum-free and feeder-free culture conditions have also been explored. In serum-free systems, a variety of specialized media may be used that include minimum essential medium-alpha (MEMα), F10, Knockout Serum Replacement (KSR), StemPro-34, B27 supplement, and Iscove's modified Dulbecco's medium (IMDM) (Kubota *et al.*, 2004a; Kanatsu-Shinohara *et al.*, 2005, 2011; Aoshima *et al.*, 2013; Kanatsu-Shinohara *et al.*, 2014; Sahare *et al.*, 2016). To replace feeder cells, MGSC have been cultured on plates coated with extracellular matrices such as laminin, gelatin, or poly-L-lysine (Sadri-Ardekani *et al.*, 2009; Kanatsu-Shinohara *et al.*, 2011; Kanatsu-Shinohara and Shinohara, 2013; Lee *et al.*, 2013; Sahare *et al.*, 2016). On the other hand, exogenous nutrients such as bovine serum albumin (BSA), growth factors, amino acids, and vitamins have been added as essential components in serum-free and feeder-free culture systems. As discussed in Chapter 2.4, a number of growth factors have been identified to regulate the proliferation and self-renewal of cultured MGSC/gonocytes including GDNF, PDGF, RA, epidermal growth factor (EGF), basic fibroblast growth factor 2 (FGF2), leukemia inhibitory factor (LIH), and stem cell factors (SCF). Thus far, serum-free and feeder-free culture systems have been developed for culturing gonocytes from rodents (Kanatsu-Shinohara *et al.*, 2011, 2014), cattle (Sahare *et al.*, 2016), humans (Sadri-Ardekani *et al.*, 2009; Piravar *et al.*, 2013), and pigs (Lee *et al.*, 2013).

### *2.3.3 Potential Derivation of Pluripotent Stem Cells*

Pluripotent stem cells (PSC) are undifferentiated cells that have the capacity for self-renewal, proliferation, and giving rise to different types of cells and tissues of all three germinal layers (*i.e.,* ectoderm, mesoderm, and endoderm). These PSC can be of embryonic origin (*i.e.,* embryonic stem -ES- cells) or artificially induced (iPSC) *in vitro* (Evans and Kaufman, 1981; Thomson *et al.*, 1998). The ES cells are collected from the inner-mass cells of embryos at the blastocyst stage, while iPSC are obtained through reprogramming of somatic cells by enforcing the expression of key pluripotency genes (*i.e., Oct3/4*, *Klf4*, *c-Myc*, *Sox2*) (Takahashi and Yamanaka, 2006; Takahashi *et al.*, 2007; Wernig *et al.*, 2007; Yu *et al.*, 2007; Lowry *et al.*, 2008; Park *et al.*, 2008; Kim *et al.*, 2016). Once induced, iPSC share many similarities with ES cells (*i.e.,* morphology,

karyotype, gene expression) and the resemblance becomes more prominent as iPSC lose their epigenetic markers over time, after multiple passages (Wernig *et al.*, 2007; Yu *et al.*, 2007; Kim *et al.*, 2010b). Therefore, iPSC offer an alternative to ES cells, where the collection is hampered by ethical issues and limited supply (Yamanaka and Blau, 2010). However, given the use of viral vectors for the induction of pluripotency genes, the clinical application of iPSC for stem cell therapy (*i.e.,* regenerative medicine) carries a risk of carcinogenicity. While iPSC can be used as a valuable tool for diseases modelling and drug screening *in vitro* (Colman and Dreesen, 2009), the search continues for alternative sources of pluripotent stem cells whose application is not hampered by ethical or carcinogen concerns.

Male germline stem cells (*i.e.,* PGC, gonocytes, SSC) may have the potential to be induced into PSC (Sabour and Schöler, 2012). The original concept was suggested in 1979 (Illmensee and Stevens, 1979), a decade before PSC were successfully obtained *in vitro* from PGC of 8.5-12.5 dpc embryos, under the influence of growth factors (*i.e.,* FGF2, SCF, LIF) (Matsui *et al.*, 1992; Resnick *et al.*, 1992). These PSC where characterized by the formation of embryoid bodies and differentiation into multiple type of cells in long-term culture, development of tumors (*i.e.,* teratomas and teratocarcinomas) upon implantation into nude mice, and contribution to germline chimeras when microinjected into blastocysts (Matsui *et al.*, 1992; Resnick *et al.*, 1992; Labosky *et al.*, 1994; Stewart *et al.*, 1994). It was initially presumed that the capability to transform into PSC was restricted to PGC, because an attempt to derive PSC from postnatal spermatogonia using the same conditions had failed (Labosky *et al.*, 1994). However, this view changed in 2003, when ES-like cells were derived from mouse SSC, which showed PCS characteristics upon culture in a newly developed long-term system (Kanatsu-Shinohara *et al.*, 2003, 2004b, 2005). Interestingly, the transformation into pluripotency state occurred without the need for 'reprograming' and in the absence of GDNF, a key factor associated with SSC self-renewal (Kanatsu-Shinohara *et al.*, 2004b). Unlike iPSC from somatic cells and ES cells (Hayashi *et al.*, 2012; Easley *et al.*, 2014), SSC-derived PSC lose their spermatogenic potential (Kanatsu-Shinohara *et al.*, 2004b, 2008b). Although SSC-derived PSC have been produced from mice of different ages (Guan *et al.*, 2006; Seandel *et al.*, 2007; Ko *et al.*, 2009), a recent study suggested that the capability of SSC to be induced pluripotent is age-dependent, where it decreases as the mouse reached adulthood (Azizi *et al.*, 2016). In addition to mouse SSC, PSC have also been derived from human, porcine, bovine,

and caprine SSC (Conrad *et al.*, 2008; Kossack *et al.*, 2009; Wang *et al.*, 2014, 2016a; Jafarnejad *et al.*, 2018).

ES-like colonies have been produced and characterized mostly in cultures using gonocytes from non-rodent models (*i.e.,* pigs, cattle, goats), because relatively large numbers of testis cells can be collected from their neonatal testes (Goel *et al.*, 2009; Kuijk *et al.*, 2009; Zheng *et al.*, 2014a). More recently, derivation of PSC from mouse and pig gonocytes has also been reported (Tanaka *et al.*, 2015; Niu *et al.*, 2016). Mechanisms underlying the formation of ES-like cells from postnatal MGSC remain to be elucidated. It was hypothesized that ES-like cells might be the remnants of pluripotent cells from the fetal stage (Kubota and Brinster, 2006); however, this possibility has been questioned because the direct derivation of ES-like cells from either ES cells or embryonic germ cells in culture conditions has been problematic (Labosky *et al.*, 1994; Kanatsu-Shinohara *et al.*, 2004b). The frequency of ES-like cells formation by postnatal MGSC is low, but treatment with glycogen synthase kinase-3 (GSK3) inhibitors and vitamin C has been found to promote the formation of ES-like cells from SSC culture (Moraveji *et al.*, 2012; Wang *et al.*, 2014). A newly-developed protocol involving depletion of two germ cell tumor candidate genes, *Trp53* and *Dmrt1* (double knockout), improved the efficiency of PSC derivation from MGSC (Takashima *et al.*, 2014; Tanaka *et al.*, 2015).

### *2.3.4 In Vitro Spermatogenesis*

*In vitro* spermatogenesis refers to an *ex vivo* production of haploid cells from diploid male germ cells in an artificial environment, which can be performed by culturing testis organ, tissue, or cells in two- (2D) or three-dimensional (3D) systems (Tesarik *et al.*, 1999; Izadyar *et al.*, 2003a; Suzuki and Sato, 2003; Stukenborg *et al.*, 2008; Sato *et al.*, 2011a; Abu Elhija *et al.*, 2012; Riboldi *et al.*, 2012; Yokonishi *et al.*, 2014). Testis organ/tissue culture involves using a whole testis or its small fragments, which ensures that the germ cells remain in their niche architecture and microenvironment throughout the culture period (Ibtisham *et al.*, 2017). However, the success of this technique relies heavily on the ability of the system to keep the tissue viable for a longer period. The use of isolated testis cells, on the other hand, involves culturing of germ cells with or without somatic or feeder cells to initiate the spermatogenic process (as described in Chapter 2.3.2).

Replicating the complex process of spermatogenesis *in vitro* has many applications that range from use as a research model to potential experimental/clinical use as an alternative for infertility treatment or conservation/preservation of endogenous spermatogenesis. Therefore, achieving *in vitro* differentiation of germ cells has been a long-standing research objective going back a century (Champy, 1920). Since then, substantial improvements have been made especially in cell culture protocols and in our understanding of the requirements of *in vitro* differentiation. The media composition and additives may play an important role during this process. Several studies have reported positive effects of FBS on *in vitro* differentiation of germ cells (Haneji *et al.*, 1983; Izadyar *et al.*, 2003b), while the effects of serum-free media have been less consistent. When KSR was used in cultures of neonatal and adult mouse testis tissues, differentiation potential was greatly improved as compared with FBS (Sato *et al.*, 2011a; Riboldi *et al.*, 2012). However, another study using fetal mouse testes reported that using KSR prevented the entry of male germ cells into mitotic arrest and caused epigenetic instabilities that raised safety concerns (Hogg and Western, 2015). *In vitro* differentiation and fertilization potential of germ cells were improved with the use of FSH and testosterone, alone or in combination, in culture systems (Tesarik *et al.*, 1998; Sousa *et al.*, 2002; Movahedin *et al.*, 2004; Vigier *et al.*, 2004; Hasegawa *et al.*, 2010; Xie *et al.*, 2010). Similarly, RA promoted *in vitro* germ cell differentiation, especially in the early steps; however, the effect on later steps requires further investigation, since the production of haploid germ cells was found to be less efficient (Wang *et al.*, 2016b).

Cryopreservation does not seem to hinder the progression of spermatogenesis *in vitro*, which has important clinical implications. Cryopreserved immature mouse testis tissue was shown to have comparable differentiation potential (SSC to secondary spermatocytes and spermatids after 2 wk of culture), and even slightly higher fertilization rate (78% *vs.* 74%) than that of fresh adult testis tissue (Suzuki and Sato, 2003). Viable offspring have also been produced from spermatids produced *in vitro* from cryopreserved testis tissue, through the use of round spermatid injection (ROSI) or intra-cytoplasmic spermatozoa injection (ICSI) (Sato *et al.*, 2011a; Yokonishi *et al.*, 2014). The differentiation efficiency appears donor age-dependent; fewer fertile haploid cells were produced when the tissue was from adult mouse testes than from neonates (Sato *et al.*, 2015).

There is no consistent or standardized incubation temperature defined for *in vitro* spermatogenesis since the temperatures used vary from 30-39 ˚C (Matte and Sasaki, 1971; Hofmann *et al.*, 1994;

Tesarik *et al.*, 1999; Izadyar *et al.*, 2003a; Sato *et al.*, 2011a). Using different incubation temperatures in a single study showed that although both germ cell proliferation and differentiation occurred steadily at 37 ˚C, conditions were more favorable for proliferation at 39 ˚C and better for differentiation at 32 ˚C (Hofmann *et al.*, 1994). In more recent years, 3D culture technology has been introduced for *in vitro* spermatogenesis, in which isolated cells or tissue fragments are cultured on/in 3D scaffolds, made from natural or synthetic polymers (*e.g.*, agarose, collagen matrix, methylcellulose) or poly lactic-co-glycolic acid (PLGA). The 3D culture system, however, seems to be more efficient than the 2D system, because it led to increased occurrence of post-meiotic cells (haploid germ cells) (Lee *et al.*, 2007a; Abu Elhija *et al.*, 2012; Khajavi *et al.*, 2014; Huleihel *et al.*, 2015).

The results of *in vitro* spermatogenesis in the literature vary greatly, and different degrees of germ cell differentiation have been reported. The results seem to be heavily affected by the source of cells/tissues (*i.e.*, prepubertal *vs.* adult *vs.* cryptorchid, or nonobstructive- *vs.* obstructive azoospermia), strains (wild-type *vs.* transgenic), species (mouse, rat, human, non-human primates, cattle), culture length (short-term *vs.* long-term), and culture systems (organ/tissue *vs.* isolated cells, or 2D *vs.* 3D). Nevertheless, more recently functional spermatozoa have been successfully produced *in vitro* using both organ/tissue and isolated cell cultures, with greater success (75%) using organ/tissue cultures (Sato *et al.*, 2011a, b; Abu Elhija *et al.*, 2012; Yokonishi *et al.*, 2014). Interestingly, these successful studies were all performed using rodent donors, in the form of tissues or cells, and 3D systems. The resultant haploid germ cells (*i.e.*, spermatids and spermatozoa) were also functional, examined through the use of ROSI or ICSI, resulting in the production of donor-derived offspring (Sato *et al.*, 2011a, b; Yokonishi *et al.*, 2014).

Thus far, there has been no report of studies achieving or specifically testing the differentiation potential of neonatal gonocytes all through the production of spermatozoa *in vitro*. Almost all available literature refers to the use of cells or tissues from immature/prepubertal to adult rodents (Matte and Sasaki, 1971; Tesarik *et al.*, 1999; Izadyar *et al.*, 2003b; Suzuki and Sato, 2003; Movahedin *et al.*, 2004; Stukenborg *et al.*, 2008; Abu Elhija *et al.*, 2012; Riboldi *et al.*, 2012). Because in mice, SSC appear as early as 3-8 dpp (Vergouwen *et al.*, 1991; Drumond *et al.*, 2011), even in the studies where the source of testes was indicated as neonates, the earliest germ cells were SSC, not gonocytes (Sato *et al.*, 2011a; Wang *et al.*, 2016b). Since differentiation of

gonocytes to SSC can be induced *in vitro* such as with RA treatment (Wang and Culty, 2007; Zhou *et al.*, 2008), *in vitro* spermatogenesis from gonocytes is theoretically achievable.

## 2.4 Involvement of Growth Factors in Testis Development

### *2.4.1 Fibroblast Growth Factors*

Members of the fibroblast growth factor (FGF) family are expressed in various cells throughout the male reproductive tract and play an important role in the development of fetal and postnatal testes. As described earlier (in Chapter 2.1.1), FGF9 is one of key regulators of sexual differentiation, in which the expression is upregulated as a result of *Sry*-activated SOX9 (Colvin *et al.*, 2001; Sekido *et al.*, 2004; Wilhelm *et al.*, 2005). Persistent expression of FGF9 is crucial in maintaining SRY and SOX9 to drive the center-to-pole (poleward expansion) of testiculogenic programs and testis cords formation in the developing gonad (Kim *et al.*, 2006a; Moniot *et al.*, 2009). The FGF9 signaling drives the proliferation of mesenchymal stem cells and the migration of mesonephric cells into the gonad, leading to formation of the interstitial compartment (Colvin *et al.*, 2001). Coordinated expression of SRY, SOX9, and FGF9 maintain the expression of testis genes, while deactivating genes involved in the ovarian development (Li *et al.,* 2014). FGF9 alone has been shown to exert antagonist effects on WNT4, a crucial factor in promoting the female gonad development (Jameson *et al.*, 2012).

Other members of the FGF family involved in testis development include FGF8, FGF1, FGF2, and FGF4. For instance, FGF8 has an important function in maturation of the seminiferous epithelium, thus its expression can decrease over time (Valve *et al.*, 1997). FGF2 and FGF4 affect somatic cells of the testis by playing an important role in the proliferation and survival of Sertoli cells, respectively (van Dissel-Emiliani *et al.*, 1996), while FGF2 and FGF1 have been associated with steroidogenesis and the normal function of Leydig cells (Sordoillet *et al.*, 1992; Laslett *et al.*, 1997). The potential direct role of the FGF family on germ cells is less clear; however, it has been suggested that the proliferation of neonatal gonocytes *in vitro* can be induced by FGF2 (van Dissel-Emiliani *et al.*, 1996). FGF2 is also a critical regulator of SSC self-renewal, where it is involved in the expression of ETV5 and BCL6B, candidate transcription factors for SSC-self renewal (Ishii *et al.*, 2012). The FGF9 signaling is also involved in mitogen-activated protein (MAP) kinase activation, which contributes to the proliferation of primitive spermatogonia and spermatogenic

meiosis during fetal and postnatal stages, respectively (Sun *et al.*, 1999). Finally, FGF4 and FGF21 exert anti- and pro-apoptotic effects on germ cells, respectively, as a potential mechanism for maintaining the germ cell pool in the testis (Yamamoto *et al.*, 2002; Hirai *et al.*, 2004).

### *2.4.2 Glial Cell-Derived Neurotrophic Factor*

The glial cell-derived neurotrophic factor (GDNF), a member of the transforming growth factor-beta (TGFß), was first identified in the media of glioma cell line cultures (Lin *et al.*, 1993). GDNF has been shown to promote the renal and neural development, while in the testis, it is produced by Sertoli cells under the influence of FSH, certain growth factors, and cytokines (Tadokoro *et al.*, 2002; Simon *et al.*, 2007). GDNF exerts its effects via the GFRα-1 and RET receptors, expressed by undifferentiated spermatogonia, to affect the establishment of stem cell niche, and to regulate SSC self-renewal and differentiation both *in vivo* and *in vitro* (Meng *et al.*, 2000; Viglietto *et al.*, 2000; Tadokoro *et al.*, 2002; Kanatsu-Shinohara *et al.*, 2003; Yomogida *et al.*, 2003; Hofmann *et al.*, 2005; Naughton *et al.*, 2006). The GDNF-receptor complex is involved in the intercellular communications between Sertoli cells and SSC, development of actin cytoskeleton, and migration of gonocytes/SSC to the stem cell niche (Dovere *et al.*, 2013). Disruptions in GDNF signaling, as observed in Ets variant gene 5 (*Etv5*) knockout mice, results in the loss of spermatogonia, due to decreased chemoattraction between Sertoli cells and SSC (Simon *et al.*, 2010), while overexpression of GDNF promotes the proliferation of spermatogonia (Meng *et al.*, 2000). Subsequent germ cell transplantation studies, where SSC from fertile donors were transplanted into GDNF knockout mice further validated these findings (Kanatsu-Shinohara *et al.*, 2003; Ogawa *et al.*, 2003; Yomogida *et al.*, 2003). In addition to the effects on germ cells, GDNF plays a role in the proliferation of Sertoli cells in the developing testis (Wu *et al.*, 2005).

GDNF was also one of the growth factors used in the establishment of a long-term culture system for the maintenance of SSC (Kanatsu-Shinohara *et al.*, 2003). The spermatogonia from neonatal mouse testes cultured on mouse embryonic fibroblasts (MEFs) in the presence of GDNF, EGF, LIH, and FGF2 supported the formation of germ cell colonies expressing SSC markers for up to 2 years. Since then, GDNF has been added as an indispensable component in long-term cultures of SSC from young and adult mice (Kanatsu-Shinohara *et al.*, 2004b; Kubota *et al.*, 2004a; Ogawa *et al.*, 2004; Ryu *et al.*, 2005). The GDNF signaling for self-renewal of SSC occurs via the activation

of phosphoinositide 3-kinase (PI3K)/AKT and mitogen-activated protein kinase/ERK1 kinase-1 (MEK) pathways (Braydich-Stolle *et al.*, 2007; Lee *et al.*, 2007b; Oatley *et al.*, 2007), which are responsible for the expression of transcription factors such as ETV5, BCL6B, EGR2 LHX1, FOXO1, ID4, POU3F1, and L-GILZ (Oatley *et al.*, 2006, 2011; Wu *et al.*, 2011; Ishii *et al.*, 2012; Romero *et al.*, 2012). Some of these factors (*e.g.,* ETV5, BCL6B, FOXO1, L-GILZ) are necessary in maintaining the expression of the RET receptor. In addition, the presence of ETV5 upregulates the expression of CXCR4, a chemokine receptor involved in the migration of PGC to the developing gonad, and SSC to the stem cell niche in the postnatal testes. Thus, the suppression of GDNF signaling pathways and their downstream transcription factors result in the failure of SSC to proliferate or survive and hence lead to depletion of spermatogenesis (Ara *et al.*, 2003; Kanatsu-Shinohara *et al.*, 2012; Kanatsu-Shinohara and Shinohara, 2013).

### *2.4.3 Stem Cell Factor*

The stem cell factor (SCF) and its receptor, the tyrosine kinase receptor c-kit (SCF/c-kit), have been shown to play an important role in the development of functional testis tissue. SCF is produced by Sertoli cells, and its expression in the adult testis can be seen at the basement membrane of seminiferous tubules and on the surface of Sertoli cells, while c-kit receptors are localized to germ cells (*i.e.,* spermatogonia, spermatids) and Leydig cells (Bokemeyer *et al.*, 1996; Unni *et al.*, 2009). Therefore, the SCF/c-kit complex provides the microenvironment necessary for spermatogenesis by exerting its effect on both the somatic and germ cell components of the testis (Bokemeyer *et al.*, 1996). Mutation of the *W* and *Sl* loci, which encode c-KIT and SCF, respectively, results in aberrations of spermatogenesis (Morrison-Graham and Takahashi, 1993; Loveland and Schlatt, 1997; Olaso and Habert, 2000). On somatic cells, the SCF/c-kit complex has been found to regulate the formation of Leydig cell populations during testis morphogenesis, support their survival, and affect testosterone synthesis during testis development (Yoshinaga *et al.*, 1991; Yan *et al.*, 2000a).

The actions of SCF/c-kit on germ cells persist throughout life; for instance, during gonadal development, expression of c-kit regulates the migration, survival, and proliferation of PGC and can be traced back to 7-12.5 dpc (Dolci *et al.*, 1991; Matsui *et al.*, 1991; Motro *et al.*, 1991). SCF/c-kit also supports the subsequent processes and events in testis development, including the

promotion of Sertoli-germ cell adhesion during testis cords formation (Marziali *et al.*, 1993). Decreases in SCF at certain stages of testis development have been associated with the mitotic arrest of spermatogonia (Mauduit *et al.*, 1999). In the postnatal testis, SCF/c-kit is known to support the differentiation of various germ cells, and survival of differentiated spermatogonia, spermatocytes, and spermatids (Yan *et al.*, 2000a) (Dolci *et al.*, 1991; Yoshinaga *et al.*, 1991; Hakovirta *et al.*, 1999; Schrans-Stassen *et al.*, 1999). This action was further highlighted in a study using telomerase-immortalized type A spermatogonia, where in the presence of SCF, these cells became capable of undergoing differentiation into haploid spermatids (Feng *et al.*, 2002).

### *2.4.4 Leukemia Inhibitory Factor*

The leukemia inhibitory factor (LIF) is a multifunctional polypeptide cytokine/growth factor of the interleukin 6 (IL-6) family, first identified for its supporting role in the maintenance of self-renewal and totipotency of mouse ES cells (Smith *et al.*, 1988). LIF is produced predominantly by the peritubular myoid cells, and in the rat testis can be detected from 13.5 dpc until adulthood (Piquet-Pellorce *et al.*, 2000). LIF receptors (LIF-R) are expressed by germ cell precursors (*i.e.,* PGC, gonocytes, spermatogonia), as well as Sertoli cells and Leydig cells. Therefore, considerable amounts of bioactive LIF can be found in both the interstitial and tubular compartments of the testis (Jenab and Morris, 1998; Piquet-Pellorce *et al.*, 2000).

*In vitro* studies have demonstrated that LIF plays a significant role in the proliferation and survival of MGSC (Matsui *et al.*, 1991; Pesce *et al.*, 1993; Cheng *et al.*, 1994; De Miguel *et al.*, 1996; Koshimizu *et al.*, 1996). LIF has been found to promote the proliferation of murine PGC *in vitro*, even in the absence of feeder cells, where the blocking of its receptor using LIF-R antiserum results in their apoptosis and death (Pesce *et al.*, 1993; Cheng *et al.*, 1994) (Godin *et al.*, 1991; Matsui *et al.*, 1991). The addition of LIF initiates the proliferation and survival of rodent gonocyte-Sertoli co-cultures (De Miguel *et al.*, 1996), enhances the formation of germ cell colonies, and promotes the differentiation of murine and bovine gonocytes to spermatogonia (Kanatsu-Shinohara *et al.*, 2007; Aponte *et al.*, 2008; Rastegar *et al.*, 2015). On the other hand, the withdrawal of LIF can disrupt the development of SSC and their colonies (Rastegar *et al.*, 2015). A role for LIF in the proliferation and survival of SSC has been shown by the increased incorporation of $^{3}$H-thymidine in spermatogonia in the micro-dissected seminiferous tubule cultures (Dorval-Coiffec *et al.*, 2005).

For somatic cells, LIF has been found to promote the survival of Sertoli cells when co-cultured with gonocytes (De Miguel *et al.*, 1996), and upregulate transcription of the c-fos gene, which is important for their differentiation in primary cultures (Jenab and Morris, 1998). LIF may also act as a regulator of testosterone production (Jenab and Morris, 1998; Yano *et al.*, 1998). Much less is known about the role of LIF in differentiated germ cells; the incubation of spermatozoa with LIF promotes their motility and survival in a dose-dependent manner (Attar *et al.*, 2003), while overexpression of LIF has been found to have detrimental effects on spermatogenesis (Hilton and Gough, 1991; Shen *et al.*, 1994; Yano *et al.*, 1998).

### *2.4.5 Vascular Endothelial Growth Factor*

The vascular endothelial growth factor (VEGF) is a very important family of growth factors for diverse functions ranging from blood vessel development and permeability to cellular migration (Ferrara *et al.*, 1996; Ferrara, 2000). The VEGF proteins are well-conserved and have several subtypes encoded in humans by five different genes including, *VEGF-A*, *VEGF-B*, *VEGF-C*, *VEGF-D*, and placental growth factors (*PLGF*). During embryonic development, the absence of even a single VEGF allele halts the development of vasculature, which is lethal for the embryo (Carmeliet *et al.*, 1996; Ferrara *et al.*, 1996). The VEGF family exert their actions via receptors known as VEGFR1 and VEGFR2, where, for instance, VEGFR1 is responsible for the development of endothelial lineage and VEGFR2 for the organization of endothelium (Fong *et al.*, 1995; Shalaby *et al.*, 1995). The role of VEGF in the testis is poorly understood because the adult tissue is not an active site of angiogenesis. VEGF expression has been detected along the male genital tract, such as in Leydig and Sertoli cells, as well as the lining of the epididymis, prostate, and vesicular glands (Carmeliet *et al.*, 1996). VEGF-A is produced by Sertoli and Leydig cells during different stages of testis development (Liu and Yang, 2004; Bott *et al.*, 2006). VEGFR2 is expressed in the testis micro-vasculature and vascular endothelium of the epididymis, while VEGFR1 is expressed in human and rodent germ cells (Ergün *et al.*, 1997; Korpelainen *et al.*, 1998; Nalbandian *et al.*, 2003; Rudolfsson *et al.*, 2004). Therefore, it is presumed that the role of VEGF in the testis may involve vascular permeability and postnatal germ cell development (Korpelainen *et al.*, 1998).

During the fetal period, VEGF-A is involved in the formation of testis cords, where it promotes and coordinates the migration of cells, including endothelial cells from the mesonephros into the

developing gonad (Bott *et al.*, 2006; Cool *et al.*, 2011). Blocking the VEGF receptors with VEGF antagonists results in disruption of seminiferous cords formation. Testis tissue xenografting and testis cell implantation studies demonstrated that VEGF is required for the normal function of germ cells, where treating the donor testis tissue and cells with VEGF (*i.e.*, VEGF-A or VEGF-164) prior to grafting/implantation promoted the proliferation, survival, and differentiation of germ cells (Schmidt *et al.*, 2006a; Dores and Dobrinski, 2014). A protective role for VEGF on germ cells has also been suggested using a 'loss-of-function' approach; VEGFR2 antagonists caused a reduction of germ cell numbers in bovine testis tissue fragments after 5 days in culture, while this number increased when VEGF-A was added (Caires *et al.*, 2009). On the other hand, the overexpression of VEGF (*e.g.*, VEGF-A120 and VEGF-A165) in transgenic mice increased the size, density, and permeability of vasculature in the testis and epididymis, but also caused infertility, likely as a result of elevated testis temperature, leading to impaired spermatogenesis (Korpelainen *et al.*, 1998; Huminiecki *et al.*, 2001).

### *2.4.6 Retinoic Acid*

Retinoic acid (RA) or tretinoin is a bioactive metabolite of retinol (vitamin A). Long known as a crucial factor for vision, RA is also involved in the development of cells and organs, and various other functions in the immune and reproductive systems (Mark *et al.*; Wang *et al.*, 1997; Gale *et al.*, 1999; White *et al.*, 2000; Doyle *et al.*, 2007; Anderson *et al.*, 2008; Chung *et al.*, 2011; Cassani *et al.*, 2012; Valli *et al.*, 2014). Because RA cannot be synthesized *in vivo* (except in the testis), it has to be acquired from the diet and stored in the liver to be delivered to target tissues via binding with retinol binding proteins. In the tissue, retinol is converted to all-trans retinal through oxidation by retinal dehydrogenase enzymes (Theodosiou *et al.*, 2010; Napoli, 2012). Thus far, several RA isomers including all-trans-RA, 9-cis-RA, 13-cis-RA, 11-cis RA and 9, and 13-di-cis-RA have been identified (Kunchala *et al.*, 2000). The molecular actions of RA are exerted through binding to heterodimers or nuclear RA receptors (RARα, β, γ) and retinoid X receptors (RAXα, β, γ). However, amongst all receptors, the expression of RARβ is known to be markedly enhanced by RA (Ghyselinck *et al.*, 2006; Cassani *et al.*, 2012; Samarut and Rochette-Egly, 2012).

The required RA in the testis is synthesized *in situ* by Sertoli cells and distributed to germ cells (Livera *et al.*, 2002), where RA receptors are found in both Sertoli cells and differentiated germ

cells (Dufour and Kim, 1999; Chung *et al.*, 2009). A number of important roles are played by RA, which include contributing to testosterone production, ensuring the integrity of the stem cell niche (*e.g.*, by maintaining the blood-testis barrier and anchoring germ cells to Sertoli cells), and assisting in the release of mature spermatozoa into the lumen of seminiferous tubules (Appling and Chytil, 1981; Huang *et al.*, 1983; Vernet *et al.*, 2006). In the fetal testis, RA appears to stimulate both the proliferation and apoptosis of gonocytes (Livera *et al.*, 2001). The expected decrease in gonocyte mitotic activity between 11.5 and 13.5 dpc was partly prevented under the influence of RA in organ culture (Trautmann *et al.*, 2008), while the number of mitotic 16.5 dpc gonocytes reduced after 6 days of culture with RA (Boulogne *et al.*, 2003). This dual action of RA is thought to be important in maintaining the fetal gonocyte pool and eliminating abnormal gonocytes. In the postnatal testis, RA has a critical role in spermatogenesis, where its lack results in impaired spermatogenesis. In the vitamin A-deficient (VAD) model, spermatogenesis is arrested at the type A spermatogonia stage in mice and at the preloptotene stage in rats, but it can be restored with the systemic administration of vitamin A (van Pelt and de Rooij, 1990; Van Pelt and de Rooij, 1991). RA has also been identified as the leading promoter of gonocyte differentiation into spermatogonia. *In vitro*-cultured neonatal mouse and rat gonocytes treated with RA show increased *Stra8* expression, an indicator of gonocyte differentiation to spermatogonia (Wang and Culty, 2007; Zhou *et al.*, 2008).

### *2.4.7 Epidermal Growth Factor*

The epidermal growth factor (EGF) is a cytokine first found in the submandibular salivary gland of mice and in human urine (also named urogastrone) (Carpenter and Cohen, 1990). However, EGF has been shown to be involved in diverse and important processes such as facilitating cell proliferation, tissue differentiation, and organogenesis (Fisher and Lakshmanan, 1990; Adamson, 1993). The localization of EGF expression in the testis varies in different species; in rodents, it is expressed predominantly in Leydig cells (Zhang *et al.*, 1997; Yan *et al.*, 1998), in boars and bulls, mainly in germ cells (Caussanel *et al.*, 1996; Kassab *et al.*, 2007), and in adult alpaca, in both germ cells and somatic cells (He *et al.*, 2009). EGF exerts its effect via EGF receptor (EGFR) mainly found on testis somatic and germ cells in rodents, humans, and non-human primates (Stubbs *et al.*, 1990; Suarez-Quain and Niklinski, 1990; Haneji *et al.*, 1991; Radhakrishnan *et al.*, 1992; Moore and Morris, 1993; Caussanel *et al.*, 1996; Nakazumi *et al.*, 1996). The role of EGF in male

reproduction was initially studied using sialoadenectomy–the removal of submandibular glands– in mice which led to a significant drop in the circulating levels of EGF, and a marked decrease in the number of mature spermatozoa in the epididymis. Treating mice with EGF restored the number of mature spermatozoa in the epididymis and spermatids in the testis to normal levels (Tsutsumi *et al.*, 1986; Liu *et al.*, 1994; Suarez-Quian *et al.*, 1994). The EGF/EGFR complex is involved in the proliferation and differentiation of germ cells, as shown by the increased incorporation of $^{3}$H-Thymidine ($^{3}$H-dT) into rat spermatogonia using cultured seminiferous tubules (Wahab-Wahlgren *et al.*, 2003). *In vitro* incubation of testis fragments from cryptorchid donor mice with EGF induced differentiation of spermatogonia type A into type B and primary spermatocytes (Haneji *et al.*, 1991). Moreover, spermatogenesis is impaired in EGFR knockout mice, although the testes appear to be of normal size (Levine *et al.*, 2000).

## 2.5 *In Vivo* Culture Systems for Male Germline Stem Cells

### *2.5.1 Male Germ Cell Transplantation*

Male germ cell transplantation (GCT) is a technique introduced in 1994, which involves the transfer of germ cells (*i.e.,* containing SSC) isolated from a fertile donor into the seminiferous tubules of infertile recipient testes. The transplanted germ cells are capable of migrating from the seminiferous tubular lumen, where they are deposited, to the basement membrane, where they colonize and undergo complete spermatogenesis; making it possible for the recipient to sire progeny using donor-derived spermatozoa (Brinster and Avarbock, 1994; Brinster and Zimmermann, 1994). Being initially established in a mouse model, the same principle has been extrapolated for using GCT in other rodents (*i.e.,* rats, hamsters), and modified for use in farm animals (*i.e.,* pigs, goats, sheep, cattle), monkeys, fish, and chicken (Jiang and Short, 1995; Clouthier *et al.*, 1996; Ogawa *et al.*, 1999; Schlatt *et al.*, 2002b; Takeuchi *et al.*, 2003; Zhang *et al.*, 2003; Honaramooz *et al.*, 2003a, b; Izadyar *et al.*, 2003b; Joerg *et al.*, 2003; Trefil *et al.*, 2006, 2010; Stockwell *et al.*, 2009; Herrid *et al.*, 2009; Hermann *et al.*, 2012; Pacchiarini *et al.*, 2014; Yoshizaki and Lee, 2018). Cross-species (heterologous) transplantation (xenotransplantation) of germ cells is also feasible, but only for closely-related species (*e.g.,* between rodent species) (Clouthier *et al.*, 1996; Ogawa *et al.*, 1999; Honaramooz *et al.*, 2002a; Zhang *et al.*, 2003). Although the initial stages of colonization can occur when transplanting donor germ cells between

phylogenetically-distant species, such as from a non-rodent donor (*i.e.*, pig, dog, cattle, horse, baboon, cat, human) into rodent recipients, spermatogenesis fails to advance (Dobrinski *et al.*, 1999; Nagano *et al.*, 2001, 2002; Kim *et al.*, 2006b). Prior to applying GCT, donor germ cells and recipient animals need to be prepared.

As with any transplantation, the success and efficiency of GCT highly depend on the number and developmental potential of donor cells. Increasing the number of transplanted donor germ cells and/or increasing the proportion of SSC in donor cells are both directly correlated with the rate of colonization by donor cells in the recipient testes (Nagano *et al.*, 1999; Shinohara *et al.*, 1999, 2001; Jiang, 2001; Buageaw *et al.*, 2005). This can be achieved by propagating and/or purifying/enriching isolated donor germ cells before use. Certain donor animals, such as the cryptorchid, VAD, and Steel mutant (*Sl*), can offer high proportions of SSC for transplantation, because in all of these animal models, the only type of germ cells remaining in the testis is undifferentiated spermatogonia (van Pelt *et al.*, 1996; Ogawa *et al.*, 2000; Shinohara *et al.*, 2000a). Another more readily available source of donor germ cells, however, is the neonatal/immature animal, which provides proportionally higher populations of MGSC (gonocytes and/or SSC) than adults (Honaramooz and Yang, 2010).

The efficiency of GCT also heavily relies on the proper preparation of the recipient testes; namely, the recipient testes must not immunologically reject the donor cells, and should ideally have sufficient unoccupied stem cell niches for colonization of donor SSC. For GCT in rodent models, immunocompatibility between donors and recipients is typically not a limiting factor, because genetically-compatible recipients (congenic) and/or immunodeficient animals are readily available (Brinster and Avarbock, 1994; Kanatsu-Shinohara *et al.*, 2003; Zhang *et al.*, 2003). For GCT in non-rodent species, although congenic or immunodeficient recipients are not readily available, surprisingly no evidence of donor testis cell rejection was observed after GCT between immunocompetent goats of different breeds (Honaramooz *et al.*, 2003b), paving way for the application of GCT in several farm species (Honaramooz *et al.*, 2002b, 2003a; Rodriguez-Sosa *et al.*, 2009; Stockwell *et al.*, 2009). The degree of donor germ cell colonization is also improved when the recipient testes contain little or no endogenous germ cells, allowing more stem cell niches to be available. Cytoablative methods such as chemotherapy or irradiation are commonly used to deplete the endogenous populations of germ cells in the recipients (Brinster and Avarbock, 1994;

Izadyar *et al.*, 2003b; Honaramooz *et al.*, 2005a; Oatley *et al.*, 2005; Mikkola *et al.*, 2006). The irradiation method was found to be a safer choice for use in farm animals, because chemotherapy agents such as busulfan can show unexpectedly high toxicity in certain strains or species, and carry various degrees of health risk for the recipients (Ogawa *et al.*, 1999; Brinster *et al.*, 2003; Honaramooz *et al.*, 2005a).

The transplantation protocols used for GCT in large animals are different from those used for rodents. In rodents, where the tunica albuginea is translucent, the donor germ cells are suspended in a dye solution to be deposited into the visible seminiferous tubules, efferent ductules, or rete testis using a glass micropipette system. The dye (*e.g.,* trypan blue) facilitates the immediate tracking of the injected solution to ensure the cells are being deposited in the targeted site (Brinster and Avarbock, 1994; Brinster and Zimmermann, 1994). In large animal, the technique had to be modified to allow transfer without direct visualization in the testes that were also hundreds of fold larger than in rodents. This led to the use of ultrasonography to visualize the needle insertion path into the centrally located rete testis, followed by tracking the injected solution through the introduction of air bubbles or an ultrasound contrast media along with the donor cell suspension (Honaramooz *et al.*, 2002b, 2003a; Izadyar *et al.*, 2003a; Joerg *et al.*, 2003; Rodriguez-Sosa and Dobrinski, 2009).

Confirmation of the proper transfer of donor cells into recipient seminiferous tubules and follow up analyses of the donor cell development can be performed using several methods. For the detection of donor cells after a short interval post-GCT, the donor cells can be labelled prior to injection using either a dye or a fluorescent agent (*e.g.,* trypan blue, carboxyfluorescein diacetate succinyl diester- CFDA-SE- and/or PKH26) (Honaramooz *et al.*, 2002b; Hill *et al.*, 2005; Rodriguez-Sosa *et al.*, 2009). For detection of the transplanted cells over long-term, however, a more permanent marker is required which can be provided by using germ cells from donors carrying inherent markers such as the *lacZ* or chloramphenicol acetyltransferase (*CAT*) that can be visualized directly *in situ* using immunohistochemical detection methods (Iwase *et al.*, 1994; Honaramooz *et al.*, 2002b; Orwig *et al.*, 2002b). A more commonly used strategy for long-term identification of donor-derived germ cells or resultant spermatozoa is based on nucleic-acid techniques to trace a transgene or donor-specific microsatellites (Honaramooz *et al.*, 2002b; Stockwell *et al.*, 2009; Hermann *et al.*, 2012). An alternative method, although less commonly

used, includes transplanting normal germ cells into the testes of recipients with a genetic aberration such as the immotile short-tail spermatozoa syndrome which is based on detection of normal donor-derived spermatozoa in the recipient ejaculates (Mikkola *et al.*, 2006). Nonetheless, the ultimate proof of GCT success is determined by the number of functional donor-derived spermatozoa produced, assessed through *in vitro* or *in vivo* fertilization, or the capability of the recipients to sire donor-derived progeny (Brinster and Avarbock, 1994; Goossens *et al.*, 2003; Honaramooz *et al.*, 2003a).

GCT has sparked considerable interest in its use as a unique means for understanding the unexplored aspects of the biology of spermatogenesis, particularly related to the stem cell potential and stem cell niche. It also offers the only available bioassay for evaluating the *in vivo* competency of putative populations of SSC (Pereira *et al.*, 1998; Nagano *et al.*, 1999; Hill and Dobrinski, 2006; Honaramooz and Yang, 2010). In terms of clinical or field applications, GCT can also be used as a tool for the conservation, preservation, or restoration of fertility (discussed in Chapter 2.6), as well as production of transgenic farm animals, because the current methods are inefficient (Brinster, 2002, 2007; Keefer, 2004; Niemann and Kues, 2007).

### *2.5.2 Testis Tissue Xenografting*

Historically, grafting of the testis tissue has been performed as early as the mid-18$^{th}$ century, although mostly as autologous (same individual) or homologous (same species), and merely to understand the biology of testis function (*i.e.,* spermatogenesis, endocrinology) or its role in male reproduction (*i.e.,* male secondary characteristics) (Setchell, 1990). Although heterologous/xenogeneic (across species) grafting (xenografting) was also attempted, the results from the early studies were subjected to controversies, and the tissue rejection was always a limiting factor that hindered success (Gunn and Seddon, 1930; Setchell, 1990). The feasibility of cross-species testis tissue grafting was highlighted only in the 1970s when a Finnish group reported that a testis tissue of human fetal origin and its germ cells (gonocytes) survived 4-8 wk post-grafting in the abdominal wall of adult nude mice. Furthermore, they showed that the developmental potential of germ cells was maintained after xenografting of rat testis tissue into mice (Povlsen *et al.*, 1974; Skakkebaek *et al.*, 1974). These findings also marked for the first time, the potential of

testis tissue xenografting (TTX) as a tool for the preservation of male genetic material; however, the progress in TTX remained stagnant.

Complete cross-species spermatogenesis and the production of functional spermatozoa from TTX were finally achieved in 2002. In this breakthrough study, small fragment (0.5-1 $mm^3$) of testis tissue from neonatal mice, pigs, and goats were ectopically grafted under the back skin of immunodeficient mice. The grafts from all three donor species survived and responded to the host mouse gonadotropins by initiating testicular development and completing all stages of spermatogenesis. At the end of the study, fertilization-competent donor-derived spermatozoa were retrieved from the grafts of all donor species, evidenced by pronuclear and polar-body formation after ICSI in mouse oocytes. In addition, when the homologous mouse embryos produced using this system were transferred into pseudo-pregnant mice, normal fetal development was observed (Honaramooz *et al.*, 2002a). As a result, the newly developed TTX system uses the recipient mice as a bio-incubator for the grafted testis tissue. The establishment of blood supplies (revascularization) from the grafts as well as surrounding tissues (recipient) allowed initiation of feedback loops between the pituitary of the mouse and the endocrine cells in grafts (Schlatt *et al.*, 2002b). The immunodeficient status of the recipients is key, ensuring the survival of the grafts, which is particularly critical for grafting from phylogenetically distant species (Paris *et al.*, 2004; Dobrinski, 2005).

Since 2002, this system has been adopted by many research groups and applied to answer various biological questions in a range of species. Currently, complete spermatogenesis after TTX from immature testis tissues of diverse species has been reported, which includes lab animals (*e.g.,* mouse, rat, hamster, rabbit), companion animals (*e.g.,* dog, cat), farm animals (*e.g.,* pig, goat, sheep, horse, cattle, alpaca), and wildlife species (*e.g.,* ferret, monkey, deer, bison) (Honaramooz *et al.*, 2002a; Schlatt *et al.*, 2002b; Shinohara *et al.*, 2002; Kaproth *et al.*, 2002; Snedaker *et al.*, 2004; Rathi *et al.*, 2008, 2005, 2006; Kim *et al.*, 2007a; Abbasi and Honaramooz, 2010a, 2012; Abrishami *et al.*, 2010a; Gourdon and Travis, 2011; Elzawam, 2013; Parvari *et al.*, 2015). Moreover, viable progenies have been produced using the spermatozoa extracted from the grafts (*i.e.*, mice, rabbits, pigs) using ICSI and embryo transfer (Schlatt *et al.*, 2002b; Shinohara *et al.*, 2002; Nakai *et al.*, 2010; Kaneko *et al.*, 2012). Several of these studies found that the maturation in the grafted tissue is accelerated, where spermatozoa could be found earlier than in intact testes.

This was particularly the case after TTX from donor pigs, monkeys, sheep, and humans (Honaramooz *et al.*, 2002b, 2004; Zeng *et al.*, 2006; Sato *et al.*, 2010). Unlike from animal donors, the grafts from human donors demonstrated poor survival, and germ cells underwent massive degeneration after TTX (Geens *et al.*, 2006; Schlatt *et al.*, 2006; Wyns *et al.*, 2007, 2008, Poels *et al.*, 2013, 2014), the reasons for which are described in Chapter 2.5.4.

### *2.5.3 Testis Cell Aggregate Implantation*

Following the establishment of GCT and TTX systems, another novel approach was introduced which involved the implantation of testis cell-aggregates (Dufour *et al.*, 2002; Gassei *et al.*, 2006; Honaramooz *et al.*, 2007; Kita *et al.*, 2007; Arregui *et al.*, 2008b; Zhang *et al.*, 2008; Campos-Junior *et al.*, 2014). Testis cell implantation (TCI) involves implanting dissociated testis cells from diverse donor species, obtained from enzymatic digestion, into immunodeficient recipient mice. Similar to TTX, the subcutaneous tissue of the back skin has been used a common site for TCI (Gassei *et al.*, 2006; Honaramooz *et al.*, 2007; Kita *et al.*, 2007; Arregui *et al.*, 2008b; Zhang *et al.*, 2008; Campos-Junior *et al.*, 2014). Upon implantation, dissociated donor cells undergo autonomous cellular reorganization, which over time leads to regeneration of a donor-derived functional testis tissue capable of supporting spermatogenesis (Honaramooz *et al.*, 2007; Kita *et al.*, 2007).

Compared with TTX, the TCI model is understudied; although it has been performed using different rodent and non-rodent mammalian and non-mammalian species (*i.e.,* pig, sheep, cattle, marmoset, fish, frog) (Dufour *et al.*, 2002; Gassei *et al.*, 2006; Kawasaki *et al.*, 2006, 2010; Honaramooz *et al.*, 2007; Kita *et al.*, 2007; Arregui *et al.*, 2008b; Zhang *et al.*, 2008; Aeckerle *et al.*, 2013; Campos-Junior *et al.*, 2014). In all these studies, the ability of the dissociated testis cells to reorganize and regenerate testis cords after ectopic implantation was retained. Complete spermatogenesis and donor-derived progenies have been reported only after TCI from donor mice (Kita *et al.*, 2007). Although, haploid germ cells (*i.e.*, spermatids/spermatozoa) have also been obtained after TCI of sheep and pig testis cells, indicating the potential of this *in vivo* system for development of testis cell aggregates from diverse species (Honaramooz *et al.*, 2007; Arregui *et al.*, 2008b; Watanabe *et al.*, 2009; Campos-Junior *et al.*, 2014). In a TCI study using bovine cells, the formation of seminiferous tubules containing some germ cells was observed; however, the

spermatogenic potential was not further evaluated since the study only lasted 3 mo (Zhang *et al.*, 2008).

When compared with TTX, the onset of germ cell differentiation and spermatogenesis is delayed after TCI (Gassei *et al.*, 2006; Honaramooz *et al.*, 2007; Arregui *et al.*, 2008b; Campos-Junior *et al.*, 2014). For example, while using sheep donor testis tissue for TTX resulted in the completion of spermatogenesis at 12 wk, comparable with the timing *in situ*, it took ~40 wk for the same event to occur after TCI (Arregui *et al.*, 2008a). In a side-by-side comparison using peccary (*Tayassu tajacu*) donors, spermatogenesis was observed at 6 mo and 8 mo, in TTX and TCI, respectively (Campos-Junior *et al.*, 2014). Although the dissociated donor cells are fully capable of rearranging and developing into testicular cords and structures that have remarkable morphological and physiological similarity to normal testis tissue, the newly developed seminiferous cords/tubules are typically void of germ cells (Gassei *et al.*, 2006; Honaramooz *et al.*, 2007; Kita *et al.*, 2007; Arregui *et al.*, 2008a). The lack of germ cells in the regenerated cords/tubules was believed to result from the very low initial number of donor germ cells used for TCI and/or a progressive degeneration of germ cells after implantation (Rathi *et al.*, 2006; Arregui *et al.*, 2008a). These differences resulted in relatively lower spermatogenic efficiency of TCI, depicted by lower production of haploid spermatids (Watanabe *et al.*, 2009; Campos-Junior *et al.*, 2014).

Since most initial TCI studies merely adopted components of the well-established GCT and TTX systems, modifications of the employed protocols (*e.g.*, cell preparation, donor species, recipient strain, implantation technique, incubation period) are expected to improve the outcomes of TCI. When the population of donor testis cells used in TCI was almost entirely comprised of somatic cells (~93% Sertoli and 2% myoid cells), *de novo* formation of testis cords still occurred, suggesting that this event is independent of germ cells (Dufour *et al.*, 2002). Since there has been no standardized protocol for the preparation of donor cells for TCI, different research groups have used different protocols for isolation of testis cells. This can lead to differences in somatic-germ cell ratios, and has likely contributed to the discrepancy in findings of many TCI studies (van der Wee and Hofmann, 1999; Gassei *et al.*, 2006; Honaramooz *et al.*, 2007; Arregui *et al.*, 2008a; Watanabe *et al.*, 2009). There has also been a lack of consistency in the number of implanted cells, especially when the procedure was performed using the conventional surgical approach (creating a small pocket in the subcutaneous fascia to be filled with donor cells) (Honaramooz *et al.*, 2007).

However, this issue can be resolved by subcutaneous injection of cells to reduce the potential leakage of cells out of the implantation site. Adding commercially-available extracellular matrices such as Matrigel, to act as a carrier for injected cell suspensions, has also been tested with varying results (Gassei *et al.*, 2006; Watanabe *et al.*, 2009; Aeckerle *et al.*, 2013; Dores and Dobrinski, 2014).

Therefore, TCI provides a unique *in vivo* culture system that is also easily accessible for the study and manipulation of potential molecular cues and cellular interactions during testis morphogenesis. Using TCI, the recipient milieu can also be controlled to better elucidate various factors involved in the regulation of spermatogenesis; thereby, using it as a previously-unavailable model to examine biological questions that are otherwise difficult to study *in situ*.

### *2.5.4 Factors Affecting the Outcome of Testis Tissue Xenografting and Testis Cell Implantation*

Since the introduction of TTX and TCI, many studies have used these models to examine the developmental potential of testis tissues and cells from various donors. A few of these studies directly or indirectly investigated several factors that affect the outcomes of these models, which included the effects of donor, recipient, tissue/cell preparation, and technique used.

The outcomes of TTX and TCI expectedly vary to a great extent based on factors related to the donor. Following TTX and TCI, the testis tissue and cells from all examined donor species have survived, developed, and initiated spermatogenesis in the recipient mouse, and given enough time, most have also shown completion of spermatogenesis (Honaramooz *et al.*, 2002a; Schlatt *et al.*, 2002b; Shinohara *et al.*, 2002; Snedaker *et al.*, 2004; Kawasaki *et al.*, 2006; Zeng *et al.*, 2006; Honaramooz *et al.*, 2007; Arregui *et al.*, 2008a; Watanabe *et al.*, 2009; Abrishami *et al.*, 2010a; Kawasaki *et al.*, 2010; Campos-Junior *et al.*, 2014). However, the extent of post-TTX/TCI development in the grafts/implants from certain donor species has been limited. In particular, TTX using human testes, regardless of the developmental stage of the donor tissue (*i.e.,* fetal, infantile, prepubertal, adult), has resulted in limited development of germ cells beyond the spermatogonial stage or even in degeneration of the tissue (Schlatt *et al.*, 2006; Yu *et al.*, 2006; Geens *et al.*, 2008; Goossens *et al.*, 2008; Wyns *et al.*, 2008; Van Saen *et al.*, 2011). Nevertheless, occasionally, generation of spermatocytes has been observed in infant testis grafts 9-12 mo post-TTX (Sato *et*

*al.*, 2010; Van Saen *et al.*, 2011). The grafts from high spermatozoa producing species (*e.g.*, pig, goat, sheep) show a higher percentage of seminiferous tubules with fully-formed spermatozoa than in some others (*e.g.,* horse, bull) (Honaramooz *et al.*, 2002a; Zeng *et al.*, 2006), (Oatley *et al.*, 2004, 2005, Rathi *et al.*, 2005, 2006; Huang *et al.*, 2008). In the former examples, the number of spermatozoa produced (per gram of tissue) in the grafts was also comparable to that in intact tissues (Honaramooz *et al.*, 2002a). The underlying reasons for differences in spermatogenic efficiency among various species remain to be elucidated. However, the development potential of testis grafts naturally relies on the compatibility and interactions between the graft and host hypothalamic-pituitary axis of the host, and this may explain some of the observed differences in spermatogenic efficiency after TTX (Arregui and Dobrinski, 2014).

Aside from the effect of donor species, TTX and TCI outcomes are known also to be donor-age dependent, where grafts from neonatal/immature donors demonstrate superior developmental potential compared with the adult/mature. In the original report and almost all subsequent TTX studies, when neonatal/immature sources were used as tissue donors, full testicular development and complete spermatogenesis were observed in the grafts (Honaramooz *et al.*, 2002a) (Schlatt *et al.*, 2002a; Shinohara *et al.*, 2002; Snedaker *et al.*, 2004; Rathi *et al.*, 2005; Kim *et al.*, 2007; Abbasi and Honaramooz, 2011, 2012; Reddy *et al.*, 2012; Elzawam, 2013). In contrast, tissues from mature sources are typically unable to survive or develop after TTX, and frequently degenerate (Schlatt *et al.*, 2006; Arregui *et al.*, 2008b; Turner *et al.*, 2010). This degeneration was found to be especially more evident in species/tissues with more intense spermatogenesis (high daily spermatozoa output per gram of testis tissue, *i.e.,* pigs and goats) or more advanced pre-grafting spermatogenesis than those with less intense/advanced spermatogenesis (*i.e.*, bulls and monkeys) (Arregui *et al.*, 2008b). This phenomenon has been associated with the vulnerability of differentiated germ cells to hypoxic conditions after grafting, as well as the poor angiogenic ability of the adult testis tissue (Rathi *et al.*, 2006; Kim *et al.*, 2007). In addition, Sertoli cells in the adult testes have reached maturity and have lost their proliferative potential (Meachem *et al.*, 2005), leading to the lack of compensatory regeneration following TTX.

Effect of donor age or the developmental status of the testis tissues used in TTX, on the progression of spermatogenesis in grafts has been examined using different donor species. The results varied, but a general theme can be inferred from these studies. For instance, optimal TTX results were

obtained if the donor cats and dogs were neonatal or were used at some time prior to the onset of puberty at ~4 mo and ~6 mo, respectively (Kim *et al.*, 2007; Abrishami *et al.*, 2010a). Using fetal testes for TTX from humans, cattle, and Cuzier's gazelle, it was concluded that the developmental potential and spermatogenic capacity are probably conserved in the fetal tissue; however, no haploid germ cells have so far been produced in the grafts (Povlsen *et al.*, 1974; Skakkebaek *et al.*, 1974; Yu *et al.*, 2006; Rodriguez-Sosa *et al.*, 2011; Arregui *et al.*, 2014). Variations observed in the developmental potential of testis grafts have been associated with differences in gene expression and cues at different ages/developmental stages (Schmidt *et al.*, 2007). The efficiency of spermatogenesis was suggested to be higher with TTX using young and immature bovine or feline tissues, compared with the neonatal (Oatley *et al.*, 2005; Kim *et al.*, 2007). The increased number of SSC prior to puberty (Orwig and Schlatt, 2005), may provide the grafts with more readily available SSC to initiate differentiation shortly after TTX (Rathi *et al.*, 2006; Kim *et al.*, 2007). Hypoxic conditions that grafts are expected to undergo in the first few hours or days post-TTX, before revascularization occurs, are thought to be responsible for the massive losses of (especially differentiated) germ cells. Therefore, having a relatively higher number of SSC prior to grafting can be advantageous to spermatogenic efficiency (Schlatt *et al.*, 2002a, b; Yu *et al.*, 2006; Arregui *et al.*, 2008b, 2012).

Although the tissue/cells to be used in TTX/TCI are ideally collected fresh, in real-world applications, they cannot always be used immediately after the collection, and may need to be stored either short-term or long-term for later use. Short-term storage of testis tissue, in the form of refrigeration for up to three days, was shown to result in comparable development after TTX using pig, cat, or rhesus monkey donor tissues. Interestingly, the percentage of tubules with differentiated germ cells was unexpectedly higher in the grafts from refrigerated than fresh tissue. Therefore, cold storage of donor tissue/cells prior to TTX at low temperatures, may in fact lead to decreased hypoxic damages by reducing the metabolism of tissue/cells (Honaramooz *et al.*, 2002a; Jahnukainen *et al.*, 2007; Zeng *et al.*, 2009; Abrishami *et al.*, 2010b; Abbasi and Honaramooz, 2011; Mota *et al.*, 2012). For long-term storage of testis tissue, different approaches (*i.e.,* slow/programed freezing or vitrification) have been introduced, although the protocols had to be modified/adjusted according to the donor species and tissue maturity (Abrishami *et al.*, 2010b; Mota *et al.*, 2012; Arregui *et al.*, 2014). Overall, cryopreserved tissue demonstrated satisfactory cellular survivability and differentiation potential, and at times similar graft recovery rates as with

fresh tissue (Honaramooz *et al.*, 2002a; Shinohara *et al.*, 2002; Jahnukainen *et al.*, 2007; Wyns *et al.*, 2008; Zeng *et al.*, 2009; Abrishami *et al.*, 2010b; Van Saen *et al.*, 2011; Poels *et al.*, 2012; Arregui *et al.*, 2014). However, similarities in viability between the fresh and frozen testis tissue should not be taken as equal developmental potential, because tissues might develop differently after grafting (Arregui *et al.*, 2014). The cryoprotectant used for cryopreservation (*e.g.,* DMSO), for instance, might have a more severe adverse effect on germ cells than somatic cells and result in delayed onset of spermatogenesis (Jahnukainen *et al.*, 2007; Zeng *et al.*, 2009; Mota *et al.*, 2012).

The type of recipient mice may also affect the outcomes of TTX. So far, two strains of immunodeficient mice have been used as recipients in the majority of TTX/TCI studies. The nude mouse (*nu/nu*), which was used in the initial development of both TTX and TCI models (Honaramooz *et al.*, 2002a, 2007) is a popular choice, while the severe combined immunodeficient (SCID) mice have also been used as an alternative to the nude mice (Snedaker *et al.*, 2004; Rathi *et al.*, 2006; Kim *et al.*, 2007; Campos-Junior *et al.*, 2014). Both strains of recipients were reported to produce comparable TTX outcomes (Snedaker *et al.*, 2004; Rathi *et al.*, 2005, 2006; Geens *et al.*, 2006; Schlatt *et al.*, 2006); however, SCID mice might have an advantage over nude mice, because their immune system is more compromised. The loss of human testis tissue grafts was less likely to happen in SCID than in nude mice (Schlatt *et al.*, 2006). On the other hand, the spermatogenic potential of porcine grafts implanted in SCID mice was reported to be significantly higher than in nude mice (Abbasi and Honaramooz, 2010b). In a study designed to compare the efficiency of TTX and TCI techniques, no significant effect of strain was found (*i.e.,* nude *vs.* SCID *vs.* NOD/Shi-SCID, IL-2Rγc$^{null}$-NOG), although SCID mice appeared to promote better reconstitution of the testis tissue (morphogenesis) and restoration of spermatogenesis (Watanabe *et al.*, 2009).

The castration of recipient mice is generally presumed to have a beneficial effect on TTX outcomes. The removal of testes from recipient mice prior to grafting results in the elimination of the androgen negative feedback on gonadotropins, causing a surge in the release of LH and FSH from the pituitary (Schlatt *et al.*, 2002b). Both FSH and LH promote graft development by initiating the proliferation of Sertoli cells and maturation of Leydig cells, which later produce testosterone to support spermatogenesis. Removing the recipient testes also terminates the growth promoting effects of mouse testosterone on its vesicular glands, where the development is androgen-

dependent (Gosden and Aubard, 1996). Thus, in castrated recipients, the physical and histological properties of the vesicular glands can be used as a bioassay for monitoring the androgenic competence of testis grafts. The effect of recipient gonadal status (castrated *vs.* intact) on TTX outcomes seems to be species-specific. While the development of immature testis tissue of horses and rhesus monkeys was compromised upon TTX into intact recipients (Honaramooz *et al.*, 2004; Rathi *et al.*, 2006), using immature tissue from rabbits, cattle, pigs, hamsters, and buffalos led to the development and production of functional spermatozoa in similarly intact recipient mice (Shinohara *et al.*, 2002; Huang *et al.*, 2008; Abbasi and Honaramooz, 2010b; Schlatt *et al.*, 2010; Reddy *et al.*, 2012). A side-by-side comparison of castrated and intact recipients showed no differences in the development of grafts between recipient types (Huang *et al.*, 2008; Abbasi and Honaramooz, 2010a; Schlatt *et al.*, 2010). The sex and age of the recipient mice were also examined for their potential effects on TTX outcomes. Although even female recipient mice with intact ovaries were fully capable of supporting the development of porcine testis grafts, the grafts in male recipients were larger in size, with higher graft recovery rate, and higher occurrence of fully developed seminiferous tubules (Abbasi and Honaramooz, 2010b). The use of mature recipients (1-year-old at grafting) led to better development of hamster testis xenografts, speculated to be due to the immunosenescence of recipients, because the grafts recovered from young recipients (1-wk-old at grafting) showed more spermatogenic loss with a high prevalence of Sertoli-cell-only tubules (Ehmcke *et al.*, 2008).

Conventionally, grafting eight fragments of testis tissue per recipient (4 on each side of the back skin) has been a common practice in TTX; however, having more grafts/implants per recipient would be advantageous because potentially more spermatozoa could be recovered from the developed grafts. When 2, 4, 8, or 16 tissue grafts were used per mouse, the recipient mice were fully capable of supporting the development of even 16 grafts. More importantly, in mice with 16 grafts, in addition to generating a greater total mass of grafted tissue, even the individual graft sizes and development observed per graft were higher when compared with mice with only 2 grafts (Abbasi and Honaramooz, 2010a).

The mouse is a social species by nature and may prefer to be housed in a group, rather than individually (Würbel, 2001; Van Loo *et al.*, 2003; Latham and Mason, 2004; Fitchett *et al.*, 2006). Grouping male mice in a single cage, on the other hand, might negatively affect the androgen levels

and other reproductive parameters (Machida *et al.*, 1981; Koyama and Kamimura, 1998). This potential effect on graft development, however, was ruled out in a study where the recipients of TTX were housed either individually or in a group; housing choice had no significant effect on the graft recovery rate, weight, microscopic development, or serum levels of androgens (Arregui *et al.*, 2008b).

The ability of grafts to establish neovascularization has also been proposed to have an impact on the graft survival and development, and hence TTX outcomes (Schmidt *et al.*, 2006b; Caires *et al.*, 2009). Treating the grafted tissue with VEGF was found to promote angiogenesis and increase the graft size and number of tubules with elongated spermatids (Schmidt *et al.*, 2006b).

As discussed earlier (Chapter 2.5.3), different outcomes might be expected from testis tissue grafts than cell implants, as exemplified by the delayed spermatogenesis and higher prevalence of tubules with no germ cells in implants from TCI (Gassei *et al.*, 2006; Honaramooz *et al.*, 2007; Arregui *et al.*, 2008b; Watanabe *et al.*, 2009; Campos-Junior *et al.*, 2014). Therefore, the effects of recipient and donor factors on the survival and development of implants would need to be examined for TCI as well, in order to improve the outcomes.

## 2.6 Application of Male Germline Stem Cells in Fertility and Conservation

As shown by the evidence presented thus far in this chapter, MGSC can be maintained using *in vitro* and *in vivo* culture systems, and induced to proliferate and differentiate into haploid germ cells. The self-renewal, proliferation, and differentiation properties of MGSC ensure that a stem cell pool remains to provide a continuous supply of spermatozoa throughout adulthood. In addition, advances in the field of MGSC and assisted reproductive technologies (ART; *e.g.,* GCT and IVF) in recent years have allowed a better understanding of MGSC biology and opened many windows of potential application in genetic conservation and male reproductive health.

At least theoretically, a combination of the aforementioned technologies can be applied to overcome fertility challenges that only two decades ago would have seemed impossible to resolve. For instance, it is now conceivable to preserve the fertility potential of prepubertal boys undergoing gonadotoxic treatments (*i.e.,* chemotherapy or total body radiotherapy), which frequently result in the depletion of germ cells. Unlike in adult men, the collection of spermatozoa for cryopreservation

is not an option for pre-pubertal males. However, cryopreservation of testis biopsies obtained prior to the onset of cytoablative cancer treatments can offer an option if decades later the donor decides to seek treatment for infertility (Wyns *et al.*, 2008, 2011; Honaramooz, 2012). Cryopreserved biopsies from immature testes that are void of haploid germ cells can then undergo maturation using the aforementioned *in vitro* or *in vivo* systems to produce spermatozoa, elongated spermatids, or even round spermatids for use in ICSI or ROSI to achieve donor-derived progeny (Schrader *et al.*, 2001). In the adult male, MGSC technologies also offer a therapeutic potential for infertility treatment, particularly those conditions that hinder the development and differentiation of SSC into advanced germ cells. Examples include chromosomal abnormalities or genetic disorders, where oligozoospermia or azoospermia is caused by the lack of certain factors or signaling pathways. Using *in vitro* systems, the missing factors or signals can be introduced, either in a pure or recombinant form, to induce *in vitro* spermatogenesis. This possibility was substantiated using the *Steel* (*Sl*) mouse model, a condition caused by c-kit ligand (KITL) mutation, which results in underdeveloped testis, low and abnormally distributed SSC, and total absence of spermatozoa (non-obstructive azoospermia). The number of SSC in the mutant testis tissue fragments was increased in a dose-dependent manner after culturing with recombinant KITL, which eventually led to successful induction of *in vitro* spermatogenesis (Sato *et al.*, 2012). It goes without saying that despite the promising perspectives and recent progress in lab animal models, the clinical application of MGSC technologies for humans is not yet feasible; aside from the ethical and safety concerns, the efficiency remains very low at the present time. Various questions, particularly related to understanding the requirements of every step involved in these technologies (*e.g.*, cryopreservation, culturing, transplantation, IVF), need to be addressed.

In recent decades, species are becoming extinct at a faster rate, mostly due to the impact of human activities. The loss of genetic diversity due to infertility and premature death of neonatal/young males adds to conservation challenges. The declining number of animals in an endangered species populations means that the genetic material of every existing individual is immensely valuable, and the ability to obtain offspring from a single male could have a significant impact on the preservation of genetic diversity within a population. Hence, MGSC can be potentially applied in genetic conservation of endangered wildlife or valuable rare breeds of livestock. When such a prized male dies, and the collection of semen or even testicular/epididymal spermatozoa is not an option, such as when the individual is neonatal/immature, then testis tissue collected even shortly after death

can be prepared for cryopreservation for future use in similar advanced reproductive technologies. This concept has also been supported, through the use of testis tissue cryopreservation and TTX using domestic mammals (*e.g.*, the sheep, goat, cattle, horse, pig, alpaca, cat, dog) as a model for endangered counterparts (*e.g.*, ungulate herbivores, equid, suid, camelid, felid, canid) (Snedaker *et al.*, 2004; Oatley *et al.*, 2005; Rathi *et al.*, 2006; Abrishami *et al.*, 2010a; Elzawam, 2013). Promising results and even donor-derived spermatozoa have also been obtained through TTX from donors of some of the target wildlife species, such as the Javan banteng, Iberian lynx, Cuvier gazelle, Mohor gazelle, white-tailed deer, and bison (Honaramooz *et al.*, 2005b; Abbasi and Honaramooz, 2011, 2012; Arregui *et al.*, 2014).

## 2.7 Conclusions

The testis plays a central role in male reproduction by providing male gametes and androgens; both of which occur via complex processes that extend continuously throughout the male adult life. These involve highly coordinated signaling between the autocrine, paracrine, and endocrine components, including the hypothalamic-pituitary-gonadal axis. Any disruption during the development or normal function of the testis may impact the male reproductive health and fertility. Despite the tremendous advances in the study of testis function, many questions pertaining to the regulation of testicular development and spermatogenesis remain unanswered and require further investigation.

MGSC form the foundation of spermatogenesis, where their capacity for self-renewal and differentiation ensure the continuity of the male germ cell lineage. Understanding the mechanisms controlling self-renewal and differentiation, provide a basis for the maintenance and manipulation of MGSC both *in vitro* and *in vivo.* Most of our knowledge about MGSC has come from the extensive studies performed using SSC. Not until recent years had gonocytes been given proper attention in MGSC studies. Being the only germ cell type present in the neonatal testis, gonocytes offer great advantage and practicality as the source of MGSC over the other types. Our knowledge of MGSC in general and gonocytes, in particular, is very limited when it comes to farm animals, especially in the pig as an important biomedical model.

The efficacy of using MGSC in clinical or biomedical research relies on our ability to prepare large numbers of enriched populations. New developments in technology and the introduction of novel

biomarkers continue to improve the identification, isolation, enrichment, and manipulation of MGSC. *In vitro* culture systems have been successful in supporting the self-renewal and differentiation of MGSC. Incorporation of growth factors that have the potential to play a part in testis culture systems either *in vitro* or *in vivo*, will also lead to a better understanding of their roles for testis development *in situ*. Using laboratory animal models, MGSC have been propagated, maintained long-term, and allowed to differentiate into even functional spermatozoa. However, the application of these culture conditions is still limited due to species differences and lack of standardized protocols. Therefore, the search for optimal culture conditions for MGSC, especially from nonrodent species demand ongoing efforts.

*In vivo* culture systems for testis tissue and cells offer an alternative for culturing MGSC that is more readily applicable to diverse donor species. GCT provides a unique bioassay to assess the competency of MGSC for establishing new colonies of spermatogenesis, and allow examination of their stem cell niche. The capability of testis tissue fragments or dissociated cells (through TTX and TCI) from distant species to develop into functional tissue and give rise to donor-derived spermatozoa in mice, has introduced new solutions to genetic and fertility preservation challenges. The autonomous reorganization and *de novo* formation of testis tissue after TCI can be used to understand the mechanisms behind testicular morphogenesis. The developmental potential and spermatogenic efficiency of TTX/TCI relies on various factors; the investigation for which will also give new insights on spermatogenesis and testis function.

Recent developments in the field of MGSC technologies have greatly impacted the fields of regenerative medicine and advanced reproductive technologies. The limitless self-renewal and proliferation potential of MGSC can be exploited as an alternative source for the generation of pluripotent stem cells for use in cell-based therapy and drug delivery studies. However, the most significant application of MGSC technology at least in the near future will be the preservation, conservation, and restoration of fertility, especially when recovery of spermatozoa is not possible.

## 2.8 Objectives and Hypotheses

The overarching hypothesis of this thesis was that *in vitro* and *in vivo* culture systems can be used to study the development of porcine testis cells and tissue. The general objectives of this thesis were to identify, examine, and manipulate potential factors associated with the development of testis cells and tissue using *in vitro* and *in vivo* culture systems. Experiments were designed to test the following specific objectives and hypotheses:

### *A. Optimization of Culture Conditions for Short-Term Maintenance, Proliferation, and Colony Formation of Porcine Gonocytes (Chapter 3)*

The objective of this study was to:

1. Optimize culture conditions (gonocyte proportion, cell seeding density, temperature, and medium changing regimen) to improve maintenance, proliferation, and colony formation of porcine gonocytes.

It was hypothesized that:

1. Optimizing culture conditions (cell seeding density and gonocyte proportion, incubation temperature, and medium changing regimen) will improve maintenance, proliferation, or colony formation of porcine gonocytes.

### *B. Live-Cell Imaging and Ultrastructural Study of Cultured Porcine Gonocytes (Chapter 4)*

The objective of this study was to:

1. Study cellular organization, movement pattern, and ultrastructure of neonatal porcine gonocytes in a prolonged culture.

It was hypothesized that:

1. Organization, movement pattern, or ultrastructure of neonatal porcine gonocytes will change over time in culture.

***C. Effect of Multiple Factors on Regeneration of Testis Tissue After Ectopic Implantation of Porcine Testis Cell Aggregates in Mice: Improved Outcomes Consistency and in Situ Monitoring (Chapter 5)***

The objectives of this study were to:

1. Establish an efficient method for implantation of neonatal porcine testis cell aggregates in mice.
2. Evaluate the potential of ultrasound biomicroscopy for *in situ* assessment of the development of testis cell aggregates after implantation in mice.

It was hypothesized that:

1. The optimized method will be more efficient than the conventional method for implantation of neonatal porcine testis cell aggregates in mice.
2. Ultrasound biomicroscopy will be utilized for assessing the development of neonatal porcine testis cell implants in mice.

***D. Effects of Growth Factors on De Novo Regeneration of Porcine Testis Tissue After Ectopic Implantation of Testis Cells in Mice (Chapter 6)***

The objective of this study was to:

1. Evaluate the effects of growth factors (EGF, RA, VEGF, FGF2, FGF9, GDNF, SCF, or LIF) on *de novo* formation of porcine testis tissue after implantation of testis cell aggregates in mice.

It was hypothesized that:

1. The addition of growth factors (EGF, RA, VEGF, FGF2, FGF9, GDNF, SCF, or LIF) to testis cell aggregates will improve *de novo* formation of porcine testis tissue after implantation in mice.

# CHAPTER 3

# OPTIMIZATION OF CULTURE CONDITIONS FOR SHORT-TERM MAINTENANCE, PROLIFERATION, AND COLONY FORMATION OF PORCINE GONOCYTES [1, 2]

## 3.1 Abstract

Gonocytes give rise to spermatogonial stem cells, and thereby play an essential role in establishing spermatogenesis. Optimized culture conditions for gonocytes provide an opportunity for their study and *in vitro* manipulation for potential application in reproductive technologies. Using six experiments in a step-wise design, we examined the effects of several culture conditions on the maintenance, proliferation, and colony formation of porcine gonocytes. Testis cells from neonatal piglets were cultured for 7 d in DMEM supplemented with 10% fetal bovine serum. The examined culture conditions included using different cell seeding densities, gonocyte proportions, incubation temperatures, sampling strategies, and medium changing regimens. Confluency of cells was optimal (>90% by ~6 d) when $3.0 \times 10^4$ testis cells/cm$^2$ containing ~40% gonocytes were used. Incubating the cells at 35 °C or 37 °C resulted in similar cell number and viability at confluency, but incubation at 35 °C resulted in a delayed confluency. In the first 2 d of culture, gonocytes remained mostly floating in the medium and gradually settled over the next 5 d. Consequently, not changing the medium for 7 d (as opposed to changing it every 2 d) led to a significant increase in the number of gonocyte colonies by reducing the loss of "floating gonocytes". We found that gonocytes require the presence of a critical minimum number of somatic cells for settlement, and can proliferate and form growing colonies even in a basic medium. Large numbers of viable gonocytes remain floating in the medium for several days. The optimized culture conditions in the

[1] This study has been published. Awang-Junaidi AH and Honaramooz A (2018). *J. Anim. Sc. Biotechnol.* 9:8. Portions of this study were also presented at the 41st American Society of Andrology Annual Meeting. The document has been reformatted from the original version for inclusion in the thesis.

[2] AHAJ contributed to the conceiving and designing of the study, performed the experiments and wrote the first draft of the manuscript.

present study included seeding with $3.0 \times 10^4$ testis cells/cm$^2$ containing ~40% gonocytes, incubating at 37 °C, and without changing the medium in the first week, which can result in improved colony formation of porcine gonocytes.

## 3.2 Introduction

Testis stem cells are a unique population of stem cells in an adult body, because in addition to their dual ability to self-renew and give rise to differentiating germ cells, they can pass the genetic information to the offspring. Among the many types of male germ cells present from the fetal period to adulthood, primordial germ cells (PGC), gonocytes, and particularly spermatogonial stem cells (SSC) are believed to possess stem cell potential and hence are referred to as male germline stem cells (MGSC) (Lehmann, 2012). An *in vivo* functional assay for confirming the stem cell potential of MGSC was provided when SSC were deposited in the lumen of seminiferous tubules of recipient testes using germ cell transplantation technique. The transplanted SSC were capable of homing to the tubule basement membrane, forming new colonies of developing germ cells, and initiating donor-derived spermatogenesis (Brinster and Avarbock, 1994; Jiang and Short, 1998; Honaramooz *et al.*, 2002b, 2003b, a; Izadyar *et al.*, 2003b). In breeding trials, some of the germ cell recipient animals of various species were capable of siring donor-derived progeny (Brinster and Avarbock, 1994; Honaramooz *et al.*, 2003a; Herrid *et al.*, 2009). There are also a few reports of using gonocytes and PGC as donor cells in germ cell transplantation leading to the establishment of spermatogenesis in the recipient testis (Jiang and Short, 1998; Chuma *et al.*, 2005; Kim *et al.*, 2014).

The choice of donor MGSC is a critical factor for the outcome of germ cell transplantation. Using PGC as donor cells has been less practical because their isolation requires collection from embryos and there are only a limited number of PGC per embryo (Jiang and Short, 1998; Ohta *et al.*, 2004). Spermatogonia can be collected from mature donor individuals and enriched for SSC at relatively high numbers. However, spermatogonia are inherently a heterogeneous population of cells and the lack of biomarkers has made unequivocal isolation of pure SSC populations difficult (De Rooij, 2001b; Orwig *et al.*, 2002c; Grisanti *et al.*, 2009). Compared with PGC and SSC, gonocytes offer a potentially more practical option. Gonocytes are transitory germ cells (between PGC and SSC) that have a distinct morphology (large round cells with large nucleus to cytoplasm ratio), and are

present during both fetal and early postnatal period for several days, months or even years, depending on the species (De Rooij and Russell, 2000; Oatley and Brinster, 2008; Culty, 2009). Perhaps more importantly, gonocytes are the only germ cells present in the testes of neonates; thus, they can be detected using most germ cell markers (*e.g.,* VASA, DAZL), pluripotency markers (*e.g.,* NANOG, OCT4), and certain surface protein markers (*e.g.,* DBA, UCHL1). These characteristics provide an opportunity for enrichment and *in vitro* manipulation of gonocytes (Goel *et al.*, 2007; Culty, 2009; Han *et al.*, 2009; Yang and Honaramooz, 2012; Zogbi *et al.*, 2012).

Gonocytes are relatively limited in numbers since they comprise only ~1.4% of cells in the testes of neonatal rats (Orwig *et al.*, 2002a) and ~7% of seminiferous cord cells in piglets (Honaramooz *et al.*, 2005a). The efficiency of colonization by the donor germ cells in the seminiferous tubules of recipients is directly proportional to the number of transplanted MGSC. Therefore, to increase the efficiency of germ cell transplantation, gonocytes must be enriched and/or propagated *in vitro* prior to transplantation, as suggested for SSC (Dobrinski *et al.*, 1999; Shinohara *et al.*, 2000b). Various strategies have been introduced to optimize the isolation, enrichment, or purification of gonocytes with differing outcomes, depending on the species (van den Ham *et al.*, 1997; Goel *et al.*, 2007; Han *et al.*, 2009; Borjigin *et al.*, 2011). Using conventional cell separation methods, no more than ~10% of isolated neonatal testis cells were gonocytes (van Dissel-Emiliani *et al.*, 1989; Li *et al.*, 1997; Orwig *et al.*, 2002a; Honaramooz *et al.*, 2005a). However, development of a three-step enzymatic digestion in our laboratory has allowed the collection of populations of cells containing ~40% gonocytes from neonatal porcine testes (Yang *et al.*, 2010). The resultant population of gonocytes can also be enriched further to ~90% using a combination of Nycodenz centrifugation and differential plating (Yang and Honaramooz, 2011).

While the pig is an important biomedical animal model, purification of porcine MGSC is still limited. The ability to obtain highly enriched populations of gonocytes from neonatal piglets (Yang *et al.*, 2010; Yang and Honaramooz, 2011), however, has provided new opportunities for using gonocytes as a model for *in vitro* propagation and manipulation of MGSC. This calls for further research on culture systems that can allow efficient large-scale propagation of gonocytes. No systematic study has examined the effects of different culture conditions on colony formation of porcine gonocytes. Therefore, given the importance of cell culture in MGSC research, the present study was designed to examine a number of culture conditions for maintenance, proliferation, and

colony formation of neonatal porcine gonocytes as a model. The objectives of the present study were to examine several aspects of porcine gonocyte culture through multiple experiments in a stepwise design. The examined factors included the gonocyte proportion and seeding density, incubation conditions, sampling, medium changing regimens, and effects of applying those optimal conditions on gonocyte colony formation.

## 3.3 Materials and Methods

### *3.3.1 Testis Collection and Preparation*

Testes from Yorkshire-cross piglets (Camborough-22 × Line 65; PIC Canada, Winnipeg, MB, Canada) less than 1 wk of age were used in this study. The testes were collected weekly (5-15 pairs per wk) through aseptic castration at the Prairie Swine Center (a university–affiliated facility). All experimental procedures involving animals were reviewed and approved by the University of Saskatchewan's Institutional Animal Care and Use Committee (Animal Use Protocol# 20080042). The testes were kept in ice-cold Dulbecco's phosphate-buffered saline (DPBS; catalogue no. 20-031-CV; Mediatech, Manassas, VA, USA), containing 1% w/v antibiotics solution (penicillin and streptomycin; catalogue no. 30-002-CI, Mediatech), and were transported within 1 h of collection to the laboratory. The testes were thoroughly rinsed three times with DPBS prior to processing. The parenchyma was separated from the tunica albuginea and excess connective tissues, and used for isolation of testicular cells.

### *3.3.2 Isolation of Testis Cells and Enrichment for Gonocytes*

Isolation of testis cells and enrichment of gonocytes were performed using methods that were established in our laboratory (three-step enzymatic digestion, Nycodenz density gradient centrifugation and extracellular matrix (ECM) differential plating; (Han *et al.*, 2009; Yang and Honaramooz, 2011). Briefly, for each batch of the three-step enzymatic digestion, ~600 mg of testis parenchyma was thoroughly minced with fine scissors for 5 min, suspended in 5 mL of DPBS, vortexed for 30 sec in a test tube shaker (Reax Top; catalogue no. 541-10000; Heidolph Instrument, Essex, UK) and digested with 1 mL of 0.2% w/v collagenase IV (catalogue no. C-153; Sigma-Aldrich, Oakville, ON, Canada), 0.1% w/v hyaluronidase (catalogue no. H-3884; Sigma-Aldrich), and 0.01% DNase (catalogue no. DN25; Sigma-Aldrich) in Dulbecco's modified Eagle's medium

(DMEM; catalogue no. 10-013-CM; Mediatech) supplemented with 1% w/v antibiotics (as above) at 37 °C for 10 min. Fetal bovine serum (FBS; catalogue no. A15-701; PAA Laboratories, Etobicoke, ON, Canada) was added to stop the digestion and the suspension was vortexed for another 30 sec and filtered through a 40 μm filter (catalogue no. 3522340; BD Biosciences, San Jose, CA, USA). The filtrate suspension was centrifuged at 500×*g* at 16 °C for 5 min and resuspended in 5 mL of DPBS supplemented with 1% w/v antibiotics. A large number of red blood cells were observed among the isolated testis cells. Therefore, erythrocyte depletion was performed by mixing the cells with 20 mL of the lysis buffer, composed of 156 mmol/L ammonium chloride ($NH_4CL$; catalogue no. A9434; Sigma-Aldrich), 10 mmol/L potassium bicarbonate ($KHCO_3$; catalogue no. 237205; Sigma-Aldrich), and 0.1 mmol/L disodium ethylenediaminetetraacetate ($Na_2EDTA$; catalogue no. E6635; Sigma-Aldrich) in sterile distilled water prior to another cycle of centrifugation (500×*g* at 16 °C for 5 min). Finally, the cell pellet was resuspended in 5 mL of DMEM supplemented with 10% v/v FBS and 1% antibiotics (designated as $DMEM^{++}$) and underwent gentle pipetting to obtain a single cell suspension.

For enrichment of gonocytes among the cells obtained from the three-step enzymatic digestion, 3 mL of 17% Nycodenz in DPBS (Histodenz; catalogue no. D2158; Sigma-Aldrich) was placed at the bottom of a 15-mL graduated conical tube. This was followed by gentle addition of 2 mL of cell suspension on top and the tube was centrifuged at 500×*g* at 4 °C for 15 min. The supernatant was discarded, and the pellet was harvested and resuspended as a single cell suspension. This was immediately followed by ECM differential plating, for which 6-well culture plates (catalogue no. 353046; BD Biosciences) were coated with 1 mL of 50 μg/mL poly-D-lysine (catalogue no. 47743-736; VWR International, Mississauga, ON, Canada) and 10 μg/mL fibronectin (catalogue no. 477743-728; VWR) in an incubator with 5% $CO_2$ at 37 °C for 1 h, and dried in a biosafety cabinet for another 1 h. The poly-D-lysine pre-coated wells were rinsed twice with DPBS before seeding the cells obtained from Nycodenz gradient density centrifugation. The cells were seeded onto the plates at a concentration of $2.5 \times 10^5$ cells/cm$^2$ in $DMEM^{++}$, and cultured in an incubator with 5% $CO_2$ at 37 °C. After 2 to 3 h, the floating cells were harvested, centrifuged at 500×*g* at 16 °C for 5 min and the pellets were collected and resuspended as a single cell suspension. These procedures lead to obtaining isolated testis cells highly enriched in gonocytes. We performed a side-by-side quantitative comparison of the cell yield, viability and loss after each progressive step. Samples were prepared from single cell suspensions obtained from each step. The suspension was smeared

onto poly-L-lysine pre-coated glass coverslips, dried overnight in a biosafety cabinet and kept at -20 °C for use in fluorescent labeling.

### *3.3.3 Simultaneous Cell Quantification and Viability Assessment*

The number of resultant cells after each isolation and enrichment step as well as after culturing was quantified, and the cell viability was assessed using the trypan blue exclusion technique. For evaluation of cells collected after isolation and enrichment, single cell suspensions were prepared as described above. For cultured cells, detachment of the adherent cells was performed by adding 1 mL of 0.25% (w/v) trypsin in Hank's balanced salt solution (HBSS) and 2.21 mmol/L EDTA (catalogue no. 25-053-CI; Mediatech) at 37 °C for 1-2 min (depending on confluency) with gentle agitation. The enzymatic digestion was stopped by adding 1 mL of undiluted FBS, and the mixture was centrifuged at 500×*g* at 16 °C for 5 min. The pellets were collected and subjected to resuspension into a single cell suspension prior to viability assessment. Trypan blue (100 µl of a 0.4% solution in saline, catalogue no. T8154; Sigma-Aldrich) was mixed (1:1 ratio) gently with the cell suspension, and 20 µl of the mixture was transferred to each hemocytometer chamber and live/dead cells were identified with the aid of a light microscope. For each replicate, two counts of live/dead cells were performed and averaged to calculate the yield and viability of cells (given as a percentage). As explained in more detail in Chapter 3.3.6, fluorescent labeling of lectin DBA was performed to confirm and quantify gonocytes, as they are the only type of germ cells present in neonatal pig testes; hence the remaining cells were categorized as somatic cells. For this staining, a minimum of 600 cells in randomly selected fields were counted in each cell smear, and the proportion (%) of gonocytes/somatic cells was calculated.

### *3.3.4 Cell Culture*

Different cell culture conditions were evaluated using a stepwise approach. The same medium ($DMEM^{++}$), culture plates (6-well plates), and incubator conditions (5% $CO_2$ and 95% humidity) were used in all experiments in order to evaluate the effects of changing other variables (*i.e.,* gonocyte proportion, incubation temperature, cell seeding density, and medium changing regimen). For all experiments, pH of the medium was adjusted to 7.4 immediately prior to using it in cell cultures. The pH of the medium was measured using a digital pH meter (catalogue no. 11288-368; model Symphony SB70P; VWR). Cell growth was monitored at least once daily using an inverted

phase contrast microscope (Nikon, Eclipse TS100). For each experiment, multiple replications were performed where cells obtained from each batch of testis tissue digestion were considered one replication. We have previously shown that the characteristics of cells obtained from 1-wk old piglets from this source remain consistent over time, both within and among litters (Yang *et al.*, 2010).

Effects of several factors on the behavior and the morphology of cultured testis cells were examined using cytology and fluorescent labeling. The examined factors included different gonocyte proportions obtained before or after each step of enrichment (40% vs. 80% vs. 86%), incubation temperature (35 °C vs. 37 °C), cell seeding density ($1.0 \times 10^5$ vs. $3.0 \times 10^5$ vs. $5.0 \times 10^5$ cells/well; each well in a 6-well plate has ~10 $cm^2$ cell growth area) and medium changing regimen (every 2 d vs. modified regimen vs. no changing of medium for up to 7 d). Confluency assessment was defined as the relative coverage of the plate surface by the mixture of testis cells, and a gonocyte colony was defined as a group of more than three gonocytes in close contact.

### *3.3.5 Cell Sampling*

For sampling of cultured cells, glass coverslips coated with 0.1% w/v poly-L-lysine were used. Glass coverslips sized 22 × 22 mm (catalogue no. 12-540B; Fisher Scientific, USA) were arranged in a sterile metal coverslip rack and immersed in 1% HCL in 70% alcohol for 10 min, followed by rinsing with sterile distilled water for 5 sec and allowed to dry for 20 min. The rack was transferred into a 0.1% w/v poly-L-lysine (catalogue no. P8920; Sigma-Aldrich) solution for 10 min and allowed to dry overnight. Finally, the glass coverslips were placed at the bottom of each well in 6-well plates. These procedures were conducted under a biosafety cabinet.

### *3.3.6 DBA Fluorescent Labeling*

Gonocytes were identified using *Dolichos biflorus* agglutinin (DBA) according to previously described protocols (Yang *et al.*, 2010; Yang and Honaramooz, 2011), with minor modifications. Briefly, the dried coverslips (with cell smears or with cells grown directly on them) were fixed in Bouin's solution (catalogue no. 1120-31; Richa Chemical Company, Pocomoke City, MD, USA) for 2-3 min. The samples were then rinsed three times with 70% alcohol to remove excess Bouin's solution followed by three rinses with DPBS. The samples were blocked with 5% bovine serum

albumin (BSA; catalogue no. 0332, Amresco, Solon, OH, USA) at 37 °C for 30 min in a humidified chamber. The blocking agent was removed and the samples were incubated with fluorescein isothiocyanate (FITC)-conjugated lectin DBA (1:100, catalogue no. FL-1031, Vector Labs, Burlington, ON, Canada) overnight at 4 °C in a humidified chamber. The samples underwent another cycle of rinsing, followed by incubation with 0.3% Sudan Black B w/v (catalogue no. S2380; Sigma-Aldrich) in 70% alcohol for 15 min, at 37 °C in a humidified chamber. The samples were rinsed with DPBS and stained with 4'6'-diamidino-2-phenyilindole (DAPI; catalogue no. D9542; Sigma-Aldrich) and observed under a fluorescence microscope. FITC-conjugated lectin DBA specifically labels gonocytes which appear green under the fluorescence microscope while DAPI stains the nuclei of all cells which appear blue (Fig. 3.1).

### *3.3.7 Statistical Analyses*

Unless stated otherwise, all data are presented as means ± standard error of mean (SEM) and analyzed using either one-way or two-way analysis of variance (ANOVA), as appropriate, followed by Tukey's HSD post-hoc test. For percentages, the data were transformed using Arcsine function prior to analysis using ANOVA. The level of significance was set at $P < 0.05$. Data were analyzed using the Statistical Package for Social Science (SPSS; Version 20.0, SPSS Inc., Chicago, IL, USA).

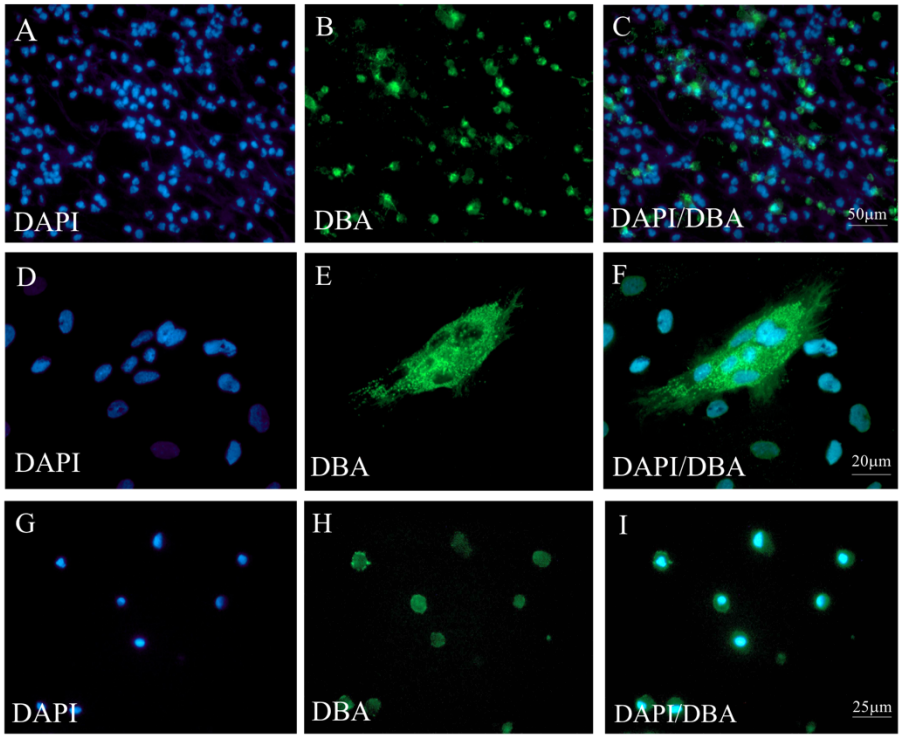


**Fig. 3.1.** *Dolichos biflorus* agglutinin (DBA) fluorescent labeling of neonatal gonocytes. (A-C) Gonocyte labeling with DBA was performed on testis cell smears collected immediately following cell isolation. (D-F) Multiple gonocytes form a colony on a somatic-cell monolayer observed at 1 wk of culture. (G-I) Floating gonocytes in the removed medium observed 4 d after incubation. (A,D,G) DAPI-stained nuclei of the cells appear blue (B,E,H). Fluorescein-conjugated DBA-labeled gonocytes appear green under the fluorescence microscope. (C,F,I) Merged images.

## 3.4 Results

As summarized in Table 3.1, enzymatic digestion of testis tissues yielded a population of testis cells containing ~41% germ cells (Fig. 3.1A-C), which at this developmental stage (~1 wk of age) are exclusively gonocytes. Gradient centrifugation by Nycodenz, followed by ECM differential plating resulted in enrichment of gonocytes to ~80% and ~86%, respectively. However, the enrichment procedures also caused significant reductions ($P < 0.05$) in cell counts after each step, resulting in ~73% and ~92% total testis cell loss and ~47% and ~83% gonocyte loss, respectively. The relatively lower gonocyte loss at each step, compared with the total cell loss, resulted in significant enrichment of gonocytes. The viability of cells was also reduced after each enrichment step (from ~93% to 84% and 82%, respectively, $P < 0.05$). When the cells were cultured ($3.0 \times 10^5$ cells/well at 37ºC with 5% $CO_2$ and the medium was changed every 2 d), only the cells used immediately after the three-step enzymatic digestion (*i.e.,* without enrichment) demonstrated growth by reaching ~90% confluency in ~6 d.

### *3.4.1 Experiment 1: Effect of Cell Seeding Density and Gonocyte Proportion*

One of the objectives of this experiment was to determine the optimal seeding density for culturing testis cells. A comparison was made by randomly assigning cells into 6-well plates at $1.0 \times 10^5$, $3.0 \times 10^5$, or $5.0 \times 10^5$ cells/well (*i.e.,* $1.0 \times 10^4$, $3.0 \times 10^4$, or $5.0 \times 10^4$ cells/cm$^2$ since each well was ~10 cm$^2$, $n = 12$ replications), in 3 mL of medium to determine the time required for the cells to reach 90% confluency. Cells were used fresh (immediately after enzymatic digestion and without enrichment, hence containing ~40% gonocytes) and cultured under similar conditions at 37 ˚C, and the medium was changed every 2 d.

As shown in Table 3.2, cells in the highest seeding density group ($5.0 \times 10^5$) became confluent earlier than other groups ($P < 0.05$), reaching >90% confluency in ~4 d, while the $3.0 \times 10^5$ seeding density group of cells were >90% confluent by ~Day 6. Cells cultured at $1.0 \times 10^5$ seeding density had slow growth and only reached ~30% confluency after 7 d in culture.

In a separate experiment, testis cells enriched for gonocytes (undergoing both Nycodenz centrifugation and ECM plating, hence containing ~86% gonocytes) were used as the source of

cells for culturing, using the same incubation conditions. Cells did not grow in plates seeded with $1.0 \times 10^5$ or $3.0 \times 10^5$ cells/well and only had limited growth in the $5.0 \times 10^5$ seeding density group after 7 d in culture (5-15% confluency, data not shown). Therefore, for the remaining experiments in this study we used testis cells without enrichment (*i.e.,* containing ~40% gonocytes), and since the $3.0 \times 10^5$ seeding density resulted in confluency of cells in ~6 d (without the need for passaging the cells within 1 wk), we used this seeding density in the subsequent experiments.

### *3.4.2 Experiment 2 : Effect of Incubation Temperature*

The objective of this experiment was to evaluate the growth of cultured testis cells using incubation temperatures of either 35 ˚C or 37 ˚C for 1 wk ($n$ = 12 replications), while other culture conditions remained the same (*e.g.,* medium, cell seeding density, and $CO_2$ levels). As shown in Table 3.3, the viability and number of cells at confluency did not differ between the two incubation temperatures ($P > 0.05$). However, the cells cultured at 35 ˚C reached confluency later than those at 37 ˚C ($P < 0.05$); therefore, for practical reasons we chose to culture the cells at 37 ˚C for subsequent experiments.

**Table 3.1.** The population of testis cells obtained after enzymatic digestion and subsequent enrichment.

| Method | Proportion (%) | | Cell count (× 106) * | | Cell loss (%) ** | | Viability (%) | Growth |
|---|---|---|---|---|---|---|---|---|
| | Gonocytes | Somatic cells | Total | Gonocytes | Total | Gonocytes | | |
| Enzymatic digestion | 40.60 ± 1.21[a] | 59.40 ± 1.21[a] | 37.84 ± 2.44[a] | 15.38 ± 1.09[a] | - | - | 92.62 ± 0.59[a] | Yes |
| Nycodenz centrifugation | 80.40 ± 1.46[b] | 19.60 ± 1.46[b] | 10.00 ± 0.41[b] | 8.00 ± 0.21[b] | 73.18 ± 1.76[a] | 46.72 ± 4.69[a] | 84.20 ± 1.06[b] | Limited |
| ECM differential plating | 86.40 ± 1.03[c] | 13.6 0 ± 1.03[c] | 3.02 ± 0.19[c] | 2.60 ± 0.2[c] | 91.62 ± 0.79[b] | 82.61 ± 1.71[b] | 81.66 ± 0.71[c] | Limited |

The results are mean ± SEM.
* Each replicate was based on the digestion of ~600 mg of testis tissue.
One-way ANOVA (or *t* test **) was used for statistical analyses, and $P < 0.05$ was considered as significant.
[abc] Within each column, data with different superscripts differ significantly ($P < 0.05$). $n = 5$ replications.

**Table 3.2.** The effect of seeding density on the growth of testis cells in culture.

| Seeding density | Maximum confluency | | |
|---|---|---|---|
| | Confluency at days | Cell count | Viability (%) |
| $1.0 \times 10^5$ | (*~30% at 7) | (*$2.98 \times 10^5 \pm 0.01$) | (*$88.4 \pm 1.02$) |
| $3.0 \times 10^5$ | >90% at $6.0 \pm 0.17^a$ | $8.10 \times 10^5 \pm 0.01$ | $91.21 \pm 0.58$ |
| $5.0 \times 10^5$ | >90% at $4.0 \pm 0.15^b$ | $8.16 \times 10^5 \pm 0.01$ | $91.62 \pm 0.56$ |

The results are mean ± SEM.
*The results from $1.0 \times 10^5$ seeding density group were excluded from statistical analysis as the cells did not reach 90% confluency.
Independent sample *t* test was used for statistical analyses.
[ab] Within each column, if data differed significantly ($P < 0.05$), they are denoted by different superscripts.
$n = 12$ replications.

**Table 3.3.** The effect of incubation temperature on the growth of testis cells in culture.

| Temperature | >90% confluency | | |
|---|---|---|---|
| | Days | Cell count | Viability (%) |
| 35 ºC | $6.42 \pm 0.15^{a}$ | $7.98 \times 10^{5} \pm 0.01$ | $89.98 \pm 0.49$ |
| 37 ºC | $5.83 \pm 0.17^{b}$ | $8.27 \times 10^{5} \pm 0.01$ | $90.04 \pm 0.49$ |

The results are mean ± SEM.
Independent sample *t* test was used for statistical analyses.
[ab] Within each column, if data differed significantly ($P < 0.05$), they are denoted by different superscripts.
$n = 12$ replications.

### *3.4.3 Experiment 3: Sampling of Cultured Testis cells for Analysis*

Various methods can be used to sample cultured cells for analysis. When sampling for applications such as immunocytochemistry, coverslips are commonly pre-coated with certain matrices to enhance adherence of cells. It is not clear whether the presence of the pre-coated coverslips in testis cell culture would affect cell growth. Furthermore, in situations where multiple samplings from each replicate are required, it would be more efficient to use all available cultured cells, including those grown on areas of the culture well not covered by the coverslip. The objectives of this experiment were to determine 1) whether the rate or pattern of testis cell growth in culture would change in the presence of glass coverslips (22 × 22 mm) coated with 0.01% poly-L-lysine, and 2) whether the growth of testis cells on the coverslips differs from those on the peripheral areas of the wells, not covered by the coverslips (Fig. 3.2).

When plates with and without poly-L-lysine-coated coverslips were compared, the number or viability of the resultant cultured cells did not differ between plates ($8.18 \pm 0.01 \times 10^5$ vs. $8.22 \pm 0.02 \times 10^5$ cells per plate, with $91.0 \pm 0.57\%$ vs. $91.3 \pm 0.87\%$ cell viability, plates with coverslips vs. plates with no coverslips, respectively, $n = 12$ replications, $P > 0.05$). When non-coated coverslips were used, little or no cell growth was observed. Furthermore, within the plates with poly-L-lysine-coated coverslips, the viability of cells grown on coverslips did not differ from those grown on the peripheral areas of the well, not covered by coverslips ($92.0 \pm 0.33\%$ vs. $92.4 \pm 0.51\%$, coverslips vs. periphery, respectively, $P > 0.05$). However, the number of cells obtained from the peripheral areas was higher than that from the coverslips ($4.59 \pm 0.14 \times 10^5$ vs. $2.99 \pm 0.06 \times 10^5$, respectively, $P < 0.05$), even though both encompassed a similar cell growth area (~4.8 $cm^2$ each).

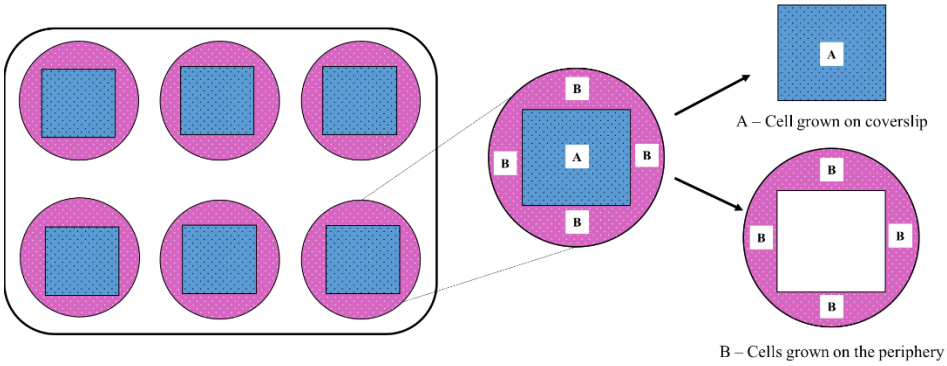


**Fig. 3.2.** Schematic representation of the areas within culture plates used for sampling in Experiment 3. The numbers and viability of cells grown on poly-L-lysine-coated coverslips (A) were compared with those grown on the peripheral areas of the wells, not covered by the coverslip (B).

### *3.4.4 Experiment 4: Short-Term Culture of Neonatal Porcine Testis Cells*

Morphological changes of neonatal porcine testis cells in culture were evaluated for 1 wk under the above-mentioned culture conditions ($3.0 \times 10^5$ seeding density, DMEM$^{++}$, 37 °C, $n = 6$ replications). The medium was changed every 2 d. Within the first 12 h of incubation, most of the cells and cell particles were still floating in the medium (Fig. 3.3A). By 24 h after incubation, small numbers of cells settled and appeared to have adhered to the plate. The early settling cells were mostly somatic cells and began to form cytoplasmic projections, creating irregularly shaped cell boundaries (Fig. 3.3B), while more cells continued to settle. After 2 d of incubation, the cells started to appear in clumps (Fig. 3.3C), and over time these groups of cells spread further and combined to create a large somatic-cell monolayer. At the same time, round cells with large nuclei, appearing bright or with a halo under phase-contrast microscopy, were seen attached onto the somatic-cell monolayer (Fig. 3.3D-E). These rounds cells were confirmed to be gonocytes using fluorescent labeling (Fig. 3.1D-F). It was also observed that while initially gonocytes were present as singles or pairs, starting at Day 5, colonies (grape-like clumps) of more than 3 cells could also be observed (Fig. 3.3D). It was noticed that gonocytes were only loosely attached to the somatic-cell monolayer, since some would detach due to slight movements of the plate. By the end of the experiment (Day 7), the number of these round cell colonies were still considerably less than expected, given that the population of testis cells at seeding contained ~41% gonocytes. The somatic cells continued to multiply and once reaching 70-80% confluency (at ~4 to 5 d), many appeared as spindle-shaped fibroblast-like cells (Fig. 3.3E).

### *3.4.5 Experiment 5: Floating Cells in the Culture Medium*

Based on the findings of Experiments 1 and 4, it was clear that gonocytes require sufficient ratios of somatic cells or feeder cells, to which they formed a loose attachment for growth in culture. We speculated that the very low number of gonocyte colonies observed by Day 7 during short-term culture (Fig. 3.3E) might be due to their loss through routine medium changes, which apparently eliminated the floating and loosely adherent gonocytes. Therefore, this experiment was designed to examine the medium removed from the plates. The results showed that indeed high numbers of round cells were present in the medium removed routinely every other day. The number of these cells was greatest in the medium removed on Day 2 ($6.81 \pm 0.63 \times 10^4$), compared with Days 4 and

6 ($1.02 \pm 0.09 \times 10^4$ and $0.4 \pm 0.07 \times 10^4$ cells/well, $P < 0.05$, $n = 5$ replications, Fig. 3.4). On the other hand, if the medium was not changed, greater numbers of floating gonocytes remained in the medium examined on Days 4 and 6 ($4.2 \pm 0.10 \times 10^4$ and $1.92 \pm 0.05 \times 10^4$ cells/well, respectively), compared with the numbers obtained on the same days when the medium was changed every other day ($P < 0.05$, $n = 5$ replications, Fig. 3.4). Based on the morphology, it was presumed that these cells were gonocytes; they were large and round in shape with prominent nuclei (large nucleus to cytoplasm ratio). The viability of these round cells remained high in all examined days (~85-97%, data not shown). Using fluorescent labeling, these round cells were later confirmed to be gonocytes (Fig. 3.1G-I).

### *3.4.6 Experiment 6: Effect of Medium Changing Regimens on Attached Gonocytes*

This experiment was designed to assess the effects of different medium changing regimens on the number and viability of attached gonocytes. The cells were cultured using the selected culture conditions ($3.0 \times 10^5$ testis cells/well containing ~40% gonocytes, $DMEM^{++}$, 37 °C) for 1 wk, and medium changing regimens were assigned to groups of plates as follows: 1) To serve as a control group, the cells were seeded with 3 mL of medium, and the medium was changed routinely, every 2 d (routine group, 3 changes in 1 wk); 2) the cells were seeded with 2 mL of medium, followed by the addition of another 1 mL after 24 h, and then every 2 d 1 mL of medium was removed from the well and replaced with 1 mL of fresh medium (modified group); or 3) the cells were seeded with 3 mL of medium but the medium was not changed (unchanged group). On Days 2, 4, 6, and 7, the cultured cells were observed under an inverted microscope and the number of gonocyte colonies in four randomly selected fields at 400× was recorded and cells were collected for evaluation of viability ($n = 5$ replications per group).

As shown in Fig. 3.5, alterations in medium changing regimens affected the number of attached gonocytes or gonocyte colonies present on the somatic-cell monolayers. Overall, the number of gonocyte colonies increased ($P < 0.05$) from Day 2 to Day 4 of culture in all medium changing regimens. However, among the medium changing regimens, the unchanged group had greater ($P < 0.05$) number of gonocyte colonies on Days 6 and 7 compared with the routine medium changing group (control).

The viability of cells in different medium changing regimens is shown in Fig. 3.6. Compared with the cell viability at seeding (~90%), there was a reduction in viability of cells at Days 4, 6, and 7 in all groups ($P < 0.05$). The cell viability was reduced further in the unchanged group on Days 6 and 7 ($P < 0.05$). Between the regimens, the viability of cells in the unchanged groups was lower ($P < 0.05$) than the routine group on Days 6 and 7 of culture.

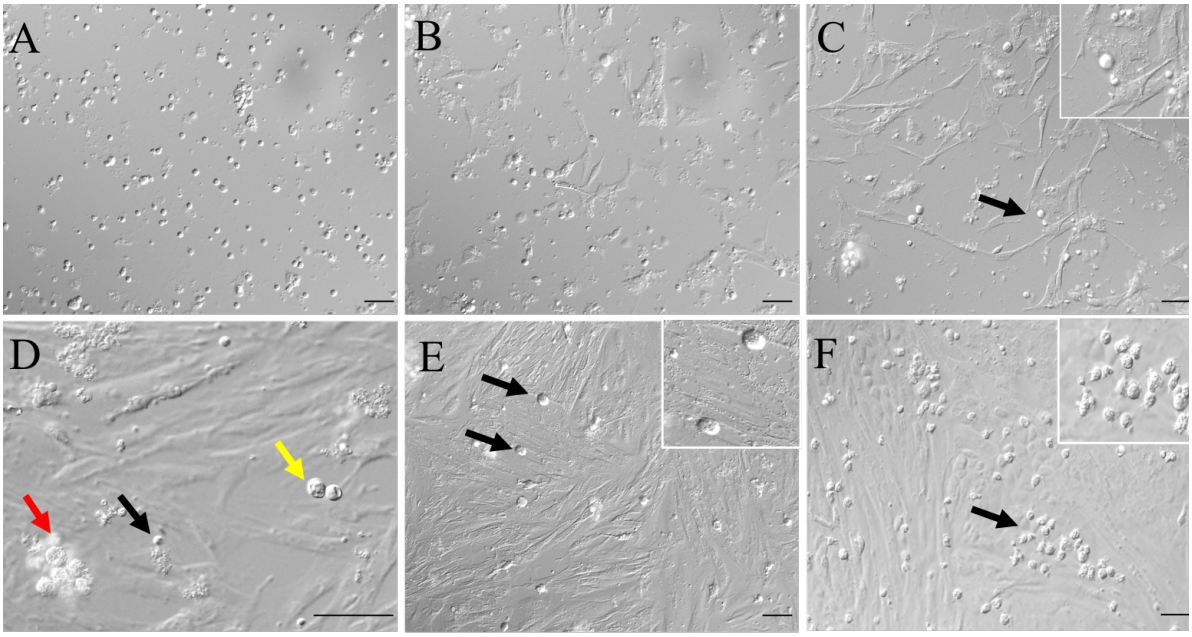


**Fig. 3.3.** Morphology of testis cells in short-term cell culture. (A) Morphology of floating cells 12 h after seeding. (B) Some somatic cells settled to the bottom of the plate within 24 h of incubation. (C) These somatic cells extended cytoplasmic projections toward one another. (C-F) Cells presumed to be gonocytes are seen attached to somatic cells (black arrows). The same gonocytes are also shown at a higher magnification (insets). (D) Gonocytes appeared as singles (black arrow), pairs (yellow arrow), or small colonies (red arrow). (E) Spindle-shaped fibroblast-like cells were more prominent when confluency reached >70%. Only a small number of gonocyte colonies were observed by Day 7 when routine medium changing regimen was applied. (F) Increased number of gonocyte colonies were observed when the medium was not changed for 7 d. (Scale bar: 50 μm).

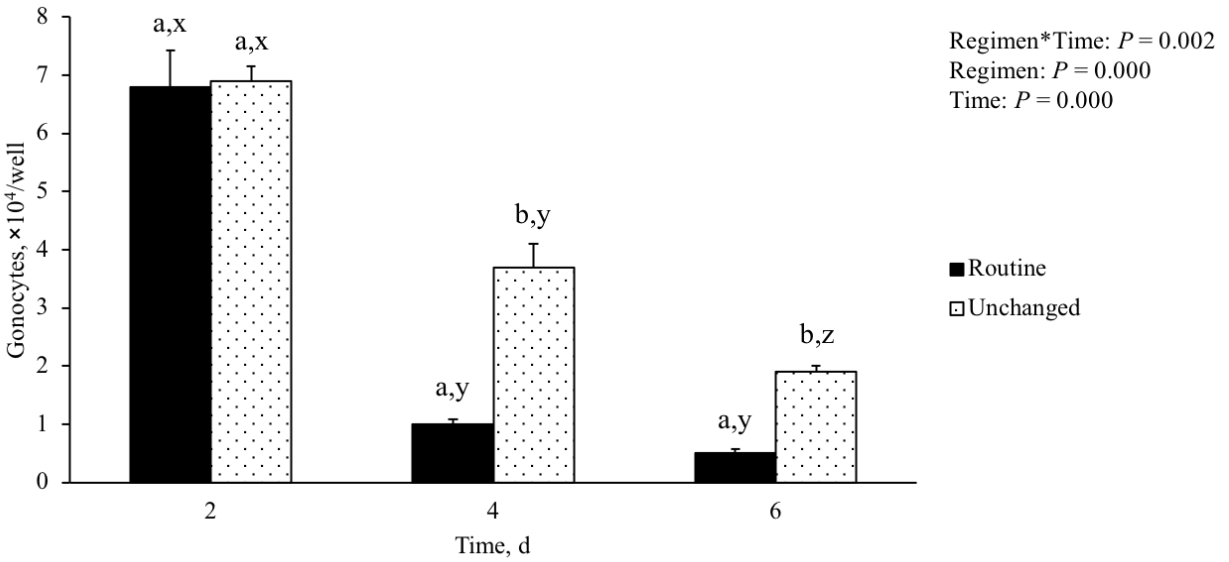


**Fig. 3.4.** Number of gonocytes upon analysis of the floating cells from the removed medium. The initial number of cells at seeding was set at $3.0 \times 10^5$ cells/well containing ~40% gonocytes and the viability was 89 ± 0.5%. The medium removed from the plates was examined and large numbers of gonocytes were seen floating in the medium on Day 2. Most of the floating gonocytes were eliminated by routine (every 2 d) medium changes (Routine), while some were present on Days 4 and 6, if the medium was not changed (Unchanged). The data are mean ± SEM. [ab] Data with different letters within each day differ significantly ($P < 0.05$). [xyz] Data with different letters within each treatment over time differ significantly ($P < 0.05$). $n$ = 5 replications.

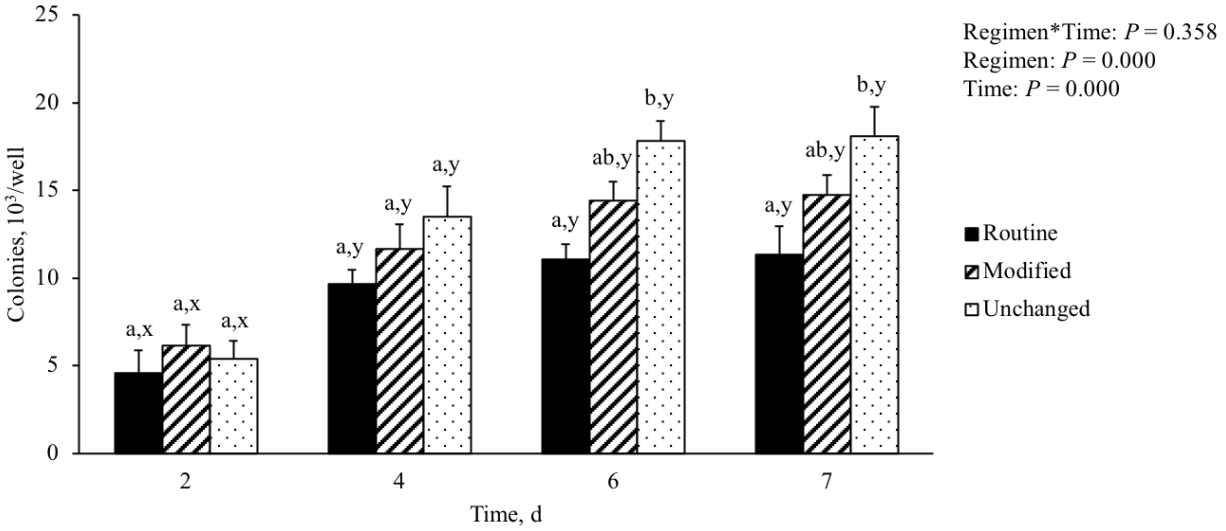


**Fig. 3.5.** Number of gonocytes or gonocyte colonies observed after applying different medium changing regimens. The cultured cells underwent one of the following medium changing regimens: 1) Seeded with 3 mL of medium and the medium was routinely changed every 2 d (Routine); 2) Seeded with 2 mL of medium, followed by the addition of another 1 mL after 24 h, and then every 2 d, 1 mL of medium was removed from the well and replaced with 1 mL of fresh medium (Modified); 3) Seeded with 3 mL of medium but the medium was not changed for 7 d (Unchanged). The data are mean ± SEM. [ab] Data with different letters within each day differ significantly ($P < 0.05$). [xy] Data with different letters within each treatment over time differ significantly ($P < 0.05$). $n = 5$ replications.

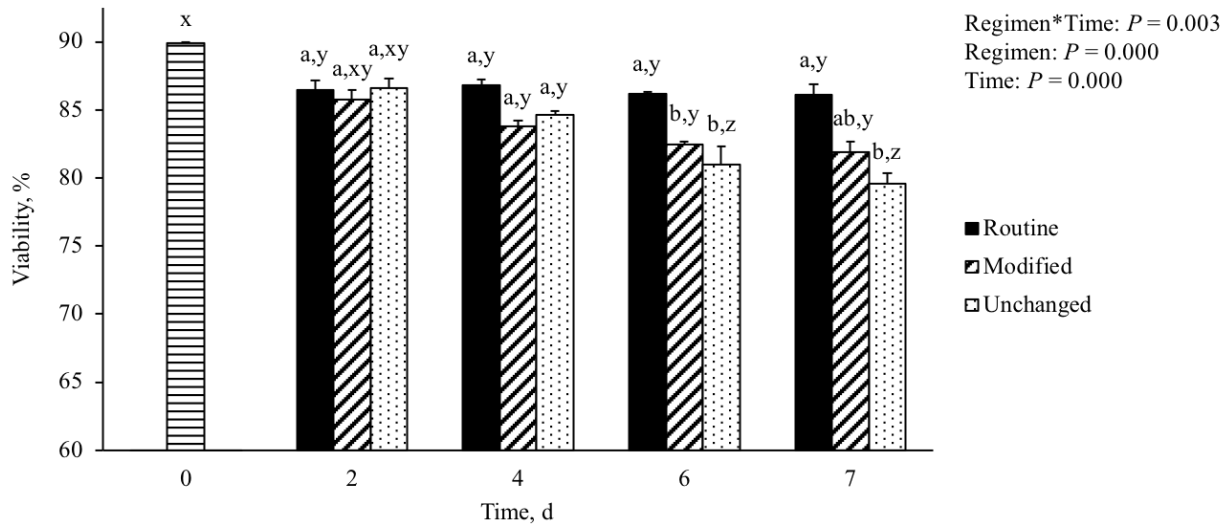


**Fig. 3.6.** Viability of cells at seeding and after applying different medium changing regimens. The cultured cells underwent one of the following medium changing regimens: 1) Seeded with 3 mL of medium and the medium was routinely changed every 2 d (Routine); 2) Seeded with 2 mL of medium, followed by the addition of another 1 mL after 24 h, and then every 2 d, 1 mL of medium was removed from the well and replaced with 1 mL of fresh medium (Modified); 3) Seeded with 3 mL of medium but the medium was not changed for 7 d (Unchanged). Viability on Day 0 represents the initial viability at seeding. The data are mean ± SEM. [ab] Data with different letters within each day differ significantly ($P < 0.05$). [xyz] Data with different letters within each treatment over time differ significantly ($P < 0.05$). $n = 5$ replications.

## 3.5 Discussion

In the neonatal testis, gonocytes represent MGSC, which have great potential applications in male reproduction research (reviewed in (Honaramooz and Yang, 2010; Honaramooz, 2012). Various methods have been established to culture MGSC to facilitate their study and manipulation or to harness their potential for downstream applications such as genetic conservation, transgenesis, or infertility treatments (Honaramooz *et al.*, 2002b, 2003b, 2008; Zeng *et al.*, 2013; Mankidy *et al.*, 2014). However, depending on the donor species, age, or developmental status, optimized culturing or enrichment of MGSC can be challenging (Yang and Honaramooz, 2010; Yang *et al.*, 2010).

Cell isolation is a critical step in preparing testis cells for culture. The number and proportion of the resultant populations of cells also vary greatly depending on the methods used to isolate the cells. As a first step in the present study, we performed a side-by-side comparison of the total testis cell yield and gonocyte proportions from three protocols (Yang *et al.*, 2010; Yang and Honaramooz, 2011). Although as expected the enrichment process resulted in highly purified populations of gonocytes (~86%), it also led to losing up to 90% of the initial number of testis cells. These findings provide a basis upon which an appropriate approach could be adopted for gonocyte isolation/enrichment in order to meet the objectives and needs of specific experiments. For example, the highly enriched populations of gonocytes could be used in studies that focus mainly on gonocytes per se, while the heterogeneous populations of testis cells obtained immediately after enzymatic digestion may be more suitable for longer-term culture or for the study of interactions between gonocytes and somatic cells.

One of the advantages of using neonatal testes as the source of germ cells is that gonocytes are the only type of germ cells present during the early postnatal stage. Gonocytes possess a distinct morphology and a unique pattern of distribution in the seminiferous cords of neonatal testes, which facilitate their identification *in situ* (Orwig *et al.*, 2002a; Goel *et al.*, 2007). Once the cells are enzymatically dissociated; however, accurate identification of gonocytes requires immunocytochemistry/fluorescent labeling. There are several biomarkers that could be used for identification of gonocytes including germ cell markers (*e.g.,* VASA and DAZL, (Reijo *et al.*, 1996; Castrillon *et al.*, 2000) and stem cell markers (*e.g.,* Nanog, SSE-A1, and OCT4, (Anderson *et al.*, 2007; Goel *et al.*, 2007; Fujihara *et al.*, 2011; Zogbi *et al.*, 2012). Two of the most commonly

used markers for neonatal porcine gonocytes are DBA (Goel *et al.*, 2007; Kim *et al.*, 2010a; Yang and Honaramooz, 2012) and ubiquitin C-terminal hydrolase L1 (UCHL1; previously known as PGP9.5) (Han *et al.*, 2009; Kim *et al.*, 2010a). DBA has a specific affinity to bind to α-D-N-acetyl-galactosamine, which is localized on the surface of porcine gonocytes (*i.e.,* primitive germ cells) (Goel *et al.*, 2007), while UCHL1 can identify both primitive and more advanced germ cells.

In the present study, the identification of gonocytes was initially hampered by autofluorescence, which was partly overcome by using a quenching protocol (Yang and Honaramooz, 2012); however, some autofluorescence remained. Autofluorescence in the tissue/cells can be due to endogenous sources (*e.g.*, lipofuscin or lipofuscin-like pigments), or acquired during processing (*e.g.,* certain fixatives). In any case, autofluorescence can interfere with specific signals by fluorescent labeling and lead to false positive results. In the present study, the autofluorescence was eliminated through modification of the quenching protocol (Yang and Honaramooz, 2012). The use of Sudan black B (SBB) has been reported to be efficient in masking autofluorescence of lipofuscins, triglycerides, and lipoproteins origin (Schnell *et al.*, 1999; Baschong *et al.*, 2001) and is a major component of the quenching protocol for testis cells (Yang and Honaramooz, 2012). In this study, as a first step in modifying the original quenching protocol, the length of incubation with SBB was extended, which led to a further reduction of the autofluorescence of testis cells, but not to its complete elimination. We then speculated that the remaining autofluorescence might have a fixative origin. The picric acid component of Bouin's solution used for fixing testis tissue has also been cited as a potential cause of autofluorescence (Hess and Moore, 1993; Howroyd *et al.*, 2005). Therefore, we applied further control measures to refine the use of fixatives in the quenching protocol. We found that the inclusion of three thorough and gentle rinses with 70% alcohol after the Bouin's fixation completely eliminated the autofluorescence problem in Bouin's fixed testis cell samples. As an alternative, we also found that to avoid the autofluorescence caused by Bouin's, cell smears or cells grown on coverslips can be fixed using methanol at -20 °C for 10 min.

Cell seeding density influences the performance of cultured cells, presumably by affecting the contact and interactions among cells (Xia *et al.*, 2011). Optimization of the cell seeding density prior to culturing cells ensures normal cell growth and allows estimation of the time to reach certain confluency levels. In the present study, the cell seeding density of $3.0 \times 10^5$/well (*i.e.,* in ~10 $cm^2$)

was found to be more practical because it allowed sampling within 1 wk without a need for passaging the cells.

Temperature may play an important role in the efficiency of testis cell culture, but the effect of incubation temperature on the proliferation of neonatal porcine testis cells has not been well studied. In Experiment 2, testis cells were cultured at either 35 or 37 °C to mimic the testis temperature *in situ*, which is normally lower than the core body temperature, ranging 38–40 °C in pigs (Ingram and Legge, 1970; Lohse *et al.*, 2010). Testis cells cultured at either 35 or 37 °C proliferated and reached a 90% confluency within 1 wk; however, those cultured at 35 °C became 90% confluent later (5.8 vs. 6.4 d, respectively, $P < 0.05$). Earlier studies using human or mouse testis cells concluded that DNA synthesis and steroidogenesis were increased when cells were cultured at 31/32 °C, compared with 37 °C, which is the core body temperature in these species (Nakamura *et al.*, 1987; Zhou *et al.*, 2008). Although these latter studies also point to the beneficial effects of culturing testis cells at lower than core body temperature, they each examined only one such temperature, making it difficult to compare the results. Results from the present study suggest that further studies will be required to determine the optimal temperature for culturing testis cells for a given species.

The use of poly-L-lysine-coated coverslips is recommended when sampling cultured testis cells. Opposing ionic charges among the cells (polyanionic) and poly-L-lysine-coated coverslip surface (polycationic) enhance efficient attachment of cells onto the coverslips. In the present study, we showed that 1) the presence of poly-L-lysine-coated coverslips had no adverse effects on the growth of cultured testis cells; 2) cells did not grow on non-coated coverslips; and 3) there was no difference in cell viability between the cells growing on coverslips and the peripheral areas of the well. Therefore, while coverslips placed at the bottom of round plate wells provide a convenient method of sampling for analyses such as immunocytochemistry, the cells at the peripheral areas could also be used for other evaluations such as monitoring of the cell viability or use in other assays. Using coverslips also offers the advantage of allowing multiple samplings from the culture dish with minimal disturbance to other cells in the same dish/plate.

*In vivo* proliferation of gonocytes is influenced by their contact or interaction with the basement membrane of the seminiferous tubule (McGuinness and Orth, 1992). It has also been suggested

that gonocytes require the presence of feeder cells in order to settle and form colonies *in vitro* (Orth and McGuinness, 1991; Hasthorpe *et al.*, 1999; Kanatsu-Shinohara *et al.*, 2003; Nagano *et al.*, 2003; Borjigin *et al.*, 2011). In the present study, testis somatic cells formed a monolayer, which provided a platform for subsequent gonocyte attachments. It also appeared that the survival and propagation of gonocytes depended on the proper ratio of gonocytes to somatic cells. This was exemplified in Experiment 1, where we used highly enriched gonocytes (~86%) for seeding and observed no or slow cell proliferation, even when the enriched gonocytes were used at the same seeding density ($3.0 \times 10^5$/well) as heterogeneous populations of testis cells. This is in agreement with a previous study by van Dissel-Emiliani *et al.*, (1993) showing that when gonocytes were cultured alone, they failed to adhere to the culture plate and instead formed gonocyte aggregates, which were subsequently lost.

In fetal and neonatal testes, gonocytes are larger than most testis cells and one would expect that among testis cells in the suspension, gonocytes would be one of the first cells to settle. This was indeed the case for mouse fetal gonocytes showing the highest sedimentation velocity of all testis cells (van Dissel-Emiliani *et al.*, 1989). In the present study, however, gonocytes settled much later than other testis cells, and could be seen floating even after several days of culture. Goel *et al.*, (2008) examined the population of floating cells after 4 h of culturing neonatal pig testis cells and concluded that they were mostly viable (~95%) and composed of mostly germ cells (91%). In the present study, although the number of floating gonocytes decreased over time, their viability remained high (78-86%) up to 6 d after culture. The extended presence of floating gonocytes may be an advantageous characteristic if they are collected to be used for gonocyte enrichment; however, it can also be disadvantageous and lead to the loss of gonocytes during medium changes, if done without due care.

Changing of medium is important to furnish nutrients and remove waste from a culture system; however, the frequency of medium-changing may affect culture conditions. Most studies on testis cell culture use a daily, every-other-day, or twice-weekly approach to medium changing (Joffre and Roche, 1988; van Dissel-Emiliani *et al.*, 1993; Majumdar *et al.*, 1995; Goel *et al.*, 2007; Han *et al.*, 2009). In the present study, routine changing of medium (every 2 d) reduced the number of attached gonocytes, prompting us to design Experiment 6 for optimizing the medium changing regimen to increase the number of gonocyte colonies. Given our observations of the floating

gonocytes, we compared gonocyte colony formation following the routine medium changing regimen (every 2 d) with the group in which the medium was not changed for 1 wk, or with the modified medium changing regimen, where a smaller volume of medium was exchanged at a time. Compared with Day 2 (~$5.0 \times 10^3$), the number of gonocytes and gonocyte colonies increased in all regimens in subsequent days (Days 4, 6, and 7; Fig. 3.5). The increased number of gonocyte colonies on Day 4 in all groups (ranging from ~$10.0 \times 10^3$ to ~$13.5 \times 10^3$, Fig. 3.5) could be taken as evidence of gonocyte proliferation in these early days of culture. This conclusion is especially based on the plates in the routine medium changing regimen which had undergone a complete medium change. As a result, this group of plates presumably should have lost all or most of its floating gonocytes, yet there was a 2-fold increase in the number of gonocyte colonies. On the other hand, the number of gonocyte colonies in subsequent days (6 and 7) were ~50% greater in the unchanged group, compared with the routine medium changing regimen (~$18.0 \times 10^3$ vs. ~$12 \times 10^3$, respectively, Fig. 3.5). This can be seen as evidence of continued settlement of gonocytes. The number of gonocyte colonies also increased over time in all groups; this increase was ~3.3 fold for the unchanged medium group (from ~$5.4 \times 10^3$ on Day 2 to ~$18.0 \times 10^3$ on Day 7, Fig. 3.5). This fold-increase in the total number of gonocyte colonies does not take into account that the number of gonocytes within each colony also increased over time (Fig. 3.3D). Therefore, these results collectively indicate that the optimized culture conditions developed in the present study improved gonocyte colony formation.

In the present study, we systematically examined the effects of several culture conditions on testis cells of the neonatal pig, as a non-rodent animal model. After each experiment, we built upon the newly obtained results and designed subsequent experiments to make successive advances in the survival, propagation, and colony formation of gonocytes. Our results are expected to facilitate further studies aiming at, for instance, investigation of specialized media for large-scale propagation of gonocytes, as a source of MGSC. Applications for MGSC range from basic to applied research, including germ cell transplantation studies in farm animals for the purpose of animal transgenesis, genetic conservation, or infertility treatment models (Honaramooz *et al.*, 2002b, 2003b, 2008; Zeng *et al.*, 2013; Mankidy *et al.*, 2014). Germ cell transplantation can also be used as a functional assay to assess the relative abundance or confirm the developmental potential of MGSC within a given population of testis cells, including cultured gonocytes (reviewed in Honaramooz, 2012).

## 3.6 Conclusions

In conclusion, the optimized culture conditions developed in the present study included seeding neonatal porcine testis cells at $3.0 \times 10^4$ testis cells/cm$^2$ containing ~40% gonocytes in DMEM$^{++}$ at 37 $^{\circ}$C, and without changing the medium in the first week. These results can be used to improve *in vitro* maintenance, proliferation, and formation of gonocyte colonies and thereby as a basis for the development of more specialized culture systems for MGSC.

## TRANSITION

The optimized culture conditions established in Chapter 3 efficiently maintained and supported the proliferation and formation of gonocyte colonies in a short-term culture. Therefore, these optimized conditions were utilized in Chapter 4 as a basis to study the organization, behavior, and ultrastructure of neonatal porcine gonocytes in a prolonged culture.

# CHAPTER 4

# LIVE-CELL IMAGING AND ULTRASTRUCTURAL STUDY OF CULTURED PORCINE GONOCYTES [3, 4]

## 4.1 Abstract

Gonocytes in the neonatal testis have male germline stem cell potential. The objective of the present study was to examine the behavior and ultrastructure of gonocytes in culture. Neonatal porcine testis cells were cultured for 4 wk and underwent live-cell imaging to explore real-time interactions among cultured cells. This included imaging every 1 h from Day 0 to Day 3, every 2 h from Day 4 to Day 7, and every 1 h for 24 h at Days 14, 21, and 28. Samples also underwent scanning electron microscopy, transmission electron microscopy, morphometric evaluations, immunostaining, and RT-PCR. Live-cell imaging revealed an active amoeboid-like movement of gonocytes, assisted by the formation of extensive cytoplasmic projections, which under scanning electron microscopy were categorized as spike-like filopodia, leaf-like lamellipodia, membrane ruffles, and cytoplasmic blebs. In the first wk of culture, gonocytes formed loose attachments on top of a somatic-cell monolayer and in Week 2 formed grape-like clusters, which over time grew in cell number. Starting at Week 3 of culture, some of the gonocyte clusters transformed into large multinucleated embryoid body-like colonies (EBLC) that expressed both gonocyte- and pluripotent-specific markers. The number and diameter of individual gonocytes, the number and density of organelles within gonocytes, as well as the number and diameter of the EBLC increased over time ($P < 0.05$). In conclusion, cultured porcine gonocytes displayed extensive migratory behavior facilitated by their

[3] The manuscript for this study has been submitted for publication in the *Journal of Cell & Tissue Research* under joint co-authorship with Eiko Kawamura, LaRhonda Sobchishin, and Ali Honaramooz.

[4] AHAJ contributed to the conceiving and designing of the study, performed the experiments, and wrote the first draft of the manuscript.

various cytoplasmic projections, propagated, and transformed into colonies that increased in size and complexity over time.

## 4.2 Introduction

Gonocytes are a transient population of germ cells that are intermediary between the primordial germ cells (PGC) and spermatogonial stem cells (SSC) (Orwig *et al.,* 2002). Gonocytes are formed during the fetal period as a morphologically-distinct group of actively proliferating large cells (also referred to as M-gonocytes) which reside at the center of seminiferous cords. Gonocytes remain largely quiescent throughout the fetal and early postnatal periods (also referred to T1-prospermatogonia), and are the only type of germ cells present during these periods (Shinohara *et al.,* 2000). At a certain species-specific developmental stage after birth, gonocytes resume proliferation and migrate to the basal membrane of the seminiferous cords, where they become known as (T2)-prospermatogonia (McGuinness and Orth 1992). Prospermatogonia later develop into undifferentiated spermatogonia which can either commit to differentiation to initiate spermatogenesis, or to self-renewal to maintain the SSC population and ensure the continuity of the germline (Oatley and Brinster 2008; De Rooij 1998). PGC, gonocytes and especially SSC possess stem cell potential and are hence referred to as male germline stem cells (MGSC) (De Rooij and Russell 2000). The distinct morphology and unique spatial and temporal distribution of gonocytes in the neonatal testis make them more accessible for identification, isolation, and manipulation, compared with their predecessors (PGC) and successors (SSC).

Studies using gonocytes have important implications for various basic and applied settings including animal conservation, experimental and/or clinical reproductive medicine (*e.g.*, fertility preservation and restoration), as well as stem cell research and therapy. For instance, testes can be collected postmortem for genetic preservation of newborn or immature males of rare/endangered species that die prior to reaching maturity. Gonocytes within the cryopreserved testis tissues can be then used as a source of MGSC to initiate spermatogenesis and produce spermatozoa using the emerging *in vitro* and *in vivo* reproductive technologies (Honaramooz 2012; 2014). Similarly, gonocytes in cryopreserved biopsies of testis tissue can be potentially used for future restoration of fertility of prepubertal boys undergoing gonadotoxic chemotherapy or irradiation (Honaramooz 2012; 2014). The study of porcine gonocytes can also provide insights for the ongoing research on

MGSC and even as a source of multipotent stem cells (Goel *et al.,* 2009; Niu *et al.,* 2016).

Gonocytes comprise a relatively small percentage of cells in the neonatal testes (*e.g.*, ~1.4% in rats) and using conventional enzymatic digestion of the neonatal pig testis tissue only ~5-10% of freshly isolated cells were gonocytes (Honaramooz *et al.,* 2003; Herrid *et al.,* 2009; Yang and Honaramooz 2011). Therefore, the number of gonocytes would need to be increased prior to their potential use in downstream applications. We have introduced a novel three-step enzymatic digestion method that results in the isolation of neonatal porcine testis cells containing ~40% gonocytes (Yang *et al.,* 2010). We have also developed efficient methods for enrichment of neonatal porcine gonocytes to ~90%, using Nycodenz gradient density centrifugation and/or extracellular matrix differential plating techniques (Yang and Honaramooz 2011). Enrichment of gonocytes in different species has also been made possible using fluorescent or magnetic cell sorting technologies (*i.e.*, FACS and MACS) (Kubota *et al.,* 2004; Shinohara *et al.,* 2000; Shinohara *et al.,* 1999). Gonocytes possess several known surface markers (*e.g.*, DBA, UCHL1, THY1) (Zheng *et al.,* 2014; Yang *et al.,* 2010; Goel *et al.,* 2007) as well as markers that are common with both germ cells (*e.g.*, DAZL, VASA) (Castrillon *et al.,* 2000; Reijo *et al.,* 2000), and stem cells (*e.g.*, POU5F1, NANOG, SOX2, SSEA) (Wang *et al.,* 2015; Fujihara *et al.,* 2011; Goel *et al.,* 2008; Perrett *et al.,* 2008; Ohmura *et al.,* 2004; Ohbo *et al.,* 2003).

Maintenance and propagation of gonocytes have been achieved in various short-term and long-term culture systems (Lee *et al.,* 2013; Borjigin *et al.,* 2011; Goel *et al.,* 2007; Kanatsu-Shinohara *et al.,* 2003; Nagano *et al.,* 2003; Larsen *et al.,* 2002). But these culture systems vary greatly depending on the species and laboratories (Sahare *et al.,* 2016; Kubota *et al.,* 2011; Hamra *et al.,* 2005; Ryu *et al.,* 2005). For instance, the type of media used in different studies varies from basic to enriched (Sahare *et al.,* 2016; Tu *et al.,* 2007), and the media may be supplemented with serum or serum-replacements (Aponte *et al.,* 2006; Izadyar *et al.,* 2003). The addition of certain growth factors and hormones were also found to be beneficial, especially for long-term maintenance of gonocytes (Tu *et al.,* 2007; Chuma *et al.,* 2005; Kubota *et al.,* 2004; Kanatsu-Shinohara *et al.,* 2003; Larsen *et al.,* 2002). Since gonocytes show limited growth when cultured alone (van Dissel-Emiliani *et al.,* 1993), they are commonly co-cultured with other testis cells (De Miguel *et al.,* 1996; van Dissel-Emiliani *et al.,* 1996; Orth and Jester, 1995; van Dissel-Emiliani *et al.,* 1993), feeder cells (Kubota *et al.*, 2004), or in the presence of extracellular matrices (*e.g.*, gelatin, collagen,

laminin) (Sahare *et al.,* 2016; Yu *et al.,* 2005; Kanatsu-Shinohara *et al.,* 2003; Hadley *et al.,*1985). Alternative serum-free or feeder-free culture systems have also been examined (Kanatsu-Shinohara *et al.,* 2014; Aoshima *et al.,* 2013; Kanatsu-Shinohara *et al.,* 2011; Ryu *et al.,* 2005; Kubota *et al.,* 2004). Gonocytes are believed to retain their self-renewal potential in long-term cultures, and are known to form various characteristic colonies, which increase in size and density over time (Lee *et al.,* 2013; Borjigin *et al.,* 2011; Goel *et al.,* 2007; Kuijk *et al.,* 2009; Hasthorpe *et al.,* 1999; van Dissel-Emiliani *et al.,*1993).

Studies on gonocytes have predominantly used rodent models (Orwig *et al.,* 2002; van den Ham *et al.,* 1997; van Dissel-Emiliani *et al.,* 1993; McGuinness and Orth, 1992); however, the growing evidence for the potential application of gonocytes in the preservation of male fertility from young individuals has promoted further studies using large animal models (Kim *et al.,* 2014; Borjigin *et al.,* 2011) and humans (Tu *et al.*, 2007; Wu *et al.*, 2009; Altman *et al.*, 2014). Despite recent advances in the study of gonocytes, there is a lack of efficient and reproducible systems to culture and propagate gonocytes from non-rodent animal models. Development of such models is critical for understanding the cellular and molecular signature of gonocytes and for using their potential. The pig is an important non-rodent animal model for biomedical research. Recently, we studied a number of factors affecting testis cell cultures and introduced an optimized system for short-term maintenance and propagation of neonatal porcine gonocytes (Awang-Junaidi and Honaramooz, 2018). This culture system allowed the optimal growth of neonatal porcine gonocytes and resulted in significant increases in the number of gonocyte colonies after 7 days of culture. The objective of the present study was to investigate the behavior and ultrastructure of neonatal porcine gonocytes in a prolonged culture using various imaging modalities. This is an important step in enhancing our understanding of the biology of porcine gonocytes and our ability to harness their potential in a large animal model.

## 4.3 Materials and Methods

### *4.3.1 Testis Collection and Preparation*

Testes were collected from ~one-wk-old Yorkshire-cross piglets ($n$ = 40) via aseptic castration, as described in more details in Chapter 3.3.1.

### *4.3.2 Isolation of Testicular Cells*

Isolation of testicular cells was performed using a three-step enzymatic digestion method that has been established in our laboratory to yield testicular cells of ~40% gonocytes proportion (Yang *et al.,* 2010). A more detailed description of the cell isolation procedures was provided in Chapter 3.3.2.

### *4.3.3 Cell Culture*

The resultant piglet testis cells were cultured using the optimized settings and conditions that we have recently reported (Awang-Junaidi and Honaramooz, 2018) and described in Chapter 3.3.4. Briefly, the cells were cultured in 6 well-plates, at a cell seeding density of $3.0 \times 10^5$ cells/well in 3 ml DMEM, supplemented with 10% FBS and 1% antibiotics. The cells were incubated at 37 °C with 5% $CO_2$ and 95% humidity ($n$ = 6 replications). The cell culture was monitored twice daily using an inverted microscope (Nikon, Eclipse TS100), the media was changed once a week, and the cells were maintained for up to 4 wk. To facilitate sampling for fluorescent labeling, a sterile coverslip (sized 22×22 mm; catalogue no. 12-540B; Fisher Scientific) coated with 0.1% poly-L-lysine was placed at the bottom of each well in 6-well plates prior to cell seeding.

### *4.3.4 Live-Cell Imaging*

Real-time interactions of the cultured testis cells were periodically assessed throughout the 4-wk period using live-cell imaging. For this purpose, the cells were cultured in glass-bottom tissue culture dishes (FluoroDish, catalogue no: FD35-100, World Precision Instruments Inc., Sarasota, FL, USA) using the same culture conditions as described above. Throughout the study, differential interference contrast (DIC) images were taken from ten randomly-selected fields using an inverted microscope (IX83, Olympus, Tokyo, Japan), equipped with a 20× objective (Numerical Aperture/N.A. = 0.75) and a DP73 camera, every 1 h from Day 0 to Day 3, every 2 h from Day 4 to Day 7, and every 1 h for 24 h at Days 14, 21, and 28. Live-cell imaging of shorter intervals (every 2.5 s) was also performed at a higher magnification using a 100× objective (N.A. = 1.4) at three randomly-selected fields for 5 min after completion of each imaging session (*i.e.*, every day from Day 1 to Day 7 and after a full day imaging at Days 14, 21, and 28). Throughout live-cell

imaging, the cells were maintained at 37 ºC and 5% $CO_2$ in a humidified incubator fitted on the microscope stage.

### *4.3.5 Fluorescent Labeling*

Fluorescent labeling was performed using a fluorescein isothiocyanate (FITC)-labelled lectin *Dolichos biflorus* agglutinin (DBA; catalogue no. FL1031; Vector Labs, Burlington, ON, Canada) to identify gonocytes, anti-UCHL1 (also known as PGP9.5) antibody (mouse monoclonal to PGP9.5; catalogue no. ab 8189; Abcam, Toronto, ON, Canada) to validate their germ cell status, anti-POU5F1 (also known as OCT4) antibody (rabbit polyclonal to POU5F1; catalogue no. ab18976; Abcam, Toronto, ON, Canada) to evaluate their pluripotency, and phalloidin-FITC (catalogue no. P5252; Sigma-Aldrich) to visualize actin filaments. Briefly, the coverslips with cell smears (fresh after isolation) or with cultured cells (samples retrieved at Days 7, 14, 21, and 28) were fixed for 2-3 min in Bouin's solution (for DBA) or 4% paraformaldehyde solution (for POU5F1 and phalloidin). For DBA staining, the samples were rinsed three times with 70% alcohol to remove excess Bouin's, followed by three rinses with DPBS. For POU5F1, UCHL1, and phalloidin fluorescent labeling, the samples were permeabilized three times with 0.1% Triton X-100 (Omnipur; catalogue no. 9400; EMD Chemical Inc, Gibbstown, NJ, USA) in DPBS for 3 min. All samples were blocked with 5% bovine serum albumin (BSA; catalogue no. 2452C055; Amresco, Solon, OH, USA) at 37 °C for 30 min in a humidified chamber, incubated with primary antibodies (1:100 for both DBA, UCHL1, and POU5F1 at 4 °C overnight, and 1:250 for phalloidin at room temperature for 45 min), and washed three times with DPBS. The UCHL1 and POU5F1 immunostaining were further continued by incubation for 1 h at room temperature with Alexa Fluor 488-conjugated donkey anti-mouse IgG (1:200, catalogue number ab150109; Abcam) and Alexa Fluor 594-conjugated goat anti-rabbit IgG (1:500; catalogue no. ab150088; Abcam). All samples were rinsed again with DPBS and mounted using hard-set antifade mounting media containing DAPI (Vectashield; catalogue no. H-1500; Vector Labs) prior to microscopic evaluation. DAPI, FITC, and Alexa 594 were imaged sequentially using an inverted microscope with 20 and 40× (N.A. = 0.95) objectives, with a DAPI filter set (catalogue no. 49000; Chroma, Bellows Falls, VT, USA; excitation 350 nm/50 nm and emission 460 nm/50 nm), a FITC filter set (catalogue no. 49002; Chroma, excitation 470 nm/40 nm and emission 525 nm/50 nm), and a Texas Red filter set

(catalogue no. 49008; Chroma, excitation 560 nm/40 nm and emission 630 nm/75 nm), respectively.

### *4.3.6 RNA Extraction and Reverse Transcription Polymerase Chain Reaction (RT-PCR)*

Total RNA was extracted and cDNA synthesized from neonatal pig testis cells as freshly-isolated and as cultured cells at Days 7, 14, 21, and 28 using the Invitrogen ™ RNAqueous Micro Total Isolation Kit (catalogue no. AM1931; Fisher Scientific, Vilnius, Lithuania) and qScript ™ XLT cDNA Supermix (catalogue no. CA10142-784; Quanta Biosciences, Gaithersburg, MD, USA) according to the manufacturer instructions. Nucleotides 719 to 918 of the POU5F1 (OCT4) coding region were amplified using Phusion® High-Fidelity DNA polymerase (catalogue no. M0530S; New England Biolabs Inc, Ipswich, MA, USA). The forward and reverse primers for the amplification were 5'-AGA GAA AGC GGA CAA GTA-3' and 5'-ATC CTC TCG TTG CGA ATA-3', respectively. The amplified PCR products were confirmed by sequencing and running through agarose gel electrophoresis for visualization. The freshly isolated cells were used as a reference, cultured porcine mesenchymal stem cells as the positive control, and no template as the negative control.

### *4.3.7 Scanning Electron Microscopy*

Scanning electron microscopy (SEM) was performed on the cultured cells at Days 7, 14, 21, and 28. The cells were fixed by immersion in 3% glutaraldehyde (catalogue no. 014; Canemco, Gore, QC, Canada) in 0.1 M sodium cacodylate buffer, pH 7.2 (NaCAC; catalogue no. C0215; Sigma-Aldrich) for 1.5 h, followed by three rinses with the same buffer. The samples were kept at 4 °C until further processing. The samples were post-fixed with 1% osmium tetroxide (catalogue no. 19110; Electron Microscopy Sciences, Hatfield, PA, USA) for 10 min followed by three rinses with distilled water. Dehydration was performed in a series of gradient ethanol (once in 30, 50, 70, 80, 90, 95%, and twice in 100%) for 10-15 min in each step. Later, the samples underwent substitution process by immersion in gradually increasing concentrations of amyl acetate (catalogue no. 3-9094; J.T Baker Chemical Co., Philipsburg, NJ, USA) (once in 25, 50, 75%, and twice in 100% amyl acetate) for 15 min in each solution. The samples then underwent critical point drying (Polaron E3000, Quorum Technologies, Lewes, UK), sputter-coating with gold (Edwards

S150B; BOC Edwards, UK), and observation under a scanning electron microscope (SU8010; Hitachi, Tokyo, Japan).

### *4.3.8 Transmission Electron Microscopy*

For transmission electron microscopy (TEM), the cultured cells were fixed at Days 7, 14, 21, and 28 with cold (4 °C) 2% glutaraldehyde in 0.1 M sodium cacodylate buffer (pH 7.2) for 3 h, immersed in 0.1 M sodium cacodylate buffer, and stored at 4 °C overnight. Post-fixation was carried out by immersion in 1% osmium tetroxide for 1 h at room temperature, followed by a rinse with distilled water. The cells were then dehydrated in a series of gradient ethanol (50, 70, 95, and 100%, 15 min at each step), immersed in two changes of absolute ethanol, and LR White resin mix (1:1 and 1:2) for 1 h, respectively, and finally in 100% resin for 2 h. The samples were sealed and polymerized at 65 °C overnight. The polymerized samples were broken down into small pieces, blocked and sectioned at 100 nm using a Leica Ultracut UCT, and viewed under a transmission electron microscope (HT7700; Hitachi) at accelerating voltage of 80Kv.

### *4.3.9 Morphometric Evaluations*

Morphometric analyses were performed on samples taken at Days 7, 14, 21, and 28 ($n$ = 4 replications). For each replicate, ten randomly-selected fields were imaged at 100, 200, and 400× and evaluated using the cellSens imaging software (Olympus, Pittsburgh, PA, USA). Quantification of gonocytes was performed by counting the number of gonocytes at 200× in five randomly-selected fields. The average diameters (X and Y axes) of at least 150 gonocytes were assessed at 400× in each of four randomly-selected fields (*i.e.*, $n$ = >600 gonocytes). The number of EBLC and their average diameters were assessed at 100× in ten randomly-selected fields. The number of gonocytes and EBLC were expressed per $cm^{2.}$

### *4.3.10 Statistical Analyses*

All numerical data were analyzed using one-way analysis of variance (ANOVA), followed by Tukey's HSD as the post-hoc test. The data are presented as mean ± standard error of mean (SEM) and the level of significance was set at $P < 0.05$. Data were analyzed using the SPSS (Version 22.0, SPSS Inc., Armonk, NY, USA).

## 4.4 Results

### *4.4.1 Organization of Neonatal Porcine Testis Cells in Culture*

Neonatal porcine testis cells were monitored during culture using live-cell imaging and conventional phase-contrast microscopy. Based on the morphology and organization, we categorized the growth and development of the cultured cells into three main stages, (a) formation of a somatic-cell monolayer, (b) establishment of gonocyte colonies, (c) and development of embryoid body-like colonies (EBLC).

#### *4.4.1.1 Formation of Somatic-cell Monolayer*

At seeding, the cells were composed of ~60% somatic cells. Within the first 7 days of culture, somatic cells contributed to the formation of a somatic-cell monolayer. Briefly, in the first 12 h after seeding, all cells appeared rounded and remained floating in the media (Fig. 4.1A and Video 1, Appendix A). Shortly after 24 h of incubation, small numbers of cells began to settle and adhere to the bottom of the plate. These settling somatic cells (identified based on morphology and later by DBA staining exclusion) flatten down and established cytoplasmic projections, forming irregular-shaped cells (Fig. 4.1B). Over time, more somatic cells settled, expanded, and formed contacts with other cells, leading to the formation of clumps within 48-52 h of incubation (Fig. 4.1C). These somatic cell clumps later spread further, formed a large somatic-cell monolayer, and reached 70-80% confluency at ~4-5 days post-seeding. Upon confluency, the morphology of somatic cells transformed from irregular with multiple cytoplasmic projections to fibroblast-like spindle-shaped (Fig. 4.1D). In addition, starting as early as Day 5 of culture, some somatic cells formed circular arrangements (Fig. 4.1D-E). Over time, these circular arrangements became more prominent, increased in diameter, and appeared to be a preferred site for gonocytes and their colonies (Fig. 4.1G-I).

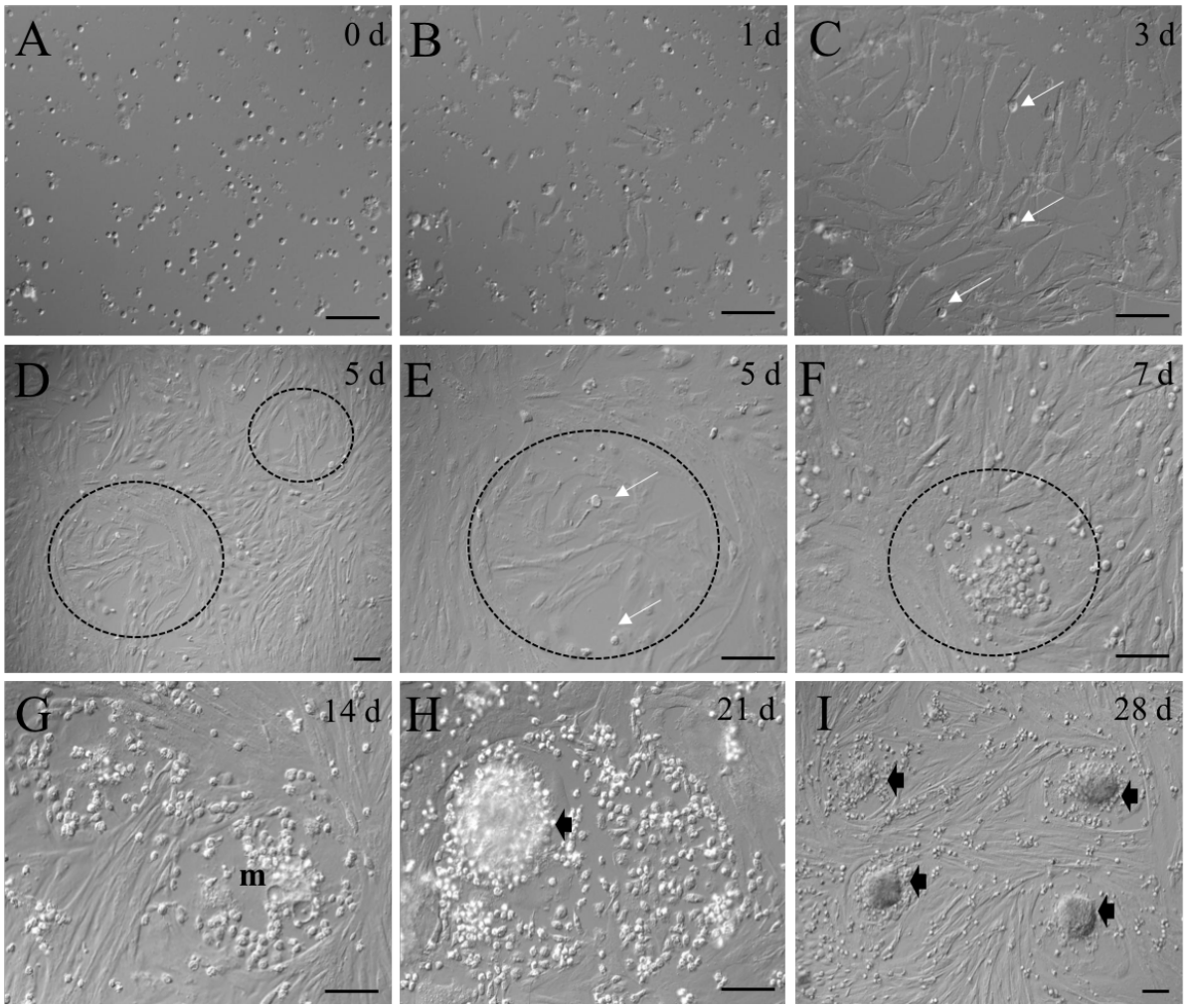


**Fig. 4.1.** Representative images showing the organization of neonatal porcine testis cells in culture over time. (A) A single-cell suspension of testis cells immediately after seeding. (B-D) Somatic cells quickly settled and adhered to the plate and then gradually expanded their cytoplasmic projections, forming a somatic-cell monolayer and becoming confluent. (E) Gonocytes (white arrows) settled on top of the somatic-cell monolayer, and (E-I) their numbers increased over time to form gonocyte colonies. (D-F) Note the organization of somatic cells into circular arrangements (CAs, some denoted by dotted circles). (F-I) The CAs appeared to be preferred sites for gonocyte cluster- and colony formations. (G) As the number of gonocytes in the culture increased, morula-like colonies were formed (**m**). (H) A morula-like colony has transformed into an embryoid body-like colony (EBLC, black arrow). (I) Multiple EBLC, each within a CA, are seen surrounded by many migrating gonocytes. (Scale bar: 50 μm (A-H) and 100 μm (I))

#### *4.4.1.2 Establishment of Gonocyte Colonies*

While the population of somatic cells started settling as early as 24 h post-seeding, gonocytes continued to float and settled down after the somatic-cell clumps or monolayer had been established. Over time, as more gonocytes settled on the somatic-cell monolayer, the number of floating gonocytes in the media decreased ($P < 0.001$; Day 2: $6.94 \pm 0.3 \times 10^4$ gonocytes/well with 84.1% ± 1.2 viability; Day 3: $3.75 \pm 0.4\ 10^4$ gonocytes/well with 72.5% ± 2.0 viability; Day 6: $1.9 \pm 0.1 \times 10^4$ gonocytes/well with 69.3% ± 1.5 viability; $n = 5$ replications). When live cell imaging was performed, an active amoeboid-like movement of gonocytes assisted by their extensive cytoplasm projections was evident (Fig. 4.2 and Video 2, Appendix A).

Once gonocytes started settling down within 48 h post-seeding, they formed loose attachments to the somatic-cell clumps and later to the somatic-cell monolayer. Morphology of the settled gonocytes changed over time. Gonocytes began losing their distinctive round shape (seen after isolation and for several hours after seeding) and started forming pseudopod-like cytoplasmic extensions. Some gonocytes, especially those that remained floating and/or failed to attach to somatic cells maintained their round morphology. Shortly after settling, gonocytes were present as singles or pairs (Fig. 4.3A), and after ~5-7 days started to also form grape-like clusters (Fig. 4.3B). During Wk 2 of culture, the grape-like clusters became more prevalent, and beginning at Wk 3, the number and diameter of grape-like clusters increased, and some clusters transformed into large morula-like colonies (Fig. 4.3C), and gradually into larger dome-shaped masses, which we termed embryoid body-like colonies (EBLC) (Fig. 4.3D). Using live-cell imaging, we documented the active process of gonocyte colony formation in real-time (Video 3, Appendix A). We observed that some gonocytes migrated toward others, forming a cluster of gonocytes, which gradually grew in size and led to the formation of larger colonies. There seemed to be a tendency for gonocytes to migrate to the center of circular arrangements formed by the somatic-cell monolayer, where they formed gonocyte clusters and colonies.

#### *4.4.1.3 Development of Embryoid Body-Like Colonies*

The transformation from morula-like colonies to EBLC was more noticeable beginning at 3 wk of culture. EBLC were characterized as large round colonies with a dome-shaped appearance and

extensive cytoplasmic projections (Fig. 4.3D-F). Under phase-contrast microscopy, EBLC exhibited a light brown appearance, which was different from the bright appearance of the earlier stage colonies and clusters. Migration of the surrounding single gonocytes towards the EBLC resulted in their joining the colony to form a multinucleated core in the EBLC (Fig. 4.3D-F). These large colonies also possessed extensive cytoplasmic projections with pulsatile outward and inward movements. The real-time live-cell observations suggested that the formation of EBLC occurs via a cell fusion process, where the migrating gonocytes approach the margin of EBLC and either anchor their cytoplasmic projections to EBLC or become entrapped by the extensive EBLC cytoplasmic projections (Fig. 4.3E).

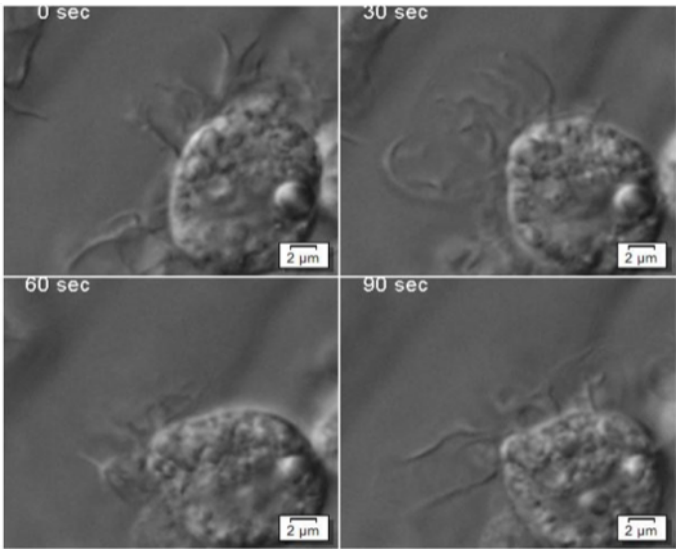


**Fig. 4.2.** Representative serial images, taken every 30 seconds (sec), from a single porcine gonocyte in culture. Sequential images depict the active movement of the cytoplasmic extensions and the changes in shape of the gonocyte over time. (Scale bar: 2 μm).

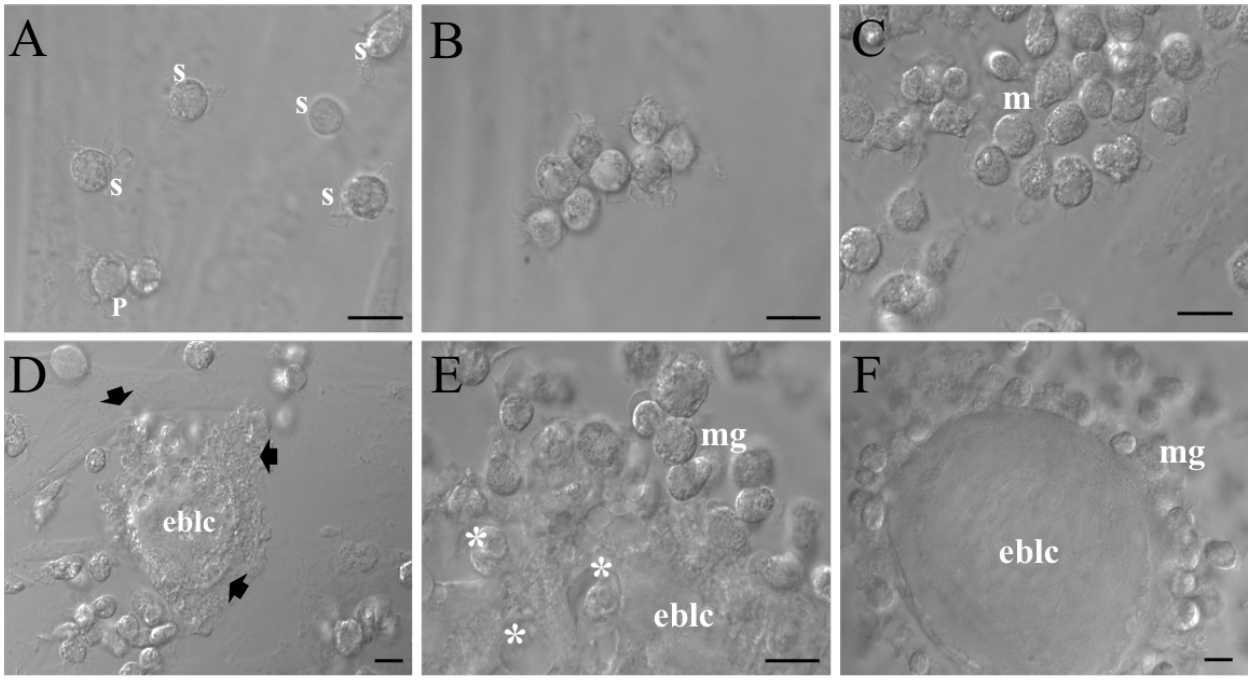


**Fig. 4.3.** Higher magnification images of neonatal porcine gonocytes in culture showing the transition to form an embryoid body-like colony (EBLC). (A) Gonocytes settled on the somatic-cell monolayer as singles (**s**) or pairs (**p**). (B) Gonocytes later formed grape-like clusters. (C) The number of gonocytes within a cluster increased over time and some formed morula-like colonies (**m**). (D) After ~14 d of culture, EBCLs (**eblc**) started to be formed. Note the presence of extensive cytoplasmic projections (black arrows) out of the EBLC which seemed to assist with their movement and attachment of migrating gonocytes. (E) Cytoplasmic fusion (∗) of adjacent gonocytes seemed to transform a morula-like colony into an EBLC. (F) Continued fusion of additional migrating gonocytes (**mg**) increased the mass of the EBLC. (Scale bar: 20 μm).

### *4.4.2 Morphometric Evaluations*

The data on the number and diameter of individual gonocytes throughout the study are summarized in Figure 4. The number of gonocytes increased over time in culture ($P < 0.001$, $n = 4$ replications) (Fig. 4.4A). Compared with Day 7 after incubation ($1.38 \pm 0.22 \times 10^4$ gonocytes/cm$^2$), the number of gonocytes increased 5.3 fold at Day 14 ($7.32 \pm 0.55 \times 10^4$ gonocytes/cm$^2$), 7.9 fold at Day 21 ($10.99 \pm 0.93 \times 10^4$ gonocytes/cm$^2$), and 8.5 fold at Day 28 ($11.74 \pm 0.64 \times 10^4$ gonocytes/cm$^2$). The size of individual gonocytes also increased over time in culture ($P < 0.001$, Fig. 4.4B). The average diameter of gonocytes was $13.37 \pm 0.11$ μm at Day 7 (ranged 10.19-19.08 μm), $14.10 \pm 0.13$ μm at Day 14 (ranged 10.29-24.05 μm), $14.36 \pm 0.89$ μm at Day 21 (ranged 10.88-20.27 μm), and $14.53 \pm 0.80$ μm at Day 28 (ranged 11.41-18.17 μm) (Fig. 4B).

The data on the number and diameter of EBLC are summarized in Table 4.1. No EBLC were yet formed at Day 7 of culture, while both the number and diameter of EBLC increased ($P < 0.001$, $n = 4$ replications) from Day 14 to Day 21 ($P < 0.05$), and remained unchanged to Day 28 (end of study). Overall, the majority of the EBLC observed at Day 14 were <100 μm in diameter, while ~70% of the EBLC at Day 21, and ~75% of the EBLC at Day 28 were >100 μm in diameter (Table 4.1).

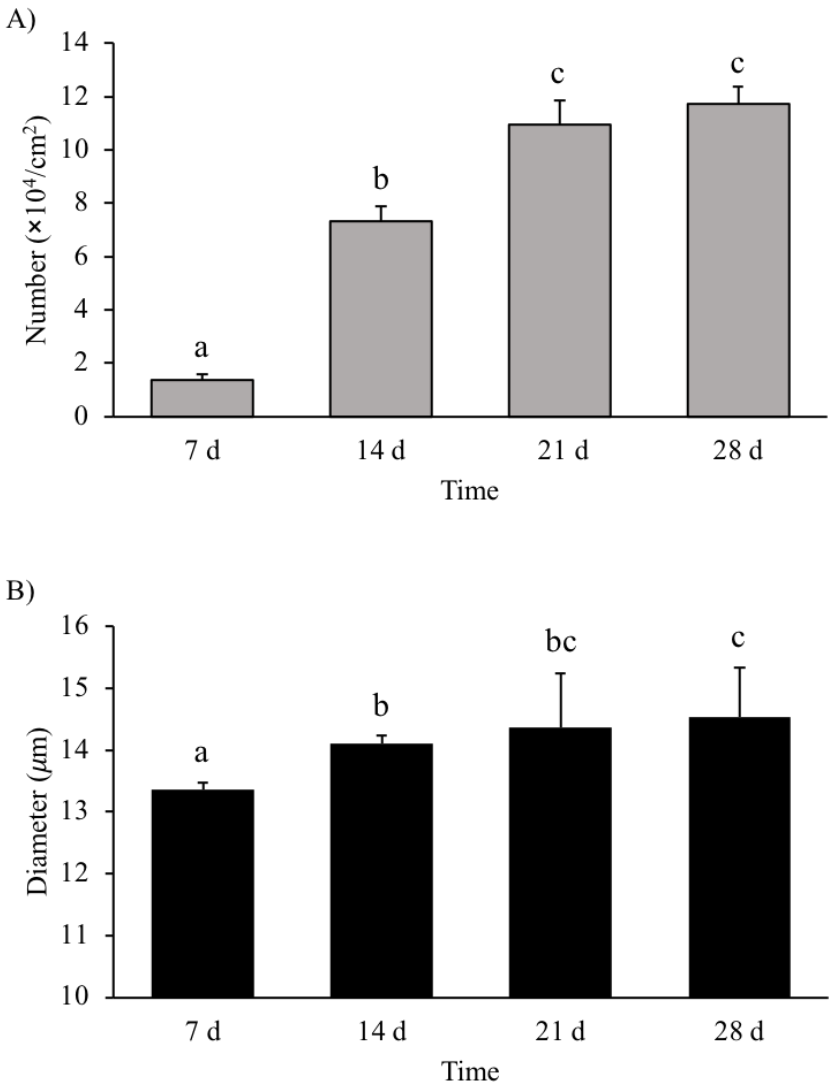


**Fig. 4.4.** Changes in the number (A) and diameter (B) of cultured porcine gonocytes over time. The data are presented as mean ± SEM. In each graph, columns with different letters differ significantly over time ($P < 0.05$).

**Table 4.1.** Changes in the number and diameter of embryoid body-like colonies (EBLC) over time.

| Time | Number of EBLC/cm$^2$ | Diameter (μm) | Diameter range (μm) | Percentage of EBLC in each diameter category (%) | | | |
|---|---|---|---|---|---|---|---|
| | | | | ≤ 99 | 100 –149 | 150 –199 | ≥ 200 |
| Day 14 | 273 ± 13.6[a] | 96 ± 1.7[a] | 59 – 167 | 58 ± 5.6 | 41 ± 5.4 | 0.1 ± 0.0 | – |
| Day 21 | 403 ± 10.1[b] | 127 ± 2.4[b] | 53 – 237 | 31 ± 3.5 | 41 ± 3.3 | 21 ± 2.6 | 7 ± 2.2 |
| Day 28 | 413 ± 9.2[b] | 131 ± 2.5[b] | 58 – 236 | 26 ± 2.7 | 43 ± 1.7 | 25 ± 1.1 | 6 ± 0.6 |

Data are mean ± SEM.
EBLC had not yet been formed at 7 d post-seeding; therefore, no data are shown for Day 7.
[ab] Within the columns for number of EBLC and diameter, values with different superscripts differ significantly ($P < 0.05$). $n = 4$ replications.

### *4.4.3 Fluorescent Labeling*

Gonocytes were identified using FITC-conjugated DBA staining as shown in Figure 5A-D. DBA-labeled gonocytes were consistently observed for the duration of the study (4 wk). DBA stained the surface and to some degree the cytoplasm of gonocytes. Expression of POU5F1 (OCT4) as a pluripotency marker was also detected for the duration of the study in both nuclear and cytoplasmic compartments of gonocytes (Fig. 4.5E-H). Gonocytes and EBLC also stained positive with phalloidin fluorescent labeling, localized in the cytoplasm (cytoplasmic projections), indicating the presence of actin filaments (F-actin) cytoskeleton (Fig. 4.5I-L).

### *4.4.4 PCR Analysis*

The expression of POU5F1 was observed in the porcine neonatal testis cells cultured at Days 7, 14, 21, and 28, but was absent in the freshly isolated cells (Fig. 4.6). The amplified region of POU5F1 also showed expression in the cultured porcine mesenchymal stem cells (as a positive control). In addition to the analysis by gel electrophoresis, amplicons were confirmed by sequencing.

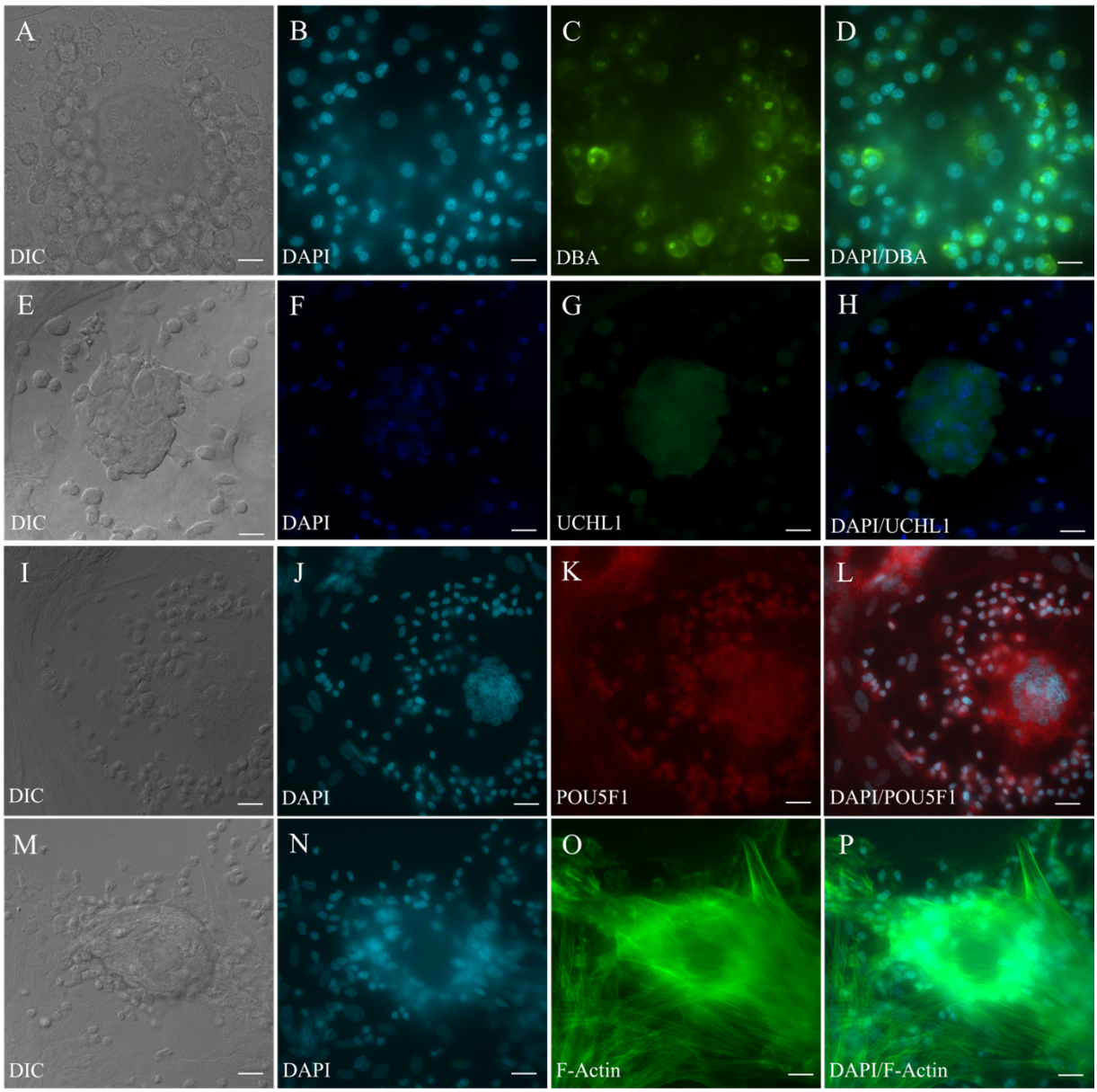


**Fig. 4.5.** Fluorescent labeling of embryoid body-like colonies (EBLC) formed in the cultures of neonatal porcine testis cells. (A-D) Fluorescent labeling using *Dolichos biflorus* agglutinin (DBA), as a gonocyte marker. (E-H) Fluorescent labeling using UCHL1, as a germline stem cell marker. (I-L) Fluorescent labeling using POU5F1, as a pluripotency marker. (M-P) Identification of actin filaments (F-actin) in cytoplasmic projections (lamellipodia) of an EBLC using phalloidin fluorescent labeling. (A, E, I, M) Differential interference contrast (DIC) images. (B, F, J, N) DAPI-stained nuclei of the cells appear blue under the fluorescence microscope. (C, G, K, O) Fluorescein-conjugated DBA-positive gonocytes and fluorescein-conjugated phalloidin-positive F-actin appear green. (D, H, L) Merged images (Scale bar: 20 μm).

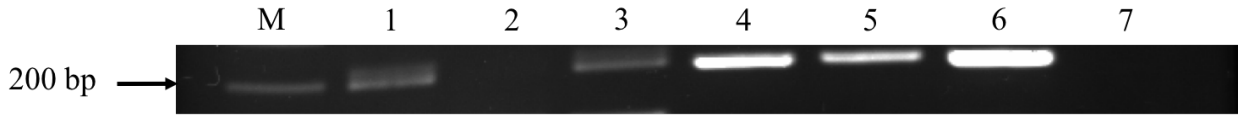


**Fig. 4.6.** Expression of the pluripotency marker POU5F1 (OCT-4) in cultured porcine testis cells. M: 100 bp molecular-weight marker; Lane 1: DNA samples from cultured porcine mesenchymal stem cells (positive control); Lane 2: DNA samples from freshly isolated porcine neonatal testis cells obtained after a 3-step enzymatic digestion (containing ~40% gonocytes); Lane 3 to 6; DNA samples from porcine neonatal testis cells cultured for 7, 14, 21, and 28 days, respectively; 7 no template control (negative control).

### *4.4.5 Ultrastructure of Gonocyte Colonies*

SEM and TEM of cultured cells were performed on samples taken at weekly intervals and the results were as follows:

#### *4.4.5.1 SEM*

Figure 6 contains representative SEM images that show in more detail the circular arrangements formed by somatic cells and provides visualization of the 3-dimensional (3-D) structure of different formations of gonocyte clusters and colonies. Individual gonocytes varied in shape from rounded to flattened (Fig. 4.7B). Round gonocytes that lacked cytoplasmic projections under live-cell imaging had a smooth surface under SEM. More importantly, SEM images showed the various forms of cytoplasmic projections of individual gonocytes, clusters, morula-like colonies, and EBLC. These cytoplasmic projections could be categorized into spike-like filopodia, leaf-like lamellipodia, membrane ruffles, and cytoplasmic blebs (Fig. 4.7B). However, as the colonies turned into EBLC, lamellipodia appeared as the most prevalent cytoplasmic projection (Fig. 4.7E). Higher magnification of the marginal areas where single gonocytes were closely attached to the EBLC showed extensive finger-like projections (Fig. 4.7G-H).

#### *4.4.5.2 TEM*

Representative TEM images of the cultured testis cells are shown in Figure 4.8. Gonocytes contained a prominent nucleus with euchromatin and heterochromatin; the latter mainly concentrated near the nuclear membrane. While the spongy-like nucleolus showed no defined membranes, the nuclear membrane was prominent with its double-layered structure (inner and outer membranes, separated by the perinuclear space) and nuclear pores (Fig. 4.8B). The nuclei of gonocytes were frequently observed in close proximity to their attachment to the somatic-cell monolayer. Where gonocytes were apposed to the somatic-cell monolayer, a certain gap was maintained (Fig. 4.8F). Closer examination of the cytoplasmic projections showed no evidence of microtubules. The organelle complexity of gonocytes seemed to increase over time. In Wk 1 samples, where gonocytes were mostly present as single cells, the organelles consisted mainly of mitochondria and rough endoplasmic reticulum (Fig. 4.8A). In samples from the following weeks when gonocytes established contacts with each other, increasing numbers of the Golgi apparatus

with vesicles, vacuole-like structures, and secretory granules were also observed, creating a dense cytoplasm (Fig. 4.8C-D). TEM examination of the EBLC cross-sections also validated the multinucleated nature of EBLC, presumed from live-cell imaging and immunostaining (Fig. 4.8E).

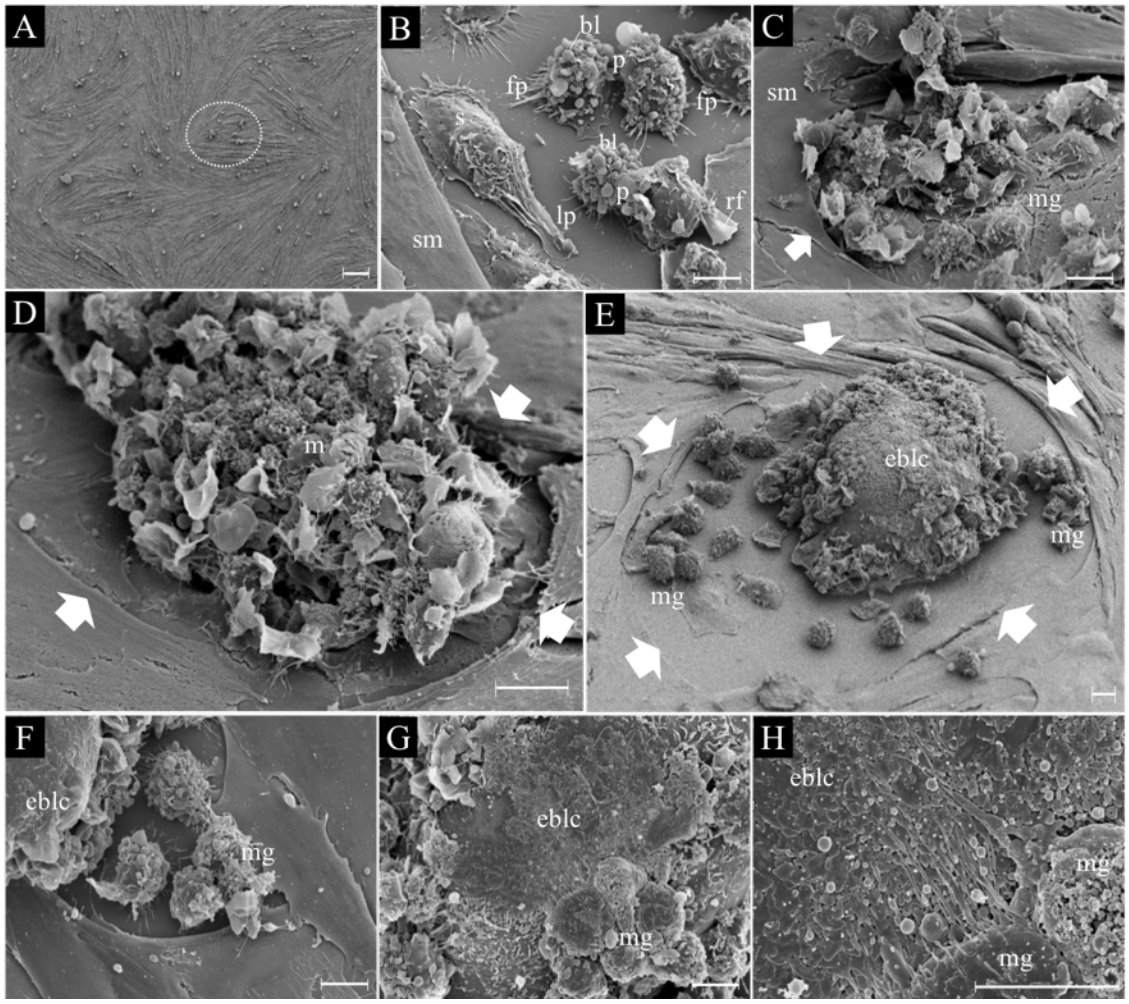


**Fig. 4.7.** Representative scanning electron microscopy (SEM) images of neonatal porcine gonocytes in culture showing the formation of embryoid body-like colonies (EBLC). (A) Gonocytes (few highlighted in a dotted circle) seen on top of the somatic-cell monolayer. (B) Within the first week after cell seeding, gonocytes were present as singles (**s**) or pairs (**p**) on the somatic-cell monolayer (**sm**). At this magnification, gonocyte cytoplasmic projections could be differentiated into spike-like filopodia (**fp**), leaf-like lamellipodia (**lp**), membrane ruffles (**rf**), and cytoplasmic blebs (**bl**). (C) Some migrating gonocytes (**mg**) formed a cluster and (D) their continued increase in numbers formed a morula-like colony (**m**). (E) Over time, the morula-like colonies transformed into EBLC (**eblc**). (C-F) Gonocytes and their colonies were primarily seen within circular arrangements (white arrows) formed by the somatic-cell monolayer. (F) A few individual gonocytes with various types of cytoplasmic projections are shown next to an EBLC with only lamellipodia. (G-H) Higher magnification images of the interface where individual gonocytes are fused with an EBLC show numerous and extensive finger-like projections (Scale bar: 100 μm (A) and 10μm (B-H)).

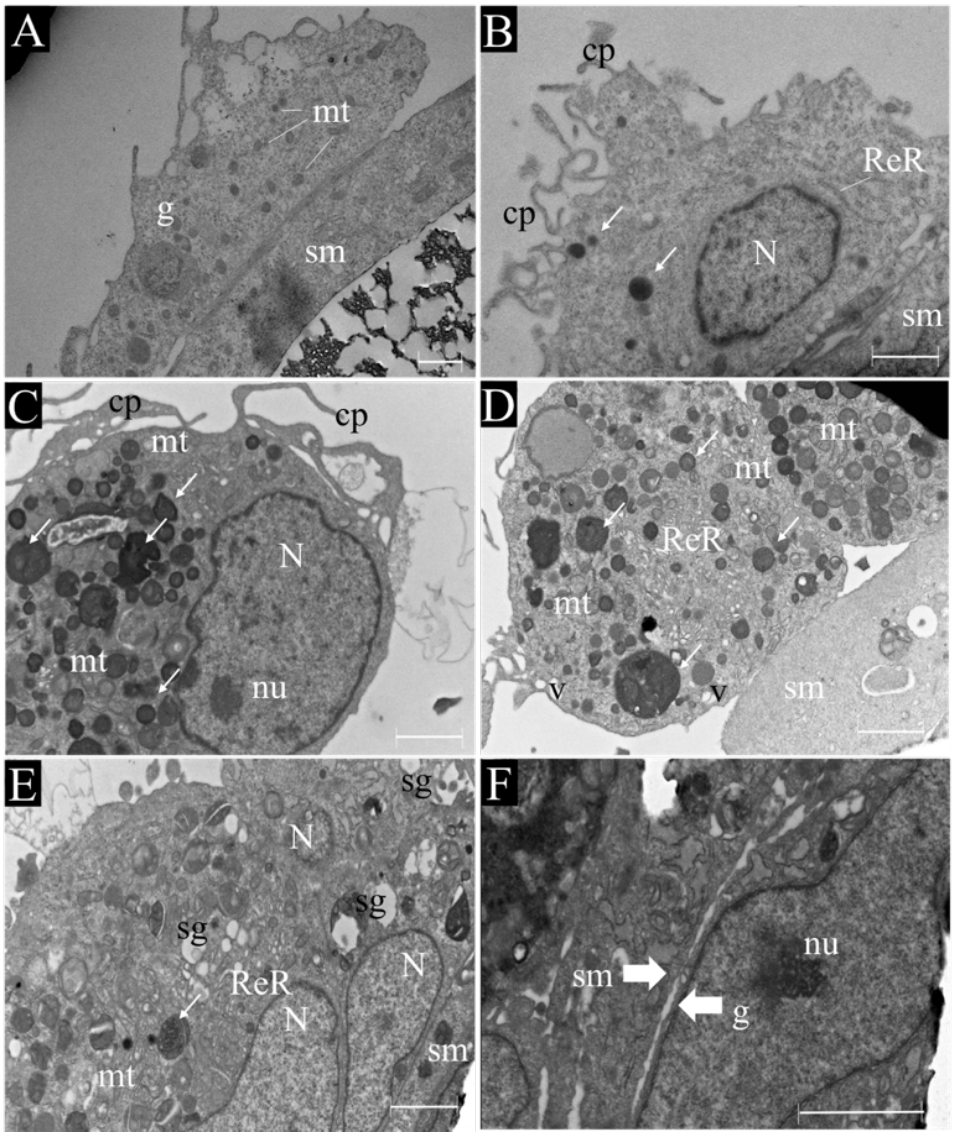


**Fig. 4.8.** Representative transmission electron microscopy (TEM) images of neonatal porcine gonocytes in culture. (A) Cross-section of a gonocyte (**g**) shown on top of a somatic-cell monolayer (**sm**). (B) A gonocyte at a higher magnification with extensive cytoplasmic projections (**cp**) and lysosomes (arrows). Also note the euchromatic and heterochromatic zones of the nucleus (**N**). (A,B) Organelles such as mitochondria (**mt**) and rough endoplasmic reticulum (**ReR**) are evident. (C) After 2 wk of culture, the number and density of cytoplasmic organelles in gonocytes were increased. The spongy appearance of the nucleolus (**nu**) is also shown. (D) Also shown are the cross-section of two adjacent gonocytes in a morula-like colony, and (E) cross-section of an embryoid body-like colony showing multiple nuclei (**N**) and the absence of a distinct border separating gonocytes. Numerous secretory granules (**sg**) are also observed. (F) Higher magnification of the interface between a gonocyte and the somatic-cell monolayer (thick arrows) shows a constant gap is maintained (Scale bar: 2 μm).

## 4.5 Discussion

Porcine testis cells have been cultured using various short-term and long-term systems that have mainly focused on their maintenance and propagation (Goel *et al.,* 2007; Han *et al.*, 2009; Lee *et al.,* 2013; Zheng *et al.,* 2014; Awang-Junaidi and Honaramooz 2018). To our knowledge, the present study is the first report on the behavior of cultured porcine testis cells using live-cell imaging. This is also the first study reporting on the ultrastructure of porcine gonocytes and their colonies. Previous studies on the ultrastructure of testis cells were conducted on tissue samples (Baillie 1964; Gondos and Hobel 1971; Tiptanavattana *et al.,* 2015). In a recent study, we examined a number of factors that could affect the maintenance, proliferation, and colony formation of porcine gonocytes in a short-term culture (*i.e.*, 7 days). The examined factors included the effects of using different cell densities, gonocyte proportions, incubation temperatures, sampling effects, and media changing regimens. We concluded that seeding of $3.0 \times 10^4/cm^2$ of neonatal porcine testis cells, containing ~40% gonocytes, culturing at 37 °C, and without changing the media in the first week, can result in improved colony formation of porcine gonocytes (Awang-Junaidi and Honaramooz 2018). Therefore, these optimized culture conditions for short-term culture were also used in the present study for a prolonged culture.

In the present study, gonocytes proliferated and formed clusters and colonies, including EBLC; the number of gonocytes increased ~8.5 fold between Days 7 and 28. This fold increase, in fact, underestimates the total increases in gonocyte numbers because our counting was based on a fixed focal plane immediately above the somatic-cell monolayer and, therefore, excluded gonocytes that formed the bulk of EBLC and gonocytes floating in different focal planes. The importance of gonocyte proliferation and EBLC formation in the present study is highlighted when considering that the culture media was basic; comprising only of DMEM+10% FBS, without additional growth factors or hormones. FBS-enriched media alone was deemed sufficient in allowing rat gonocytes to initiate growth (Hasthorpe *et al.,* 1999; Hasthorpe *et al.,* 2000). However, the formation of ES-like cells and/or colonies from the neonatal and/or adult testes of mice, humans, and pigs required stem cell-specific media or supplementation with various growth factors (*e.g.*, LIF, GDNF), which carry safety concerns over their use in potential cell replacement therapies (reviewed in Goel and Imai 2011; Hermann and Orwig 2011).

Gonocytes are considered non-adherent to glass or plastic, making their culture as a pure population a challenge (van Dissel-Emiliani *et al.,* 1993), requiring co-culture with supporting/feeder cells to improve survival and proliferation (De Miguel *et al.,* 1996; McGuinness and Orth 1992; van Dissel-Emiliani *et al.,* 1993). In the present study, the population of testis cells at seeding contained ~60% somatic cells, which led to the establishment of a somatic-cell monolayer acting as feeder cells to support proliferation and colony formation of gonocytes. Our results, therefore, differ from studies using the rat model that concluded the somatic-cell underlay had no enhancing effects or even had inhibitory effects on gonocyte colony formation (Hasthorpe *et al.,* 2000; Hasthorpe 2003; Orth and Boehm 1990).

Sertoli cells promote *in vitro* survival of gonocytes by establishing specific contacts with gonocytes, even in the presence of other testis somatic cells (van Dissel-Emiliani *et al.,* 1993). Rat Sertoli cells were reported to became senescent after 20-24 days in culture (Buzzard *et al.,* 2002). In the present study, the cultured testis cells were not passaged, and somatic cells were allowed to continue growing, forming a monolayer which became confluent in about a week, after which time their growth slowed. Not having to passage the cells was convenient and avoided disruption of gonocyte colony formation or their potential loss during passaging. Co-culturing gonocytes with their somatic cell counterparts (from the same donor) can be advantageous in preventing cross-contamination with xenogeneic cells, pathogens, or metabolites, which may arise from the use of established feeder cell lines (frequently originating from other species such as mice; Llames *et al.,* 2015).

We observed the formation of circular arrangements by the somatic-cell monolayer, which commonly coincided with gonocyte colony formations. A similar arrangement has been described when enriched populations of rat Sertoli cells were cultured on extracellular matrix-containing gels, indicating that it was driven by interactions amongst Sertoli cells (Hadley *et al.,* 1985). However, to our knowledge, Sertoli cell circular arrangements becoming a preferred site for gonocytes colonies *in vitro* has not been described. We have previously reported that when neonatal testis cell suspensions were implanted under the back skin of immunodeficient mice, they showed an unexpected ability to regenerate functional testis tissue *de novo*. Within a few days after implantation, extensive cellular rearrangements were evident, and by the second week post-implantation, seminiferous cords were fully formed and housed gonocytes in their center.

Continued development of the implanted cells eventually led to the formation of a regenerated testis tissue capable of producing androgens, differentiating germ cells, and even spermatozoa (Arregui *et al.,* 2008; Honaramooz *et al.,* 2007). Therefore, it may be postulated that the observed somatic cell circular arrangements in the present study were formed as a result of an innate tendency of testis somatic cells to organize themselves in such a way to enclose gonocytes. While an *in vivo* culture system allows the implanted cells to move more freely to form 3-D seminiferous cords, the *in vitro* culture system is understandably more limited to 2-D formations.

In the present study, in addition to gonocytes typically showing cytoplasmic projections (pseudopodia), we observed a smaller population of gonocytes that lacked cytoplasmic projections and displayed a round shape with a smooth surface. The morphology of gonocytes has been related to their potential fate in the spermatogenic lineage. When rat gonocytes with or without pseudopodia were transplanted into the testes of infertile recipient mice, only the gonocytes with pseudopodia had the competency to initiate donor-derived colonies of spermatogenesis (Orwig *et al.,* 2002). In the developing testis, gonocytes migrate from the center to the periphery of the seminiferous cords, via amoeboid movements and this migratory event is believed to be crucial for gonocyte survival, since their failure to move to the periphery results in apoptosis (McGuinness and Orth 1992; Nagano *et al.,* 2000; Orwig *et al.,* 2002). Therefore, in the present study, gonocytes with pseudopodia that were observed to be motile and later developed other cytoplasmic projections may represent the functional population of gonocytes, while those lacking pseudopodia likely represent the apoptotic or dead gonocytes. This conclusion also highlights the importance of the present study in examining gonocyte cytoplasmic projections and migratory behavior.

In the present study, we also documented that cytoplasmic projections assisted gonocytes in their movement/migration, and later contributed to their formation of colonies. Our phalloidin fluorescent labeling confirmed that these cytoplasmic projections were composed of a dense and dynamic actin meshwork. Polymerization (via ATP hydrolysis) of the actin meshwork has been shown to induce protrusions (continuous growth of actin filaments) towards the leading edge, which along with retraction of the rear end, results in cell movement (Korn *et al.,* 1987; Lauffenburger and Horwitz 1996). Our TEM observations revealed the presence of a constant gap at the interface between the basolateral membrane of gonocytes and the somatic-cell monolayer. The continuous movement of gonocytes on top of the somatic-cell monolayer, documented by our

real-time imaging of live cultured cells, may explain the need for such a constant gap between gonocytes and somatic cells.

In the present study, gonocytes proliferated to form clusters, morulae-like colonies, and EBLC. The formation of germ cell colonies by cultured testis cells has been reported for different species (Goel *et al.,* 2007; Kuijk *et al.,* 2009; Hasthorpe *et al.,* 1999; van Dissel-Emiliani *et al.,* 1993; Lee *et al.,* 2013), which at times formed 3-D structures that resembled embryoid bodies typical of those made by pluripotent embryonic stem (ES) cells when cultured *in vitro* (Sahare et al 2016; Bratt-Leal *et al.,* 2009). Given the great therapeutic potential of pluripotent stem cells, extensive research is underway mainly using either ES cells or induced pluripotent stem cells (iPSC); although significant ethical concerns and carcinogenic risks have limited their clinical application. This further highlights the importance of research on MGSC, including gonocytes, as a potential alternative source of multipotent stem cells.

Using fluorescent labeling and RT-PCR, we confirmed that EBLC maintained both their primitive germ cell status (positive for DBA and UCHL1, a gonocyte marker) and stem cell characteristics (expressed POU5F/OCT4, a pluripotency marker). This is an important finding because unlike in all previous studies, the EBLC in our study were spontaneously formed in a simple media. Therefore, our results are also of interest for the field of therapeutic potential of pluripotent stem cells. This is because the use of additional growth factors in culture of these cells can carry carcinogenic risks which would limit their clinical application. The exact mechanism of EBLC formation in the present study is not clear. The formation of embryoid bodies has been shown to occur via cell-to-cell adhesion receptors, involving hemophilic binding of E-cadherin, which is highly expressed in undifferentiated embryonic stem cells (Dang *et al.,* 2004; Dasgupta *et al.,* 2005; Fok and Zandstra 2005; Kurosawa 2007; Park *et al.,* 2003). This mechanism may explain our live-cell observations in which gonocytes established contacts with each other, leading to their aggregation and creating a center for attraction of more gonocytes to form larger colonies and ultimately EBLC.

In the present study, POU5F1 (OCT4) expression was observed in all weekly samples of cultured cells, but was absent in the freshly isolated cells, consistent with a previous report using neonatal pig testis cells (Goel *et al.,* 2008). In humans, downregulation of POU5F1 during the fetal to

neonatal transition has been associated with differentiation of gonocytes into more advanced germ cell stages (Rajpert-De Meyts *et al.,* 2004). On the other hands, POU5F1 expression in PGP9.5-positive cultured neonatal porcine gonocytes (from 5-day old donors) and in more advanced spermatogonia (from 10 wk old donors) suggested that POU5F1 is upregulated in the culture environment (Lee *et al.,* 2013; Luo *et al.,* 2006). The expression of POU5F1 is deemed crucial for the survival, self-renewal, and pluripotency of male germline stem cells *in vitro*, as shown in studies involving mouse spermatogonia (Pesce *et al.,* 1993; Dann *et al.,* 2008). Transplantation of cultured porcine gonocytes expressing POU5F1, as well as other stem cell markers such as NANOG, PLZF, and THY1 into the testes of immunodeficient recipient mice has been shown to result in successful colonization at the basement membrane of the seminiferous tubules (Lee *et al.,* 2013). The ability to induce functional pluripotent male germline stem cells *in vitro* would have important cell-based therapy applications.

In the present study, using live-cell imaging and TEM, we also found that gonocyte-derived EBLC are multinucleated structures, where multiple gonocytes share a cytoplasm. There are no closely related comparable observations to compare with our results. In human testis tissue, the presence of multinucleated germ cells (*e.g.*, spermatogonia and spermatocytes), occurring via cell-to-cell fusion has been associated with senescent of seminiferous tubule epithelium or pathological conditions (Miething 1993; 1995). These multinucleated germ cells usually degenerate, in contrast to EBLC in our culture which demonstrated increased diameters to 4 wk (end of study).

In the present study, we also found that over time gonocytes increased in size and underwent complex transformations at the subcellular levels. There are no published reports on the size of gonocytes in culture to compare with our observations. Increases in cell volume and size *in vitro* have been associated with aging (Cristofalo and Kritchevsky 1969; Schneider and Fowlkes 1976; Schneider and Mitsui 1976; Yang *et al.,* 2011). Aging cells have a low proliferative capability, and large size cells have been shown to have a shorter lifespan (Bowman *et al.,* 1975; Zadrag-Tecza *et al.,* 2009). However, all of these conclusions are derived from studies involving mammalian somatic cells, mostly fibroblasts. Stem cells are known to be capable of long-term and sustained self-renewal. Gonocytes have been successfully maintained and propagated in long-term culture (3-5 months) in an enriched system (Kanatsu-Shinohara *et al.,* 2003; Jeong *et al.,* 2003). Considering that gonocytes in the present study were kept for only 4 wk and were mitotically active,

these morphological transformations are unlikely to be indicative of aging or degenerative changes. We also speculate that the increased size of gonocytes was likely due to their tendency to elongate, flatten, and spread their cytoplasm during migration.

## 4.6 Conclusions

In conclusion, live-cell imaging allowed non-invasive monitoring of neonatal porcine testis cells *in vitro*. Gonocytes migrated freely atop the somatic-cell monolayer, assisted by the presence of various cytoplasmic projection, delineated through SEM imaging. Gonocytes gradually established clusters and colonies, which increased in size and complexity over time, and some transformed into EBLC where a number of gonocytes shared a cytoplasm. These observations demonstrated remarkable migratory behavior and colony formation of neonatal porcine gonocytes in culture.

## TRANSITION

The results of live-cell imaging and electron microscopy in Chapter 4 allowed detailed study of neonatal porcine gonocytes and their colony-formation patterns in an *in vitro* culture system. Having addressed our primary objectives related to the study of testis cells *in vitro* in Chapters 3 and 4, we designed the experiments in Chapter 5 to expand our study of testis cells by examining their potential for *de novo* formation of testis tissue after implantation in recipient mice, as an *in vivo* culture system.

# CHAPTER 5

# EFFECTS OF MULTIPLE FACTORS ON REGENERATION OF TESTIS TISSUE AFTER ECTOPIC IMPLANTATION OF PORCINE TESTIS CELL AGGREGATES IN MICE: IMPROVED OUTCOMES CONSISTENCY AND *IN SITU* MONITORING [5, 6]

## 5.1 Abstract

Ectopic implantation of donor testis cell aggregates in recipient mice results in *de novo* formation/regeneration of testis tissue, and as such provides a unique *in vivo* model for the study of testis development. However, the results are inconsistent, and the efficiency of the model remains low. This study was designed to 1) examine several factors that can potentially improve the consistency and efficiency of this model, and 2) explore the use of ultrasound biomicroscopy (UBM) for the non-invasive *in vivo* evaluation of implants. Testis cell aggregates, containing ~40% gonocytes from 1-wk old donor piglet, were implanted under the back skin of immunodeficient mice through skin incisions and using gel matrices or through subcutaneous injections and without using gel matrices. The addition of gel matrices led to inconsistent tissue development, where the outcomes were dependent on the gel type; gelatin had the greatest development, followed by collagen, and agarose resulted in poor development. The results also depended on the implanted cell numbers, where implants with $100 \times 10^6$ cells were larger than those with $50 \times 10^6$ cells. The injection approach for cell implantation was less invasive and resulted in more consistent and efficient testis tissue development. UBM provided promising results as a means for non-invasive monitoring of implants and prediction of the outcomes, and hence improved the implantation model further.

[5] The manuscript for this study has been submitted for publication in the Journal of *Reproduction, Fertility and Development* under joint co-authorship with Jaswant Singh and Ali Honaramooz.

[6] AHAJ contributed to the conceiving and designing of the study, performed the experiments, and wrote the first draft of the manuscript.

## 5.2 Introduction

Implantation of dissociated neonatal porcine testis cells into immunodeficient mice led to *de novo* formation/regeneration of testis tissue (Honaramooz *et al.,* 2007). The testis cell implantation (TCI) procedure involved enzymatic digestion of the neonatal pig testis tissue to obtain single-cell suspensions, followed by centrifugation to obtain concentrated cell aggregates for ectopic implantation under the back skin of immunodeficient mice. Within 4 d post-TCI, some cells displayed organized alignments, which by 7 d formed extensive cellular rearrangements leading to the formation of cord-like structures. By 2 wk, the newly formed testis cords resembled the seminiferous cords typical of those seen in neonatal pig testes. The extensive rearrangements of cells and structures in the regenerated tissue included the usual polarization of Sertoli cells (with their nuclei facing the basal membrane of the cords), localization of gonocytes in the center of cords, and formation of the interstitial tissue in the intertubular areas. When given enough time, the *de novo* formed testis tissues underwent complete development to result in morphologically normal spermatogenesis, at times indistinguishable from age-matched pig testis tissue *in situ*. These regenerated xenogeneic porcine testis tissues were also capable of releasing sufficient androgens to restore the vesicular gland weights of the castrated recipient mice to the range of values seen in intact mice (Honaramooz *et al.,* 2007).

The unexpected morphogenic capacity of isolated cells from a postnatal donor to undergo autonomous rearrangements to form a structurally- and functionally-complex tissue such as the testis tissue is remarkable. Testicular morphogenesis has also been shown to occur using dissociated cells from other donor species such as the mouse, sheep, and cattle (Kita *et al.,* 2007, Arregui *et al.,* 2008b, Zhang *et al.,* 2008). This unique *in vivo* culture system provides an ideal microenvironment, and an accessible model for the study and manipulation of testis morphogenesis and spermatogonial stem cell niche formation (Honaramooz *et al.,* 2007; Dores and Dobrinski 2014). The TCI model may also be viewed as a unique approach to allow preservation of fertility potential of prepubertal boys undergoing gonadotoxic cancer treatments. This, for instance, would involve cell sorting to exclude cancerous cells out of isolated testis cells obtained from testis tissue biopsies of prepubertal cancer patients, followed by formation of the tissue using *in vitro* or *in vivo* culture systems.

Despites its great potential, the application of TCI model for *de novo* tissue formation has been somewhat limited due to the lack of an optimized protocol to provide more efficient and consistent outcomes (Dores and Dobrinski, 2014). For instance, the commonly used testis cell isolation techniques (*e.g.*, conventional two-step enzymatic digestion) yield testis cell suspensions of low germ cell numbers (*e.g.*, ~7%), resulting in a lack of germ cells in many regenerated seminiferous cords/tubules, and hence leading to low spermatogenic efficiency (Honaramooz et al., 2007; Kita *et al.,* 2007). In these previous studies, the implantation of dissociated testis cells under the back skin of recipient mice required transferring loose cell aggregates/pellets into pockets of subcutaneous fascia and closing the incisions with sutures or metal wound clips. The drawbacks of this approach included the lack of control over the number of transferred implanted cells (since cells could remain attached to the holding vials or transferring probes) and also a tendency of the cells to leak out of the skin incisions prior to or after wound closure. The inflammation due to skin incisions could also affect the fate of implanted cells and the formation of tissue. Thus, a comparison of alternative methods for implantation of cell aggregates was needed to provide more consistent and efficient strategies to overcome the aforementioned problems.

To address some of the limitations associated with low germ cell numbers in the donor cell populations, we have introduced improvements in the isolation of neonatal testis cells to allow obtaining donor cell populations with a high proportion of gonocytes (~40%, using a new 3-step enzymatic digestion method; Yang and Honaramooz 2010), which could be further enriched (to ~90%, using a combination of Nycodenz centrifugation and differential plating) (Yang *et al.,* 2011).

Our findings in another implantation model, testis tissue xenografting (TTX), have also provided a better understanding of various factors affecting the efficiency of implantation/grafting. For instance, TTX studies indicate that using testis tissue from immature donors results in higher graft survival and better support of spermatogenesis than tissue from more mature donors (Schlatt *et al.,* 2002b; Honaramooz *et al.,* 2007; Arregui *et al.,* 2008b; Rathi *et al.,* 2008). The efficiency of spermatogenesis in xenografts is also dependent on the donor species. Studies in various species demonstrated variations in the response of graft development. Although complete spermatogenesis has been observed in grafts from the pig, goat (Honaramooz *et al.,* 2002b, 2003b), cattle (Oatley *et al.,* 2005; Schmidt *et al.,* 2006), sheep (Arregui *et al.,* 2008a), cats (Kim *et al.,* 2007), rhesus

monkeys (Honaramooz *et al.,* 2004), and horses (Rathi *et al.,* 2006), the spermatogenic efficiency has been inconsistent among donor species. In term of recipients, there are indications of considerable differences among immunodeficient mice used as a recipient choice (Paris *et al.,* 2004; Honaramooz *et al.,* 2007). The use of SCID mice for TTX was found to be more advantageous than nude mice (Abbasi and Honaramooz, 2010b), thus suggesting the strain of immunodeficient mice used as recipients for TCI may also affect the outcomes. The effect of recipient mouse sex on TTX outcomes was also examined, in which and males (regardless of the strain) gave rise to significantly higher graft development when compared with female recipients (Abbasi and Honaramooz, 2010b). The effect of gonadectomy on graft development, however, remains less clear. While some studies suggested that castration of recipients prior to TTX led to a higher development of grafts over intact recipients (Schlatt *et al.,* 2002a; Rathi *et al.,* 2006), these findings contradicted the observations in earlier studies (Shinohara *et al.,* 2002; Abbasi and Honaramooz, 2010a). The results from our laboratory showed no beneficial effect of gonadectomy (orchidectomy or ovariectomy) for TTX (Abbasi and Honaramooz, 2010a). In addition to recipient factors, the number of transplanted grafts, their size, as well as their implantation site have also been shown to affect TTX outcomes and therefore these same factors may also influence tissue formation in the TCI model (Schlatt *et al.,* 2002b; Shinohara *et al.,* 2002; Rathi *et al.,* 2006; Abbasi and Honaramooz, 2010b).

Gel matrices have been widely used as binders or scaffolds in cell delivery systems, mostly in tissue engineering and regenerative medicine applications (Fan *et al.,* 2008; Nicodemus and Bryant, 2008; Park *et al.,* 2009). The biocompatible properties of these materials (*i.e.,* being inert and absorbable) reduce the risk of rejection when applied as the carrier for drugs and cells. The use of Matrigel (a gelatinous protein mixture obtained from a mouse sarcoma cell line), as a binder/scaffold for TCI has been reported (Dores and Dobrinski, 2014). However, the presence of a host of known and unknown growth factors and other proteins in Matrigel makes its use less suitable for cell implantation studies aimed at investigating the effects of different factors on the TCI outcome. To date, basic gel-based matrices (without additives) have not been tested as potential carriers or scaffolds for TCI.

Moreover, evaluation of TCI and TTX outcomes have thus far been limited to the post-mortem/post-retrieval examination of implants/grafts. Therefore, in the present study, we also

tested the feasibility of using ultrasound biomicroscopy (UBM), as a non-invasive tool to monitor the development of testis cell aggregates prior to their retrieval. UBM is a high-resolution ultrasound imaging tool allowing real-time *in vivo* assessment of structures, tissues, and organs and hence has been used in a range of clinical and research applications. However, UBM has not been previously used in the assessment of TTX or TCI models. Therefore, the objectives of the present study were to examine various factors related to the TCI model, and to test UBM for non-invasive evaluation of the implants prior to their retrieval.

## 5.3 Materials and Methods

### *5.3.1 Study Design*

The present study consisted of two experiments, the design of which is schematically illustrated in Fig. 5.1. In Experiment 1, we studied the effects of using different basic gel matrices (gelatin, agarose, or collagen, without additives) and different cell numbers ($50 \times 10^6$ or $100 \times 10^6$ cells) on *de novo* formation of testis tissue after TCI of neonatal porcine cell aggregates under the back skin of immunodeficient mice. The implantation was performed using a previously described surgical approach involving the transfer of cell aggregates through skin incisions (Honaramooz *et al.,* 2007). At 2 wk post-TCI, the mice were euthanized and the implants retrieved for gross and microscopic analyses. In Experiment 2, a less-invasive method of implantation through subcutaneous injection of testis cell aggregates was evaluated. We also examined the effects of gonadal status (intact *vs.* castrated) and implantation site under the back skin on the TCI outcomes. For both experiments, the implants were imaged *in vivo* using UBM, before their retrieval.

### *5.3.2 Testis Collection and Preparation*

Neonatal testes were collected through aseptic castration of Yorkshire-cross piglets (Camborough-22 × Line 65) aged <1 wk ($n$ = 160), as described in more details in Chapter 3.3.1.

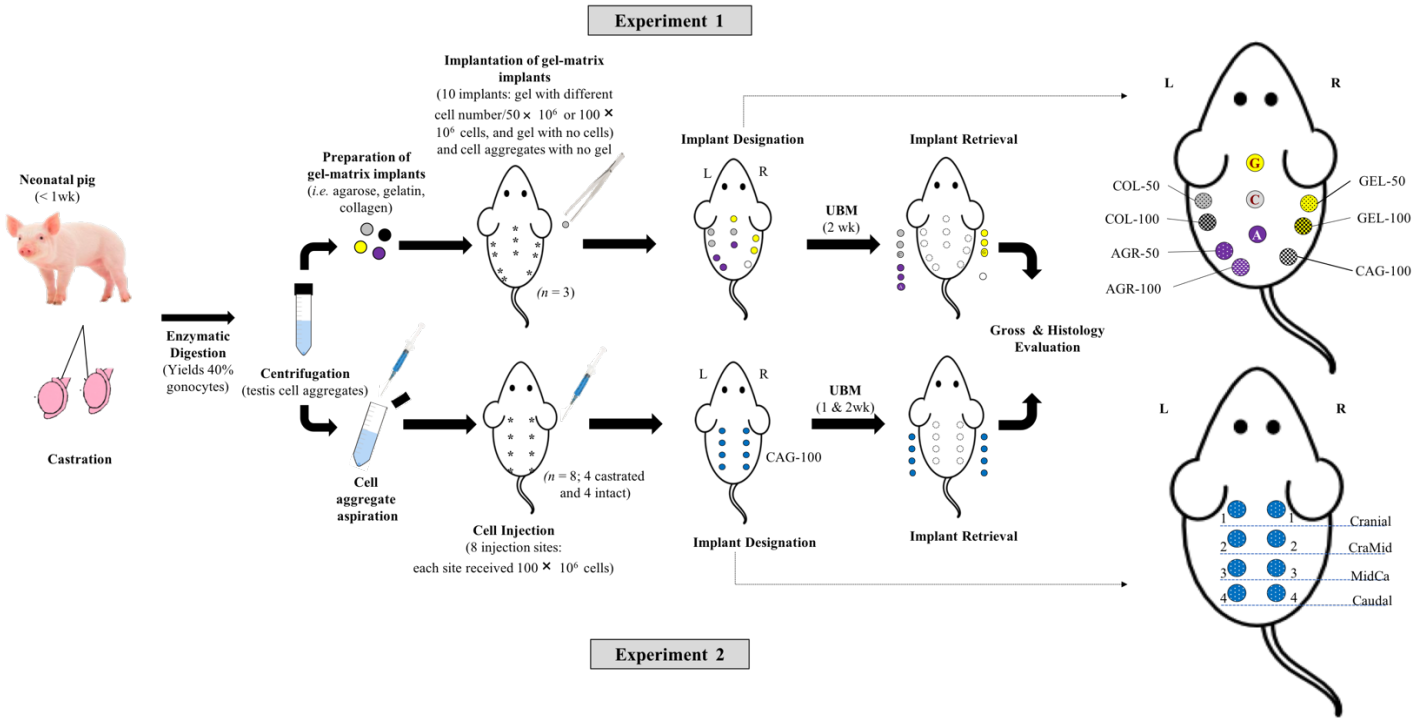


**Fig. 5.1.** Schematic overview of the study design for Experiments 1 and 2. In Experiment 1, three types of gel-based implants (*i.e.*, gelatin, agarose, and collagen) containing either 50 × $10^6$ or 100 × $10^6$ testis cells were implanted surgically under the back skin of recipient mice ($n$ = 3) via the creation of pockets in subcutaneous fascia by blunt dissection. Implants void of testis cells from each of the three gel types and a cell pellet (100 ×$10^6$ cells) without gels were also implanted as controls. The 10 implants in each mouse were labeled as GEL-50 or GEL-100 (gelatin with 50 × $10^6$ or 100 × $10^6$ cells), AGR-50 or AGR-100 (agarose with 50 × $10^6$ or 100 × $10^6$ cells), COL-50 or COL-100 (collagen with 50 × $10^6$ or 100 × $10^6$ cells), GEL-0, COL-0, or AGR-0 (agarose, collagen, or gelatin with no cells, as negative controls), and CAG-100 (cell aggregate containing 100 × $10^6$ cells without gel matrices, as a positive control). In Experiment 2, cell aggregates were injected into 8 sites (100 ×$10^6$ cells per implantation site) under the back skin of recipient mice ($n$ = 8), which were either castrated ($n$ = 4) or intact ($n$ = 4). The implant sites were assigned based on location on each side of the recipient as L1, L2, L3, and L4 or R1, R2, R3, and R4. For ease of analysis, the implantation sites were also grouped based on the relative craniocaudal location as Cranial (L1 and R1), CraMid (L2 and R2), MidCa (L3 and R3), and Caudal (L4 and R4). The implants were scanned using ultrasound biomicroscopy (UBM) at 2 wk for Experiment 1 and at both 1 and 2 wk for Experiment 2. The mice were euthanized and the implants retrieved at 2 wk post-implantation in both experiments.

### *5.3.3 Isolation of Testis Cells*

Isolation of testis cells was performed using methods that have been previously established in our laboratory (three-step enzymatic digestion, Yang *et al*., 2010), with minor modifications as described in Chapter 3.3.2. The final cell pellet, containing ~40% gonocytes and a mixture of testis somatic cells, was re-suspended in 30 mL of DMEM supplemented with 10% FBS and 1% antibiotics and underwent gentle pipetting to obtain a single cell suspension.

### *5.3.4 Experiment 1 – Evaluation of Basic Gel-Based Matrices as Carriers for Implantation of Testis Cell Aggregates*

#### *5.3.4.1 Preparation of Gel-Based Matrices*

Three types of basic (without additives) gel-based matrices were evaluated, which included agarose, gelatin, and collagen. Preliminary experiments were performed to determine the optimal composition for each gel matrix by assessing its physical properties at different temperatures as well as its effect on the viability of cultured testis cells (data not shown). The optimal composition was determined to be 10% (w/v) for gelatin, 0.05% (w/v) for agarose, and 5 mg/mL for collagen type I.

Briefly, for the preparation of 10% gelatin, 1.0 g of gelatin (catalogue no. D2500, Sigma-Aldrich) was dissolved in 10 mL of DPBS containing 1% antibiotics and kept at room temperature (21 °C) for 30 min. The mixture was then heated on a magnetic stirring hot plate to 60-70 °C, transferred into a 15-mL test tube, and incubated in a 37 °C-water bath. At the same time, the cell suspensions were placed in an incubator for 10 min to bring the temperature up to 37 °C. The cell suspension was aliquoted into 1.5 mL micro-centrifuge tubes to a total of either $50 \times 10^6$ or $100 \times 10^6$ cells per tube. The aliquots were centrifuged for 5 min at 500×*g* at 16 °C, and the supernatant was removed, leaving behind the cell pellets. Immediately, 100 µl of 10% gelatin was mixed with the cell pellet and gently pipetted up and down to homogenize the mixture. The gelatin-cell mixture was then pipetted onto a sterile Parafilm in a petri dish and kept in a refrigerator (4 °C) for 10 min to solidify. Parafilm was used to prevent adherence of gel-based matrices to the dish. Prior to implanting the gelatin-based cell aggregates they were kept in an ice-cold container.

For the preparation of 0.05% agarose, 500 µg of agarose (catalogue no. 11388983001, Sigma-Aldrich) was mixed with 10 mL of DPBS with 1% antibiotics, and the mixture was heated and stirred at 60 °C for 5 min. Once the mixture was homogenized, it was incubated at 37 °C for 5 min and immediately mixed with the cell pellet. The remaining procedures continued as described for gelatin.

For the preparation of collagen, 200 µl of 5 mg/mL collagen type I (catalogue no. 50201, Ibidi, Fitchburg, WI, USA) was added to the cell pellet, and the mixture was homogenized before pipetting onto a Parafilm. The end product for all preparations was a sphere-shaped (~1.0 cm in diameter) gel-based testis cell aggregate.

#### *5.3.4.2 Implantation of Gel Matrix-Based Neonatal Testis Cell Aggregates via the Surgical Method*

The recipients were double-homozygous severe combined immunodeficient hairless outbred mice (SHO mice, Crl:SHO-*Prkdc*$^{scid}$*Hr*$^{hr}$, strain code 474; Charles River, Montreal, Canada, $n = 3$), aged 8 wk at time of surgery. The mice were housed in sterile Plexiglas micro-isolator individual cages, maintained under controlled photoperiod (lights on 0600-1800), and handled aseptically. Sterile water and food were provided *ad libitum*. The mice were acclimatized for 1 wk prior to the procedures, and anesthetized using 5% isoflurane in oxygen for induction and 2% isoflurane in oxygen for maintenance throughout the surgery. After the surgical preparation of the skin, the mice were castrated and received 10 longitudinal linear skin incisions on their backs. Using blunt dissection through each incision, a subcutaneous pocket was created and an implant was inserted into each pocket. For each mouse, the implants included a gelatin-based sphere with $50 \times 10^6$ cells (GEL-50), one with $100 \times 10^6$ cells (GEL-100), an agarose-based sphere with $50 \times 10^6$ cells (AGR-50), one with $100 \times 10^6$ cells (AGR-100), a collagen-based sphere with $50 \times 10^6$ cells (COL-50), and one with $100 \times 10^6$ cells (COL-100). In addition, a gel-based sphere with no cells from each of the 3 matrices as negative controls (*i.e.*, GEL-0, COL-0, AGR-0), and a cell aggregate containing $100 \times 10^6$ cells without any matrices, as a positive control for cell aggregates (CAG-100), were also implanted (*i.e.*, 10 implants per mouse). The incisions were sutured using 6-0 coated, non-absorbable braided silk (Sofsilk, catalogue no. SS1639G, Syneture, Norwalk, USA). All experimental procedures involving animals were reviewed and approved by the University of

Saskatchewan's Institutional Animal Care and Use Committee (Animal Use Protocol# 20080042). A schematic representation of the study design and designation of implant placement is illustrated in Fig. 5.1.

### *5.3.5 Experiment 2 – Development of an Alternative Method for Implantation of Neonatal Testis Cell Aggregates*

#### *5.3.5.1 Implantation of Neonatal Testis Cell Aggregates via an Injection Method*

Based on the results of Experiment 1, an injection method for TCI was evaluated in this experiment. The recipient mice and anesthesia procedure were as described for Experiment 1. The mice were either castrated ($n$ = 4) or remained intact ($n$ = 4), and each mouse received 8 implants in the form of injected cell aggregate. Testis cells were isolated as described above, maintained at 4 °C overnight, and centrifuged at 500×*g* for 5 min at 16 °C to obtain cell aggregates for injection. Cell aggregates were highly concentrated (100 × $10^6$ cells per 0.1 mL), 0.8 mL of which was drawn into a 1-mL syringe and a 22-gauge needle was attached. The skin was lifted to create a tent, and 0.1 mL of the cell aggregate was gently injected into the subcutaneous tissue. To keep track of implants at analyses, the implantation sites were categorized as being on the left (L) or right (R), and from 1 through 4 (*i.e.,* L1, L2, L3, and L4 or R1, R2, R3, and R4), corresponding to the craniocaudal positioning, respectively (*i.e.*, Cranial, CraMid, MidCau, Caudal; Fig. 5.1). The mice were housed and cared for under similar conditions as described in Experiment 1.

#### *5.3.5.2 Ultrasound Biomicroscopy (UBM) Assessment*

We also evaluated the potential application of an ultrasound biomicroscope (UBM; 40 MHz, VEVO 3100, Visual Sonics, Toronto, ON, Canada), as a non-invasive tool for the assessment of implants *in vivo*. For Experiment 1, this assessment was performed at 2 wk post-TCI (prior to euthanasia) and, for Experiment 2, at 1- and 2 wk post-TCI. The mice underwent anesthesia using a mixture of ketamine at 100 mg/kg and xylazine at 10 mg/kg, injected intraperitoneally, were placed in sternal recumbency on the UBM stage and the ultrasound gel lubricant (EcoGel 200; catalogue no 40JB; Eco-Med Pharmaceutical Inc, Mississauga, ON, Canada) was applied on the skin. The transducer, which was prefixed onto a custom-designed holder, was lowered into contact with the surface of the skin covering the implant. The platform was then moved craniocaudally

until the implant was visualized, at which time the platform was steered slowly from cranial to caudal aspect of the implant and images were digitally recorded. The same procedure was repeated to image the remaining implants.

Dimensions of each implant were measured using the 2D (B-mode) and 3D functions of UBM. We also used the color flow Doppler function to evaluate the blood vessels supplying the implants (performed only in Experiment 2). The machine settings, based on previous reports (Mircea *et al.,* 2009; Cervantes *et al.,* 2013), used for obtaining images of implants included: transducer with a 50-MHz central frequency (MX Transducer, MX700, Visual Sonics), power 100%, radio frequency 2 kHz, master gain 38 dB, delay 1.0 mm, field of view 9 mm × 10 mm, frame rate 19 fps, and range 70 dB. At 50 MHz central frequency, the axial resolution was 30 μm and the maximum imaging depth was 10 mm. The fixed focal point was set at 4.5 mm from the transducer surface.

To examine the accuracy/fidelity of UBM measurements of implants in live mice, we compared the UBM data with the measurements of implants retrieved post-mortem. The length and width of implants were calculated from the recorded UBM images and videos, and compared with those from the photographs of the implants after the mice were euthanized, and while the implants were still attached to the skin (measured using ImageJ, U.S. National Institutes of Health, Bethesda, Maryland, USA). The implant length (along the transverse plane or Y-axis) was calculated based on the UBM probe displacement from the cranial to caudal border, and the implant width (along the sagittal plane or X-axis) based on the lateromedial dimension. The implant thickness/height (Z-axis) was measured as the vertical dimension between the ventral and dorsal borders of the implant, at the halfway point between the cranial and caudal borders. For UBM, the images were recorded continuously at 0.5 mm intervals (slices), thus multiplying the total number of images from an implant by the thickness of slices produced an estimate of the implant dimensions.

#### *5.3.5.3 Implant Retrieval and Gross Evaluation*

The implants were retrieved at 2 wk post-TCI in both experiments. Based on the previous reports (Honaramooz *et al.,* 2007; Arregui *et al.,* 2008b; Zhang *et al.,* 2008), this duration was sufficient for the reorganization of the cells, and formation of testis cords. Mice were euthanized using an overdose of isoflurane anesthesia, followed by bilateral thoracotomy to ensure death. Necropsy

was performed and the implant recovery rates, dimensions, weights, and gross features were recorded. The vesicular glands of recipient mice were excised and weighed to calculate the vesicular gland index as follows:

$$Vesicular\ gland\ index = \frac{Weight\ of\ vesicular\ glands}{Live\ weight\ of\ the\ mouse} \times 100$$

### *5.3.6 Histological Evaluation*

The retrieved implants were fixed in Bouin's solution overnight, rinsed with and preserved in 70% ethanol until processing in an automated tissue processor (Tissue Tek, Sakura Finetek USA Inc, Torrance, USA). Processed tissues were then paraffin embedded, sectioned at a thickness of 5 µm, and stained with hematoxylin and eosin (H&E) and Masson's trichrome. Histological assessment was performed using a microscope equipped with digital photomicrography (Northern Eclipse Image Analysis software version 7.0, Empix Imaging, Mississauga, ON, Canada). The degree of *de novo* tissue formation was assessed by calculating the relative area of the grafts occupied by the seminiferous cords. In addition, the average number of gonocytes per 1,000 Sertoli cells was also counted in five randomly-selected fields per slide (at 400× magnification). For comparison, this relative number of gonocytes was also calculated for testis tissue samples of age-matched 1, 2, and 3 wk old piglets.

### *5.3.7 Statistical Analyses*

All data are presented as means ± standard error of mean (SEM). Unless stated otherwise, all data were analyzed using independent *t-tests*, one-way, or two-way analysis of variance (ANOVA) as appropriate. For percentages, the data were transformed using Arcsine function prior to analysis using ANOVA. The level of significance was set at $P < 0.05$. Data were analyzed using the SPSS (Version 22.0, SPSS Inc., Armonk, NY, USA).

## 5.4 Results

### *5.4.1 Feasibility of Using UBM for Assessment of Implants*

As part of Experiment 1, we evaluated the feasibility of using UBM in monitoring the gel-based implants *in vivo* prior to their retrieval at 2 wk post-TCI. The implants were readily identifiable and clearly defined upon ultrasonography, allowing their measurements across the X, Y, and Z-axes. As shown in Fig. 5.2, the implants had a hyperechoic line outlining the periphery, and their core showed different degrees of echogenicity, presumably indicative of differential cellular organization or testis cord formation among different types of implants.

The degree of echogenicity appeared to be related to the original number of cells incorporated in the implants. In contrast to the relatively homogenous echogenicity seen in the cell-only implants (Fig. 5.2A), anechogenic texture (lack of echogenicity) was evident in the agarose-only implants (Fig. 5.2B). Echogenicity seemed to also differ depending on the gel composition. The echogenicity in the gelatin-based implants (Fig. 5.2C) was greater than that of the agarose-based implants (Fig. 5.2D), although both contained the same number of cells (*i.e.*, $100 \times 10^6$ cells).

The number of implanted cells also influenced the size of the implants since the same collagen-based implants with fewer cells ($50 \times 10^6$ cells, Fig. 5.2E) appeared smaller than those with a greater number of cells ($100 \times 10^6$ cells, Fig. 5.2F). Judging from the heterogeneous texture of implants through UBM images, we predicted higher cellular organization and testis cord formation in the gelatin- and collagen-based implants. This was also dependent on the number of incorporated cells, and little or no cellular activity or tissue formation was evident in the agarose-based implants. However, not all implants could be found using UBM; the negative control implants (*i.e.*, no-cell gelatin and no-cell collagen) were not detected, indicating they might have undergone complete absorption (Table 5.1). Finally, we also observed pulsatile movement at the periphery of the implants via UBM, suggesting the presence of blood vessels. However, this observation occurred only twice out of all observations (2/27).

The UBM examination at 1- and 2 wk post-TCI in Experiment 2 allowed assessment of the implants over time. The results indicated that the encapsulation of the implant by a hyperechoic layer was also detectable at 1 wk. (Fig. 5.3). The implants at 1 wk post-TCI appeared less echogenic than

those at 2 wk (Fig 5.3A-B). Additional assessments included using the color Doppler mode and 3D imaging to visualize the blood supply, which appeared limited to the periphery of the implants at 1 wk post-TCI but was extended into the implants at 2 wk (Fig. 5.3C-D*)*.

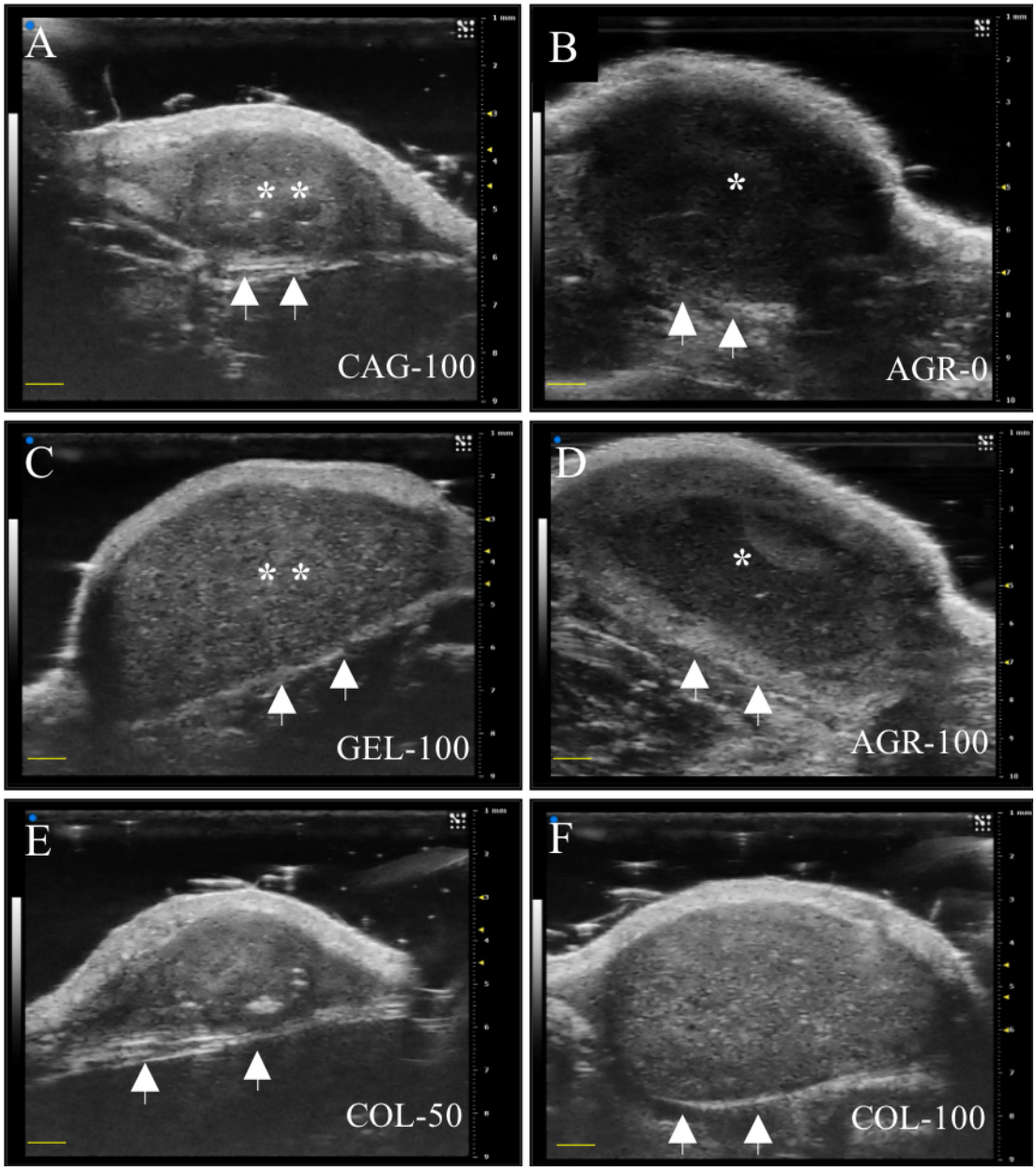


**Fig. 5.2.** Representative *in vivo* images of gel-based implants obtained using ultrasound biomicroscopy (UBM). Depicted implants include (A) cell aggregates with $100 \times 10^6$ cells but no gels (CAG-100, as a positive control), (B) agarose with no cells (AGR-0, as a negative control for agarose), (C) gelatin with $100 \times 10^6$ cells (GEL-100), (D) agarose with $100 \times 10^6$ cells (AGR-100), (E) collagen with $50 \times 10^6$ cells (COL-50), and (F) collagen with $100 \times 10^6$ cells (COL-100). UBM was performed at 2 wk post-implantation using the B-mode. Note the presence of a capsule (arrowheads) surrounding the implants and the echogenic appearance presumed to represent cellular activity or testis cord formation. One or two asterisks (*) represent the varying opacity of implants (A-D). Evidence of cellular activity or testis cord formation was observed in collagen-based implants in a cell number-dependent manner (E-F). (Scale bar: 1 mm).

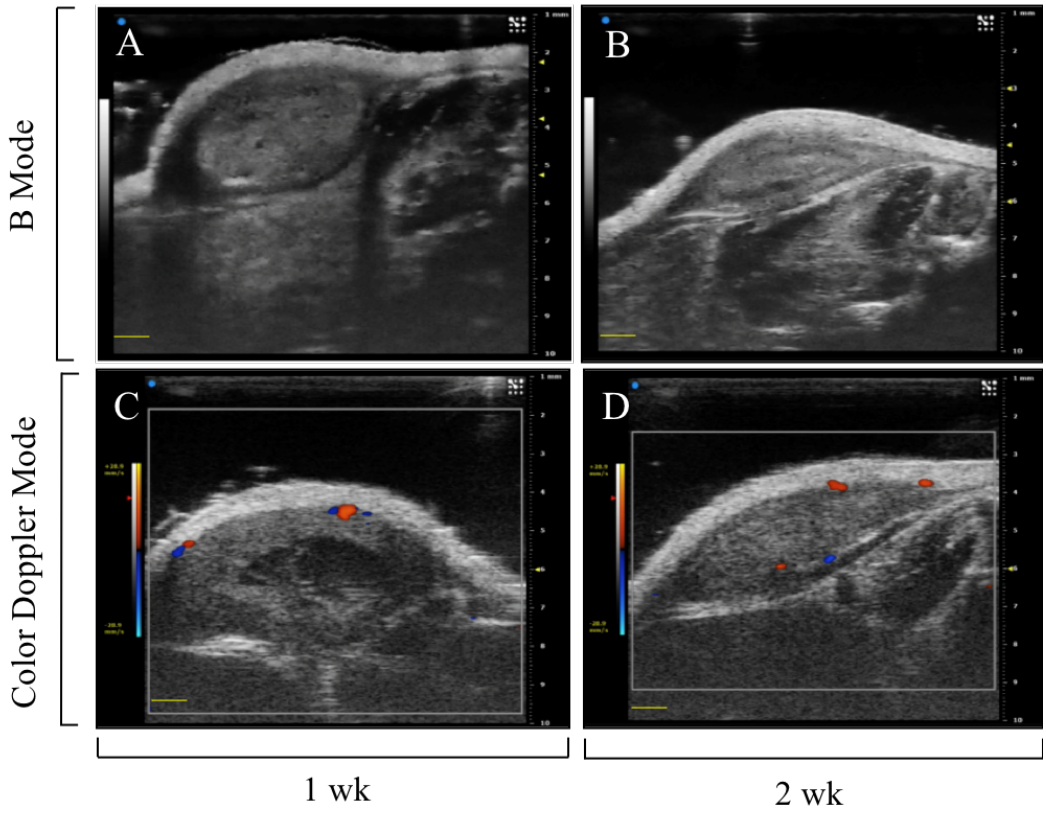


**Fig. 5.3.** Representative *in vivo* images of cell injection implants obtained using ultrasound biomicroscopy (UBM). UBM was performed at 1- and 2 wk post-implantation, using the B- (A-B) and color Doppler modes (C-D). Note the changes in the size and shape of the implants (A-D). The distribution of blood vessels in the implants could be assessed by UBM via color Doppler mode (C-D). The blood vessels appeared as blue or red pseudo-colors indicating different directions of the blood flow; blue indicating the blood flowing away from the transducer (towards the implants) and red indicating the blood flow towards the transducer (away from the implants). Note the blood vessels were primarily present at the periphery of the implant at 1 wk and extended into the implants at 2 wk post-implantation. (Scale bar: 1 mm).

**Table 5.1.** The number of implants upon retrieval at 2 wk post-implantation in Experiment 1.

| Implants | Cell no. ($\times 10^6$) | Mouse 1 | Mouse 2 | Mouse 3 | Total |
|---|---|---|---|---|---|
| Collagen-based | 100 | + | + | + | 3/3 |
| | 50 | + | + | - | 2/3 |
| | 0 | - | - | - | 0/3 |
| Gelatin-based | 100 | + | + | + | 3/3 |
| | 50 | + | + | + | 3/3 |
| | 0 | - | - | - | 0/3 |
| Agarose-based | 100 | + | + | + | 3/3 |
| | 50 | + | + | + | 3/3 |
| | 0 | + | + | + | 3/3 |
| Cell aggregates | 100 | + | + | + | 3/3 |
| Total | | 8/10 | 8/10 | 7/10 | |

[+] Indicates the implants were present at retrieval at 2 wk post-implantation.
[-] Indicates the absence of implants at retrieval at 2 wk post-implantation.

### *5.4.2 Fidelity of UBM Measures for Predicting the Size of Implants Prior to Retrieval*

The length and width of implants measured *in vivo* using UBM were consistently greater (by 21% and 18%, respectively, $P < 0.05$) than those measured using image analyses of post-mortem implants. There were positive correlations among the measurements (Table 5.2).

### *5.4.3 Gross Evaluation of Implants*

In Experiment 1, upon opening the back skin, the implants were readily identifiable while being adhered to the subcutaneous layer of the skin. The presence of blood vessels leading to the implants and encapsulation of the implants by thin fibrous connective tissues were also detectable (Fig. 5.4A-C). Some of the implants were not visible/retrieved, leading to a recovery rate of 8/10 implants in two mice, and 7/10 in the third mouse (Table 5.1). While all collagen- and gelatin-only (negative control) implants were absent in all mice, all the implants with cells were retrieved, except for one implant (*i.e.*, COL-50) in one mouse. The positive control implants (CAG-100) were present in all mice.

In Experiment 2, at euthanasia, vascularization and encapsulation of the implants were observed to be similar to those in Experiment 1 (Fig 5.4D-F); however, 100% of implants were retrieved from all recipients (*i.e.*, 64/64 implants). Less variation in size and shape was observed in implants retrieved in Experiment 2, compared with the implants in Experiment 1 with the same number of cells ($100 \times 10^6$ cells; CAG-100). Overall, the implants from Experiment 2 were heavier ($37.95 \pm 2.15$ mg, $n$=64; $P < 0.05$) than comparable cell-only implants ($100 \times 10^6$ cells, CAG-100) retrieved in Experiment 1 ($19.1 \pm 9.32$ mg, $n = 3$).

**Table 5.2.** Relationships between the implant dimensions measured either *in vivo* using ultrasound biomicroscopy (UBM) or *post-mortem* after implants were visualized while still attached to the skin.

| Dimension | Method | Mean ± SEM (mm) | *Correlation* | |
|---|---|---|---|---|
| | | | *r* | *P-value* |
| Length | *In vivo* | 8.55 ± 0.25 | 0.224 | 0.075 |
| | Post-mortem | 7.09 ± 0.22 | | |
| Width | *In vivo* | 6.15 ± 0.13 | 0.250 | 0.047 |
| | Post-mortem | 5.20 ± 0.15 | | |

Data are mean ± SEM ($n$ = 64 implants).
Pearson's product-moment correlation coefficients ($r$) were calculated between the two methods of dimension measurements.
Correlation coefficients were considered significant when $P < 0.05$.

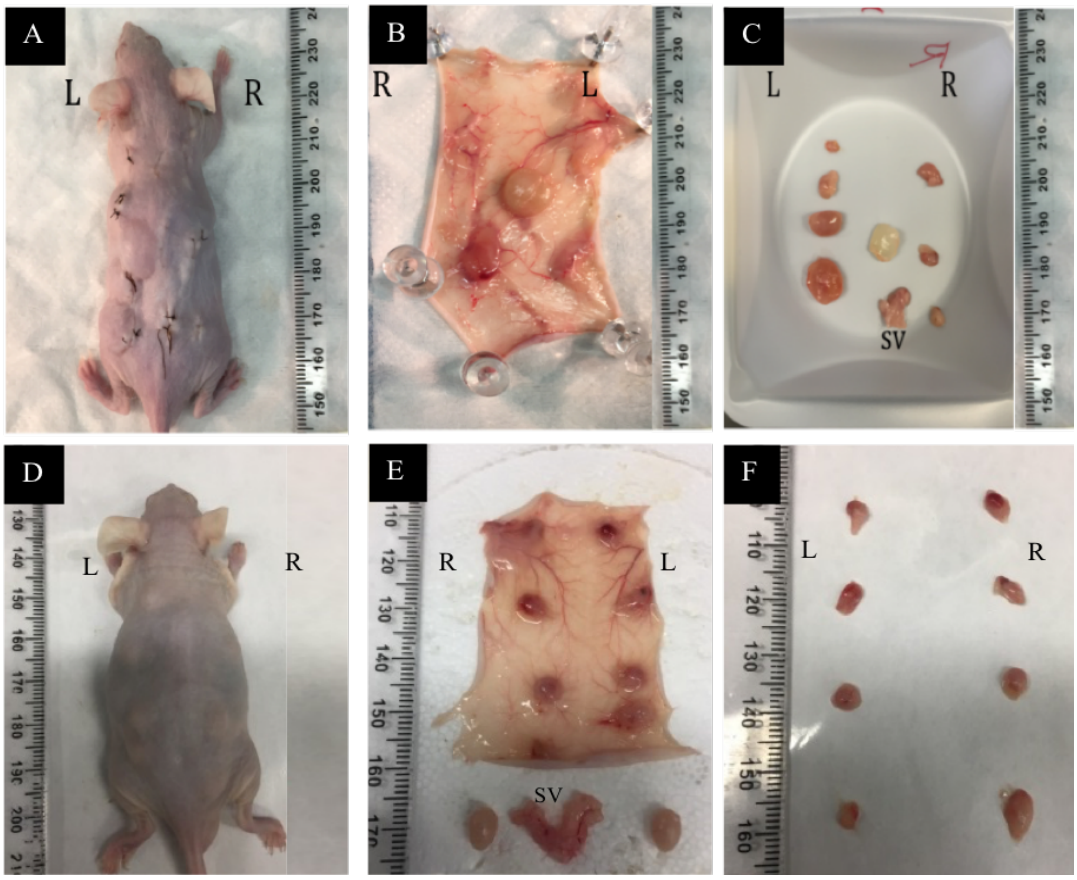


**Fig. 5.4.** Representative photomacrographs showing implants before and after retrieval at 2 wk post-implantation in Experiments 1 and 2. The appearance of implants (A, D) under the skin, prior to retrieval, (B, E) still attached to the skin, and (E, F) after retrieval in Experiment 1 (A-C) and Experiment 2 (D-F). Note the presence of blood vessels directed toward the implants (B, E). Vesicular glands (SV) are also shown.

### *5.4.4 Histological Evaluation of Implants*

Histological examination of the implants in Experiment 1 showed the organization of cells and *de novo* formation of testis cords in the collagen- (Fig. 5.5C-D) and gelatin-based implants (Fig. 5.5G-H), as well as cell-only implants (positive control/no-gel; Fig. 5.5A). Qualitatively, the development of cords was most complete in the gelatin-based implants. No cord development was observed in the agarose-based implants with $50 \times 10^6$ cells (AGR-50), where only necrotic cells were found (Fig. 5.5E). However, in the agarose-based implants with $100 \times 10^6$ cells (AGR-100), a small degree of cellular organization was observed but without formation of cords (Fig. 5.5F). No cellular activities were observed in the retrieved negative control implants for agarose (AGR-0), which only contained a vacuolated/empty space (Fig. 5.5B).

In Experiment 2, a number of common histological patterns were observable in all implants (Fig. 5.6A-B). For instance, cross-sections of the implants collected at 2 wk post-TCI could be categorized into three zones/areas: 1) The external capsule made of fibrous connective tissue (capsular area); 2) areas of cellular activity or testis cord formation (tissue formation area); and 3) areas void of cellular activities in some implants, primarily associated with vacuolation/fluid-filled cavity in the center of the implant (vacuolar area). Vascularization was evident by the presence of blood vessels (visualized with the aid of Masson's trichrome staining) both at the capsular and tissue formation areas (Fig. 5.6E-F), supporting the UBM observations (Fig. 5.3C-D).

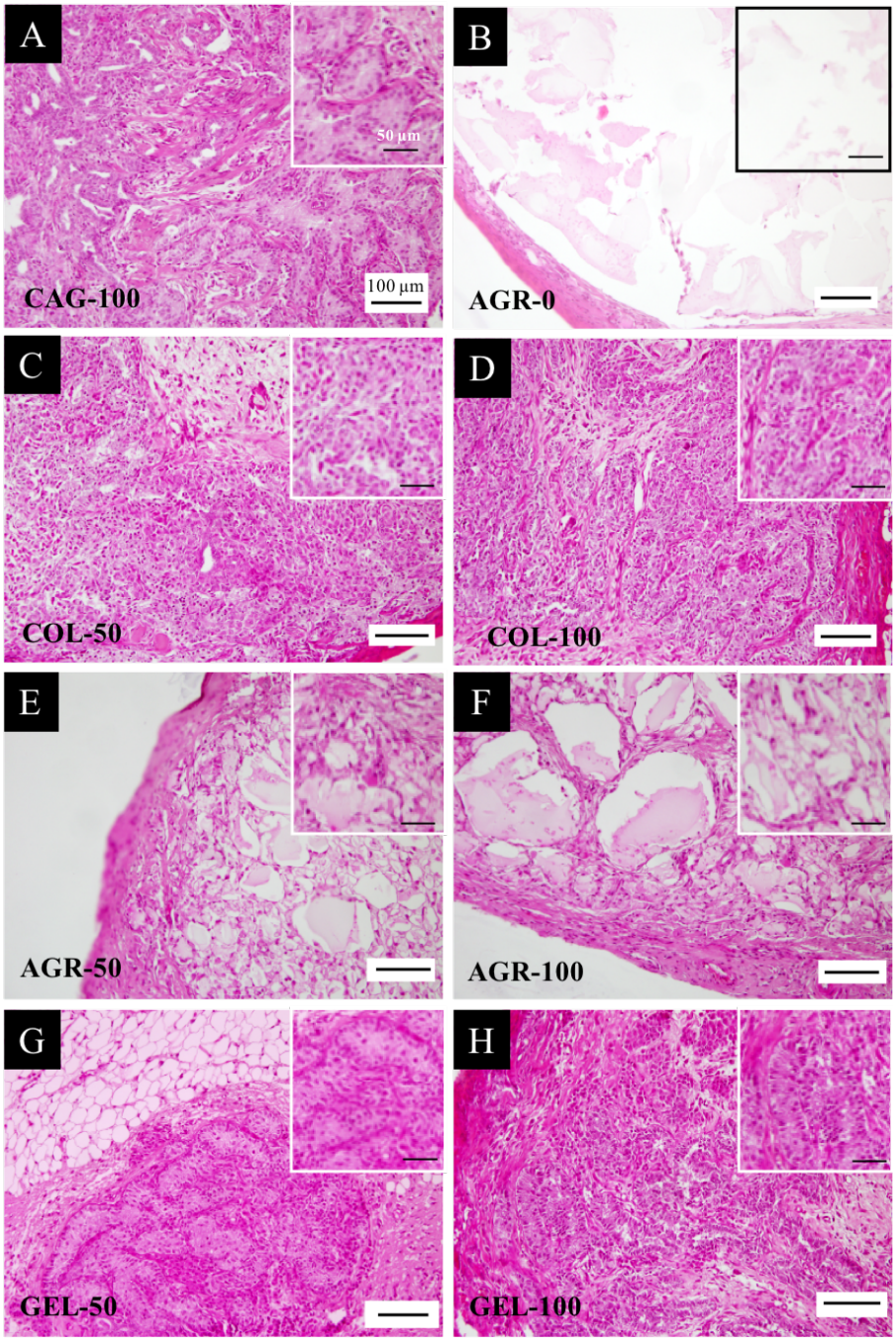


**Fig. 5.5.** Representative histological photomicrographs of implants from Experiment 1 at 2 wk post-implantation. *De novo* testis cord formation was observed in (A) the positive control implant (CAG-100, cell aggregates with $100 \times 10^6$ but no gels). A similar development is present in (C-D) collagen (COL)-based and (G-H) gelatin (GEL)-based implants, and the degree of *de novo* testis cord formation is correlated with the number of cells (*i.e.*, higher with $100 \times 10^6$ *vs.* $50 \times 10^6$ cells). In contrast, no or limited development was observed in agarose (AGR)-based implants, including (B) the negative control with agarose-only, and (E-F) agarose with $50 \times 10^6$ or $100 \times 10^6$ cells. (Scale bars: 50 and 100 µm, H&E staining).

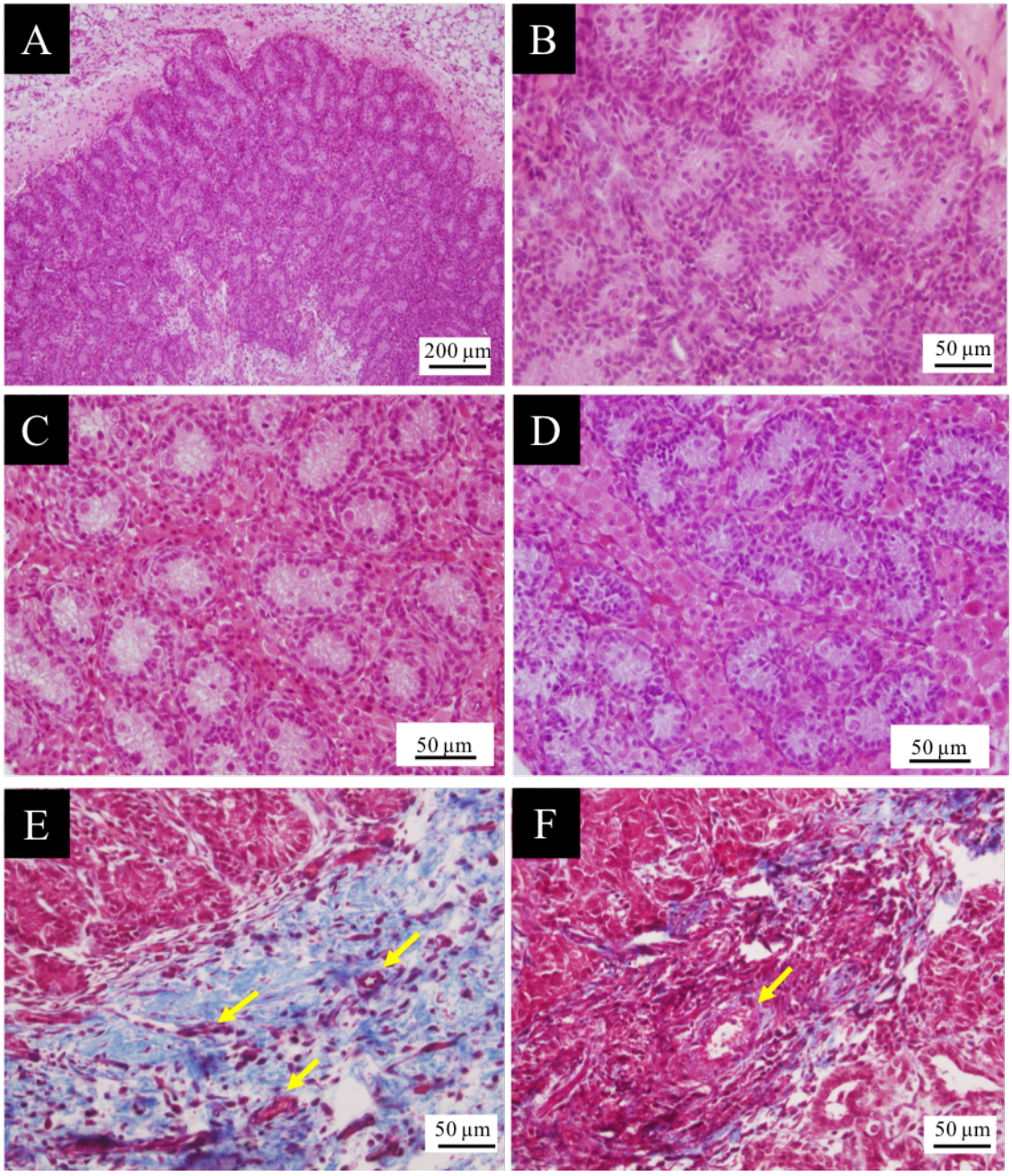


**Fig. 5.6.** Representative histological photomicrographs of implants from Experiment 2 at 2 wk post-implantation. *De novo* testis cord formation is evident in implants at (A) low and (B) high magnifications. Morphology of intact testis tissue of (C) 1 wk and (D) 3 wk old piglets for comparison (H&E staining). Blood vessels (arrows) are observed at the (E) periphery of the implants and (F) within the areas of cord formation (Masson's trichrome staining), consistent with ultrasound biomicroscopy observations.

### *5.4.5 The Effect of Gonadal Status of the Recipient Mice on Development of Implants*

The SHO mice used in this study are a new immunodeficient strain, which have not been previously used in TTX or TCI studies. Therefore, as an added comparison in Experiment 2, we subjected half of the recipient mice to castration while leaving the remaining mice intact, and compared the effect of gonadal status on the following parameters:

#### *5.4.5.1 Vesicular Gland Index and Implant Weight*

The weight of the vesicular glands relative to the body weight (vesicular gland index) did not differ between the castrated and intact groups of recipient mice ($P > 0.05$; 0.58 ± 0.04% *vs.* 0.52 ± 0.02%, respectively, $n = 4$ mice/group). Similarly, the weight of the implants did not differ between the castrated and intact mice ($P > 0.05$; 41.3 ± 2.8 mg *vs.* 34.60 ± 3.2 mg, respectively, $n = 32$ implants/group).

#### *5.4.5.2 De Novo Formation of Testis Tissue*

Histomorphometric analyses were performed on cross-sectioned samples and the following criteria were measured: the total area of implant parenchyma (all areas excluding the capsule, *P*), the area of tissue formation (areas with evidence of cellular activity and tissue formation, *T*), and the area of complete cord formation (areas with complete cords only, *C*). The total parenchymal area (*P*) did not differ between implants from castrated and intact recipients ($P > 0.05$; 7.34 ± 0.55 $mm^2$, $n = 29$ and 6.67 ± 0.47 $mm^2$, $n = 27$, respectively). Similarly, the relative area of tissue formation to the total parenchymal area ($T/P \times 100$) did not differ between the two groups ($P > 0.05$; 33.77 ± 3.21% *vs.* 33.56 ± 3.86%, in castrated *vs.* intact, respectively). The relative area of complete cord formation ($C/P \times 100$) also did not differ between the castrated and intact groups ($P > 0.05$; 26.37 ± 2.77% *vs.* 19.12 ± 2.36%). However, the relative area of complete cord formation to the area of tissue formation ($C/T \times 100$) was greater in the castrated group ($P < 0.05$; 81.14 ± 4.53% *vs.* 57.04 ± 5.40%, respectively). The relative number of gonocytes per 1,000 Sertoli cells in the implants also did not differ between castrated and intact recipients ($P > 0.05$; 44 ± 5.8, $n = 4$ and 43 ± 3.5, $n = 4$, respectively). The combined relative number of gonocytes in all implants (44 ± 3.1, $n = 8$) was lower ($P < 0.05$) than the relative number of gonocytes in 1-, 2-, or 3 wk old pig testis reference samples (126 ± 8.2, 103 ± 3.3, or 87 ± 3.4, respectively, $n = 5$/age; Fig. 5.6C-D).

#### *5.4.5.3 The Effect of Implantation Site*

When the implant weight data were analyzed for the effects of gonadal status (intact *vs.* castrated) and implantation site (Cranial *vs*. CraMid *vs.* MidCa *vs.* Caudal), no main effect of gonadal status ($P > 0.05$) or interactions were detected ($P > 0.05$). However, the main effect of implantation site was significant ($P < 0.05$) and the implants retrieved from the Cranial (L1 and R1; 52.2 ± 6.2 mg, $n = 16$) and CraMid sites (L2 and R2, 43.2 ± 3.3 mg, $n = 16$) were heavier ($P < 0.05$) than those from the caudal sites (L4 and R4; 22.6 ± 3.1 mg, $n = 16$) (Fig. 5.7). Moreover, the weight of implants retrieved from the right side (R1, R2, R3, and R4; 38.29 ± 3.4 mg, $n = 16$) did not differ ($P > 0.05$) from those of the left side (LI, L2, L3, and L4; 37.61 ± 2.7 mg, $n = 16$).

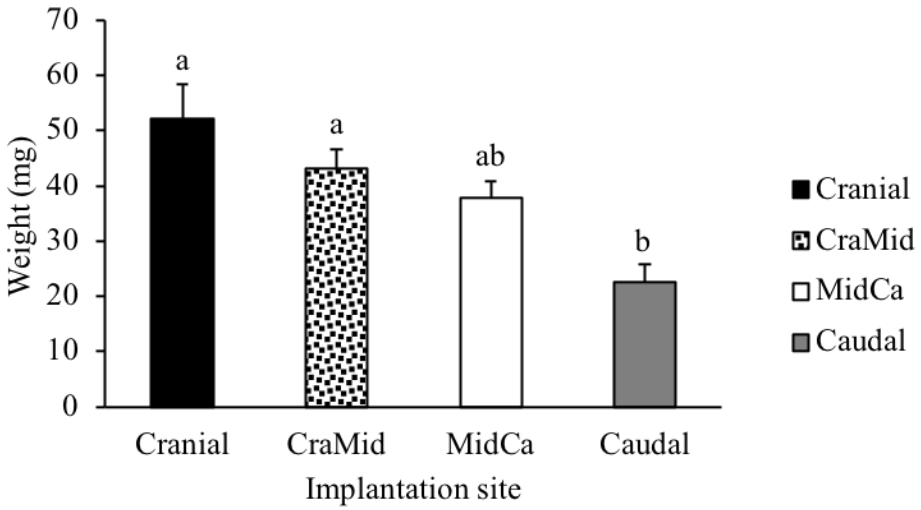


**Fig. 5.7.** Weight of the retrieved implants from Experiment 2 based on the site of implantation. Each mouse received 8 testis cell aggregate implants (4 on each side), which were labelled craniocaudally as: Cranial (L1 and R1), CraMid (L2 and R2), MidCa (L3 and R3), and Caudal (L4 and R4). Data are mean ± SEM. Data with different letters differ significantly between groups ($P < 0.05$).

## 5.5 Discussion

Testis cell implantation (TCI) from a range of donor species under the back skin of recipient mice has provided a unique model for the study of testis regeneration (Dufour *et al.,* 2002; Gassei *et al.,* 2006; Honaramooz *et al.,* 2007; Kita *et al.,* 2007; Arregui *et al.,* 2008b; Zhang *et al.,* 2008; Campos-Junior *et al.,* 2014). In the present study, we used neonatal porcine testis cells to examine several factors that can potentially affect the efficiency and consistency of TCI outcomes. The examined effects included increasing the proportion of gonocytes, comparing the number of implanted cells, employing different gel-based matrices, comparing implantation methods, using a new strain of recipient mice, comparing the gonadal status of the recipients, comparing the implantation sites, and using UBM to assess the growth and development of implants.

First, we addressed the importance of testis cell composition and number for use in TCI. In earlier TCI studies (Honaramooz *et al.,* 2007; Kita *et al.,* 2007; Arregui *et al.,* 2008b; Zhang *et al.,* 2008), a conventional two-step digestion protocol (Honaramooz *et al.,* 2002b; 2003) was used to isolate testis cells which yields a low proportion of germ cells (*e.g.*, 4.5%) (Honaramooz *et al.,* 2007). To date, all TCI studies have reported *de novo*-generated seminiferous cords/tubules that typically lack germ cells (*i.e.*, few have germ cells but most only have Sertoli cells) and consequently TCI results have been associated with a low spermatogenic efficiency (Honaramooz *et al.,* 2007; Kita *et al.,* 2007; Arregui *et al.,* 2008b; Zhang *et al.,* 2008; Dores and Dobrinski 2014). The low number/proportion of germ cells in the donor cells may be a contributing factor in the observed Sertoli cell-only tubules and low spermatogenic efficiency. The lack of a specialized cell isolation method to preferentially select germ cells was a major limitation. In response to this limitation, our lab has developed a 3-step enzymatic digestion strategy for neonatal donor testes which results in high numbers of testis cells containing ~40% gonocytes, which can be further enriched to 80-90% (Yang *et al.,* 2010; Yang and Honaramooz 2011). Recently, we determined that for *in vitro* culture of neonatal testis cells, the proportion of 40% gonocytes were better suited compared with much lower or much higher gonocyte proportions (Chapter 3) (Awang-Junaidi and Honaramooz, 2018). Therefore, in the present study, we used a similar population of neonatal testis cells (with 40% gonocytes). The relative number of gonocytes (per 1,000 Sertoli cells) in 2 wk implants was lower than that in intact piglet testes of related ages (4% in implants *vs.* 13% in 1 wk, 10% in 2 wk, and 9% in 3 wk old intact testes). There are no comparative data using pig donors at these ages to assess

how the number of gonocytes in the implants in the present study compare with those after conventional procedures.

In the present study, we also addressed another limitation of conventional TCI, namely the inconsistency due to a lack of control over the actual number of implanted cells because of the inaccurate means of cell transfer (using pipet tips) and post-implantation leakage of cells from skin wounds (Honaramooz *et al.,* 2007). This implantation of a defined number of testis cells using subcutaneous injection in the present study (Experiment 2) was aimed at overcoming this limitation, and the improved consistency of TCI outcomes (*i.e.*, implant size, shape, and weight) supported this application. Additionally, our injection method can reduce cell preparation time (compared with gel-based implants), surgery time and costs, and the potential risk of infection. Therefore, the injection method is more efficient and suitable for the delivery or implantation of testis cell aggregates, while the conventional implantation technique is more suitable for implanting solid gel-based spheres or testis tissue fragments.

There have been no standardized provisions for the assessment of testis tissues or cell aggregate implants prior to their retrieval from the recipients. In the present study, we addressed this limitation through the application of UBM. There are several reports of the use of UBM for visualization of organs (Hinton *et al.,* 2008; Shen *et al.,* 2008; Mancini *et al.,* 2009), embryology (Foster, 2003; Spurney *et al.,* 2006), oncology (Manning *et al.,* 2008; Greco *et al.,* 2010), clinical ophthalmology (Dada *et al.,* 2011; Mannino *et al.,* 2016), cardiology (Springer *et al.,* 2005), and assessment of tissue repair (Töyräs *et al.,* 2003; Schöne *et al.,* 2016). However, to our knowledge, this is the first attempt to evaluate the feasibility of UBM to monitor the development of testis cell aggregate implants in a recipient mouse model. Based on our results, not only is UBM simple and non-invasive, it also provides high-resolution data and allows real-time *in vivo* assessment of implants over time without the need of sacrificing the recipients at different time points. UBM provided valuable information such as the survival and development of implants prior to their retrieval. Varying cellular activity or tissue formation among different types of implants were indicated through changes in echogenicity. In addition, the response of the recipients towards implants (*i.e.*, through assessment of neovascularization and encapsulation) could be used as a biocompatibility indicator. Our UBM assessment findings were also consistent with our gross observations of implants (*i.e.*, their survival, morphology, and the presence of blood vessels) and

their histological attributes (*i.e.*, the degree of cellular activities and tissue formation). Furthermore, the UBM estimations of implant size and growth prior to their retrieval were correlated with the post-mortem measurements. The decreasing trend in length (21%) and width (18%) of post-mortem retrieved implants would have been expected since the shape and dimensions of the implants change after detachment from the surrounding tissues and skin. Therefore, our results paved the way for the use of UBM for non-invasive and repeated pre-retrieval assessment of implants in future TCI and testis tissue xenografting (TTX) studies; thereby, reducing the number of recipient mice needed for such studies.

Here, we also investigated the addition of different gel matrices (*i.e.*, gelatin, agarose, or collagen) as a binder or carrier of neonatal testis cell aggregates (Experiment 1). This approach, known as cell microencapsulation, has been widely used in tissue engineering, including transplantation of mesenchymal stem cells, and has also been reported in regenerative medicine (Liu and Chang, 2010) Lund *et al.,* 2008; Gasperini *et al.,* 2014; Tzouanas *et al.,* 2014). The rationale for encapsulation of cells by gel-based matrices is to provide a scaffold to facilitate cell movements and interaction by mimicking the *in vivo* 3D arrangement of cells, and provide a semi-permeable medium that allows the exchange of beneficial molecules (*e.g.*, oxygen, nutrients, and growth factors), while eliminating waste products. In addition, the bio-inert attribute of these gel-based matrices also provides a temporary protective barrier that prevents immediate absorption of implanted cells or their rejection (Murua *et al.,* 2008). In the present study, *de novo* tissue formation by neonatal testis cell aggregates encapsulated with certain basic gel based-matrices (gelatin and collagen) points to the potential of using these known matrices as an economical alternative to commercially available matrices with an unknown composition of growth factors.

In Experiment 1, not all implants were retrieved because some had undergone complete absorption. Almost all of these untraceable implants were from the gel-only controls (no cells). No signs of rejection were observed in either experiment. *De novo* testis tissue formation in implanted gel-based matrices containing cells indicates that the added gel-based matrices are safe, biocompatible, and biodegradable. From a qualitative standpoint based on gross morphology and histological assessment, we concluded that collagen and gelatin are more suitable as an encapsulation and binding agent than agarose.

Neovascularization or angiogenesis is a key step in successful incorporation of any graft or implant in the new environment. In this present study, the presence of blood vessels as early as 1 wk after implantation was observed through UBM, and subsequently at gross and histological evaluations. The presence of peripheral blood vessels at 1 wk post-implantation and within the implants at 2 wk post-implantation are evidence of angiogenic progression, indicating that these vessels were of the recipient origin. Timely formation of blood vessels ensures the survival of implanted cells and support of the developing tissues. Although the exact mechanisms of neovascularization in this model have not been determined, it is likely initiated due to the ischemic conditions at the time of implantation, triggering the release of vascular endothelial growth factors (VEGF), as a potent promoter of new blood vessel formation and migration (Ferrara, 2000; Neufeld *et al.,* 1999). VEGF is upregulated in hypoxic conditions to restore the inadequate supply of oxygen to the tissues (Shweiki *et al.,* 1992). When VEGF was used in a TTX study, it promoted a better development of grafts by increasing the graft weight, the number of seminiferous tubules, and presence of advanced germ cells (Schmidt *et al.,* 2006). The promising results of the present TCI study provide an excellent model for the examination of various growth factors on the development of testis tissue.

Severe combined immunodeficient (SCID) mice have been widely used in TTX studies where the lack of both T- and B lymphocytes provides a more conducive environment for the development of grafts (Ito *et al.,* 2002), without compromising the outcomes (Rathi *et al.,* 2006; Goossens *et al.,* 2008; Watanabe *et al.,* 2009). To our knowledge, hairless SCID mice (also designated SHO) have not been used as recipients in TTX or TCI. This mouse strain is a promising new model because in addition to being immunodeficient to the same degree as conventional SCID mice, has the advantage of being hairless which allows better visualization of developing implants and grafts, similar to nude mice. In the present study, we also evaluated the effect of castration on the outcomes of neonatal testis cell implantation in this new recipient model. Immediately after castration of the recipient, serum levels of gonadotropins increase, which theoretically should stimulate the development of newly grafted testis tissues (Honaramooz *et al.,* 2002a; Schlatt *et al.,* 2002a, b; Paris and Schlatt, 2007; Rodriguez-Sosa and Dobrinski, 2009). However, a comprehensive study using SCID and nude mice showed that the recipient gonadal status had no significant effects on the development of neonatal testis tissue (Shinohara *et al.,* 2002; Abbasi and Honaramooz, 2010b). This was also the case in the present study using SHO mice.

The vesicular glands, as with other accessory male glands, rely for their maintenance on continued exposure to testosterone, and thereby become considerably smaller as early as 2 wk after castration (Schlatt *et al.,* 2002a). The size of the vesicular glands hence provides a bioindicator for the levels of circulating testosterone (Honaramooz *et al.,* 2007; Arregui *et al.,* 2012). While in intact recipient mice the circulating testosterone can be from both endogenous (own testes) and xenogeneic sources, any circulating testosterone in castrated mice is solely from the implants. Thus, the difference in the testosterone levels between these two groups would be reflected in the vesicular glands mass. In the present study, no effects of castration on the vesicular gland indices were observed at 2 wk post-implantation, indicating that the implants were capable of supplying sufficient testosterone to the host.

In the present study, we found that the implantation site can affect the growth of implants, where implants located more cranially on the back of mice grew larger compared with those of the caudal region. This rather surprising observation has not been previously reported and the reasons for such a difference are not known. However, differences in relative abundance of blood vessels or relative laxity of the subcutaneous tissue between different regions of the back skin might be a potential cause. Due to the observed effect of implantation site on the growth of implants, randomization of implants sampling can be recommended for future studies to reduce the potential confounding effects of the implantation site within the same mouse.

## 5.6 Conclusions

In conclusion, in the present study, we established an improved method for implantation of neonatal porcine testis cell aggregates which allows more consistent outcomes for *de novo* testis tissue formation. The use of gel matrices as a binder for cell implants led to inconsistent tissue development, and the outcomes were gel-type and cell number-dependent. The injection approach offers a simple and less invasive technique and results in more consistency and greater *de novo* testis tissue formation. Finally, UBM was found to be applicable as a non-invasive monitoring tool, allowing the prediction of implantation outcomes.

## TRANSITION

Subcutaneous injection of porcine testis cell aggregates under the back skin of recipient mice as described in Chapter 5 offers an efficient model for *de novo* formation of testis tissue and results in more consistent implantation outcomes. Therefore, we used this model in Chapter 6 to study the effects of brief pre-implantation exposure of testis cells to various growth factors on the development of testis tissue in the resultant implants.

# CHAPTER 6

# EFFECTS OF GROWTH FACTORS ON *DE NOVO* REGENERATION OF PORCINE TESTIS TISSUE AFTER ECTOPIC IMPLANTATION OF TESTIS CELLS IN MICE [7]

## 6.1 Abstract

The role of growth factors during normal testis development is difficult to assess *in situ*, especially in non-rodents. Ectopic implantation of neonatal pig testis cell aggregates under the back skin of recipient mice results in *de novo* formation/regeneration of testis tissue, hence provides a powerful model for the study of testis formation. In the present study, we used this model to study the effects of exposing donor porcine testis cell aggregates to various growth factors. Each recipient mouse (n = 7 mice/group) was implanted with eight porcine testis cell aggregates (~$100 \times 10^6$ cells/implant) that were exposed to a given dose of different growth factors. A total of 11 groups were examined: EGF (20 ng/mL of cell aggregates: EGF-L or 2μg/mL: EGF-H), GDNF (20 ng/mL: GDNF-L or 2 μg/mL: GDNF-H), FGF2: 1 μg/mL, FGF9: 5 μg/mL, VEGF: 3.5 μg/mL, LIF: 5 μg/mL, SCF: 3.5 μg/mL, RA: $3.5\times10^{-5}$ M, or no growth factors (Control). Two randomly-selected implants were removed from each mouse at 1, 2, and 4 wk, and the remaining implants were retrieved at euthanasia at 8 wk post-implantation. The overall implant recovery rate was 95% and did not differ among groups. The main effects of treatments on *de novo* tissue morphogenesis were enhanced implant weight (FGF2 and LIF), implant area (FGF2, EGF-L, and SCF), and seminiferous cord area (FGF2 and GDNF-L). RA promoted the formation of enlarged cords, GDNF-H led to irregular cords, and FGF2 resulted in the highest ratio of regular cords and lowest ratio of aberrant cords. RA also promoted the number of gonocytes in the implants. The use of higher doses of EGF and GDNF did not improve the results compared with their lower doses. Overall, the use of FGF9 and VEFG had no effects on formation of cords. Rete testis formation occurred earlier in the implants

[7] AHAJ contributed to the conceiving and designing of the study, performed the experiments, and wrote the first draft of the manuscript.

treated with EGF-L, GDNF-H, FGF2, FGF9, or LIF. The results show that even brief pre-implantation exposure of testis cells to growth factors can have profound effects on the formation of testis tissue using the testis cell aggregate implantation model.

## 6.2 Introduction

Ectopic implantation of testis cell aggregates from neonatal donor piglets in recipient mice was shown to result in *de novo* formation/regeneration of testis tissue (Honaramooz *et al.*, 2007). Similar results have also been obtained using other donor species (Dufour *et al.*, 2002; Gassei *et al.*, 2006; Kawasaki *et al.*, 2006, 2010; Arregui *et al.*, 2008). In this testis cell implantation (TCI) model, cells obtained after enzymatic dissociation of donor testes are implanted under the back skin of immunodeficient mice. The heterogeneous population of donor testis cells undergo autonomous rearrangements to form seminiferous cords that are morphologically similar to those of the intact testis. Over time, the newly-developed testis tissue can further develop into a functional testis tissue, capable of supporting spermatogenesis and steroidogenesis (Honaramooz *et al.*, 2007). This unexpected morphogenic capacity of dissociated testis cells to regenerate a functional testis tissue suggests that factors involved in the process of testis development are retained even shortly after birth. Therefore, this unique *in vivo* culture system offers a promising model for the study and manipulation of various potential factors involved in testis development and formation. This can include the study of putative growth factors and molecular cues in the process, which otherwise are inherently difficult to study *in situ*, especially in non-rodent target species.

Testis tissue morphogenesis is a complex process which involves coordinated endocrine, paracrine, and autocrine signaling (Lamb, 1993; Huleihel and Lunenfeld, 2004). Several paracrine, growth, and differentiation factors are believed to play a key role in tissue patterning and organogenesis during the gonadal development. For instance, the presence of fibroblast growth factor 9 (FGF9) is crucial during sex determination (DiNapoli *et al.*, 2006; Kim *et al.*, 2006a), where it regulates Sertoli cell proliferation and testis cord formation, leading to the suppression of genes that are responsible for ovarian development (Park and Jameson, 2005; Jameson *et al.*, 2012). Disruption of FGF9 and its receptors have been shown to result in termination of testis development, which can lead to sex reversal. The vascular endothelial growth factor (VEGF), in addition to being vital

for vasculature development in the embryo (Carmeliet *et al.*, 1996; Ferrara *et al.*, 1996), contributes to the formation of testis cords, as well as promotion and coordination of cell migration from the mesonephros to the developing gonad (Bott *et al.*, 2006; Baltes-Breitwisch *et al.*, 2010; Cool *et al.*, 2011).

The basic fibroblast growth factor 2 (FGF2) and epidermal growth factors (EGF) regulate Leydig cell proliferation and steroidogenesis (Gonzalez *et al.*, 1990; Sordoillet *et al.*, 1991, 1992; Han *et al.*, 1993). On the other hand, certain growth factors are thought to act primarily on germ cells, including the glial cell-derived neurotrophic factor (GDNF), leukemia inhibitory factor (LIF), stem cell factor (SCF), and retinoic acid (RA) (De Miguel *et al.*, 1996; Mauduit *et al.*, 1999; Meng *et al.*, 2000; Kubota *et al.*, 2004a; Hofmann *et al.*, 2005; Wu *et al.*, 2005; Aponte *et al.*, 2006; Zhou *et al.*, 2008; Chung *et al.*, 2009). The GDNF produced by Sertoli cells is an integral part of the stem cell niche within the seminiferous tubules, and promotes the self-renewal of spermatogonial stem cells (SSC) (Meng *et al.*, 2000; Viglietto *et al.*, 2000; Chuma *et al.*, 2005; Hofmann *et al.*, 2005). The SCF and LIF exert their action on germ cells throughout life, ensuring the survival, proliferation, and differentiation of developing germ cells (Matsui *et al.*, 1991; Pesce *et al.*, 1993; Mauduit *et al.*, 1999; Yan *et al.*, 2000a; Aponte *et al.*, 2008). Additionally, RA is responsible for maintaining the pool of fetal gonocytes and promoting their differentiation to spermatogonia after birth (Wang and Culty, 2007; Zhou *et al.*, 2008; Manku *et al.*, 2015). Role of the aforementioned factors in testis development and function has been deciphered primarily using knockout mice and *in vitro* models, with considerably less data on non-rodent species.

The limited literature on the ectopic TCI model has thus far been primarily focused on describing the potential of this model, survival of the implants, formation of testis tissue, and progression of spermatogenesis. The lack of a defined protocol, inconsistency in results, and the low rate of spermatogenic efficiency have limited the application of this potentially powerful model (Gassei *et al.*, 2006; Kita *et al.*, 2007; Arregui *et al.*, 2008a; Campos-Junior *et al.*, 2014; Honaramooz *et al.*, 2007; Arregui *et al.*, 2008a; Dores and Dobrinski, 2014). A single previous study has employed this model to examine the effect of a growth factor on post-implantation testis tissue formation, where treatment with VEGF led to improved outcomes ( Schmidt *et al.*, 2006b; Dores and Dobrinski, 2014). In this latter study, the beneficial effects of VEGF were attributed to its

angiogenic promoting effect, because it is believed that in the early days post-implantation, the implants are likely exposed to ischemic conditions, before blood supply is established.

Despite the regeneration of a functional testis tissue, the implants resulting from this model commonly display low spermatogenic efficiency, because most seminiferous cords/tubules lack germ cells (Honaramooz *et al.*, 2007; Arregui *et al.*, 2008a; Watanabe *et al.*, 2009; Campos-Junior *et al.*, 2014). The reasons for the observed low number of germ cells in the newly developed tubules are not clear, but a low proportion of germ cells in the donor cell populations or subsequent loss of germ cells during development have been proposed as likely causes (Honaramooz *et al.*, 2007; Arregui *et al.*, 2008a). For example, in a study where the donor cell aggregates comprised of ~5% germ cells, only ~11% of the resultant seminiferous tubules contained complete spermatogenesis at 30 wk post-implantation (Honaramooz *et al.*, 2007). To address the potential lack of sufficient germ cells in the donor cell populations, our lab has previously established a three-step enzymatic testis cell isolation protocol that yields ~40% germ cells from donor neonatal pig testes (Yang *et al.*, 2010). We have recently also examined several potential factors that can improve the consistency of the results and spermatogenic efficiency of the TCI model (Chapter 5). Taking advantage of the improved TCI model, the present study was designed to investigate the effect of various growth factors (*i.e.,* EGF, GDNF, FGF2, FGF9, VEGF, LIF, SCF, and RA) on *de novo* formation of porcine testis tissue.

## 6.3 Materials and Methods

### *6.3.1 Animal and Experimental Design*

A total of 165 male piglets of ~2 wk of age were used as donors of testis cells to be implanted under the back skin of recipient mice. Each recipient mouse ($n$ = 7 mice/group, total $n$ = 77) received eight cell aggregate implants (each containing 100 × $10^6$ cells). Immediately prior to implantation (within an hour), cell aggregates were exposed to a designated growth factor/dose. In total, there were 11 groups as follows: EGF (20 ng/mL of cell aggregates: EGF-L or 2μg/mL: EGF-H), GDNF (20 ng/mL: GDNF-L or 2 μg/mL: GDNF-H), FGF2: 1 μg/mL, FGF9: 5 μg/mL, VEGF: 3.5 μg/mL, LIF: 5 μg/mL, SCF: 3.5 μg/mL, RA: $3.5\times10^{-5}$ M, or no growth factors (Control). Two randomly-selected implants were removed from each mouse at 1, 2, and 4 wk, and the remaining

implants retrieved at euthanasia at 8 wk post-implantation. The growth factors used, number of recipients, and implants in each group are summarized in Table 6.1. The recipient mice were double-homozygous severe combined immunodeficient hairless outbred mice (SHO), their housing, handling, anesthesia, and cell aggregate injections were as described in Chapter 5.3.4.2, Chapter 5.3.5.1, and shown in Figure 6.1A. All recipient mice were males and remained intact (were not castrated).

**Table 6.1.** Summary of the growth factors, recipients, and implants in each treatment group.

| Growth factors | Catalogue no. | Manufacturer | Dose | No. implants/mouse (*n*) | No. mice/group (*n*) | Total no. implants/group (*n*) |
|---|---|---|---|---|---|---|
| Epidermal Growth Factor (EGF) | 236-EG-200 | R&D Systems, Inc., Minneapolis, USA. | 20 ng/mL (low) | 8 | 7 | 56 |
| | | | 2 µg/mL (high) | 8 | 7 | 56 |
| Glial Cell Derived Neurotrophic Factor (GDNF) | 212-GD-010 | " | 20 ng/mL (low) | 8 | 7 | 56 |
| | | | 2 µg/mL (high) | 8 | 7 | 56 |
| Fibroblast Growth Factor basic 146 aa (FGF2) | 233-FB-025 | " | 1 µg/mL | 8 | 7 | 56 |
| Fibroblast Growth Factor 9 (FGF9) | 273-F9-025 | " | 5 µg/mL | 8 | 7 | 56 |
| Vascular Endothelial Growth Factor 165 (VEGF) | 293-VE-010 | " | 3.5 µg/mL | 8 | 7 | 56 |
| Leukemia Inhibitory Factor (LIF) | 7734-LF-025 | " | 5 µg/mL | 8 | 7 | 56 |
| Stem Cell Factor (SCF)/c-Kit Ligand | 255-SC-010 | " | 3.5 µg/mL | 8 | 7 | 56 |
| Retinoic Acid (RA) | 0695 | Tocris Bio-Techne, Ontario, CA | $3.5 \times 10^{-5}$ M | 8 | 7 | 56 |

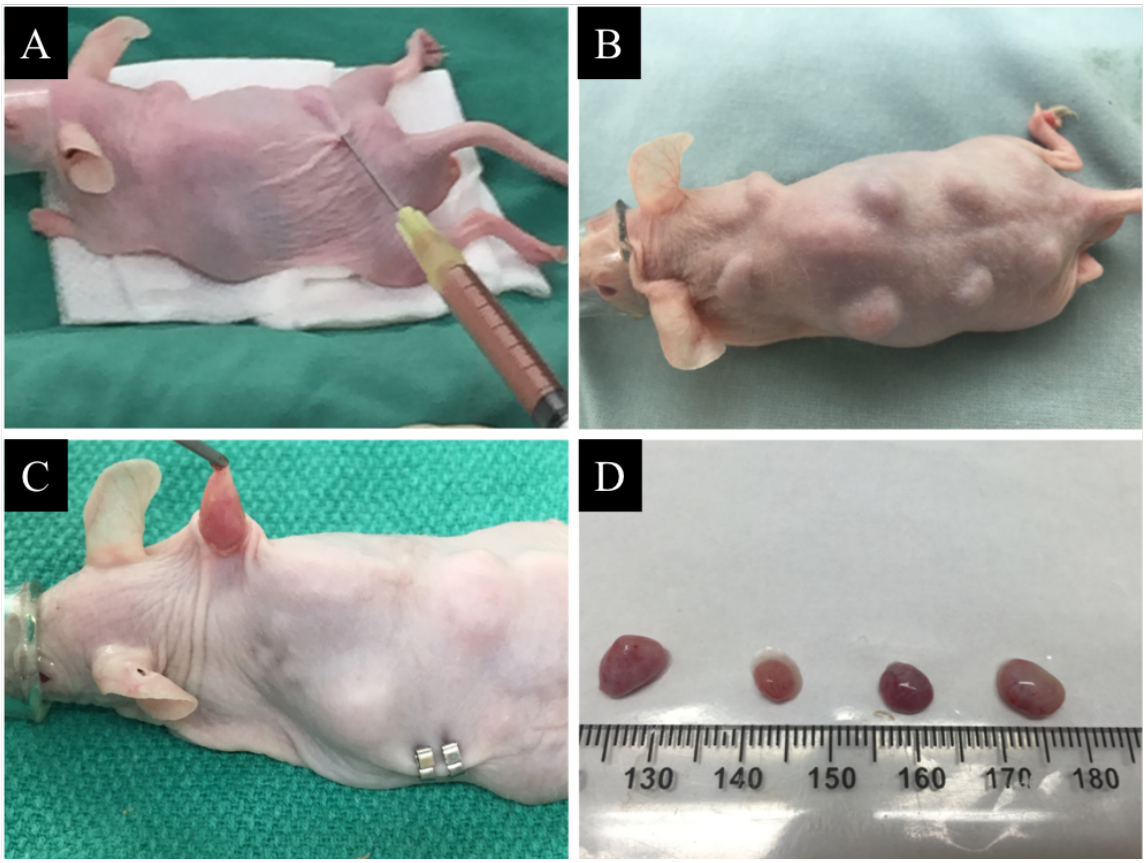


**Fig. 6.1.** Representative photomacrographs demonstrating the recipient mice undergoing ectopic implantation of testis cell aggregates. (A) Testis cell aggregates were injected under the back skin of immunodeficient mice, where each injection site received ~100 × $10^6$ cells in a volume of 0.1 mL. (B) Each mouse received eight subcutaneous implants, four on each side of the midline. (C) Two randomly-selected implants were retrieved at 1, 2, and 4 wk post-implantation, followed by the final retrieval at 8 wk at the time of euthanasia. (D) Individual implants after retrieval.

### *6.3.2 Testis Collection and Preparation*

Donor testes were obtained through aseptic castration of 2 wk old Yorkshire-cross piglets from the Prairie Swine Centre, performed 24 h prior to each implantation day (15 pairs of donor testes/group of mice; hence *n*=165 piglets). The testes were prepared and processed for the isolation of testis cells as described in Chapter 3.3.1.

### *6.3.3 Isolation of Testis Cells*

Isolation of testis cells was performed using a three-step enzymatic digestion method that has been established in our laboratory (Yang *et al.*, 2010; Yang and Honaramooz, 2011). Briefly, the testis parenchyma was pooled to obtain a sufficient number of cells. For the ease and efficiency of isolation, the parenchyma was divided equally into 5 portions, where each portion was transferred into a 14 mL polypropylene round-tube and thoroughly minced with fine scissors for 10 min. Other detailed were as described in Chapter 3.3.2. The resultant cell pellet was resuspended and stored at 4 °C overnight.

### *6.3.4 Cell Aggregate Preparation*

On the day of implantation, the cells were resuspended, filtered, centrifuged at 500×*g* at 16 °C for 10 min, and the media was discarded to yield a compact cell aggregate. The volume of cell aggregates was standardized to 8 mL in a 50 mL falcon test tube, the total dose of a designated growth factor in 0.5 mL was added, and the suspension was gently pipetted to ensure homogeneity. Most growth factors were used as a single dose, while EGF and GDNF were used in two doses (Table 6.1). Except for the RA, all growth factors were of the human recombinant origin (Table 6.1). Preparation of growth factors was according to the manufacturers recommendations. For the controls, the cell aggregates were mixed with 0.5 mL of sterile Dulbecco's phosphate-buffered saline (DPBS; catalogue no. 20-031-CV; Mediatech, Manassas, VA, USA).

### *6.3.5 Cell Aggregate Implantation*

The mouse anesthesia and preparation for cell implantation were as described in Chapter 5.3.5.1. Approximately 0.8 mL of the designated cell aggregates for each mouse was aspirated into a 1-mL syringe, the skin was lifted to create a 'tent' (Fig. 6.1C), the needle (22-gauge) was inserted

subcutaneously on either side of the back skin, and 0.1 mL of the cell aggregates was injected into each site. The cell aggregates were prepared to contain ~100 × $10^6$ cells per 0.1 mL.

### *6.3.6 Retrieval of Implants*

Two implants were randomly retrieved from each mouse at 1, 2, and 4 wk post-implantation, performed under general anesthesia (as described in Chapter 5.3.5.3). A transverse linear skin incision was created adjacent to the edge of an implant, and the implant was gently severed from the skin and surrounding subcutaneous tissue. The incision was then closed with metal wound clips (Michel clips; catalogue no. 12-460-179; Miltex Inc., York, PA, USA) (Fig. 6.1E). The remaining implants were retrieved at 8 wk post-implantation at the time of euthanasia; performed using an overdose of isoflurane, followed by bilateral thoracotomy to ensure death.

### *6.3.7 Tissue Processing and Histology*

The retrieved implants were fixed, processed, embedded in paraffin blocks, sectioned, and stained with hematoxylin and eosin (H&E) as described in Chapter 5.3.6.

### *6.3.8 Gross and Histological Analysis*

The weight of each implant was recorded immediately after retrieval. During the final implant retrieval at euthanasia, the vesicular glands were also removed and their weight index calculated (%; relative to body weight). The histology slides were subjected to histomorphometric analysis, where each mouse (unless stated otherwise) was treated as the experimental unit. From each implant, digital micrographs were captured using a light microscope equipped with digital photomicrography (Northern Eclipse Image Analysis software version 7.0; Empix Imaging, Mississauga, ON, Canada). The obtained images included 40× magnification for general observation of the implants (1 image) and 400× magnification (5 randomly-selected fields) for detailed morphometric analysis. The histomorphometric evaluations of implants included their general development, seminiferous cords (SC), and prevalence of germ cells. The collected data included the number of recovered implants, implants showing *de novo* morphogenesis, SC development, rete testis-like structures (RT), and fluid-filled cavities (FFC); expressed as their prevalence and percentage (%). The surface area measurements included the total implant area

($mm^2$), the total area occupied by SC (%; relative to total implant area), the relative area of SC by category (*i.e.,* % of regular SC, irregular SC, enlarged SC, and aberrant SC; relative to total SC occupied area). The relative number of gonocytes (per 1,000 Sertoli cells) in 2 wk samples was also counted in five randomly-selected fields per slide (at 400× magnification). All the measurements and counting were performed using ImageJ software (National Institutes of Health, Bethesda, Maryland, USA).

### *6.3.9 Statistical Analyses*

All data are presented as mean ± standard error of mean (SEM). Unless otherwise stated, the statistical analyses were performed using repeated measures analysis of variance (ANOVA) and Chi-square tests. For percentage expression, the data were transformed using the Arcsin function prior to analysis. The level of significance was set at $P < 0.05$. Data were analyzed using the SPSS (Version 22.0, SPSS Inc., Armonk, NY, USA).

## 6.4 Results

### *6.4.1 Gross Evaluations*

#### *6.4.1.1 Recipient Mouse Body Weight and Vesicular Gland Index*

Five out of the 77 recipient mice died prior to the scheduled time of euthanasia; they were from different groups and died at various time points post-implantation. The body weight (BW) and vesicular gland (VG) index of the mice, recorded at the time of euthanasia (8 wk post-implantation), did not differ among all groups ($P > 0.05$, treatment *vs.* control or low *vs.* high dose) (Table 6.2).

#### *6.4.1.2 Implant Recovery and Implant Weight*

We retrieved a total of 563 identifiable implants from the remaining 596 potential implants, which included recovery of some samples from the mice that died prematurely. Therefore, the overall implant recovery rate was ~95%, which ranged between 84% and 98%, but did not differ among the groups ($P > 0.05$, Table 6.2). The effect of time on implant weight was significant for all treatment groups ($P < 0.05$), except EGF-H, which only showed a tendency when compared with the control ($P = 0.054$; Fig. 6.2 and 6.3). The implant weight increased over time in most groups, except in EGF-H, GDNF-H, and RA groups. The effect of treatment on implant weight was significant only for FGF2 and LIF groups ($P < 0.05$), where the implant weight in FGF2 group at 4 wk (99.3 ± 8.3 mg) was greater than that of the control (66.5 ± 10.1 mg; $P < 0.05$; Fig. 6.3A and 6.3D). Interactions were also observed between the effects of time and treatment for implants weight in control *vs.* EGF-H, EGF-L *vs.* EGF-H, GDNF-L *vs.* GDNF-H and control *vs.* RA groups ($P < 0.05$; Fig. 6.2B, 6.2C, 6.2F, and 6.3F, respectively). Among these groups, unlike the control, the implant weight in EGF-H and RA groups did not differ over time ($P > 0.05$). Weight of implants in the EGF-H group was greater than EGF-L at 1- and 2 wk, and than control at 2 wk, while in the RA group was less than control at 8 wk ($P < 0.05$; Fig. 6.2 and 6.3). The weight of implants retrieved at 8 wk negatively correlated with the VG index in EGF-H and GDNF-L groups, as well as overall (Table 6.3).

**Table 6.2.** The recipient mouse body weight, vesicular gland index, and the relative number of implants retrieved at the time of euthanasia.

| Group | Mouse BW (g) | VG index (%) | No. implant retrieved/total (%) |
|---|---|---|---|
| Control | 32.32 ± 1.2 | 0.69 ± 0.40 | 42/46 (91) |
| EGF-L | 33.62 ± 0.9 | 0.61 ± 0.10 | 53/54 (93) |
| EGF-H | 34.99 ± 1.4 | 0.77 ± 0.04 | 55/56 (98) |
| GDNF-L | 32.60 ± 1.3 | 0.70 ± 0.10 | 47/50 (94) |
| GDNF-H | 31.79 ± 0.5 | 0.78 ± 0.03 | 47/56 (84) |
| FGF2 | 33.56 ± 1.1 | 0.67 ± 0.03 | 54/56 (96) |
| FGF9 | 33.73 ± 0.7 | 0.79 ± 0.05 | 55/56 (98) |
| VEGF | 33.95 ± 0.9 | 0.64 ± 0.10 | 52/54 (96) |
| LIF | 34.20 ± 0.9 | 0.69 ± 0.04 | 53/56 (95) |
| SCF | 32.04 ± 0.5 | 0.73 ± 0.04 | 52/56 (93) |
| RA | 30.90 ± 0.8 | 0.77 ± 0.01 | 53/56 (95) |
| | | Total | 563/596 (94.5) |

Mouse body weight (BW: g); vesicular gland index (VG: % weight of VG/BW); epidermal growth factor (EGF); glial-derived neurotrophic factor (GDNF); fibroblast growth factor (FGF2); fibroblast growth factor 9 (FGF9); vascular endothelial growth factor (VEGF); leukemia inhibitory factor (LIF); stem cell factor (SCF); retinoic acid (RA).
Each group was compared with the control.
The high (H) and low (L) doses of the same growth factor groups were compared with each other.
BW and VG index data were analyzed using independent t-tests.
Implant % were analyzed using the Chi-square tests.
The data did not differ *(P* > 0.05) among all compared groups.

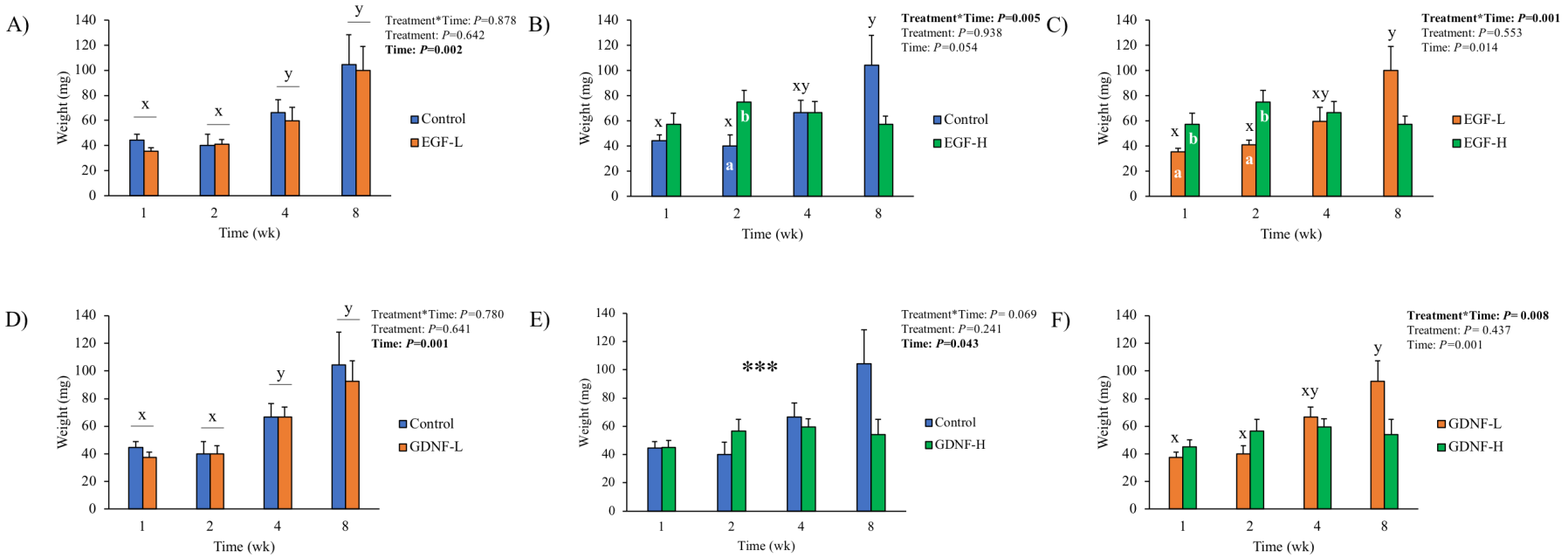


**Fig. 6.2.** The weight of implants (mg) in (A-C) the epidermal growth factor (EGF) and (D-F) glial-derived neurotrophic growth factor (GDNF) groups over time. Two doses of each growth factor were evaluated, low dose (20 ng/mL of cells): (A) EGF-L and (D) GDNF-L, and high dose (2 mg/mL of cells): (B) EGF-H and (E) GDNF-H. The weight of implants was compared with the control and between the doses (low *vs.* high) (C) and (F). The growth factors were added to the neonatal porcine testis cell aggregates (~100 $\times 10^6$ cells) before implantation under the back skin of recipient mice ($n$ = 7 per group). The control implants received no growth factor. Implants were retrieved at 1, 2, 4, and 8 wk post-implantation. Data are mean ± SEM. [ab] Data with different letters between treatments differ significantly ($P < 0.05$). [xy] Data with different letters over time differ significantly ($P < 0.05$). [***]The main effect of time was significant ($P < 0.05$), but no individual group differed ($P > 0.05$) at post-hoc analysis.

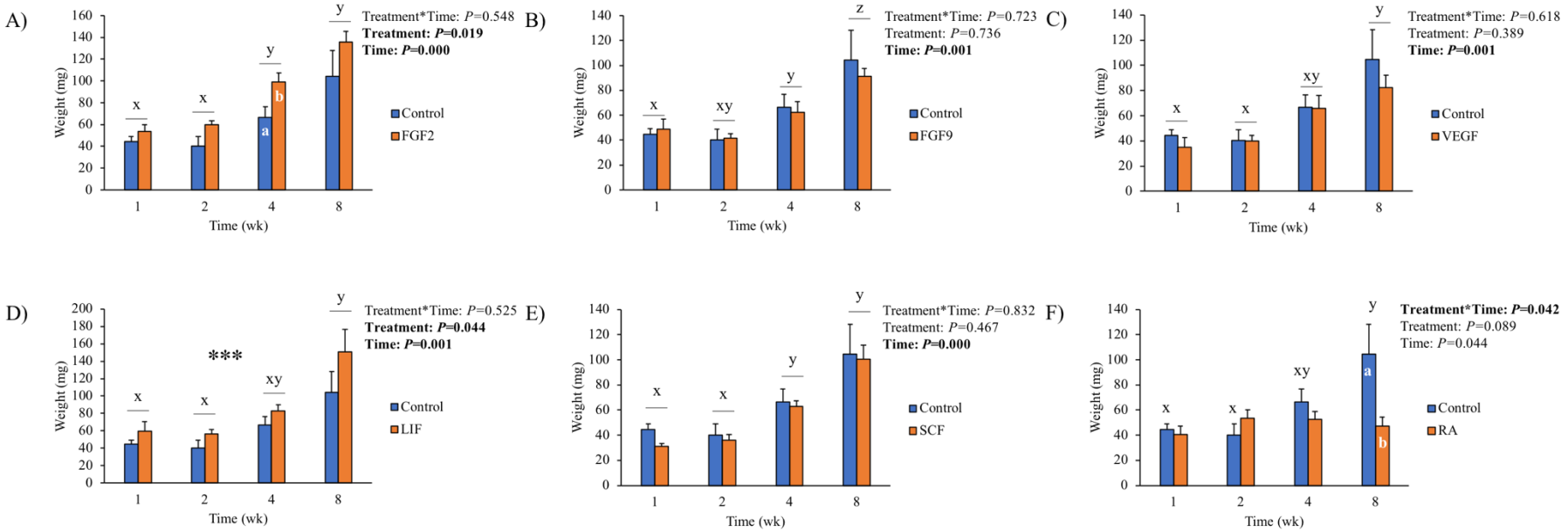


**Fig. 6.3.** The weight of implants (mg) in the (A) basic fibroblast growth factor (FGF2), (B) fibroblast growth factor 9 (FGF9), (C) vascular endothelial growth factor (VEGF), (D) leukemia inhibitory factor (LIF), (E) stem cell factor (SCF), and (F) retinoic acid (RA) groups over time. The implants weight was compared with the control and over time. The growth factors were added to the neonatal porcine testis cell aggregates (~100 $\times 10^6$ cells) before implantation under the back skin of recipient mice ($n$ = 7 per group). The control implants received no growth factor. Implants were retrieved at 1, 2, 4, and 8 wk post-implantation. Data are mean ± SEM. $^{ab}$ Data with different letters between treatments differ significantly ($P < 0.05$). $^{xyz}$ Data with different letters over time differ significantly ($P < 0.05$). $^{***}$The main effect of treatment was significant ($P < 0.05$), but no individual group differed ($P > 0.05$) at post-hoc analysis.

**Table 6.3.** Relationships among the recipient mouse vesicular gland index, implant weight, implant area, and seminiferous cord area at euthanasia (8 wk post-implantation) in EGF and GDNF groups of implants.

| Group (No. mice) | Variable | VG Index (%) | | Implant weight (mg) | | Implant area ($mm^2$) | | SC area ($mm^2$) | |
|---|---|---|---|---|---|---|---|---|---|
| | | *r* | *P* | *r* | *P* | *r* | *P* | *r* | *P* |
| Overall (*n* = 72) | VG Index | - | - | **-0.29** | **0.01** | -0.12 | 0.28 | -0.18 | 0.12 |
| | Implant weight | **-0.29** | **0.01** | - | - | **0.32** | **0.00** | 0.01 | 0.97 |
| | Implant area | -0.12 | 0.28 | **0.32** | **0.00** | - | - | **0.37** | **0.01** |
| | SC area | -0.18 | 0.12 | 0.01 | 0.97 | **0.37** | **0.01** | - | - |
| Control (*n* = 5) | VG Index | - | - | 0.02 | 0.98 | 0.41 | 0.37 | 0.24 | 0.61 |
| | Implant weight | 0.02 | 0.98 | - | - | **-0.83** | **0.02** | **-0.88** | **0.01** |
| | Implant area | 0.41 | 0.37 | **-0.83** | **0.02** | - | - | **0.89** | **0.01** |
| | SC area | 0.24 | 0.61 | **-0.88** | **0.01** | **0.89** | **0.01** | - | - |
| EGF-L (*n* = 6) | VG Index | - | - | -0.57 | 0.19 | -0.07 | 0.89 | -0.36 | 0.42 |
| | Implant weight | -0.57 | 0.19 | - | - | -0.64 | 0.12 | -0.51 | 0.25 |
| | Implant area | -0.07 | 0.89 | -0.64 | 0.12 | - | - | **0.92** | **0.00** |
| | SC area | -0.36 | 0.42 | -0.51 | 0.25 | **0.92** | **0.00** | - | - |
| EGF-H (*n* = 7) | VG Index | - | - | **-0.79** | **0.04** | -0.70 | 0.08 | **-0.42** | **0.04** |
| | Implant weight | **-0.79** | **0.04** | - | - | 0.53 | 0.22 | 0.45 | 0.31 |
| | Implant area | -0.70 | 0.08 | 0.53 | 0.22 | - | - | -0.16 | 0.74 |
| | SC area | **-0.42** | **0.04** | 0.45 | 0.31 | -0.16 | 0.74 | - | - |
| GDNF-L (*n* = 7) | VG Index | - | - | **-0.86** | **0.01** | 0.35 | 0.45 | 0.27 | 0.56 |
| | Implant weight | **-0.86** | **0.01** | - | - | 0.05 | 0.92 | 0.04 | 0.93 |
| | Implant area | 0.35 | 0.45 | 0.05 | 0.92 | - | - | 0.01 | 0.98 |
| | SC area | 0.27 | 0.56 | 0.04 | 0.93 | 0.01 | 0.98 | - | - |
| GDNF-H (*n* = 6) | VG Index | - | - | 0.64 | 0.12 | **0.92** | **0.00** | -0.32 | 0.49 |
| | Implant weight | 0.64 | 0.12 | - | - | 0.47 | 0.28 | -0.47 | 0.28 |
| | Implant area | **0.92** | **0.00** | 0.47 | 0.28 | - | - | -0.48 | 0.28 |
| | SC area | -0.32 | 0.49 | -0.47 | 0.28 | -0.48 | 0.28 | - | - |

Vesicular gland (VG) index (% weight of VG/body weight); epidermal growth factor (EGF); glial-derived neurotrophic factor (GDNF).
The high (H) and low (L) doses of the same growth factor groups were compared with each other.
Each group was also compared with the control.
Pearson's correlation coefficients (*r*) were considered significant when $P < 0.05$.

### *6.4.2 Histological Evaluations*

#### *6.4.2.1 Implant Area*

An effect of time on implant area, measured at the widest cross-section of the samples, was observed in all groups ($P < 0.05$; Fig. 6.4 and 6.5). Overall, the implant area of 1 and 2 wk samples was smaller ($P < 0.05$) than that of 4 and 8 wk samples. An effect of treatment on implant area was observed in EGF-L, FGF2, and SCF groups, and in GDNF-L *vs.* GDNF-H groups ($P < 0.05$; Fig. 6.4A, 6.5A, 6.5E, and 6.4F, respectively). Among groups, the implant area in EGF-L and SCF groups at 8 wk was larger than that in control ($7.60 \pm 0.4$ mm$^2$; $P < 0.05$; Fig. 6.4A and 6.5E). Interactions were observed between the effects of time and treatment for implants area in control *vs.* GDNF-H, EGF-L *vs.* EGF-H, and GDNF-L *vs.* GDNF-H ($P < 0.05$; Fig. 6.4E, 6.4C, and 6.4F, respectively). The area of implants was larger in EGF-H than EGF-L at 2 wk and larger in GDNF-H than control at 1 wk, while at 8 wk it was smaller in GDNF-H than both GDNF-L and control ($P < 0.05$; Fig. 6.4). At 8 wk, the overall area of implants positively correlated with the implants weight ($r = 0.32$; $P < 0.05$). Among individual groups, this correlation was strongly negative in the control ($r = - 0.83$; $P < 0.05$), while it was strongly positive in LIF ($r = 0.88$; $P < 0.05$; Tables 6.3 and 6.4). The implant area and VG index were correlated only in GDNF-H group ($r = 0.92$; $P < 0.005$) and VEGF ($r = -0.87$; $P < 0.05$; Table 6.3 and 6.4).

#### *6.4.2.2 General Development/Regeneration of Testis Tissue*

Upon histological examination, a total of 500 out of 563 retrieved implants (89%) had at least some level of *de novo* regenerated testis parenchyma. Typical development observed in implants at 1 wk included enclosure within a defined connective tissue capsule, and the presence of random cellular arrangements (Fig. 6.6A). In some implants at 1 wk post-implantation, the formation of seminiferous cords (SC) was also evident, which first appeared at the periphery of implants. At 2 wk post-implantation, individual implants typically had both random cellular arrangements and SC formations at the same time (Fig. 6.6B). At 4 wk, the area covered by random cellular arrangements was reduced and, especially at 8 wk, was replaced by cordal/tubular structures, and occasionally by rete testis-like formations (Fig. 6.6C-D). The overall percentage of implants with regenerated

testis tissue ranged from 82% to 93%, which did not differ among groups or over time ($P > 0.05$; Table 6.5).

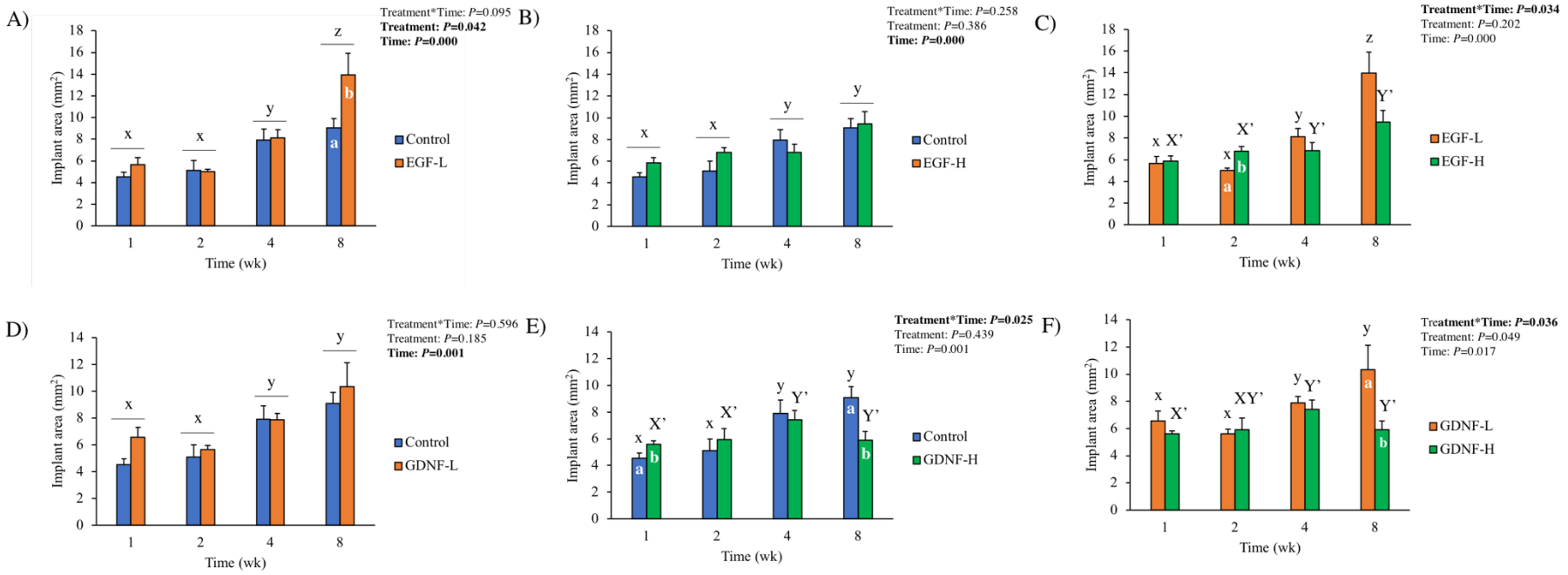


**Fig. 6.4.** The implant areas ($mm^2$) measured at the widest cross-section in (A-C) epidermal growth factor (EGF) and (D-F) glial-derived neurotrophic factor (GDNF) samples over time. Two doses of each growth factor were evaluated, low dose (20 ng/mL of cells): (A) EGF-L and (D) GDNF-L, and high dose (2 mg/mL of cells): (B) EGF-H and (E) GDNF-H. The implant areas were compared with the control and between the doses (low *vs.* high) (C) and (F). The growth factors were added to the neonatal porcine testis cell aggregates (~100 $\times 10^6$ cells) before implantation under the back skin of recipient mice ($n = 7$ per group). The control implants received no growth factor. Implants were retrieved at 1, 2, 4, and 8 wk post-implantation. Data are mean ± SEM. $^{ab}$ Data with different letters between treatments differ significantly ($P < 0.05$). $^{xyz/X'Y'}$ Data with different letters over time differ significantly ($P < 0.05$).

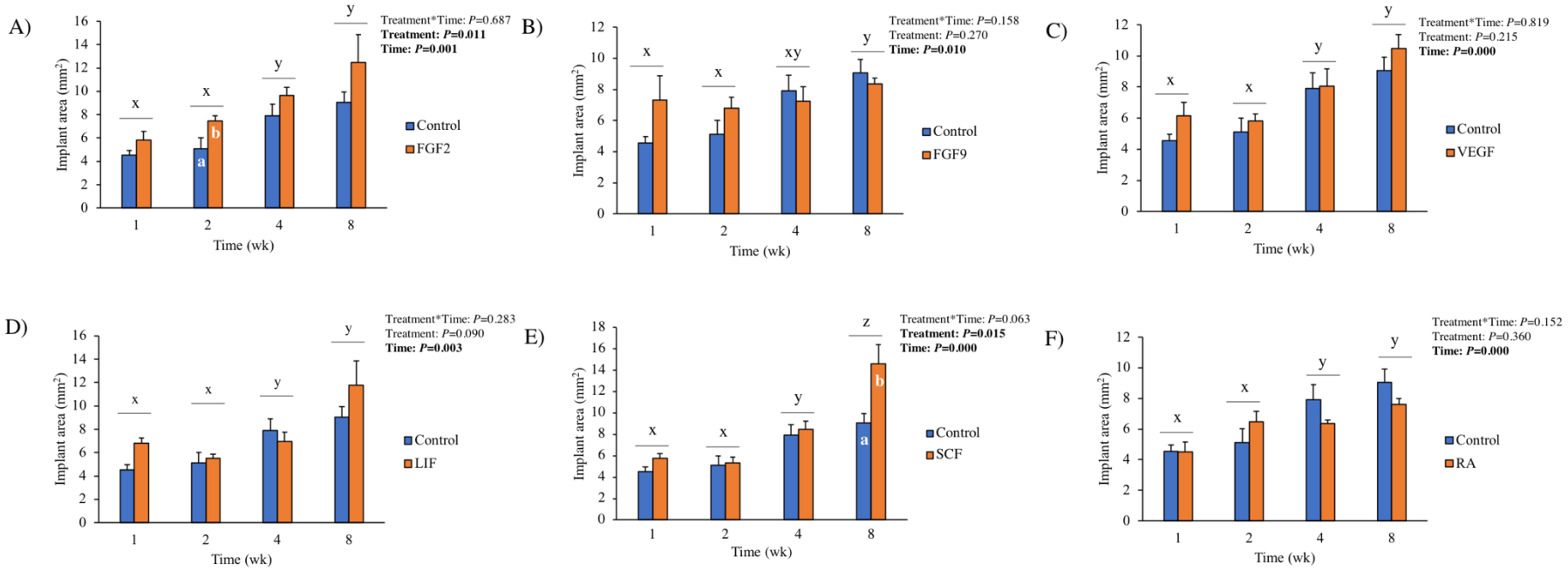


**Fig. 6.5.** The implant areas ($mm^2$) measured at the widest cross-section in the (A) basic fibroblast growth factor (FGF2), (B) fibroblast growth factor 9 (FGF9), (C) vascular endothelial growth factor (VEGF), (D) leukemia inhibitory factor (LIF), (E) stem cell factor (SCF), and (F) retinoic acid (RA) groups over time. The implant areas were compared with the control and over time. The growth factors were added to the neonatal porcine testis cell aggregates (~100 $\times 10^6$ cells) before implantation under the back skin of recipient mice ($n = 7$ per group). The control implants received no growth factor. Implants were retrieved at 1, 2, 4, and 8 wk post-implantation. Data are mean ± SEM. $^{ab}$ Data with different letters between treatments differ significantly ($P < 0.05$). $^{xyz}$ Data with different letters over time differ significantly ($P < 0.05$).

**Table 6.4.** Relationships among the recipient mouse vesicular gland index, implant weight, implant area, and seminiferous cord area at euthanasia (8 wk post-implantation) in FGF2, FGF9, LIF, SCF, and RA groups of implants.

| Group (No. mice) | Variable | VG Index (%) | | Implant weight (mg) | | Implant area ($mm^2$) | | SC area ($mm^2$) | |
|---|---|---|---|---|---|---|---|---|---|
| | | *r* | *P* | *r* | *P* | *r* | *P* | *r* | *P* |
| FGF2 (*n* = 7) | VG Index | - | - | 0.18 | 0.70 | 0.69 | 0.09 | -0.18 | 0.70 |
| | Implant weight | 0.18 | 0.70 | - | - | 0.43 | 0.34 | 0.19 | 0.68 |
| | Implant area | 0.69 | 0.09 | 0.43 | 0.34 | - | - | 0.46 | 0.30 |
| | SC area | -0.18 | 0.70 | 0.19 | 0.68 | 0.46 | 0.30 | - | - |
| FGF9 (*n* = 7) | VG Index | - | - | -0.27 | 0.56 | -0.05 | 0.92 | 0.21 | 0.65 |
| | Implant weight | -0.27 | 0.56 | - | - | 0.26 | 0.57 | -0.26 | 0.58 |
| | Implant area | -0.05 | 0.92 | 0.26 | 0.57 | - | - | -0.68 | 0.09 |
| | SC area | 0.21 | 0.65 | -0.26 | 0.58 | -0.68 | 0.09 | - | - |
| VEGF (*n* = 6) | VG Index | - | - | 0.19 | 0.69 | **-0.87** | **0.11** | 0.25 | 0.59 |
| | Implant weight | 0.19 | 0.69 | - | - | -0.09 | 0.85 | 0.25 | 0.59 |
| | Implant area | **-0.87** | **0.11** | -0.09 | 0.85 | - | - | -0.48 | 0.27 |
| | SC area | 0.25 | 0.59 | 0.25 | 0.59 | -0.48 | 0.27 | - | - |
| LIF (*n* = 7) | VG Index | - | - | 0.44 | 0.32 | 0.24 | 0.61 | -0.02 | 0.97 |
| | Implant weight | 0.44 | 0.32 | - | - | **0.88** | **0.01** | 0.14 | 0.77 |
| | Implant area | 0.24 | 0.61 | **0.88** | **0.01** | - | - | 0.42 | 0.35 |
| | SC area | -0.02 | 0.97 | 0.42 | 0.35 | 0.42 | 0.35 | - | - |
| SCF (*n* = 7) | VG Index | - | - | -0.37 | 0.41 | 0.05 | 0.92 | 0.26 | 0.58 |
| | Implant weight | -0.37 | 0.41 | - | - | 0.32 | 0.49 | -0.16 | 0.73 |
| | Implant area | 0.05 | 0.92 | 0.32 | 0.49 | - | - | 0.45 | 0.31 |
| | SC area | 0.26 | 0.58 | -0.16 | 0.73 | 0.45 | 0.31 | - | - |
| RA (*n* = 7) | VG Index | - | - | 0.06 | 0.90 | -0.69 | 0.09 | -0.46 | 0.30 |
| | Implant weight | 0.06 | 0.90 | - | - | 0.21 | 0.65 | 0.35 | 0.44 |
| | Implant area | -0.69 | 0.09 | 0.21 | 0.65 | - | - | 0.16 | 0.73 |
| | SC area | -0.46 | 0.30 | 0.35 | 0.44 | 0.16 | 0.73 | - | - |

Vesicular gland (VG) index (% weight of VG/body weight); fibroblast growth factor (FGF2); fibroblast growth factor 9 (FGF9); vascular endothelial growth factor (VEGF); leukemia inhibitory factor (LIF); stem cell factor (SCF); retinoic acid (RA).
Each group was compared with the control.
Pearson's correlation coefficients (*r*) were considered significant when $P < 0.05$.
Data for the control group is already included in Table 6.3.

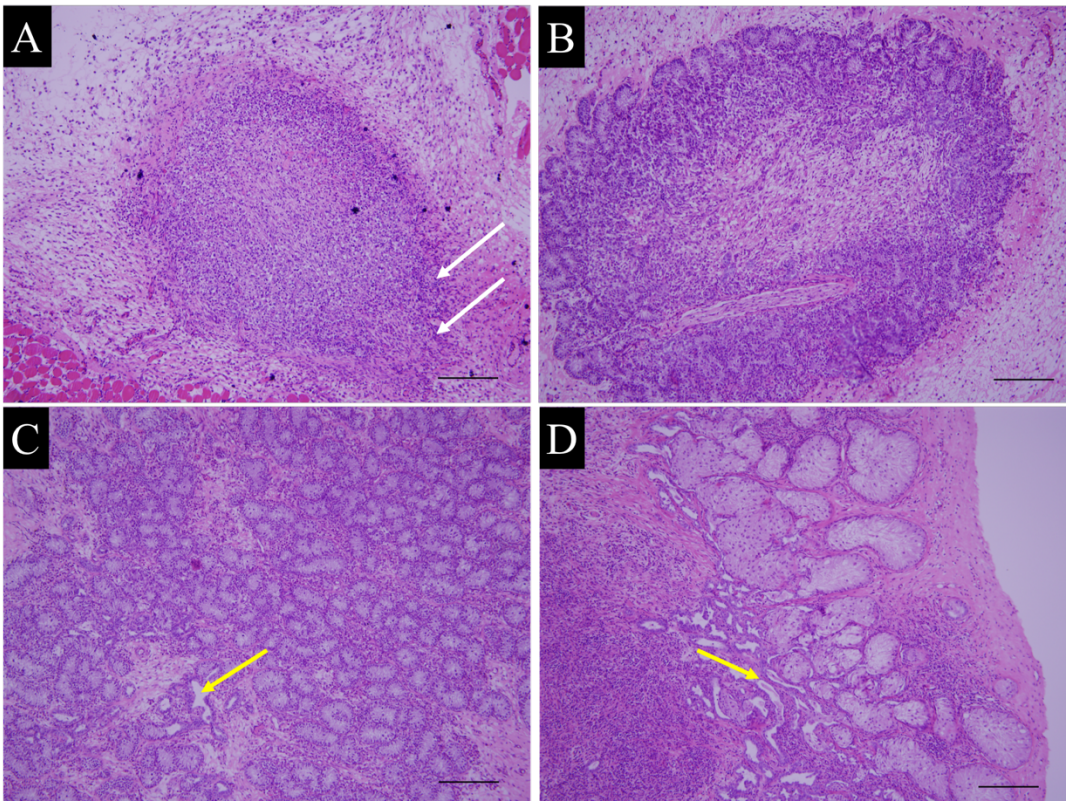


**Fig. 6.6.** Representative histological photomicrographs demonstrating *de novo* morphogenesis of porcine testis tissue after implantation of porcine testis cell aggregates under the back skin of recipient mice. Each image represents a typical morphology observed at 1, 2, 4, and 8 wk post-implantation. (A) The morphogenesis at 1 wk was characterized by random cellular formations, demarcated in encapsulated areas. Note the initial formation of seminiferous cords starting from the periphery of the implants (white arrows). (B) More defined formation of seminiferous cords seen at 2 wk post-implantation; overall morphology of the cords starting to resemble seminiferous cords in intact testis tissue. The area occupied by the cords also continuously increased. (C) The random cellular formations diminished at 4 wk, and the implant area was almost entirely occupied by seminiferous cords. (D) The testis tissue underwent extensive morphological changes over time. The presence of large and irregularly shaped seminiferous cords become especially prominent at 8 wk post-implantation. Note also the presence of the rete testis-like structures, which initially developed in the center of implants and then branched radially over time (yellow arrows). (H&E Staining, Scale bar: 200 μm).

**Table 6.5.** The prevalence of testis tissue regeneration among implants of different groups and over time.

| Group | No. implants with regenerated testis tissue/total implants (%) | | | | |
|---|---|---|---|---|---|
| | 1 wk | 2 wk | 4 wk | 8 wk | Overall |
| Control | 10/13 (77) | 10/11(91) | 9/10 (90) | 8/8 (100) | 37/42 (88) |
| EGF-L | 14/14 (100) | 13/14 (93) | 10/13 (77) | 12/12 (100) | 49/53 (93) |
| EGF-H | 14/14 (100) | 12/14 (86) | 8/13 (62) | 13/14 (93) | 47/55 (86) |
| GDNF-L | 14/14 (100) | 9/11 (82) | 9/10 (90) | 11/12 (92) | 43/47 (92) |
| GDNF-H | 9/11 (82) | 9/13 (69) | 10/12 (83) | 11/11 (100) | 39/47 (83) |
| FGF2 | 11/12 (92) | 12/14 (86) | 12/14 (86) | 14/14 (100) | 49/54 (91) |
| FGF9 | 13/13 (100) | 11/14 (79) | 13/14 (93) | 12/14 (86) | 49/55 (89) |
| VEGF | 12/14 (86) | 13/14 (93) | 11/12 (92) | 12/12 (100) | 48/52 (92) |
| LIF | 10/13 (77) | 13/13 (100) | 11/13 (85) | 14/14 (100) | 48/53 (91) |
| SCF | 9/14 (64) | 13/14 (93) | 9/12 (75) | 12/12 (100) | 43/52 (83) |
| RA | 12/13 (92) | 11/14 (79) | 12/13 (92) | 13/13 (100) | 48/53 (91) |
| Total | 128/145 (88.2) | 126/146 (85.1) | 114/136 (83.8) | 132/136 (97.1) | 500/563 (88.8) |

Data are the number and % of implants showing *de novo* morphogenesis of testis tissue among the retrieved samples at each time point.
Epidermal growth factor (EGF); glial-derived neurotrophic factor (GDNF); fibroblast growth factor (FGF2); fibroblast growth factor 9 (FGF9); vascular endothelial growth factor (VEGF); leukemia inhibitory factor (LIF); stem cell factor (SCF); retinoic acid (RA).
The high (H) and low (L) doses of the same growth factor groups were compared with each other.
Each group was also compared with the control.
The data were compared using the Chi-square tests.
The data did not differ ($P > 0.05$) among all compared groups.

#### *6.4.2.3 Formation of Seminiferous Cords (SC)*

##### *6.4.2.3.1 First Appearance and Prevalence of SC in Implants*

Implants displaying SC formation appeared as early as 1 wk post-implantation (earliest) in implants from recipient mice of all groups, except RA, in which the earliest implants with SC were observed at 2 wk (Table 6.6). Compared with the control, first appearance of SC in implants was advanced in all groups, except LIF and RA groups. All implants in all group contained SC by 4 wk, except those in RA group with some implants showing SC as late as 8 wk. Although, the overall number of implants with SC did not differ among groups ($P > 0.05$), 1 wk implants in RA group contained no SC (0%), which was different from the control (30%, $P < 0.05$), and those in EGF-L group had less SC (14%) than EGF-H (64%, $P < 0.01$). At 2 wk, more implants in RA and FGF2 groups had developed SC than in controls (91% and 92%, respectively *vs.* 50%; Table 6.6).

##### *6.4.2.3.2 SC Area in Implants*

The area occupied by SC in implants (%, relative to the total implant area) increased at each examined time point (*i.e.*, from 2 to 4 wk, and from 4 to 8 wk) in all groups ($P < 0.05$; Fig. 6.7 and 6.8). An effect of treatment on the SC area was observed for GDNF-L, FGF2 groups and in GDNF-L *vs.* GDNF-H groups ($P < 0.05$; Fig. 6.7D, 6.8A, and 6.7F, respectively). The SC area in 2 and 4 wk GDNF-L implants was larger than both the control and GDNF-H groups (Fig. 6.7D and 6.7F). Overall, there was a positive correlation between SC area and implant area ($r = 0.37$; $P < 0.05$). Among the groups, this correlation was strongly positive for the control ($r = 0.89$; $P < 0.01$) and EGF-L groups ($r = 0.92$; $P < 0.01$). However, SC area in control implants had a strongly negative correlation with implants weight ($r = -0.88$; $P < 0.05$; Table 6.3).

**Table 6.6.** The prevalence and first appearance of seminiferous cord formations among implants from different groups.

| Group | No. implants with SC/total implants (%) | | | | | First appearance (wk) | | |
|---|---|---|---|---|---|---|---|---|
| | 1 wk | 2 wk | 4 wk | 8 wk | Overall | Earliest | Median | Latest |
| Control | 3/10 (30) | 5/10 (50) | 9/9 (100) | 8/8 (100) | 25/37 (68) | 1 | 4 | 4 |
| EGF-L | 2/14 (14) | 10/13 (77) | 10/10 (100) | 12/12 (100) | 34/49 (69) | 1 | 2 | 4 |
| EGF-H | **9/14 (64)††** | 6/12 (50) | 8/8 (100) | 13/13 (100) | 36/47 (77) | 1 | 2 | 4 |
| GDNF-L | 9/14 (64) | 8/9 (89) | 9/9 (100) | 11/11 (100) | 37/43 (86) | 1 | 2 | 4 |
| GDNF-H | 5/9 (56) | 6/9 (67) | 10/10 (100) | 11/11 (100) | 32/39 (82) | 1 | 2 | 4 |
| FGF2 | 4/11 (36) | **11/12 (92)*** | 12/12 (100) | 14/14 (100) | 41/49 (84) | 1 | 2 | 4 |
| FGF9 | 5/13 (39) | 9/11 (82) | 13/13 (100) | 12/12 (100) | 39/49 (80) | 1 | 2 | 4 |
| VEGF | 5/12 (42) | 10/13 (77) | 11/11 (100) | 12/12 (100) | 38/48 (79) | 1 | 2 | 4 |
| LIF | 3/10 (30) | 8/13 (62) | 10/11 (91) | 14/14 (100) | 35/48 (73) | 1 | 4 | 8 |
| SCF | 3/9 (33) | 8/13 (62) | 9/9 (100) | 12/12 (100) | 32/43 (74) | 1 | 2 | 4 |
| RA | **0/12 (0)*** | **10/11(91)*** | 12/12 (100) | 13/13 (100) | 35/48 (73) | 2 | 4 | 4 |
| Total | 48/128 (37.5) | 91/126 (72.2) | 113/114 (99.1) | 132/132 (100) | 384/500 (76.8) | | | |

Data are the prevalence of seminiferous cord (SC) formations and their first appearance among implants showing *de novo* morphogenesis of testis tissue at each time point.
Epidermal growth factor (EGF); glial-derived neurotrophic factor (GDNF); fibroblast growth factor (FGF2); fibroblast growth factor 9 (FGF9); vascular endothelial growth factor (VEGF); leukemia inhibitory factor (LIF); stem cell factor (SCF); retinoic acid (RA).
The high (H) and low (L) doses of the same growth factor groups were compared with each other.
Each group was also compared with the control.
The data were compared using the Chi-square tests
The first appearance of SC was assessed based on their first occurrence; earliest, the midpoint of occurrence; median, and the last occurrence from all implant retrieved in a single recipient.
* $P < 0.05$ compared to the control.
†† $P < 0.01$ compared to the lower dose.

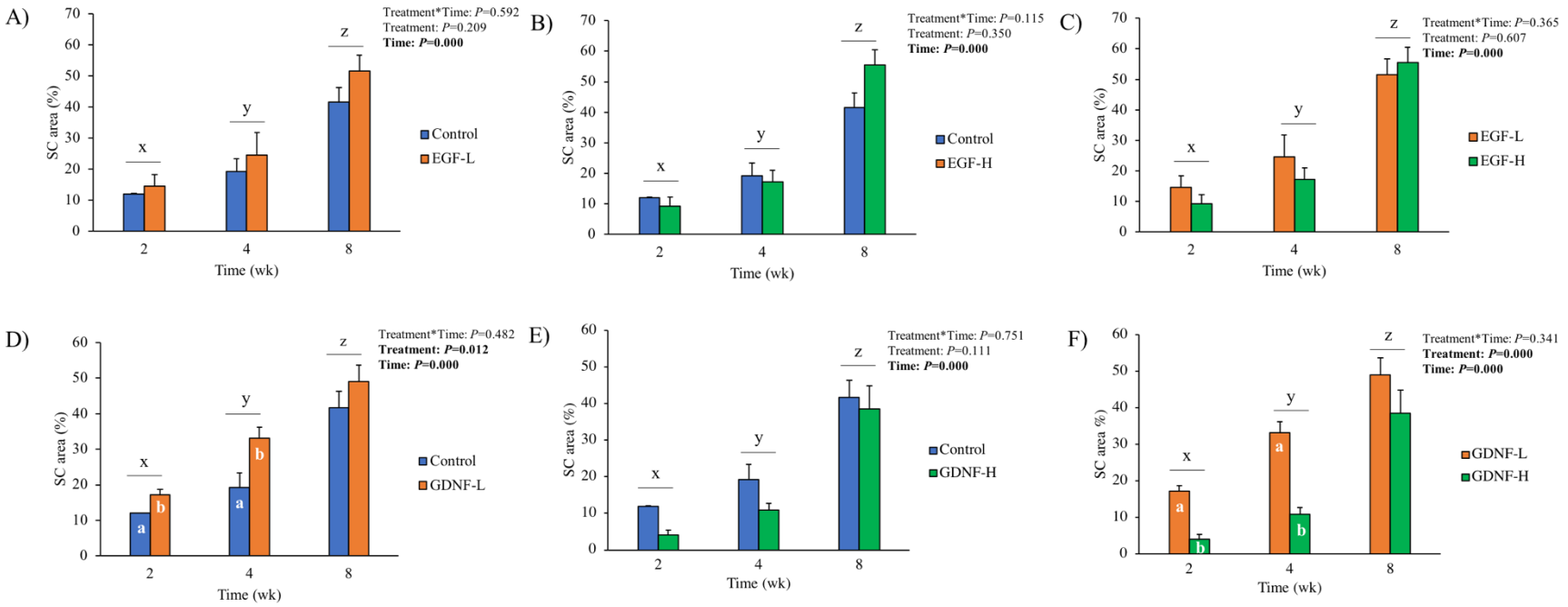


**Fig. 6.7.** The area occupied by seminiferous cords (SC) relative to the total implant area (%), measured at the widest cross-section of samples over time in (A-C) epidermal growth factor (EGF) and (D-F) glial-derived neurotrophic factor (GDNF) groups. Two doses of each growth factor were evaluated, low dose (20 ng/mL of cells): (A) EGF-L and (D) GDNF-L, and high dose (2 mg/mL of cells): (B) EGF-H and (E) GDNF-H. The SC% areas were compared with the control and between the doses (low *vs.* high) (C) and (F). The growth factors were added to the neonatal porcine testis cell aggregates (~100 $\times 10^6$ cells) before implantation under the back skin of recipient mice ($n$ = 7 per group). The control implants received no growth factor. Implants were retrieved at 1, 2, 4, and 8 wk post-implantation, although the SC area developed in implants retrieved at 1 wk was excluded in this analysis. Data are mean ± SEM. $^{ab}$ Data with different letters between treatments differ significantly ($P < 0.05$). $^{xyz}$ Data with different letters over time differ significantly ($P < 0.05$).

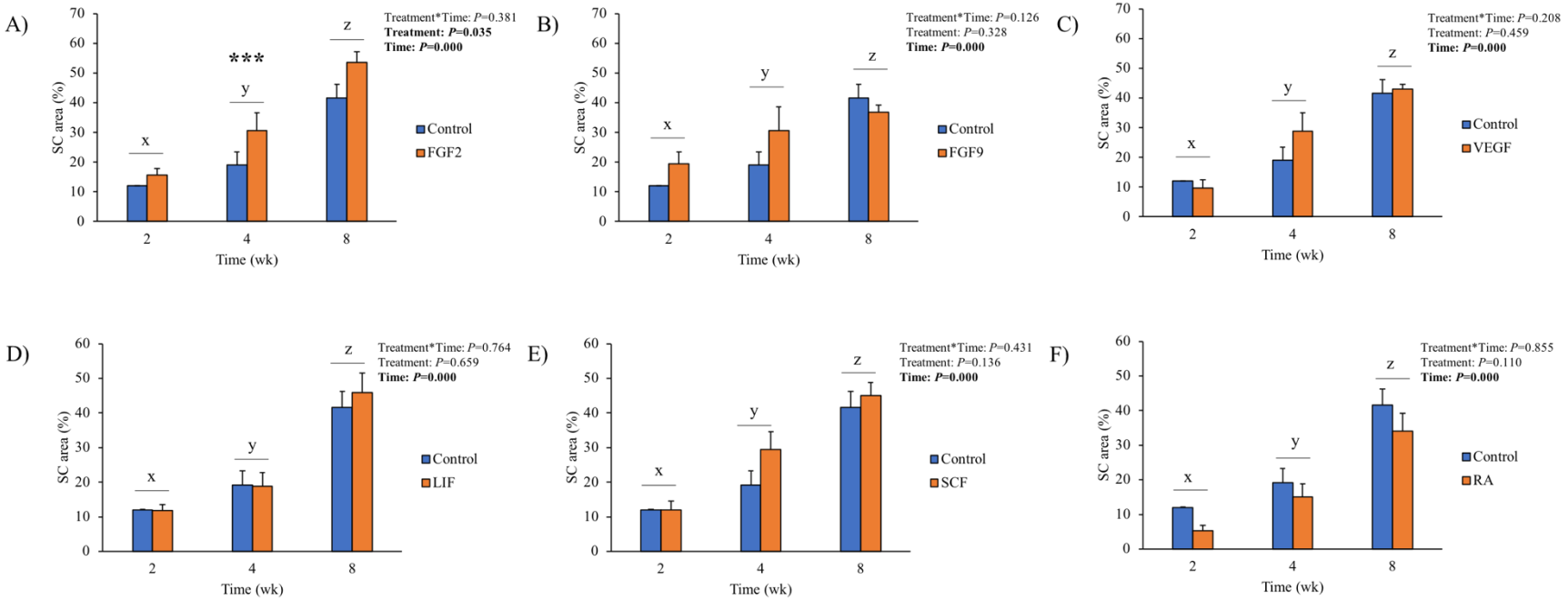


**Fig. 6.8.** The area occupied by seminiferous cords (SC) relative to the total implant area (%),measured at the widest cross-section of samples over time in the (A) basic fibroblast growth factor (FGF2), (B) fibroblast growth factor 9 (FGF9), (C) vascular endothelial growth factor (VEGF), (D) leukemia inhibitory factor (LIF), (E) stem cell factor (SCF), and (F) retinoic acid (RA) groups. The SC% areas of each group were compared with the control. The growth factors were added to the neonatal porcine testis cell aggregates (~100 $\times 10^6$ cells) before implantation under the back skin of recipient mice ($n = 7$ per group). The control implants received no growth factor. Implants were retrieved at 1, 2, 4, and 8 wk post-implantation, although the SC area developed in implants retrieved at 1 wk was excluded in this analysis. Data are mean ± SEM. $^{ab}$ Data with different letters between treatments differ significantly ($P < 0.05$). $^{xyz}$ Data with different letters over time differ significantly ($P < 0.05$). $^{***}$ The main effect of treatment was significant ($P < 0.05$), but no individual group differed ($P > 0.05$) at post-hoc analysis.

#### *6.4.2.3.3 Classification of SC*

Upon histological examination, SC within the retrieved implants displayed various morphology which could be classified into four types: 1) *regular* SC, referring to those with a normal morphology, typical of SC in the donor neonatal porcine testis tissue (diameter: 48.7 ± 0.2 μm, range: 34.4-57.4 μm, $n$ = 500 SC; Fig. 6.9A); 2) *irregular* SC, with obvious branching, not normally observed in the donor testis tissue (149.7 ± 1.6 μm, 76.8-259.2 μm, $n$ = 500; Fig. 6.9B); 3) *enlarged* SC, characterized by considerably larger diameter than age-matched regular SC (132.4 ± 1.0 μm, 63.3-237.2 μm, $n$ = 500; Fig. 6.9C); and 4) *aberrant* SC, or SC-like structures completely or partially enclosed by a cuboidal cell lining (94.7 ± 1.6 μm, 38.6-199.9 μm , $n$ = 500; Fig. 6.9D). Relative prevalence of each SC type within implants ranged from 0% to 100%. When the relative prevalence of SC types within implants of all examined time points were combined (*i.e.*, 2, 4, and 8 wk, $n$ = 822), regular and enlarged SC were more prevalent (~30% each, $P < 0.005$) than irregular and aberrant SC (23% and 18%, respectively) (Fig. 6.10A). Similarly, the overall area of implants covered by regular SC was greatest (39 ± 2%, $P < 0.0005$), followed irregular and enlarged SC (26 ± 2% and 25 ± 2%, respectively), and aberrant SC (10 ± 1%) (Fig. 6.10C).

***(a) Regular SC***

The overall prevalence of the regular type of SC was 100% (41/41 implants) at 1 wk, and 97% (88/91) at 2 wk, but dropped ($P < 0.0005$) to 45% of implants at 4 wk post-implantation. Among different groups at 4 wk, this prevalence was lower (0%, $P < 0.0005$) in both GDNF-H and RA groups than in control (78%), and also lower in GNDF-H than in GNDF-L group (0% *vs.* 78%, $P < 0.0005$). At 8 wk, the prevalence of regular SC was higher in FGF2, VEGF, LIF, and SCF groups than in control ($P < 0.05$; Fig. 6.10B and Table 6.7).

The overall area occupied by regular SC decreased over time ($P < 0.0005$), from 91% at 2 wk to 21% and 19% at 4 and 8 wk, respectively ($P < 0.005$). Among individual groups at 4 wk, this area was smaller ($P < 0.01$) in FGF9, GDNF-H, and RA groups than in control, and also smaller ($P < 0.005$) in GDNF-H than GDNF-L group. At 8 wk, this area was larger ($P < 0.005$) in FGF2 group than in control, and greater in EGF-L than EGF-H group (Fig. 6.10D and Table 6.7).

***(b) Irregular SC***

The first irregular SC was observed at 2 wk in only ~1% of implants (1/91), but their prevalence rapidly increased ($P < 0.005$) to 70% and 83% at 4 and 8 wk, respectively. Consequently, compared with regular SC, the prevalence of irregular SC was lower ($P < 0.005$) at 2 wk, but higher ($P < 0.005$) at 4 and 8 wk post-implantation. Irregular SC were conspicuously absent in RA (0% of implants) at 4 wk and therefore lower ($P < 0.005$) than the control (89%). On the other hand, this prevalence at 8 wk was 100% for both GDNF-L and RA, and hence higher than the control (63%; $P < 0.005$; Fig. 6.10B and Table 6.7).

The overall area of implants occupied by irregular SC increased over time ($P < 0.0005$), from 1 wk (1%) to 4 and 8 wk (35%), where at 8 wk it was highest among all SC types ($P < 0.0005$; Fig. 6.10D). Among individual groups at 8 wk, this area was larger ($P < 0.005$) in both EGF-H and GDNF-H groups than in their respective low-dose groups (Fig. 6.10D and Table 6.7).

***(c) Enlarged SC***

The overall prevalence of enlarged SC in implants was highest at 4 wk (97%), followed by 8 wk (89%, $P < 0.05$), and was lowest at 2 wk (20%, $P < 0.0005$) (Fig. 6.10B). Compared with regular SC, enlarged SC were also less prevalent at 2 wk ($P < 0.0005$), but most prevalent at both 4 and 8 wk ($P < 0005$). At 2 wk, no enlarged SC were observed in implants of RA, GDNF-L, EGF-H, and FGF9 groups, while their prevalence ranged between 13% and 60% among other groups. At 2 wk, more implants had enlarged SC in EGF-L than in EGF-H ($P < 0.04$). At 8 wk, multiple groups had enlarged SC in all (100%) their implants (*i.e.*, GDNF-L, FGF2, LIF, SCF, and RA) and therefore differed from the control (63%; $P < 0.005$; Fig. 6.10B and Table 6.7).

The overall area of implants containing enlarged SC was larger ($P < 0.005$) at 4 wk (43%) than at 2 wk (8%) and 8 wk (23%). At 4 wk, enlarged SC covered the largest area ($P < 0.0005$) among all SC types. Among individual groups, this area was larger in RA (100%) than in the control (28%, $P < 0.0005$; Fig. 6.10D and Table 6.7).

***(d) Aberrant SC***

The aberrant type of SC first appeared at 4 wk in 22% of combined implants but this prevalence increased to 91% at 8 wk ($P < 0.0005$). Compared with regular SC, the prevalence of aberrant SC was lower at 4 wk ($P < 0.0005$) and higher at 8 wk ($P < 0.0005$). At 4 wk, while no aberrant SC (0%) were observed in implants of the control, GDNF-L, or RA groups, this prevalence was higher ($P < 0.05$) in EGF-H (30%), SCF (44%), and FGF9 (69%) groups, as compared with the control. At 8 wk, implants of all groups had aberrant SC, ranging from 71% to 100%, which did not differ among groups ($P < 0.05$; Fig. 6.10B and Table 6.7).

The area of aberrant SC in combined implants at 4 wk was only 1%, but increased to 23% at 8 wk ($P < 0.0005$). Compared with the area of other SC types at 4 wk, aberrant SC covered the least area ($P < 0.05$). Among the groups at 8 wk, the area of aberrant SC was smaller ($P < 0.05$) in FGF2 (5%), LIF (10%), and RA (10%) groups than in the control (35%; Fig. 6.10D and Table 6.7).

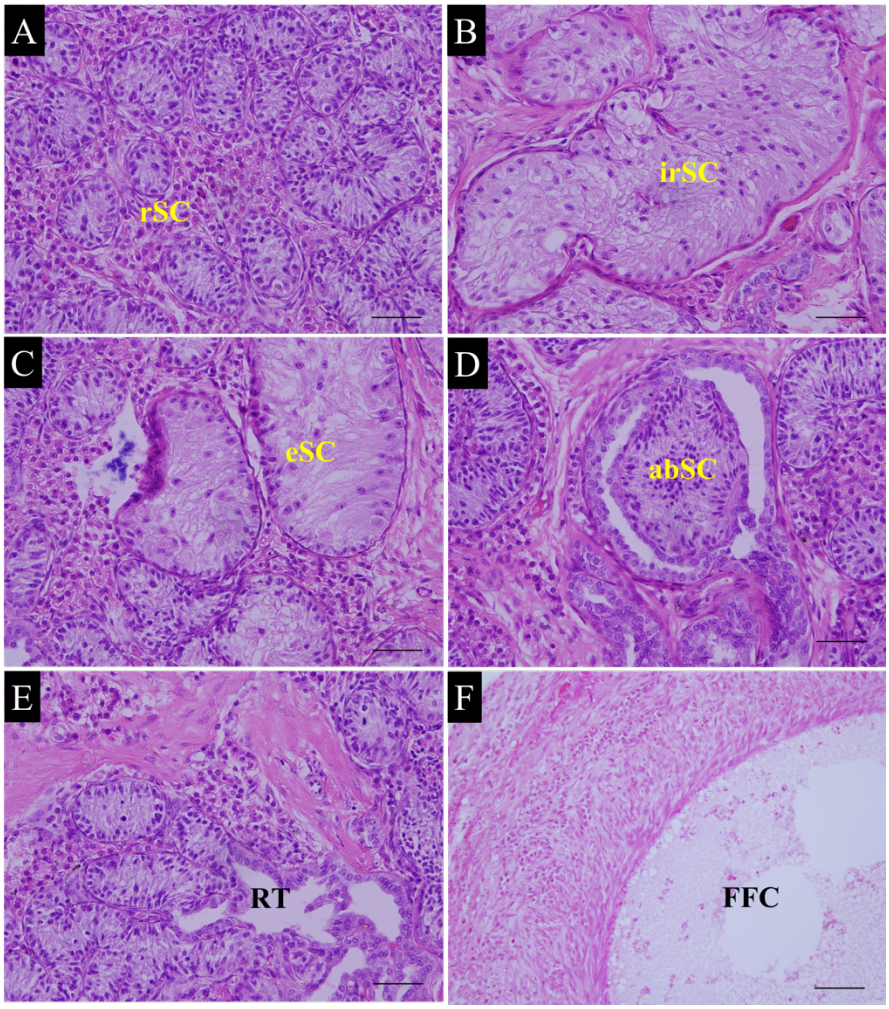


**Fig. 6.9.** Representative histological photomicrographs demonstrating typical morphology of seminiferous cords (SC) classified into: (A) regular (rSC), (B) irregular (irSC), (C) enlarged (eSC), and (D) aberrant seminiferous cords (abSC). Additional observed structures in the implants included (E) rete testis-like structure (RT) and (F) fluid-filled cavities (FFC). (H&E Staining, Scale bar: 50μm (A-E) and 200 μm (F)). Also see Appendix B.1 for representative normal morphology of testis tissue cross-sections from pigs at different developmental stages.

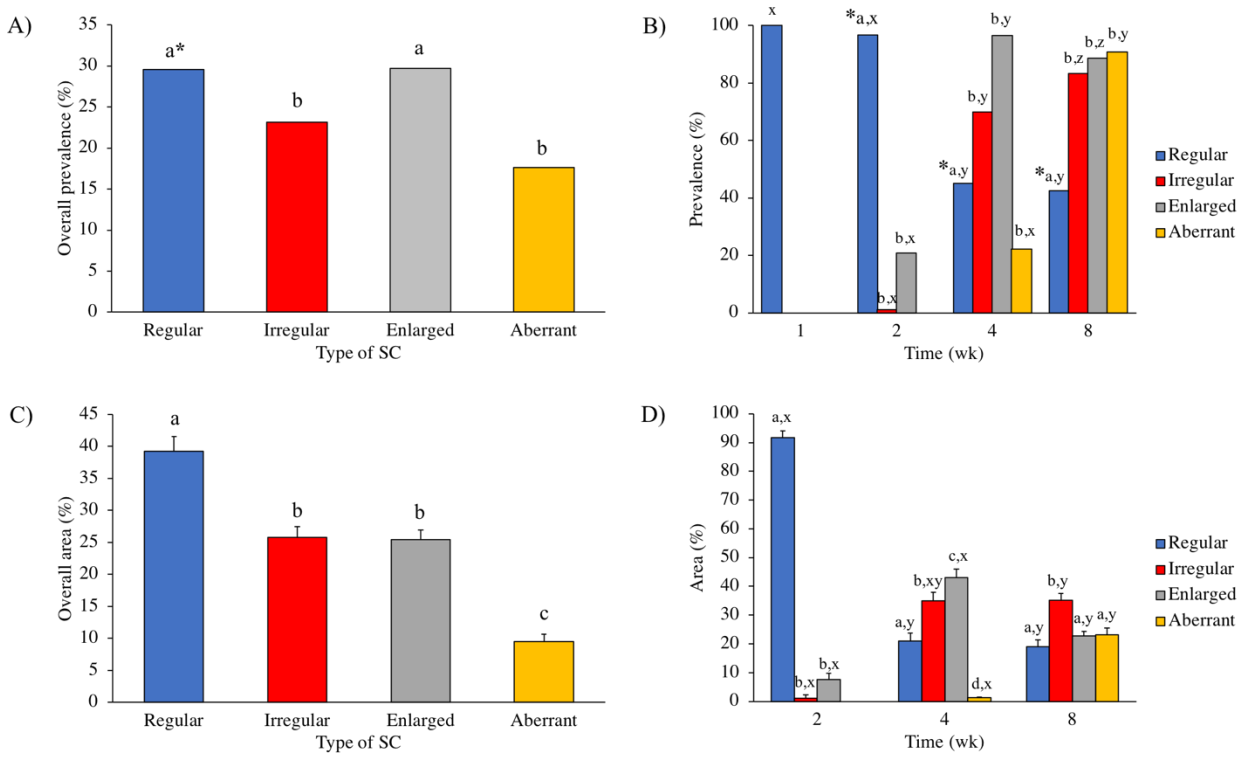


**Fig. 6.10.** The prevalence (%) of different types of seminiferous cords (SC) as well as their relative area (%, compared with the total implant area), measured at the widest cross-section of samples. (A) The overall prevalence (%) of different types of SC in all implants, and (B) their prevalence at each time point. (C) The overall relative area occupied by different types of SC in all implants, and (D) their relative area at each time point. The data for the prevalence and area were analyzed using Chi-Square test and one-way ANOVA, respectively. Data are the relative number of observations (% ± SEM). * The regular type of SC as the basis of comparison. $^{abc}$ Data with different letters between treatments differ significantly ($P < 0.05$). $^{xyz}$ Data with different letters differ significantly over time ($P < 0.05$).

**Table 6.7.** The prevalence of each type of seminiferous cords and their relative area among implants of different groups.

| | | Type of SC | | | | | | | |
|---|---|---|---|---|---|---|---|---|---|
| | | Regular | | Irregular | | Enlarged | | Aberrant | |
| Group | Wk | No. (%) | Area (%) | No. (%) | Area (%) | No. (%) | Area (%) | No. (%) | Area (%) |
| Control | 2 | 5/5 (100) | 90 ± 10 | 0/5 (0) | 0 | 1/5 (20) | 10 | 0/5 (0) | 0 |
| | 4 | 7/9 (78) | 32 ± 9 | 8/9 (89) | 36 ± 8 | 9/9 (100) | 33 ± 7 | 0/9 (0) | 0 |
| | 8 | 1/8 (13) | 6 | 5/8 (63) | 31 ± 12 | 5/8 (63) | 28 ± 9 | 7/8 (88) | 35 ± 12 |
| EGF-L | 2 | 9/10 (90) | 78 ± 11 | 0/10 (0) | 0 | 5/10 (50) | 22 ± 8 | 0/10 (0) | 0 |
| | 4 | 5/10 (50) | 29 ± 11 | 9/10 (90) | 42 ± 10 | 9/10 (90) | 28 ± 7 | 3/10 (30) | 4 ± 1 |
| | 8 | 6/12 (50) | 24 ± 9 | 6/12 (50) | 16 ± 7 | 7/12 (58) | 15 ± 6 | 12/12 (100) | 45 ± 10 |
| EGF-H | 2 | 6/6 (100) | 100 | 0/6 (0) | - (-) | 0/6 (0) | 0 | 0/6 (0) | 0 |
| | 4 | 5/8 (63) | 10 ± 6 | 4/8(50) | 36 ± 14 | **8/8 (100)†** | 53 ± 14 | **3/8 (38)*** | 1 ± 0.4 |
| | 8 | 3/13 (23) | **4 ± 3†** | 11/13 (85) | **49 ± 9††** | 11/13 (84) | 14 ± 4 | 13/13 (100) | 37 ± 10 |
| GDNF-L | 2 | 8/8 (100) | 100 | 0/8 (0) | 0 | 0/8 (0) | 0 | 0/8 (0) | 0 |
| | 4 | 7/9 (78) | 46 ± 11 | 6/9 (67) | 36 ± 12 | 9/9 (100) | 18 ± 3 | 0/9 (0) | 0 |
| | 8 | 4/11 (36) | 14 ± 7 | **11/11 (100)*** | 29 ± 4 | **11/11 (100)*** | 27 ± 6 | 10/11 (91) | 31 ± 9 |
| GDNF-H | 2 | 6/6 (100) | 92 ± 8 | 0/6 (0) | 0 | 1/6 (17) | 8 | 0/6 (0) | 0 |
| | 4 | **0/10 (0)**††** | **0**†† | 9/10 (90) | 59 ± 10 | 9/10 (90) | 33 ± 10 | 1/10 (10) | 0.30 |
| | 8 | 2/11 (19) | 13 ± 9 | 10/11(91) | **52 ± 10†** | 10/11 (91) | 24 ± 8 | 9/11 (82) | 12 ± 3 |
| FGF2 | 2 | 11/11 (100) | 98 ± 1 | 0/11 (0) | 0 | 3/11 (27) | 2 ± 1 | 0/11 (0) | 0 |
| | 4 | 6/12 (50) | 22 ± 9 | 9/10 (90) | 30 ± 9 | 12/12 (100) | 47 ± 7 | 2/12 (17) | 1 ± 1 |
| | 8 | **14/14 (100)**** | **53 ± 6**** | 12/14 (86) | 21 ± 5 | **14/14 (100)*** | 20 ± 3 | 12/14 (86) | **5 ± 1**** |
| FGF9 | 2 | 9/9 (100) | 100 | 0/9 (0) | 0 | 0/9 (0) | 0 | 0/9 (0) | 0 |
| | 4 | 5/13 (39) | **11 ± 4*** | 12/13 (92) | 33 ± 6 | 13/13 (100) | 52 ± 6 | **9/13 (69)**** | 4 ± 1 |
| | 8 | 3/12 (25) | 9 ± 5 | 9/12 (75) | 33 ± 7 | 10/12 (83) | 21 ± 5 | 12/12 (100) | 37 ± 10 |
| VEGF | 2 | 9/10 (90) | 70 ± 12 | 1/10 (10) | 10 | 6/10 (60) | 21 ± 9 | 0/10 | 0 |
| | 4 | 5/11 (46) | 32 ± 12 | 6/11 (55) | 33 ± 11 | 11/11 (100) | 35 ± 7 | 2/11 (18) | 1 ± 1 |
| | 8 | **7/12 (58)*** | 21 ± 8 | 11/12 (92) | 32 ± 7 | 10/12 (83) | 19 ± 4 | 11/12 (92) | 29 ± 7 |
| LIF | 2 | 7/8 (88) | 88 ± 13 | 0/8 (0) | 0 | 1/8 (13) | 13 | 0/8 (0) | 0 |
| | 4 | 5/10 (50) | 24 ± 8 | 10/10 (100) | 54 ± 10 | 8/10 (80) | 22 ± 9 | 1/10 (10) | 1 |
| | 8 | **9/14 (64)*** | 29 ± 9 | 11/14 (79) | 37 ± 9 | **14/14 (100)*** | 24 ± 4 | 10/14 (71) | **10 ± 3*** |
| SCF | 2 | 8/8 (100) | 99 ± 1 | 0/8 (0) | 0 | 1/8 (13) | 1 | 0/8 (0) | 0 |
| | 4 | 6/9 (67) | 35 ± 12 | 8/9 (89) | 35 ± 9 | 9/9 (100) | 27 ± 6 | **4/9 (44)*** | 3 ± 2 |
| | 8 | **7/12 (58)*** | 26 ± 9 | 11/12 (92) | 26 ± 6 | **12/12 (100)*** | 28 ± 4 | 11/12 (92) | 20 ± 5 |
| RA | 2 | 10/10 (100) | 100 | 0/10 (0) | 0 | 0/10 (0) | 0 | 0/10 (0) | 0 |
| | 4 | **0/12 (0)**** | **0**** | **0/12 (0)**** | **0**** | 12/12 (100) | **100**** | 0/12 (0) | 0 |
| | 8 | 0/13 (0) | 0 | **13/13 (100)*** | 58 ± 6 | **13/13 (100)*** | 32 ± 7 | 13/13 (100) | **10 ± 3*** |

Data are the prevalence (%) of different types of seminiferous cord (SC) and their relative area (%, compared with the total implant area), measured at the widest cross-section of samples.
Epidermal growth factor (EGF); glial-derived neurotrophic factor (GDNF); fibroblast growth factor (FGF2); fibroblast growth factor 9 (FGF9); vascular endothelial growth factor (VEGF); leukemia inhibitory factor (LIF); stem cell factor (SCF); retinoic acid (RA).
The high (H) and low (L) doses of the same growth factor groups were compared with each other.
Each group was also compared with the control.
Data are mean ± SEM.
The data were compared using the Chi-square and independent t-tests for the prevalence and area data, respectively.
* $P < 0.05$ compared to the control.
** $P < 0.01$ compared to the control.
† $P < 0.05$ compared to the lower dose treatment.
†† $P < 0.01$ compared to the lower dose treatment.

#### *6.4.2.3.4 Predominant Type of SC Per Group*

We also combined the area covered by the same type of SC from different time points to determine the predominant type of SC per treatment group. Since SC development in most implants first appeared at 2 wk, we compared the overall area of SC types among groups by combing data from 2, 4, and 8 wk (1st approach). Because the high prevalence of regular SC at 2 wk masked the overall effect of other SC types, we also determined the predominant SC type for each group by combining the data from only 4 and 8 wk (2nd approach) (Table 6.8).

Analysis using the 1st approach showed that, with few exceptions, the overall area occupied by various types of SC in a given treatment group differed ($P < 0.05$), where regular SC were the predominant type, making up 34-56% of all SC in EGF-L, GDNF-L, FGF2, FGF9, VEGF, LIF, and SCF groups ($P < 0.05$). The exceptions included a lack of a difference for the overall area of SC types in EGF-H and control groups ($P > 0.05$), and the predominance of irregular SC and enlarged SC types in GDNF-H and RA groups, respectively ($P < 0.05$; Table 6.8).

Using the 2nd approach, the overall area occupied by various types of SC differed in most treatment groups ($P < 0.05$), in which the predominant SC type was distributed among irregular SC (in EGF-H, GDNF-H, and LIF), enlarged SC (in FGF9 and RA), and regular SC (in FGF2), while regular and irregular SC had covered equal areas (each 30% in SCF; $P < 0.05$). The overall area of SC types did not differ in implants of the control, EGF-L, GDNF-L, and VEGF groups ($P > 0.05$). RA was the only group that lacked regular SC (0%) and instead had the highest area of enlarged SC among all groups, and differed from the control ($P < 0.005$; Table 6.8).

### *6.4.2.4 Relative Number of Gonocytes*

The number of gonocytes relative to the number of Sertoli cells was calculated in 2 wk implants, because at this time point the implants had the most number of regular SC. The relative number of gonocytes in control was 15 ± 2 per 1,000 Sertoli cells, and while it was numerically higher in all other groups, it was significantly higher only in RA (27 ± 3) compared with the control ($P < 0.05$; Fig. 6.11).

**Table 6.8.** The predominant type of seminiferous cords per group, calculated based on two different approaches.

| Group | 1st Approach: Overall at 2, 4, and 8 wk | | | | | 2nd Approach: Overall at 4 and 8 wk | | | | |
|---|---|---|---|---|---|---|---|---|---|---|
| | *P* | Type of SC (%) | | | | *P* | Type of SC (%) | | | |
| | | Regular | Irregular | Enlarged | Aberrant | | Regular | Irregular | Enlarged | Aberrant |
| Control | 0.10 | 36 ± 8 | 26 ± 6 | 26 ± 5 | 13 ± 6 | 0.36 | 20 ± 6 | 33 ± 7 | 31 ± 5 | 17 ± 7 |
| EGF-L | 0.01 | 41 ± 7$^{a}$ | 19 ± 5$^{b}$ | 22 ± 5$^{b}$ | 17 ± 5$^{b}$ | 0.84 | 26 ± 7 | 28 ± 6 | 21 ± 5 | 25 ± 7 |
| EGF-H | 0.41 | 27 ± 8 | 34 ± 7 | 23 ± 6 | 16 ± 6 | 0.01 | **6 ± 3$^{b}$*††** | 44 ± 8$^{a}$ | 29 ± 7$^{ab}$ | 20 ± 7$^{b}$ |
| GDNF-L | 0.00 | 49 ± 8$^{a}$ | 23 ± 5$^{b}$ | 17 ± 3$^{b}$ | 12 ± 4$^{b}$ | 0.28 | 28 ± 7 | 32 ± 6 | 23 ± 3 | 17 ± 6 |
| GDNF-H | 0.00 | 26 ± 8$^{a}$ | **43 ± 7$^{a}$†** | 27 ± 6$^{ab}$ | 5 ± 2$^{b}$ | 0.00 | **7 ± 5$^{c}$††** | **55 ± 7$^{a}$††** | 32 ± 7$^{b}$ | 6 ± 2$^{c}$ |
| FGF2 | 0.00 | 56 ± 6$^{a}$ | 18 ± 4$^{b}$ | 23 ± 4$^{b}$ | **2 ± 1$^{c}$*** | 0.00 | **39 ± 6$^{a}$*** | 25 ± 5$^{a}$ | 32 ± 4$^{a}$ | **3 ± 1$^{b}$*** |
| FGF9 | 0.03 | 34 ± 7$^{a}$ | 24 ± 4$^{ab}$ | 27 ± 5$^{ab}$ | 15 ± 4$^{b}$ | 0.00 | 10 ± 3$^{a}$ | 33 ± 5$^{b}$ | 37 ± 5$^{b}$ | 20 ± 6$^{ab}$ |
| VEGF | 0.00 | 39 ± 7$^{a}$ | 25± 4$^{ab}$ | 25 ± 5$^{ab}$ | 11 ± 2$^{b}$ | 0.22 | 26 ± 5 | 32 ± 7 | 26 ± 6 | 15 ± 3 |
| LIF | 0.00 | 42 ± 7$^{a}$ | 33 ± 6$^{ab}$ | 20 ± 4$^{bc}$ | 4 ± 2$^{c}$ | 0.00 | 27 ± 6$^{ab}$ | 44 ± 7$^{a}$ | 23 ± 4$^{b}$ | 6 ± 2$^{b}$ |
| SCF | 0.00 | 49 ± 8$^{a}$ | 22 ± 5$^{b}$ | 20 ± 3$^{b}$ | 9 ± 3$^{b}$ | 0.00 | 30 ± 7$^{ab}$ | 30 ± 5$^{a}$ | 28 ± 3$^{ab}$ | 13 ± 4$^{b}$ |
| RA | 0.00 | 29 ± 8$^{ab}$ | 22 ± 5$^{bc}$ | **46 ± 7$^{a}$*** | 4 ± 1$^{b}$ | 0.00 | 0$^{c}$ | 30 ± 7$^{b}$ | **64 ± 8$^{a}$**** | 5 ± 2$^{bc}$ |

Data are the predominant type of seminiferous cords (SC) per group, defined as the combined relative area (%) covered by the same type of SC from different time points, measured at the widest cross-section of samples.
Two different approaches were used to calculate the values.
Epidermal growth factor (EGF); glial-derived neurotrophic factor (GDNF); fibroblast growth factor (FGF2); fibroblast growth factor 9 (FGF9); vascular endothelial growth factor (VEGF); leukemia inhibitory factor (LIF); stem cell factor (SCF); retinoic acid (RA).
Data are mean ± SEM.
The high (H) and low (L) doses of the same growth factor groups were compared with each other: independent *t*-test..
Each group was also compared with the control: independent *t*-test..
Data from within the treatment groups were compared among SC types: one way ANOVA.
* $P < 0.05$ compared to the control.
** $P < 0.01$ compared to the control.
† $P < 0.05$ compared to the lower dose treatment.
†† $P < 0.01$ compared to the lower dose treatment.

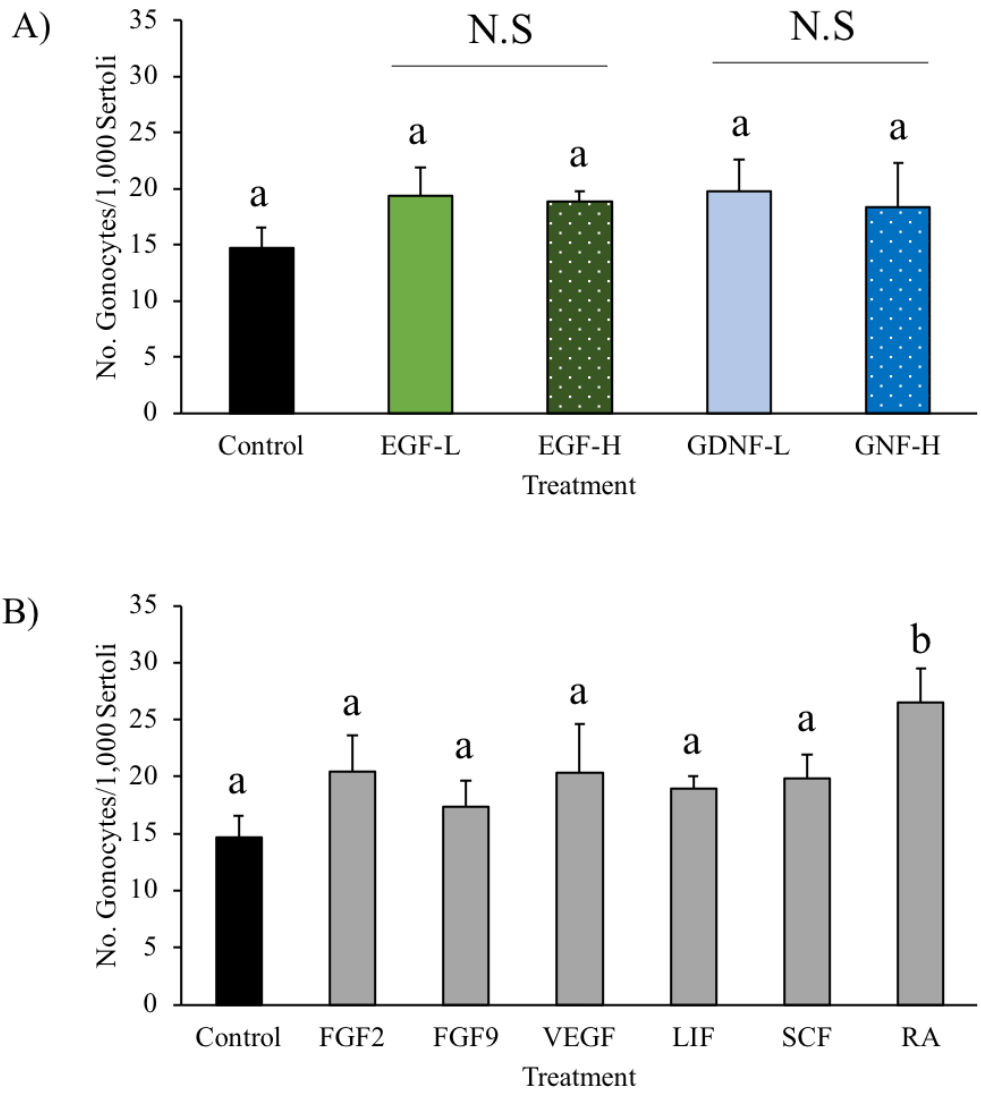


**Fig. 6.11.** The relative number of gonocytes (per 1,000 Sertoli cells) in implants retrieved from different groups. (A) The gonocyte numbers were compared among implants treated with the epidermal growth factor (EGF) or glial-derived neurotrophic factor (GDNF) at either low doses (20 ng/mL of cells; EGF-L and GDNF-L), or high doses (2 mg/mL of cells; EGF-H and GDNF-H). The gonocyte numbers were compared with the control and between the doses (low *vs.* high). (B) The gonocyte numbers were also compared among implants treated with the basic fibroblast growth factor (FGF2), fibroblast growth factor 9 (FGF9), vascular endothelial growth factor (VEGF), leukemia inhibitory factor (LIF), stem cell factor (SCF), or retinoic acid (RA). The relative number of gonocytes in each group was compared with the control. The growth factors were added to the neonatal porcine testis cell aggregates (~100 $\times 10^6$ cells) before implantation under the back skin of recipient mice ($n$ = 7 per group). The control implants received no growth factor. Implants were retrieved at 1, 2, 4, and 8 wk post-implantation, although the relative number of gonocytes was determined only in the implants retrieved at 2 wk. Data are expressed as mean ± SEM. $^{ab}$ Data with different letters differ significantly ($P < 0.05$). $^{N.S}$ No significant difference ($P > 0.05$ ) was observed between the low *vs.* high dose.

#### *6.4.2.5 Rete Testis-Like Formation*

In addition to the formation of SC, the implanted cells underwent reorganizations to form structures resembling the rete-testis (RT) and efferent ductules. The RT formations were typically observed at the center of implants, over time branched out radially, and were lined by cuboidal epithelial cells (Fig. 6.9E). Although not significantly different among groups ($P > 0.05$), RT appeared as early as 2 wk in implants of about half of the groups, the median point for RT appearance was 4 or 8 wk, and by 8 wk (latest) most but not all retrieved implants had RT. When data from different time points were pooled for each group, the prevalence of RT did not differ ($P > 0.05$) among groups, and RT was evident in 27-56% of implants in all groups. However, at 4 wk, more implants in GDNF-H group (100%) had RT than in control (67%), and more in EGF-L (80%) than in its high dose group ($P < 0.05$; Table 6.9).

#### *6.4.2.6 Fluid-Filled Cavities*

Fluid-filled cavities (FFC) were atypical morphological features observed in some implants, characterized by a space void of cellular organizations (originating from implanted cells), filled with fluid or occasionally with red blood cells (RBC) (Fig. 6.9F). The FFC were observed in ~10% of all implants (49/500) that displayed regeneration of testis tissue. The majority of FFC were only present at 1 wk, comprising 32% (41/128) of implants at this time point, or 84% (41/49) of all implants with FFC. Over time, the number and the diameter of FFC decreased ($P < 0.05$); they were present in 5% (6/126) of 2 wk implants or 12% of all implants with FFC, in 2% (2/114) of 4 wk implants or 4% of all implants with FFC, and none among the 8 wk implants. However, the overall prevalence of FFC, or that of individual groups *vs.* control, or among high *vs.* low dose groups did not differ ($P > 0.05$; Table 6.10).

**Table 6.9.** The prevalence and first appearance of rete testis formations among implants from different groups.

| | No. implants with RT/total implants (%) | | | | | First appearance (wk) | | |
|---|---|---|---|---|---|---|---|---|
| Group | 1 wk | 2 wk | 4 wk | 8 wk | Overall | Earliest | Median | Latest |
| Control | 0/10 (0) | 0/10 (0) | 6/9 (67) | 7/8 (88) | 13/37 (35) | 4 | 4 | NA |
| EGF-L | 0/14 (0) | 3/13 (23) | 8/10 (80) | 12/12 (100) | 23/49 (47) | 2 | 8 | 8 |
| EGF-H | 0/14 (0) | 0/12 | **2/8 (25)**† | 13/13 (100) | 15/47 (32) | 4 | 8 | 8 |
| GDNF-L | 0/14 (0) | 0/9 (0) | 8/9 (89) | 11/11 (100) | 19/43 (44) | 4 | 8 | 8 |
| GDNF-H | 0/9 (0) | 1/9 (11) | **10/10 (100)*** | 11/11 (100) | 22/39 (56) | 2 | 4 | 4 |
| FGF2 | 0/11 (0) | 2/12 (17) | 8/12 (67) | 14/14 (100) | 24/49 (49) | 2 | 8 | 8 |
| FGF9 | 0/13 (0) | 2/11 (18) | 10/13 (77) | 12/12 (100) | 24/49 (49) | 2 | 4 | 8 |
| VEGF | 0/12 (0) | 0/13 (0) | 6/11 (55) | 12/12 (100) | 18/48 (38) | 4 | 8 | 8 |
| LIF | 0/10 (0) | 1/13 (8) | 5/11 (46) | 13/14 (93) | 19/48 (40) | 2 | 4 | NA |
| SCF | 0/9 (0) | 0/13 (0) | 8/9 (89) | 12/12 (100) | 20/43 (47) | 4 | 8 | 8 |
| RA | 0/12 (0) | 0/11 (0) | 3/12 (25) | 10/13 (77) | 13/48 (27) | 4 | 8 | NA |
| Total | 0/128 (0) | 9/126 (7.14) | 74/114 (64.91) | 127/132 (96.21) | 210/500 (42) | | | |

Data are the prevalence of rete testis (RT) formations and their first appearance among implants showing *de novo* morphogenesis of testis tissue at each time point.
Epidermal growth factor (EGF); glial-derived neurotrophic factor (GDNF); fibroblast growth factor (FGF2); fibroblast growth factor 9 (FGF9); vascular endothelial growth factor (VEGF); leukemia inhibitory factor (LIF); stem cell factor (SCF); retinoic acid (RA).
The high (H) and low (L) doses of the same growth factor groups were compared with each other.
Each group was also compared with the control.
The data were compared using the Chi-square tests
The first appearance of RT was assessed based on their first occurrence; earliest, the midpoint of occurrence; median, and the last occurrence from all implant retrieved in a single recipient.
* $P < 0.05$ compared to the control.
† $P < 0.05$ compared to the lower dose.

**Table 6.10.** The prevalence of fluid-filled cavities among implants of different groups and over time.

| Group | No. implants with FFC/total implants (%) | | | | |
|---|---|---|---|---|---|
| | 1 wk | 2 wk | 4 wk | 8 wk | Overall |
| Control | 2/10 (20) | 2/10 (20) | 0/9 (0) | 0/8(0) | 4/37 (11) |
| EGF-L | 8/14 (57) | 0/13 (0) | 0/10 (0) | 0/12 (0) | 8/49 (16) |
| EGF-H | 2/14 (14) | 0/12 (0) | 0/8 (0) | 0/13 (0) | 2/47 (4) |
| GDNF-L | 7/14 (50) | 0/9 (0) | 0/9 (0) | 0/11(0) | 7/43 (16) |
| GDNF-H | 4/9 (44) | 0/9 (0) | 0/10 (0) | 0/11(0) | 4/39 (10) |
| FGF2 | 0/11 (0) | 0/12 (0) | 0/12 (0) | 0/14 (0) | 0/49 (0) |
| FGF9 | 6/13 (46) | 1/11 (9.10) | 0/13 (0) | 0/12 (0) | 7/49 (14) |
| VEGF | 7/12 (58) | 0/13(0) | 0/11(0) | 0/12 (0) | 7/48 (15) |
| LIF | 3/10 (30) | 0/13 (0) | 0/11(0) | 0/14 (0) | 3/48 (6) |
| SCF | 2/9 (22) | 3/13 (23) | 0/9 (0) | 0/12 (0) | 5/43 (12) |
| RA | 0/12 (0) | 0/11(0) | 2/12 (17) | 0/13(0) | 2/48 (4) |
| Total | 41/128 (32.03) | 6/126 (4.76) | 2/114 (1.75) | 0/132 (0) | 49/500 (9.8) |

Data are the number and % of implants showing fluid-filled cavities (FFC) among the retrieved samples at each time point.
Epidermal growth factor (EGF); glial-derived neurotrophic factor (GDNF); fibroblast growth factor (FGF2); fibroblast growth factor 9 (FGF9); vascular endothelial growth factor (VEGF); leukemia inhibitory factor (LIF); stem cell factor (SCF); retinoic acid (RA).
The high (H) and low (L) doses of the same growth factor groups were compared with each other.
Each group was also compared with the control.
The data were compared using the Chi-square tests.
The data did not differ ($P > 0.05$) among all compared groups.

## 6.5 Discussion

In the present study, we investigated the effects of several growth factors on *de novo* morphogenesis of testis tissue after implantation of neonatal porcine testis cell aggregates in mice. With the exception of VEGF (Schmidt *et al.*, 2006b; Dores and Dobrinski, 2014), the examined growth factors had not been previously studied using the TCI model. Hence, there was a lack of background information on choosing suitable doses of these growth factors, their efficient mode of treatment, or the expected outcomes. The growth factors we evaluated in this study are known to play an important role in testis development (Sordoillet *et al.*, 1991; Mauduit *et al.*, 1999; DiNapoli *et al.*, 2006; Kim *et al.*, 2006a; Zhou *et al.*, 2008; Baltes-Breitwisch *et al.*, 2010; Cool *et al.*, 2011; Svingen and Koopman, 2013). Some of these growth factors, such as GDNF, FGF2, EGF, and LIF have long been used for *in vitro* maintenance and propagation of SSC (Kanatsu-Shinohara *et al.*, 2003; Kubota *et al.*, 2004a; Ryu *et al.*, 2005; Kanatsu-Shinohara *et al.*, 2007; Aponte *et al.*, 2008). Due to a lack of comparable *in vivo* studies, the doses of growth factors applied in the present study were chosen to be higher than those commonly used *in vitro*, taking into account the obvious differences between the two systems and the brief exposure of growth factors to cells prior to implantation. For example, our doses of EGF, GNDF, and FGF2 were 2–100 fold higher than those used for *in vitro* SSC culture systems (Kanatsu-Shinohara *et al.*, 2003; Kubota *et al.*, 2004a; Kanatsu-Shinohara *et al.*, 2007). For VEGF, which had been used in the ectopic TCI model with modest effects, we aimed to augment potential effects, simulating overexpression of VEGF; hence, its dose was 35 fold higher than the previously used dose/cell (Dores and Dobrinski, 2014). In addition, the higher dose was also deemed crucial to ensure sufficient amounts of VEGF being applied given the short exposure to the high number of cells used in our study.

In this chapter, we applied the modifications for testis cell implantation that we established in Chapter 5. The injection technique for testis cell implantation allowed manipulation of the cell number, effective and accurate placement of cells in the implantation site, and minimized the potential cell leakage experienced using the conventional surgical implantation technique (Honaramooz *et al.*, 2007). Using our improved protocol, ~100 $\times 10^6$ testis cells were injected per implantation site in this study, which is 2–50 fold higher than the previously used numbers (Arregui *et al.*, 2008a; Watanabe *et al.*, 2009; Campos-Junior *et al.*, 2014; Dores and Dobrinski, 2014). The

overall implant recovery rate in our study was very high (95% of 596 implants), which compares favorably and exceeds comparable earlier reports using donor pig testis cells (78–82% of 96 implants) (Honaramooz *et al.*, 2007; Campos-Junior *et al.*, 2014) or donor sheep testis cells (92% of 96 implants) (Arregui *et al.*, 2008a). This high recovery rate alone indicates that our modifications have been effective, especially considering that we used a much higher number of recipient mice in our study than in previous studies (77 mice *vs.* typically up to 12). In a single previous study using the same model to evaluate the effect of VEGF (Dores and Dobrinski, 2014), the proportion of developed implants (92%) treated with VEGF was similar, albeit their use of a cell carrier (Matrigel matrix) for implantation and different cell numbers.

From the perspective of gross and histological evaluations, FGF2 had significant effects on the implant weight, implant area, and SC area; these parameters were consistently higher than in the control at all retrieval points. These findings, coupled with the positive correlations between all the parameters (although not significantly), lead to the conclusion that FGF2 has an effect on *de novo* morphogenesis of testis tissue, by giving rise to larger implants and greater SC formation. Proliferative and protective (improved survival) effects of FGF2 on pig Sertoli cells have been demonstrated in several *in vitro* studies (Jaillard *et al.*, 1987; van Dissel-Emiliani *et al.*, 1996). Therefore, we speculate that in our *in vivo* model, FGF2 also exerts its effects on the somatic cells of implants, especially Sertoli cells, by promoting their proliferation. The protective role of FGF2 on Sertoli cells may also have helped to maintain the Sertoli cell pool to support the initiation of seminiferous cord formation. It has also been shown that FGF2 is abundantly expressed in the testis, where it peaks in the prepubertal testis and decreases over time (Mullaney and Skinner, 1992; Cancilla *et al.*, 2000; Abd-Elmaksoud *et al.*, 2005). Thus, in our study, the effects of FGF2 were potentiated because in addition to the exogenous FGF2 (from our treatment), endogenous FGF2 was already highly expressed in the implanted testis cells since they were from neonatal donors.

Several growth factors showed a significant overall effect on at least one of the evaluated gross or histological parameters (*i.e.*, implant weight, implant area, or SC area), including the effects of LIF on implant weight, EGF-L and SCF on implant area, and GDNF-L on SC area. Therefore, we further analyzed the data for potential correlations and focused on the outcomes at 8 wk post-implantation. For LIF, the overall treatment effect on the implant weight was significant, and there were correlations between implant weight and area. For EGF-L, the implant area was significantly

correlated with the SC area. The effects of EGF, LIF, and SCF are thought to be on both the somatic and germ cells components of the testis (Dolci *et al.*, 1991; Sordoillet *et al.*, 1991; De Miguel *et al.*, 1996; Levine *et al.*, 2000; Piquet-Pellorce *et al.*, 2000; Yan *et al.*, 2000a, b; Wahab-Wahlgren *et al.*, 2003; Tu *et al.*, 2007; Rastegar *et al.*, 2015). Thus, we suggest that the observed effects of these growth factors in our *in vivo* model could be due to a combination of their effects on both somatic and germ cells for the promotion of *de novo* morphogenesis. Such potential effects of EGF-L and LIF on *de novo* testis tissue morphogenesis can be delineated in the future studies.

Based on the SC area alone, we concluded that GDNF-L has a significant effect on the development of SC. Measuring SC area is a more reliable criteria than implant area for assessing *de novo* testis tissue morphogenesis because it excludes non-tubular compartments within the implant. Aside from its important role in SSC self-renewal in the testis (Meng *et al.*, 2000; Kubota *et al.*, 2004b, 2011; Oatley *et al.*, 2007), GDNF has been shown to have proliferative effects on immature Sertoli cells *in vitro* (Hu *et al.*, 1999; Yang and Han, 2010). In addition, GDNF has been identified as one of the factors that promote tubulogenesis during testis and even kidney development (Popsueva *et al.*, 2003; Costantini and Shakya, 2006). Therefore, we propose that the observed effects of GDNF in our *in vivo* model is exerted through its promotion of Sertoli cell proliferation and tubulogenesis, giving rise to implants with improved SC development.

Here, we highlighted the presence of different types of SC and their developmental pattern over time (in terms of both prevalence and area). In the limited available literature on the ectopic TCI model, detailed examination of SC morphology in *de novo* testis tissue formation is lacking, instead the endpoints have been focused on spermatogenic efficiency. We observed that SC can be found in different patterns; while initially regular SC are the predominant type at 2 wk, enlarged and irregular SC develop and become more prominent at 4 and 8 wk post-implantation. The development of enlarged seminiferous tubules has been described previously in the TTX model, where the enlargements coincided with the increased size of the seminiferous tubular lumen (Schlatt *et al.*, 2002b; Rathi *et al.*, 2005). The absence of efferent ducts in the grafts leading to accumulation of the Sertoli cell secretions has been proposed as the causative mechanism (Schlatt *et al.*, 2002b; Arregui *et al.*, 2008a). However, many of the implants in the present study developed both efferent ducts and rete testis-like structure. Since we retrieved the implants prior to their potential development of a seminiferous lumen, we could not determine whether these structures

would contribute to the absorption of such secretions. Moreover, the nature of enlarged SC in early implants is different from that of the late stage grafts, and the cause of their formation remains to be elucidated in future studies. Reasons for the development of irregular SC are not known but can be attributed to the less than optimal conditions in which the implants are being formed. Similarly, the causes of aberrant SC formation remain unknown but given that they are usually seen in the proximity of rete testis, it could be hypothesized that the hyperplastic rete testis cells entrap some of the neighboring parenchyma undergoing SC development. This is further supported by the presence of cuboidal epithelial lining, typical of rete testis cells, surrounding the aberrant SC.

Several growth factors were found to enhance the development of a specific type of SC. Considering both approaches for determining the predominant type of SC among groups, we propose that FGF2, GDNF-H, and RA enhance the formation of regular, irregular, and enlarged SC, respectively. This is also generally supported by evaluations of the prevalence of different SC types and implant area. Compared with the control, FGF2 treatment led to development of most regular and least aberrant SC. The RA treatment led to the presence of enlarged SC in 100% and ~32% of implants at 4 and 8 wk, respectively. Meanwhile, in the GDNF-H group, irregular SC were seen in >90% of the implants at 4 and 8 wk, where they occupied >50% (range 52-59%) of the implant area.

This was the only histomorphometric study using the TCI model that evaluated the survival of gonocytes in implants. We evaluated the effect of various growth factors on the relative number of gonocytes using only 2-wk samples, because gonocytes were morphologically more distinctive at this time point, compared with those in implants of earlier or later stages. Compared with the control, RA was the only group that increased the relative number of gonocytes in SC. There are no comparable *in vivo* studies, but our results seem to contrast several *in vitro* studies (*i.e.*, organ or cell culture) showing an apoptotic effect of RA on neonatal gonocyte numbers, although mitosis had also resumed in the remaining gonocytes (Livera *et al.*, 2000a; Boulogne *et al.*, 2003). In the postnatal testis, gonocytes migrate to the seminiferous basement membrane prior to their resumption of mitosis and differentiation to SSC; failure to migrate leads to gonocyte apoptosis (Roosen-Runge and Leik, 1968; Orwig *et al.*, 2002a). To achieve migration, gonocytes must actively interact and bind to Sertoli cells; a process that has been shown to be promoted by RA (Griswold *et al.*, 1989; Orth and Jester, 1995; Vernet *et al.*, 2006). In the pig, gonocyte migration

occurs at 4-8 weeks. Considering that the donor pigs were already 2 wk old and the examined implants were 2 wk post-implantation, the timing of RA treatment in our study may have coincided with intrinsic timing of events at this stage of testis development. Therefore, although the mechanism for the observed effect of RA in our study is unknown, it could be hypothesized that RA is involved in either direct promotion of gonocyte survival or indirect promotion of the gonocyte-Sertoli cell interactions during the SC morphogenesis.

A limitation of the earlier TCI studies was the low proportion of germ cells among the donor cells (*e.g.*, 4.5%), resulting in *de novo* formation of seminiferous cords/tubules that typically lacked germ cells (Honaramooz *et al.,* 2007; Kita *et al.,* 2007; Arregui *et al.,* 2008b; Zhang *et al.,* 2008; Dores and Dobrinski 2014). In the present study, the implanted testis cells had ~40% gonocytes; however, the number of gonocytes in implants examined at 2 wk was low, ranging from ~1.5% to 2.6% relative to Sertoli cells. Therefore, there is an obvious disconnect between the ratio of gonocytes at implantation and that at retrieval, even as early as 2 wk after implantation. This may be due to either a massive reduction in gonocyte numbers or a substantial increase in the relative number of somatic cells. In the short-term *in vitro* culture study (Chapter 3), we observed a rapid expansion of somatic cells to full confluency within a week, while gonocyte numbers did not increase nearly as much. Therefore, the observed decrease in gonocyte ratio in implants of the present study is more likely due to the much higher rate of somatic cell proliferation that overtakes gonocyte numbers. In a study by Dores and Dobrinski (2014), implantation of testis cells with relative enrichment of spermatogonia (*i.e.,* 25% *vs.* 3-4%) did not improve the spermatogenic efficiency, defined as the number of seminiferous tubules containing germ cells at 40 wk post-implantation. There are no comparable data from the previous studies, but judging from the histological images presented in some of these earlier studies (Honaramooz *et al.*, 2007; Arregui *et al.*, 2008), the relative number of gonocytes in the present study appears to be improved. Thus, the ideal proportion of gonocytes among donor cells to be implanted would need to be further investigated. On the other hand, the relative number of gonocytes in the present study are almost half of that in our previous study in Chapter 5 (~2% *vs.* ~4%). We used the same testis cell isolation protocol for both studies, but the donor pigs were 2 wk old in the present study and 1 wk old in Chapter 5: therefore, at least part of the difference between these results is due to using donors of different age. This is supported by a study using TTX, where the development of grafts was donor age-dependent, even among very young donors (Schmidt *et al.*, 2006a).

The development of rete testis or rete testis-like structures during *de novo* testis tissue morphogenesis has not been previously reported. In this study, the rete testis was one of the frequently occurring features (observed in ~40% of all implants), regardless of the treatment. Although there were generally no differences in the prevalence of rete testis formation among the groups, this formation occurred earlier in the implants treated with EGF-L, GDNF-H, FGF2, FGF9, or LIF. The expression of EGF, FGF2, and their receptors (EGFRs and FGFRs) have been localized in the straight tubules and rete testis of bulls (Abd-Elmaksoud *et al.*, 2005; Kassab *et al.*, 2007). In addition to GDNF, as describe previously, EGF, FGF2, and FGF9 are involved in promoting tubulogenesis in the developing gonad and kidney (Taub *et al.*, 1990; Humes and Cieslinski, 1992; Castrillon *et al.*, 2000; Popsueva *et al.*, 2003; Combes *et al.*, 2009; Svingen and Koopman, 2013; Li *et al.*, 2014). Given that previous reports failed to mention the development of rete testis in implants, it is unclear whether this widespread rete testis formation in the present study was due to the contamination of the parenchymal testis cell isolates with the mediastinal cells or other mechanisms. Therefore, these findings should be further investigated. In addition, the relationship between the rete testis development and formation of aberrant SC would also warrant further studies.

In the present study, the FFC were a non-pathological feature found in many implants, likely occurring as a result of the remnant fluid within the cell aggregates (*i.e.,* from the added media or growth factor diluents). In addition, the needle insertion may have also caused bleeding, which explains the presence of RBC within FFC observed through histological assessments. The FFC were transient, with high prevalence at 1 wk post-implantation, where they were present in >50% of the samples in multiple groups.

In addition, overall, the use of FGF9 and VEGF in the present study had no discernable effect on *de novo* testis tissue morphogenesis. This was surprising, because these two growth factors have been shown to have important roles during fetal testis development (Ergün *et al.*, 1997; Willerton *et al.*, 2004; Kim *et al.*, 2006a; Cool *et al.*, 2011), and exert supportive effects on both somatic and germ cells *in vitro* (El Ramy *et al.*, 2005; DiNapoli *et al.*, 2006; Schmidt *et al.*, 2006b; Caires *et al.*, 2009). We also found that the use of a higher dose of EGF and GDNF was not advantageous, and in the case of GDNF, in fact, led to a lower implant development. This observation reinforced

the fact that the expected outcomes of studies using growth factors are not simply a function of their relative dose.

## 6.6 Conclusions

In this exploratory study, the effects of multiple growth factors on *de novo* testis tissue morphogenesis were evaluated for the first time. Our findings suggest that even brief pre-implantation exposure of testis cells to growth factors can have profound and long-term effects on the development of both somatic and germ cells in the implants. Growth factors also caused unique SC formation patterns which may influence the spermatogenic and steroidogenic efficiency of the implants. Therefore, our findings provided a basis for future studies using the TCI model where background information was lacking.

# CHAPTER 7

# GENERAL DISCUSSION AND FUTURE DIRECTIONS

## 7.1 General Discussion

*In vitro* and *in vivo* culture systems are two important tools in the study of testicular function and spermatogenesis. The knowledge obtained from the studies based on these two systems has significantly improved our understanding of the factors involved in the regulation of testis development and spermatozoa production. The studies presented in this thesis were designed to focus on *in vitro* and *in vivo* culture systems for the development of testis cells and tissue using pigs as a model. The following is a discussion of the common themes and findings among different experiments as well as general conclusions that can be drawn from them.

### *7.1.1 Optimized Culture Conditions for Maintenance, Proliferation, and Colony Formation of Porcine Gonocytes*

Through a step-wise approach, optimized culture conditions for the short-term maintenance, proliferation, and colony formation of porcine gonocytes were established (Chapter 3). These optimized conditions were then utilized to study the *in vitro* development of porcine testis cells in a prolonged culture (Chapter 4). One of the most important findings to emerge from the first study (Chapter 3), aside from the optimized culture conditions, was that gonocytes require the presence of feeder cells (which were present in the form of ~60% mixed testis somatic cells) for their survival and growth *in vitro*. This finding was further supported by the poor cell growth when we attempted to culture an enriched population of gonocytes (~80-90%). The observed requirement of feeder cells presence for gonocyte growth in culture was consistent with previously reports (van Dissel-Emiliani *et al.*, 1993). On the other hand, the 'floating' nature of gonocytes, especially during the first few days of culture (Chapter 3), indicated that infrequent media changes can avoid the unnecessary losses of gonocytes during media changes. This conclusion was strongly supported by evidence of highly viable floating gonocytes (>85% viability) in the removed media after several

days of culture, which increased the number of gonocytes settling on the somatic cell monolayer after the infrequent media change routine was adapted. Overall, these findings contributed in several ways to our understanding of neonatal porcine gonocytes and provided a basis for future *in vitro* studies.

### *7.1.2 Development of Neonatal Porcine Testis Cells and Colonies In Vitro*

Using the optimized culture conditions established in our first *in vitro* study (Chapter 3), we evaluated the *in vitro* behavior, colony formation, and ultrastructure of gonocytes, with the aid of various imaging techniques (*i.e.*, live-cell imaging, SEM and TEM) and fluorescent labeling in a second *in vitro* study (Chapter 4). To our knowledge, this latter study was the first to trace the development of neonatal porcine testis cells in real-time and thoroughly examine their ultrastructural changes over time. However, given that our optimized culture conditions (Chapter 3) were using a basic culture system, it was not clear whether they could support the development of neonatal porcine testis cells in a prolonged culture.

In Chapter 4, we highlighted the unique organization of somatic cells to form areas of circular arrangements, which we presumed to be a preferred site for the establishment of gonocyte colonies. We are not certain whether the formation of these circular structures is indeed as a result of somatic cell-germ cell interactions. Currently, there are no closely-related studies to support our assumption. The most intriguing observation in this study was the formation of EBLC by gonocytes, which was tracked stage-by-stage (*i.e.*, singles, paired, clusters, morula-like colonies, and EBLC) via live-cell imaging. The formation of the EBLC, or commonly reported as embryoid bodies, is a common feature of gonocytes and other MGSC *in vitro,* and their developmental stages have been well described (van Dissel-Emiliani *et al.*, 1993; Hasthorpe *et al.*, 2000; Goel *et al.*, 2007, 2009; Han *et al.*, 2009; Kuijk *et al.*, 2009; Matsui *et al.*, 2014). Real-time observations revealed that the formation of EBLC relies on the ability of gonocytes to establish contact with each other, leading to their aggregation, and creation of a center for the attraction of more gonocytes to form bigger colonies and finally EBLC. This is achieved via their active movement, assisted by the cytoplasmic projections, which based on SEM examinations could be categorized into lamellipodia, filopodia, membrane blebs, and membrane ruffles. The formation of cytoplasmic projections in migrating cells is driven by the polymerization of actin cytoskeletal, promoted by

the expression of GDNF (Korn *et al.*, 1987; Dovere *et al.*, 2013; Tang and Gerlach, 2017), as was confirmed in this study by F-actin fluorescent labeling.

The multinucleated nature of EBLC and the events leading to their transformation via cellular fusion were proposed in this study for the first time. In fact, these multinucleated EBLC also possessed extensive cytoplasmic projections and motility at a slow rate. The present study adds to a growing body of research that indicates the importance of cytoplasmic projection (or pseudopods) during the migration of gonocytes to the basement membrane of seminiferous tubules prior to their differentiation into SSC (McGuinness and Orth, 1992; Nagano *et al.*, 2000; Orwig *et al.*, 2002a). We also noted the presence of round gonocytes among the populations of gonocytes with cytoplasmic projections. These immotile and non-viable gonocytes, confirmed using live-cell imaging and trypan-blue assays, respectively, represent the cells that had undergone apoptosis or were dead. This finding complimented the previous observations by Orwig *et al.*, (2002a) that compared the developmental competency of two subpopulations of gonocytes (pseudopod *vs.* round gonocytes), using a germ cell transplantation assay.

One of the ultimate goals of *in vitro* culture systems for MGSC is to expand their numbers while maintaining their 'stemness' long-term. Using the same basic culture system developed in Chapter 3, we were able to propagate gonocytes up to ~9 fold by the end of our study in Chapter 4 (4 wk). The pluripotent nature of the propagated gonocytes and EBLC, as shown by the expression of POU5F1, suggests that they have the capacity to undergo infinite self-renewal, and potentially give rise to any cells and tissues of the three germinal layers. These findings might also have clinical implications in fertility preservation, where high numbers of MGSC are required for efficient germ cell transplantation and cell-based therapy. Therefore, our findings in Chapter 4 adequately addressed the question posed earlier in this section as to whether basic culture conditions can support the maintenance and propagation of gonocytes in a prolonged culture condition.

### *7.1.3 The Ectopic Testis Cell Implantation (TCI) Model*

The experiments designed in Chapter 5 focused on the development of an efficient technique for implantation of testis cells in an ectopic implantation model. In a pioneering study by Honaramooz *et al.*, (2007), a surgical implantation technique was developed, which coupled with the low number of germ cells in the population of donor cells resulted in inconsistent implant development with

low spermatogenic efficiency. The issue of low number of germ cells among the donor cells had been addressed by the establishment of a three-step enzymatic digestion method in our lab and was applied in Chapter 3. Two implantation approaches were examined in two separate experiments, the conventional surgical approach (but with the added gel-based matrices as a cell carrier) and a subcutaneous injection method of cell aggregates (without cell carriers). Other examined variables included the cell number and the implantation site. This study was the first study to examine various gel-based matrices (*i.e.,* gelatin, collagen, and agarose) for cell implantation, which adds to the literature where the only other studies had used the commercially available Matrigel matrix (Watanabe *et al.*, 2009; Dores and Dobrinski, 2014). This study found that both approaches offer advantages over the conventional implantation technique used in the previous reports (Honaramooz *et al.*, 2007; Arregui *et al.*, 2008b). The use of gel-based matrices as a cell carrier enables manipulation of the number of cells to be implanted (50 - 100 $\times$ $10^6$ cells per implant/site) and efficient placement of cells at the implantation site. Although *de novo* morphogenesis of testis tissue from the gel-based matrix implants (*i.e.,* gelatin and collagen) was not compromised and performed slightly better than the control, the consistency of the outcomes, control over the transferred cells, as well as being less invasive led us to adopt the subcutaneous injection technique for our next experiments in Chapter 6.

In these experiments (Chapter 5), we also examined for the first time the potential of ultrasound biomicroscopy (UBM) for monitoring the implants prior to their retrieval. The use of UBM via 2D and 3D modes allowed visualization of the implants, estimation of their degree of tissue formation, and neovascularization *in situ*. However, the most obvious advantage of using UBM is that it allows basic measurements of implants (*e.g.,* length, width, and height), through which the data could be manipulated to derive other useful information (*e.g.*, volume and cross-sectional area), with the aid of its software. As proof of principle, we compared the UBM measurements (*i.e.*, length and width) with physical measurements when the implants were retrieved, and found high fidelity between the two methods. This finding has significant implications for future studies in the areas of testis cell implantation as well as testis tissue xenografting, where UBM could be used to assess the development of implants and grafts over time, potentially reducing the number of required samples and recipient mice.

The findings in Chapter 5 also highlighted for the first time the effect of implantation site on the development of testis cell implants. The developmental potential of implants as indicated by their weight decreased from cranial to caudal sites. This important finding will influence the way we sample implants in the future, especially during the early period post-grafting, pointing to a need to also randomize our sampling based on the implant site. Finally, we also evaluated the effect of gonadal status on the development of testis cell implants and found no apparent gross or histomorphometric differences between the intact and castrated recipients, consistent with previous reports (Shinohara *et al.*, 2002; Abbasi and Honaramooz, 2010b). Learning from the latter two findings from Chapter 5, we randomized our sampling and used intact recipient in our subsequent study in Chapter 6.

### *7.1.4 The Effect of Growth Factors on De Novo Porcine Testis Tissue Morphogenesis In Vivo*

The final study in this thesis (Chapter 6) provides the first comprehensive assessment of the effect of growth factors on *de novo* morphogenesis of porcine testis tissue in an ectopic implantation model. In this study, we examined the effect of brief exposure of cell aggregates to various growth factors (*i.e.*, EGF, GDNF, FGF2, FGF9, VEGF, SCF, LIF, or RA). The selected growth factors are known to have a significant role in testis development (De Miguel *et al.*, 1996; Mauduit *et al.*, 1999; Meng *et al.*, 2000; Kubota *et al.*, 2004a; Wu *et al.*, 2005; Hofmann *et al.*, 2005; Aponte *et al.*, 2006; Bott *et al.*, 2006; DiNapoli *et al.*, 2006; Kim *et al.*, 2006a; Wang and Culty, 2007; Zhou *et al.*, 2008; Chung *et al.*, 2009; Baltes-Breitwisch *et al.*, 2010; Cool *et al.*, 2011; Manku *et al.*, 2015). Due to a lack of background *in vivo* studies, the dosage of each growth factor was set higher than those applied *in vitro*, and where there was widespread disagreement in the range of such doses, a low and a high dose group were included (*i.e.*, EGF-L, EGF-H and GDNF-L, GDNF-H). The growth factors were added to the testis cell aggregates immediately prior to implantation, using the subcutaneous injection technique that was optimized in Chapter 5.

This exploratory study showed that indeed the TCI model could be used to examine potential factors involved in testis development because *de novo* morphogenesis of the testis tissue could be manipulated in the presence of growth factors. The FGF2 appeared to be the only growth factor to have an impact on both the physical and histological development of implants, while several other growth factors had an effect on either parameter (*i.e.*, LIF, SCF, EGF, and GDNF-L). We

speculated that these growth factors enhanced *de novo* testis tissue morphogenesis via promoting the survival of implanted testis cells and later by regulating their proliferation and differentiation, reflected by their roles in the testis development *in situ* (Gonzalez *et al.*, 1990; Sordoillet *et al.*, 1991, 1992; Matsui *et al.*, 1991; Pesce *et al.*, 1993; Han *et al.*, 1993; De Miguel *et al.*, 1996; Mauduit *et al.*, 1999; Meng *et al.*, 2000; Yan *et al.*, 2000a; Hirai *et al.*, 2004; Wu *et al.*, 2005; Hofmann *et al.*, 2005; Aponte *et al.*, 2006, 2008; Chung *et al.*, 2009a). We found unique temporospatial changes in the morphology of SC, where the prevalence of regular, enlarged, irregular, and aberrant types of SC changed over time, which were accentuated by different growth factors. The accumulation of secretions from Sertoli cells was suggested as a cause of the formation of dilated/enlarged SC (Arregui *et al.*, 2008b). However, the presence of efferent ductules and rete testis in the developed tissue, reported for the first time here in this study, might debunk that assumption. Adding to this interesting finding was the tendency of certain growth factors to support the development of rete testis and/or a specific type of SC. The exact mechanism underlying these morphological changes and their association with specific growth factors remain to be explored. Other than VEGF, which has been examined in a single study using the same model (Dores and Dobrinski, 2014), there are no closely-related studies to compare with our observations. Therefore, this large-scale study provided several important findings to further our insights into *de novo* testis tissue morphogenesis, and many more leads into the potential effects of various growth factors to guide future research in this field.

One of the limitations of the TCI model was the low spermatogenic efficiency, likely as a consequence of the low number of donor germ cells in the developed implants (Honaramooz *et al.*, 2007; Arregui *et al.*, 2008a; Campos-Junior *et al.*, 2014; Dores and Dobrinski, 2014). Thus, in this study, we addressed this problem by implanting cell aggregates of high germ cell proportions (~40% gonocytes). Although direct comparison of results is not possible, in previous studies most SC in implants lacked germ cells, while we observe gonocytes in almost all SC. Despite being higher than in the previous reports, the relative number of gonocytes was lower in the implants than in intact age-matched testes. The RA treatment appeared to be the only growth factor to have a significant effect on the relative number of gonocytes. The hypoxic conditions, prior to the establishment of blood supplies, have been proposed as a causative factor for germ cell losses in implants (Schmidt *et al.*, 2006b; Arregui *et al.*, 2014; Dores and Dobrinski, 2014). However, considering the fact that adding VEGF, as an angiogenesis promoter, had no apparent effect on the

relative number of gonocytes, we propose that germ cell losses post-implantation are not because of the hypoxic effects on germ cells but likely due to other intrinsic factors that remain to be elucidated. For instance, reduced proportion of gonocytes may in fact have nothing to do with their losses but instead with the disproportional proliferation rate of somatic cells over gonocytes.

Finally, the data in Chapter 6 showed no advantage of using higher doses of EGF and GDNF over lower doses on the development of implants. In fact surprisingly, this development in the high dose groups appeared repressed and even less than the control. The reasons for such observations are not clear but indicate the need for more extensive studies using this model to elucidate the effect of each growth factor in more details.

## 7.2 Future Directions

### *7.2.1 Manipulation of Culture Conditions for Long-Term Maintenance and Propagation of Porcine Gonocytes*

The optimized culture system developed in this thesis (Chapter 3) can be further examined and potentially modified for use in long-term maintenance and propagation of gonocytes. This basic culture system could be utilized as a tool to examine the effects of other conditions that are known to have beneficial effects (*i.e.*, survival, self-renewal, or proliferation) on gonocytes. Such conditions can include the use of other media and serum alternatives (*e.g.*, DMEM/F12 or KSR), growth factors (such as some of those described in Chapter 6), hormones (*e.g.*, LH, FSH, testosterone, or progesterone), and other additives (*e.g.,* amino acids, proteins, or vitamins). For this purpose, the already established culture systems, such as those for long-term maintenance and propagation of SSC, could be used as a study baseline (Kanatsu-Shinohara *et al.*, 2003, 2005, 2008a; Kubota *et al.*, 2004b; Ryu *et al.*, 2005). To address the concern of the negative effect of testis somatic cells on the pluripotency of gonocytes, mitotically inactivated cells (*e.g.*, STO and MEF) should also be considered as alternative feeder cells. A study performed by Lee *et al.*, (2013) showed that porcine SSC could be optimally cultured at 31 °C, demonstrating marked pluripotency compared with those cultured at 34 °C and 37 °C. Thus, the effect of temperature on gonocytes could be re-examined by testing lowered temperatures (*i.e.*, <35 °C), along with the addition of analyses for DNA synthesis and proliferation to the routine evaluations for growth rate.

### *7.2.2 Motility and Pluripotency of Porcine Gonocytes and EBLC*

Establishment of the cytoplasmic projections is crucial for the survival and migration of gonocytes (McGuinness and Orth, 1992; Nagano *et al.*, 2000; Orwig *et al.*, 2002a). Thus, identifying the molecular cues regulating the formation of these projections is of high importance in the study of gonocytes. Two candidate growth factors, GDNF and SCF/c-kit ligand (Orth *et al.*, 1997; Basciani *et al.*, 2008; Dovere *et al.*, 2013) have been proposed to promote the development of actin cytoskeleton and migration of gonocytes to the basement membrane of the SC, and could be included in deciphering the motility of gonocytes *in vitro*. In addition, live-cell imaging could be utilized to further understand the kinetics of gonocyte proliferation and migration *in vitro.* It will be interesting to see whether improving the population of motile gonocytes (with cytoplasmic projections/pseudopods) would indeed benefit their stem cell potential for application in germ cell transplantation, because the efficiency of gonocyte migration and subsequent colonization of the SC are thought to rely on the number of motile gonocytes (Orwig *et al.*, 2002a).

The MGSC can be manipulated to produce pluripotent stem cells and offer a useful tool for cell-based therapy and regenerative medicine (Geijsen and Jones, 2008). The application of pluripotent stem cells of MGSC origin for human use is favored over the iPSC of somatic cell origin, due to their autologous nature, their superior genomic integrity, and close resemblance to ESC (Ko *et al.*, 2009; Kim and Izpisua Belmonte, 2011). In addition, the pluripotent state of MGSC could be induced spontaneously under specific culture conditions (Kanatsu-Shinohara *et al.*, 2004b; Ko *et al.*, 2009), without the need of forced biophysical reprograming such as that for the iPSC (Takahashi *et al.*, 2007; Lowry *et al.*, 2008; Kim *et al.*, 2016). However, the progress in germline-derived pluripotent stem cells (GPS) has been hindered by the poor understanding of factors behind this spontaneous pluripotency, and the inefficiency of the isolation and propagation of MGSC (Kim and Izpisua Belmonte, 2011). Accordingly, the neonatal porcine gonocytes offer a great advantage to be used as a model to study GPS, especially now that they can be isolated, enriched, and propagated efficiently with the available technologies described or established in this thesis. Future studies should focus on how to improve and identify the molecular cues regulating the pluripotency of gonocytes. The SCF and LIF are two growth factors that have been proposed to be essential for the maintenance of gonocyte pluripotency i*n vitro* (Kanatsu-Shinohara *et al.*, 2007; Tu *et al.*, 2007).

Comprehensive investigation of the role of these and other growth factors in regulating the pluripotency of gonocytes will provide insight into GPS.

In this study, the pluripotency of gonocytes and EBLC was determined using a single marker, POU5F1. Future studies should examine the expression of other pluripotency markers, such as the SSEA-1 and NANOG homeobox (NANOG). The multipotency of gonocytes and EBLC could be investigated *in vitro* by providing specific culture conditions that direct their transformation into any cells and tissues of the three germinal layers, as previously shown for SSC from adult mouse testes (Guan *et al.*, 2006). Transfer of cultured gonocytes and EBLC *in vivo* is another approach that could be performed in the future to assess their multipotency. Teratoma formation, as an indicator of multipotency, has been observed after subcutaneous implantation of cultured piglets gonocytes (Hoei-Hansen *et al.*, 2005; Tu *et al.*, 2007; Goel *et al.*, 2009; Niu *et al.*, 2016).

### *7.2.3 Incorporating UBM in TTX and TCI Studies*

Future studies could utilize UBM for monitoring the development of grafts/implants in between designated retrieval points. In addition to visualizing gross features of grafts/implants (*i.e.*, size, shape, and dimension), the UBM data could be extrapolated to gain additional information on the development of grafts/implants. The ability to detect blood vessels at implantation sites should be incorporated in the study of angiogenesis and hemodynamics of grafts/implants. The ability of the UBM to measure the oxygen saturation level should be further studied to assess the hypoxic environment and its effect on graft/implant survival. With the aid of a software, 3D remodeling of grafts/implants and their blood supply could also be constructed. Future studies should also explore the relationship/correlation between the echogenicity of implants and their histology. This will be useful as a preliminary indicator of *de novo* morphogenesis, especially during the early phases of grafting/implanting. The UBM also allows for image-guided injections in future studies, especially in the studies designed to evaluate the application of a series of treatments over time (*i.e.*, growth factors, drugs, or hormones) to the grafts/implants.

### *7.2.4 Utilizing De Novo Morphogenesis of Testis Tissue for the Study of Testiculogenesis and Spermatogenesis*

Despite the lack of extensive background information and poor spermatogenic efficiency, *de novo* morphogenesis of testis tissue remains one of the only and most promising bioassays for the study of testis development and spermatogenesis. This model has a unique advantage for elucidating the molecular cues and cellular interactions during the process of testis development, where it offers an accessible route for manipulating both the somatic and germ cell components of the testis. However, further studies are needed to standardize the protocols and improve the consistency of the outcomes, before this bioassay can be fully utilized. Nevertheless, the effect of growth factors on *de novo* morphogenesis of testis tissue should be further investigated for future studies. The findings presented in this thesis, provide a basis for designing future experiments to examine new growth factors, dosage/regimen of treatment, as well as assessment criteria. The growth factors that displayed significant effects on gross and/or histomorphometric evaluations in this study (*i.e.,* FGF2, RA, GDNF, LIF, SCF, and EGF) could be further studied in detail. We also suggest re-examining other growth factors that were not found effective, using other treatment doses/regimens. One of the approaches that could be implemented to evaluate the effect of a given growth factor is by performing loss-of-function or gain-of-function studies. Future studies should also manipulate the growth factor dose, regimen, interval, and duration of exposure. Finally, it would also be interesting to uncover the underlying factors leading to the temporospatial changes of the SC and their long-term effect on the spermatogenic efficiency and tissue function. The source and mechanism of the rete testis and efferent ductules development in the implants and their impact on the structural growth of the resultant testis tissue should also be investigated.

## REFERENCES


**Abbasi S and Honaramooz A** (2010a) The number of grafted fragments affects the outcome of testis tissue xenografting from piglets into recipient mice. *Veterinary Medicine International* **2011** 20–23.

**Abbasi S and Honaramooz A** (2010b) Effects of recipient mouse strain, sex and gonadal status on the outcome of testis tissue xenografting. *Reproduction, Fertility & Development* **22** 1279–1286.

**Abbasi S and Honaramooz A** (2011) Xenografting of testis tissue from bison calf donors into recipient mice as a strategy for salvaging genetic material. *Theriogenology* **76** 607–614.

**Abbasi S and Honaramooz A** (2012) Feasibility of salvaging genetic potential of post-mortem fawns: Production of sperm in testis tissue xenografts from immature donor white-tailed deer (*Odocoileus virginianu*s) in recipient mice. *Animal Reproduction Science* **135** 47–52.

**Abbasi H, Tahmoorespur M, Hosseini SM, Nasiri Z, Bahadorani M, Hajian M, Nasiri MR and Nasr-Esfahani MH** (2013) THY1 as a reliable marker for enrichment of undifferentiated spermatogonia in the goat. *Theriogenology* **80** 923–932.

**Abd-Elmaksoud A, Vermehren M, Nützel F, Habermann FA and Sinowatz F** (2005) Analysis of fibroblast growth factor 2 (FGF2) gene transcription and protein distribution in the bovine testis. *Growth Factors* **23** 295–301.

**Abel MH, Wootton AN, Wilkins V, Huhtaniemi I, Knight PG and Charlton HM** (2000) The effect of a null mutation in the follicle-stimulating hormone receptor gene on mouse reproduction. *Endocrinology* **141** 1795–1803.

**Abel MH, Baker PJ, Charlton HM, Monteiro A, Verhoeven G, De Gendt K, Guillou F and O'Shaughnessy PJ** (2008) Spermatogenesis and sertoli cell activity in mice lacking sertoli cell receptors for follicle-stimulating hormone and androgen. *Endocrinology* **149** 3279–3285.

**Abrishami M, Abbasi S and Honaramooz A** (2010a) The effect of donor age on progression of spermatogenesis in canine testicular tissue after xenografting into immunodeficient mice. *Theriogenology* **73** 512–522.

**Abrishami M, Anzar M, Yang Y and Honaramooz A** (2010b) Cryopreservation of immature porcine testis tissue to maintain its developmental potential after xenografting into recipient mice. *Theriogenology* **73** 86–96.

**Abu Elhija M, Lunenfeld E, Schlatt S and Huleihel M** (2012) Differentiation of murine male germ cells to spermatozoa in a soft agar culture system. *Asian Journal of Andrology* **14** 285–293.

**Adams IR and McLaren A** (2002) Sexually dimorphic development of mouse primordial germ cells: Switching from oogenesis to spermatogenesis. *Development* **129** 1155–1164.

**Adamson ED** (1993) Growth factors and their receptors in development. *Developmental Genetics* **14** 159–164.

**Aeckerle N, Dressel R and Behr R** (2013) Grafting of neonatal marmoset monkey testicular single-cell suspensions into immunodeficient mice leads to ex situ testicular cord neomorphogenesis. *Cells, Tissues, Organs* **198** 209–220.

**Almeida FFL, Leal MC and França LR** (2006) Testis morphometry, duration of spermatogenesis, and spermatogenic efficiency in the wild boar (*Sus scrofa scrofa*). *Biology of Reproduction* **75** 792–799.

**Altman E, Yango P, Moustafa R, Smith JF, Klatsky PC and Tran ND** (2014) Characterization of human spermatogonial stem cell markers in fetal, pediatric, and adult testicular tissues. *Reproduction* **148** 417–427.

**Anderson R, Copeland TK, Schöler H, Heasman J and Wylie C** (2000) The onset of germ cell migration in the mouse embryo. *Mechanisms of Development* **91** 61–68.

**Anderson R, Fulton N, Cowan G, Coutts S and Saunders PT** (2007) Conserved and divergent patterns of expression of DAZL, VASA and OCT4 in the germ cells of the human fetal ovary and testis. *BMC Developmental Biology* **7** 136.

**Anderson EL, Baltus AE, Roepers-Gajadien HL, Hassold TJ, de Rooij DG, van Pelt AMM and Page DC** (2008) Stra8 and its inducer, retinoic acid, regulate meiotic initiation in both spermatogenesis and oogenesis in mice. *Proceedings of the National Academy of Sciences* **105** 14976–14980.

**Aoshima K, Baba A, Makino Y, Okada Y and Sun Y** (2013) Establishment of alternative culture method for spermatogonial stem cells using knockout serum replacement. *PLoS ONE* **8** e77715.

**Aponte PM, Van Bragt MPA, De Rooij DG and Van Pelt AMM** (2005) Spermatogonial stem cells: Characteristics and experimental possibilities. *Acta Pathologica, Microbiologica, et immunologica Scandinavica* **113** 727–742.

**Aponte PM, Soda T, van de Kant HJG and de Rooij DG** (2006) Basic features of bovine spermatogonial culture and effects of glial cell line-derived neurotrophic factor. *Theriogenology* **65** 1828–1847.

**Aponte PM, Soda T, Teerds KJ, Mizrak SC, van de Kant HJG and de Rooij DG** (2008) Propagation of bovine spermatogonial stem cells *in vitro*. *Reproduction* **136** 543–557.

**Appling DR and Chytil F** (1981) Evidence of a role for retinoic acid (Vitamin A-Acid) in the maintenance of testosterone production in male rats. *Endocrinology* **108** 2120–2123.

**Ara T, Nakamura Y, Egawa T, Sugiyama T, Abe K, Kishimoto T, Matsui Y and Nagasawa T** (2003) Impaired colonization of the gonads by primordial germ cells in mice lacking a chemokine, stromal cell-derived factor-1 (SDF-1). *Proceedings of the National Academy of Sciences* **100** 5319–5323.

**Arregui L and Dobrinski I** (2014) Xenografting of testicular tissue pieces: 12 years of an *in vivo* spermatogenesis system. *Reproduction* **148** R71–84.

**Arregui L, Rathi R, Megee SO, Honaramooz A, Gomendio M, Roldan ERS and Dobrinski I** (2008a) Xenografting of sheep testis tissue and isolated cells as a model for preservation of genetic material from endangered ungulates. *Reproduction* **136** 85–93.

**Arregui L, Rathi R, Zeng W, Honaramooz A, Gomendio M, Roldan ERS and Dobrinski I** (2008b) Xenografting of adult mammalian testis tissue. *Animal Reproduction Science* **106** 65–76.

**Arregui L, Rathi R, Modelski M, Zeng W, Roldan ERS and Dobrinski I** (2012) Suppression of spermatogenesis before grafting increases survival and supports resurgence of spermatogenesis in adult mouse testis. *Fertility & Sterility* **97** 1422–1429.

**Arregui L, Dobrinski I and Roldan ERS** (2014) Germ cell survival and differentiation after xenotransplantation of testis tissue from three endangered species: Iberian lynx (*Lynx pardinus*), Cuvier's gazelle (Gazella cuvieri) and Mohor gazelle (*G. dama mhorr*). *Reproduction, Fertility & Development* **26** 817.

**Asatiani K, Gromoll J, Eckardstein S V, Zitzmann M, Nieschlag E and Simoni M** (2002) Distribution and function of FSH receptor genetic variants in normal men. *Andrologia* **34** 172–176.

**Attar E, Ozsait B, Bulgurcuoglu S, Serdaroglu H and Arici A** (2003) Effect of leukaemia inhibitory factor on long-term sperm motility and survival. *Reproductive BioMedicine Online* **7** 71–74.

**Awang-Junaidi AH and Honaramooz A** (2018) Optimization of culture conditions for short-term maintenance, proliferation, and colony formation of porcine gonocytes. *Journal of Animal Science & Biotechnology* **9** 8.

**Azizi H, Conrad S, Hinz U, Asgari B, Nanus D, Peterziel H, Hajizadeh Moghaddam A, Baharvand H and Skutella T** (2016) Derivation of pluripotent cells from mouse sscs seems to be age dependent. *Stem Cells International* **2016** 1–13.

**Bahadorani M, Hosseini SM, Abedi P, Hajian M, Hosseini SE, Vahdati A, Baharvand H and Nasr-Esfahani MH** (2012) Short-term in-vitro culture of goat enriched spermatogonial stem cells using different serum concentrations. *Journal of Assisted Reproduction & Genetics* **29** 39–46.

**Baillie AH** (1964) The histochemistry and ultrastructure of the gonocyte. *Journal of Anatomy* **98** 641–645.

**Baker PJ and O'Shaughnessy PJ** (2001) Role of gonadotrophins in regulating numbers of Leydig and Sertoli cells during fetal and postnatal development in mice. *Reproduction* **122** 227–234.

**Baltes-Breitwisch MM, Artac RA, Bott RC, McFee RM, Kerl JG, Clopton DT and Cupp AS** (2010) Neutralization of vascular endothelial growth factor antiangiogenic isoforms or administration of proangiogenic isoforms stimulates vascular development in the rat testis. *Reproduction* **140** 319–329.

**Barrionuevo F, Bagheri-Fam S, Klattig J, Kist R, Taketo MM, Englert C and Scherer G** (2006) Homozygous inactivation of Sox9 causes complete XY sex reversal in mice. *Biology of Reproduction* **74** 195–201.

**Bartlett JMS, Weinbauer GF and Nieschlag E** (1989) Differential effects of FSH and testosterone on the maintenance of spermatogenesis in the adult hypophysectomized rat. *The Journal of Endocrinology* **121** 49–58.

**Baschong W, Suetterlin R and Laeng RH** (2001) Control of autofluorescence of archival formaldehyde-fixed, paraffin-embedded tissue in confocal laser scanning microscopy (CLSM). *The Journal of Histochemistry & Cytochemistry* **49** 1565–1572.

**Basciani S, De Luca G, Dolci S, Brama M, Arizzi M, Mariani S, Rosano G, Spera G and Gnessi L** (2008) Platelet-derived growth factor receptor β-subtype regulates proliferation and migration of gonocytes. *Endocrinology* **149** 6226–6235.

**Bendel–Stenzel M, Anderson R, Heasman J and Wylie C** (1998) The origin and migration of primordial germ cells in the mouse. *Seminars in Cell & Developmental Biology* **9** 393–400.

**Billig H, Furuta I, Rivier C, Tapanainen J, Parvinen M and Hsueh AJ** (1995) Apoptosis in testis germ cells: Developmental changes in gonadotropin dependence and localization to selective tubule stages. *Endocrinology* **136** 5–12.

**Birkhead T., Buchanan KL, Devoogd T., Pellatt E., Székely T and Catchpole CK** (1997) Song, sperm quality and testes asymmetry in the sedge warbler. *Animal Behaviour* **53** 965–971.

**Boepple PA, Hayes FJ, Dwyer AA, Raivio T, Lee H, Crowley WF, Pitteloud N and Pitteloud N** (2008) Relative roles of inhibin B and sex steroids in the negative feedback regulation of follicle-stimulating hormone in men across the full spectrum of seminiferous epithelium function. *The Journal of Clinical Endocrinology & Metabolism* **93** 1809–1814.

**Bokemeyer C, Kuczyk MA, Dunn T, Serth J, Hartmann K, Jonasson J, Pietsch T, Jonas U and Schmoll HJ** (1996) Expression of stem-cell factor and its receptor c-kit protein in normal testicular tissue and malignant germ-cell tumours. *Journal of Cancer Research & Clinical Oncology* **122** 301–306.

**Borjigin U, Zhou X, Han X, Li R, Herrid M and Bou S** (2011) Enrichment and short term culture of the ovine gonocyte. *Journal of Animal & Veterinary Advances* **10** 2936–2942.

**Bott RC, McFee RM, Clopton DT, Toombs C and Cupp AS** (2006) Vascular endothelial growth factor and kinase domain region receptor are involved in both seminiferous cord formation and vascular development during testis morphogenesis in the rat. *Biology of Reproduction* **75** 56–67.

**Boulogne B, Habert R and Levacher C** (2003) Regulation of the proliferation of cocultured gonocytes and sertoli cells by retinoids, triiodothyronine, and intracellular signaling factors: Differences between fetal and neonatal cells. *Molecular Reproduction & Development* **65** 194–203.

**Bowles J, Knight D, Smith C, Wilhelm D, Richman J, Mamiya S, Yashiro K, Chawengsaksophak K, Wilson MJ, Rossant J *et al.*** (2006) Retinoid Signaling determines germ cell fate in mice. *Science* **312** 596–600.

**Bowman PD, Meek RL and Daniel CW** (1975) Aging of human fibroblasts *in vitro*. Correlations between DNA synthetic ability and cell size. *Experimental Cell Research* **93** 184–190.

**Bratt-Leal AM, Carpenedo RL and McDevitt TC** (2009) Engineering the embryoid body microenvironment to direct embryonic stem cell differentiation. *Biotechnology Progress* **25** 43–51.

**Braydich-Stolle L, Kostereva N, Dym M and Hofmann MC** (2007) Role of Src family kinases and N-Myc in spermatogonial stem cell proliferation. *Developmental Biology* **304** 34–45.

**Brinster RL** (2002) Germline stem cell transplantation and transgenesis. *Science* **296** 2174–2176.

**Brinster RL** (2007) Male germline stem cells: From mice to men. *Science* **316** 404–405.

**Brinster RL and Avarbock MR** (1994) Germline transmission of donor haplotype following spermatogonial transplantation. *Proceedings of the National Academy of Sciences of the United States of America* **91** 11303–11307.

**Brinster RL and Zimmermann JW** (1994) Spermatogenesis following male germ-cell transplantation. *Proceedings of the National Academy of Sciences of the United States of America* **91** 11298–11302.

**Brinster CJ, Ryu BY, Avarbock MR, Karagenc L, Brinster RL and Orwig KE** (2003) Restoration of fertility by germ cell transplantation requires effective recipient preparation. *Biology of Reproduction* **69** 412–420.

**Bryant JM, Meyer-Ficca ML, Dang VM, Berger SL and Meyer RG** (2013) Separation of spermatogenic cell types using STA-PUT velocity sedimentation. *Journal of Visualized Experiments : JoVE*.

**Buaas FW, Val P and Swain A** (2009) The transcription co-factor CITED2 functions during sex determination and early gonad development. *Human Molecular Genetics* **18** 2989–3001.

**Buageaw A, Sukhwani M, Ben-Yehudah A, Ehmcke J, Rawe VY, Pholpramool C, Orwig KE and Schlatt S** (2005) GDNF family receptor alpha1 phenotype of spermatogonial stem cells in immature mouse testes. *Biology of Reproduction* **73** 1011–1016.

**Buzzard JJ, Wreford NG and Morrison JR** (2002) Marked extension of proliferation of rat Sertoli cells in culture using recombinant human FSH. *Reproduction* **124** 633–641.

**Caires KC, de Avila J and McLean DJ** (2009) Vascular endothelial growth factor regulates germ cell survival during establishment of spermatogenesis in the bovine testis. *Reproduction* **138** 667–677.

**Campos-Junior PHA, Costa GMJ, Avelar GF, Lacerda SMSN, Da Costa NN, Ohashi OM, Miranda MDS, Barcelos LS, Jorge ÉC, Guimarães DA *et al.*** (2014) Derivation of sperm from xenografted testis cells and tissues of the peccary (*Tayassu tajacu*). *Reproduction* **147** 291–299.

**Cancilla B, Davies A, Ford-Perriss M and Risbridger GP** (2000) Discrete cell- and stage-specific localisation of fibroblast growth factors and receptor expression during testis development. *The Journal of Endocrinology* **164** 149–159.

**Carmeliet P, Ferreira V, Breier G, Pollefeyt S, Kieckens L, Gertsenstein M, Fahrig M, Vandenhoeck A, Harpal K, Eberhardt C *et al.*** (1996) Abnormal blood vessel development and lethality in embryos lacking a single VEGF allele. *Nature* **380** 435–439.

**Carpenter G and Cohen S** (1990) Epidermal growth factor. *The Journal of Biological Chemistry* **265** 7709–7712.

**Cassani B, Villablanca EJ, De Calisto J, Wang S and Mora JR** (2012) Vitamin A and immune regulation: Role of retinoic acid in gut-associated dendritic cell education, immune protection and tolerance. *Molecular Aspects of Medicine* **33** 63–76.

**Castrillon DH, Quade BJ, Wang TY, Quigley C and Crum CP** (2000) The human VASA gene is specifically expressed in the germ cell lineage. *Proceedings of the National Academy of Sciences of the United States of America* **97** 9585–9590.

**Cattanach BM, Iddon CA, Charlton HM, Chiappa SA and Fink G** (1977) Gonadotrophin-releasing hormone deficiency in a mutant mouse with hypogonadism. *Nature* **269** 338–340.

**Caussanel V, Tabone E, Mauduit C, Dacheux F and Benahmed M** (1996) Cellular distribution of EGF, TGFα and their receptor during postnatal development and spermatogenesis of the boar testis. *Molecular & Cellular Endocrinology* **123** 61–69.

**Cervantes MP, Singh J, Palomino JM and Adams GP** (2013) Surgical translocation and ultrasound bio-microscopy of the ovaries in rabbits. *Animal Reproduction Science* **138** 133–141.

**Champy C** (1920) Quelques re´sultats de la me´thode de culture des tissus. *Archives de Zoologie Expérimentale et Générale.* **60** 461–500.

**Chen S-R and Liu YX** (2015) Regulation of spermatogonial stem cell self-renewal and spermatocyte meiosis by Sertoli cell signaling. *Reproduction* **149** R159-67.

**Chen HH, Welling M, Bloch DB, Muñoz J, Mientjes E, Chen X, Tramp C, Wu J, Yabuuchi A, Chou YF *et al.*** (2014) DAZL limits pluripotency, differentiation, and apoptosis in developing primordial germ cells. *Stem Cell Reports* **3** 892–904.

**Cheng L, Gearing DP, White LS, Compton DL, Schooley K and Donovan PJ** (1994) Role of leukemia inhibitory factor and its receptor in mouse primordial germ cell growth. *Development* **120** 3145–3153.

**Childs AJ, Saunders PTK and Anderson RA** (2008) Modelling germ cell development *in vitro*. *Molecular Human Reproduction* **14** 501–511.

**Chiquoine AD** (1954) The identification, origin, and migration of the primordial germ cells in the mouse embryo. *The Anatomical Record* **118** 135–146.

**Chuma S, Kanatsu-Shinohara M, Inoue K, Ogonuki N, Miki H, Toyokuni S, Hosokawa M, Nakatsuji N, Ogura A and Shinohara T** (2005) Spermatogenesis from epiblast and primordial germ cells following transplantation into postnatal mouse testis. *Development* **132** 117–122.

**Chung SSW, Wang X and Wolgemuth DJ** (2009) Expression of retinoic acid receptor alpha in the germline is essential for proper cellular association and spermiogenesis during spermatogenesis. *Development* **136** 2091–2100.

**Chung SSW, Wang X, Roberts SS, Griffey SM, Reczek PR and Wolgemuth DJ** (2011) Oral administration of a retinoic acid receptor antagonist reversibly inhibits spermatogenesis in mice. *Endocrinology* **152** 2492–2502.

**Clouthier DE, Avarbock MR, Maika SD, Hammer RE and Brinster RL** (1996) Rat spermatogenesis in mouse testis. *Nature* **381** 418–421.

**Colman A and Dreesen O** (2009) Pluripotent stem cells and disease modeling. *Cell Stem Cell* **5** 244–247.

**Colvin JS, Green RP, Schmahl J, Capel B and Ornitz DM** (2001) Male-to-female sex reversal in mice lacking fibroblast growth factor 9. *Cell* **104** 875–889.

**Combes AN, Lesieur E, Harley VR, Sinclair AH, Little MH, Wilhelm D and Koopman P** (2009) Three-dimensional visualization of testis cord morphogenesis, a novel tubulogenic mechanism in development. *Developmental Dynamics* **238** 1033–1041.

**Conrad S, Renninger M, Hennenlotter J, Wiesner T, Just L, Bonin M, Aicher W, Bühring HJ, Mattheus U, Mack A *et al.*** (2008) Generation of pluripotent stem cells from adult human testis. *Nature* **456** 344–349.

**Cool J, DeFalco TJ and Capel B** (2011) Vascular-mesenchymal cross-talk through Vegf and Pdgf drives organ patterning. *Proceedings of the National Academy of Sciences* **108** 167–172.

**Costantini F and Shakya R** (2006) GDNF/Ret signaling and the development of the kidney. *BioEssays* **28** 117–127.

**Coucouvanis E, Sherwood SW, Carswell-Crumpton C, Spack EG and Jones PP** (1993) Evidence that the mechanism of prenatal germ cell death in the mouse is apoptosis. *Experimental Cell Research* **209** 238–247.

**Couse JF, Lindzey J, Grandien K, Gustafsson JÅ and Korach KS** (1997) Tissue distribution and quantitative analysis of estrogen receptor-α (ERα) and estrogen receptor-β (ERβ) messenger ribonucleic acid in the wild-type and ERα-knockout mouse. *Endocrinology* **138** 4613–4621.

**Cristofalo VJ and Kritchevsky D** (1969) Cell size and nucleic acid content in the diploid human cell line WI-38 during aging. *Medicina Experimentalis: International Journal of Experimental Medicine* **19** 313–320.

**Culty M** (2009) Gonocytes, the forgotten cells of the germ cell lineage. *Birth Defects Research Part C - Embryo Today: Reviews* **87** 1–6.

**Culty M** (2013) Gonocytes, from the fifties to the present: Is there a reason to change the name?. *Biology of Reproduction* **89** 46.

**Dada T, Gadia R, Sharma A, Ichhpujani P, Bali SJ, Bhartiya S and Panda A** (2011) Ultrasound biomicroscopy in glaucoma. *Survey of Ophthalmology* **56** 433–450.

**Dalgaard L** (2015) Comparison of minipig, dog, monkey and human drug metabolism and disposition. *Journal of Pharmacological & Toxicological Methods* **74** 80–92.

**Dang SM, Gerecht-Nir S, Chen J, Itskovitz-Eldor J and Zandstra PW** (2004) Controlled, scalable embryonic stem cell differentiation culture. *Stem Cells* **22** 275–282.

**Dann CT, Alvarado AL, Molyneux LA, Denard BS, Garbers DL and Porteus MH** (2008) Spermatogonial stem cell self-renewal requires oct4, a factor downregulated during retinoic acid-induced differentiation. *Stem Cells* **26** 2928–2937.

**Dasgupta A, Hughey R, Lancin P, Larue L and Moghe P V.** (2005) E-cadherin synergistically induces hepatospecific phenotype and maturation of embryonic stem cells in conjunction with hepatotrophic factors. *Biotechnology & Bioengineering* **92** 257–266.

**Delbès G, Levacher C, Pairault C, Racine C, Duquenne C, Krust A and Habert R** (2004) Estrogen receptor beta-mediated inhibition of male germ cell line development in mice by endogenous estrogens during perinatal life. *Endocrinology* **145** 3395–3403.

**Dierich A, Sairam MR, Monaco L, Fimia GM, Gansmuller A, LeMeur M and Sassone-Corsi P** (1998) Impairing follicle-stimulating hormone (FSH) signaling *in vivo*: Targeted disruption of the FSH receptor leads to aberrant gametogenesis and hormonal imbalance. *Proceedings of the National Academy of Sciences of the United States of America* **95** 13612–13617.

**DiNapoli L, Batchvarov J and Capel B** (2006) FGF9 promotes survival of germ cells in the fetal testis. *Development* **133** 1519–1527.

**van Dissel-Emiliani FM, Boer-Brouwer M, Spek E, Donk J and de Rooij D** (1993) Survival and proliferation of rat gonoeytes *in vitro*. *Cell & Tissue Research* 141–147.

**van Dissel-Emiliani FM, Grootenhuis AJJ, De Jong FHH and de Rooij DGG** (1989) Inhibin reduces spermatogonial numbers in testes of adult mice and Chinese hamsters. *Endocrinology* **125** 1898–1903.

**van Dissel-Emiliani FM, De Boer-Brouwer M and De Rooij DG** (1996) Effect of fibroblast growth factor-2 on Sertoli cells and gonocytes in coculture during the perinatal period. *Endocrinology* **137** 647–654.

**Dobrinski I** (2005) Germ cell transplantation and testis tissue xenografting in domestic animals. *Animal Reproduction Science* **89** 137–145.

**Dobrinski I, Avarbock MR and Brinster RL** (1999) Transplantation of germ cells from rabbits and dogs into mouse testes. *Biology of Reproduction* **61** 1331–1339.

**Dolci S and De Felici M** (1990) A study of meiosis in chimeric mouse fetal gonads. *Development* **109** 37–40.

**Dolci S, Williams DE, Ernst MK, Resnick JL, Brannan CI, Lock LF, Lyman SD, Boswell HS and Donovan PJ** (1991) Requirement for mast cell growth factor for primordial germ cell survival in culture. *Nature* **352** 809–811.

**Donovan PJ, Stott D, Cairns LA, Heasman J and Wylie CC** (1986) Migratory and postmigratory mouse primordial germ cells behave differently in culture. *Cell* **44** 831–838.

**Dores C and Dobrinski I** (2014) *De novo* morphogenesis of testis tissue: An improved bioassay to investigate the role of VEGF165 during testis formation. *Reproduction* **148** 109–117.

**Dorrington JH, Fritz IB and Armstrong DT** (1978) Control of testicular estrogen synthesis. **18** 55–64.

**Dorval-Coiffec I, Delcros JG, Hakovirta H, Toppari J, Jégou B and Piquet-Pellorce C** (2005) Identification of the leukemia inhibitory factor cell targets within the rat testis. *Biology of Reproduction* **72** 602–611.

**Dovere L, Fera S, Grasso M, Lamberti D, Gargioli C, Muciaccia B, Lustri AM, Stefanini M and Vicini E** (2013) The niche-derived glial cell line-derived neurotrophic factor (GDNF) induces migration of mouse spermatogonial stem/progenitor cells. *PloS One* **8** e59431.

**Doyle TJ, Braun KW, McLean DJ, Wright RW, Griswold MD and Kim KH** (2007) Potential functions of retinoic acid receptor A in sertoli cells and germ cells during spermatogenesis. *Annals of the New York Academy of Sciences* **1120** 114–130.

**Drumond AL, Meistrich ML and Chiarini-Garcia H** (2011) Spermatogonial morphology and kinetics during testis development in mice: A high-resolution light microscopy approach. *Reproduction* **142** 145–155.

**Dufour JM and Kim KH** (1999) Cellular and subcellular localization of six retinoid receptors in rat testis during postnatal development: Identification of potential heterodimeric receptors. *Biology of Reproduction* **61** 1300–1308.

**Dufour JM, Rajotte R V. and Korbutt GS** (2002) Development of an *in vivo* model to study testicular morphogenesis. *Journal of Andrology* **23** 635–644.

**Dym M** (1994) Spermatogonial stem cells of the testis. *Proceedings of the National Academy of Sciences of the United States of America* **91** 11287–11289.

**Easley CA, Simerly CR, Schatten G and Schatten G** (2014) Gamete derivation from embryonic stem cells, induced pluripotent stem cells or somatic cell nuclear transfer-derived embryonic stem cells: State of the art. *Reproduction, Fertility & Development* **27** 89–92.

**Eddy EM, Washburn TF, Bunch DO, Goulding EH, Gladen BC, Lubahn DB and Korach KS** (1996) Targeted disruption of the estrogen receptor gene in male mice causes alteration of spermatogenesis and infertility. *Endocrinology* **137** 4796–4805.

**Ehmcke J, Gassei K and Schlatt S** (2008) Ectopic testicular xenografts from newborn hamsters (*Phodopus sungorus*) show better spermatogenic activity in aged compared with young recipients. *Journal of Experimental Zoology Part A: Ecological Genetics & Physiology* **309** 278–287.

**Elzawam AZ** (2013) Establishment of spermatogenesis following testicular tissue ectopic xenografting in alpaca. PhD Thesis Washington State University.

**Enders GC and May JJ** (1994) Developmentally regulated expression of a mouse germ cell nuclear antigen examined from embryonic day 11 to adult in male and female mice. *Developmental Biology* **163** 331–340.

**Ergün S, Kiliç N, Fiedler W and Mukhopadhyay A.** (1997) Vascular endothelial growth factor and its receptors in normal human testicular tissue. *Molecular & Cellular Endocrinology* **131** 9–20.

**Escalante-Alcalde D and Merchant-Larios H** (1992) Somatic and germ cell interactions during histogenetic aggregation of mouse fetal testes. *Experimental Cell Research* **198** 150–158.

**Evans MJ and Kaufman MH** (1981) Establishment in culture of pluripotential cells from mouse embryos. *Nature* **292** 154–156.

**Falin LI** (1969) The development of genital glands and the origin of germ cells in human embryogenesis. *Acta Anatomica* **72** 195–232.

**Fan H, Zhang C, Li J, Bi L, Qin L, Wu H and Hu Y** (2008) Gelatin microspheres containing TGF-beta3 enhance the chondrogenesis of mesenchymal stem cells in modified pellet culture. *Biomacromolecules* **9** 927–934.

**Faria MJS, Simões ZLP, Lunardi LO and Hartfelder K** (2003) Apoptosis process in mouse leydig cells during postnatal development. *Microscopy & Microanalysis* **9** 68–73.

**Feng LX, Chen Y, Dettin L, Pera RAR, Herr JC, Goldberg E and Dym M** (2002) Generation and *in vitro* differentiation of a spermatogonial cell line. *Science* **297** 392–395.

**Ferrara N** (2000) Vascular endothelial growth factor and the regulation of angiogenesis. *Recent Progress in Hormone Research* **55** 15–36 .

**Ferrara N, Carver-Moore K, Chen H, Dowd M, Lu L, O'Shea KS, Powell-Braxton L, Hillan KJ and Moore MW** (1996) Heterozygous embryonic lethality induced by targeted inactivation of the VEGF gene. *Nature* **380** 439–442.

**Fisher DA and Lakshmanan J** (1990) Metabolism and effects of epidermal growth factor and related growth factors in mammals. *Endocrine Reviews* **11** 418–442.

**Fitchett AE, Barnard CJ and Cassaday HJ** (2006) There's no place like home: Cage odours and place preference in subordinate CD-1 male mice. *Physiology & Behavior* **87** 955–962.

**Fok EYL and Zandstra PW** (2005) Shear-controlled single-step mouse embryonic stem cell expansion and embryoid body-based differentiation. *Stem Cells* **23** 1333–1342.

**Fong GH, Rossant J, Gertsenstein M and Breitman ML** (1995) Role of the Flt-1 receptor tyrosine kinase in regulating the assembly of vascular endothelium. *Nature* **376** 66–70.

**Foster FS** (2003) *In vivo* imaging of embryonic development in the mouse eye by ultrasound biomicroscopy. *Investigative Ophthalmology & Visual Science* **44** 2361–2366.

**Francavilla S, Cordeschi G, Properzi G, Concordia N, Cappa F and Pozzi V** (1990) Ultrastructure of fetal human gonad before sexual differentiation and during early testicular and ovarian development. *Journal of Submicroscopic Cytology & Pathology* **22** 389–400.

**Fujihara M, Goel S, Minami N, Yamada M and Imai H** (2008) Cryopreservation in liquid nitrogen of gonocytes from neonatal porcine testes stored at 4°C. *Reproductive Medicine & Biology* **7** 153–160.

**Fujihara M, Kim SM, Minami N, Yamada M and Imai H** (2011) Characterization and *in vitro* culture of male germ cells from developing bovine testis. *The Journal of Reproduction & Development* **57** 355–364.

**Gale E, Zile M and Maden M** (1999) Hindbrain respecification in the retinoid-deficient quail. *Mechanisms of Development* **89** 43–54.

**Gartner LP and Hiatt JL** (2006) Male Reproductive System. In *Color Textbook of Histology* (Eds Gartner LP and Hiatt JL), pp 489–510. Philadelphia, PA: Saunders.

**Gasperini L, Mano JF and Reis RL** (2014) Natural polymers for the microencapsulation of cells. *Journal of the Royal Society Interface* **11** 20140817.

**Gassei K, Schlatt S and Ehmcke J** (2006) *De novo* morphogenesis of seminiferous tubules from dissociated immature rat testicular cells in xenografts. *Journal of Andrology* **27** 611–618.

**Ge R and Hardy MP** (1997) Decreased Cyclin $A_2$ and increased Cyclin $G_1$ levels coincide with loss of proliferative capacity in rat leydig cells during pubertal development. *Endocrinology* **138** 3719–3726.

**Geens M, De Block G, Goossens E, Frederickx V, Van Steirteghem A and Tournaye H** (2006) Spermatogonial survival after grafting human testicular tissue to immunodeficient mice. *Human Reproduction* **21** 390–396.

**Geens M, Goossens E, De Block G, Ning L, Van Saen D and Tournaye H** (2008) Autologous spermatogonial stem cell transplantation in man: Current obstacles for a future clinical application. *Human Reproduction* **14** 121–130.

**Geijsen N and Jones DL** (2008) Seminal discoveries in regenerative medicine: Contributions of the male germ line to understanding pluripotency. *Human Molecular Genetics* **17** R16–R22.

**De Gendt K, Swinnen JV, Saunders PTK, Schoonjans L, Dewerchin M, Devos A, Tan K, Atanassova N, Claessens F, Lecureuil C *et al.*** (2004) A Sertoli cell-selective knockout of the androgen receptor causes spermatogenic arrest in meiosis. *Proceedings of the National Academy of Sciences* **101** 1327–1332.

**Ghyselinck NB, Vernet N, Dennefeld C, Giese N, Nau H, Chambon P, Viville S and Mark M** (2006) Retinoids and spermatogenesis: Lessons from mutant mice lacking the plasma retinol binding protein. *Developmental Dynamics* **235** 1608–1622.

**Gilbert SF** (2000) Spermatogenesis. In *Developmental Biology*. Sunderland, MA. Sinauer Associates Inc.

**Gill ME, Hu YC, Lin Y and Page DC** (2011) Licensing of gametogenesis, dependent on RNA binding protein DAZL, as a gateway to sexual differentiation of fetal germ cells. *Proceedings of the National Academy of Sciences of the United States of America* **108** 7443–7448.

**Ginsburg M, Snow MH and McLaren A** (1990) Primordial germ cells in the mouse embryo during gastrulation. *Development* **110** 521–528.

**Godin I, Deed R, Cooke J, Zsebo K, Dexter M and Wylie CC** (1991) Effects of the steel gene product on mouse primordial germ cells in culture. *Nature* **352** 807–809.

**Goel S and Imai H** (2011) Pluripotent Stem Cells from Testis. In *Embryonic Stem Cells - Differentiation and Pluripotent Alternatives*. InTech.

**Goel S, Sugimoto M, Minami N, Yamada M, Kume S and Imai H** (2007) Identification, isolation, and *in vitro* culture of porcine gonocytes. *Biology of Reproduction* **77** 127–137.

**Goel S, Fujihara M, Minami N, Yamada M and Imai H** (2008) Expression of NANOG, but not POU5F1, points to the stem cell potential of primitive germ cells in neonatal pig testis. *Reproduction* **135** 785–795.

**Goel S, Fujihara M, Tsuchiya K, Takagi Y, Minami N, Yamada M and Imai H** (2009) Multipotential ability of primitive germ cells from neonatal pig testis cultured *in vitro*. *Reproduction, Fertility & Development* **21** 696.

**Gondos B and Hobel CJ** (1971) Ultrastructure of germ cell development in the human fetal testis. *Zeitschrift Fur Zellforschung Und Mikroskopische Anatomie (Vienna, Austria : 1948)* **119** 1–20.

**Gonzalez AM, Buscaglia M, Ong M and Baird A** (1990) Distribution of basic fibroblast growth factor in the 18-day rat fetus: Localization in the basement membranes of diverse tissues. *The Journal of Cell Biology* **110** 753–765.

**Goossens E, Frederickx V, de Block G, Van Steirteghem AC and Tournaye H** (2003) Reproductive capacity of sperm obtained after germ cell transplantation in a mouse model. *Human Reproduction* **18** 1874–1880.

**Goossens E, Geens M, de Block G and Tournaye H** (2008) Spermatogonial survival in long-term human prepubertal xenografts. *Fertility & Sterility* **90** 2019–2022.

**Gosden R and Aubard Y** (1996) Transplantation of testicular tissues. In *Transplantation of Ovarian and Testicular Tissues* (Eds Gosden R and Aubard Y) , pp 89–97. Austin, TX: Landes Bioscience.

**Gourdon JC and Travis AJ** (2011) Spermatogenesis in ferret testis xenografts: A new model. *Comparative Medicine* **61** 145–149.

**Greco A, Di Benedetto A, Howard CM, Kelly S, Nande R, Dementieva Y, Miranda M, Brunetti A, Salvatore M, Claudio L *et al.*** (2010) Eradication of Therapy-resistant Human Prostate Tumors Using an Ultrasound-guided Site-specific Cancer Terminator Virus Delivery Approach. *Molecular Therapy* **18** 295–306.

**Grisanti L, Falciatori I, Grasso M, Dovere L, Fera S, Muciaccia B, Fuso A, Berno V, Boitani C, Stefanini M *et al.*** (2009) Identification of spermatogonial stem cell subsets by morphological analysis and prospective isolation. *Stem Cells* **27** 3043–3052.

**Griswold MD** (1998) The central role of Sertoli cells in spermatogenesis. *Seminars in Cell & Developmental Biology* **9** 411–416.

**Griswold MD, Bishop PD, Kim KH, Ping R, Siiteri JE and Morales C** (1989) Function of vitamin A in normal and synchronized seminiferous tubules. *Annals of the New York Academy of Sciences* **564** 154–172.

**Guan K, Nayernia K, Maier LS, Wagner S, Dressel R, Lee JH, Nolte J, Wolf F, Li M, Engel W *et al.*** (2006) Pluripotency of spermatogonial stem cells from adult mouse testis. *Nature* **440** 1199–1203.

**Gubbay J, Collignon J, Koopman P, Capel B, Economou A, Münsterberg A, Vivian N, Goodfellow P and Lovell-Badge R** (1990) A gene mapping to the sex-determining region of the mouse Y chromosome is a member of a novel family of embryonically expressed genes. *Nature* **346** 245–250.

**Gunn RM. and Seddon H.** (1930) Testicular grafts on rams. *The Australian Veterinary Journal* **6** 132–145.

**Hadley MA, Byers SW, Suárez-Quian CA, Kleinman HK and Dym M** (1985) Extracellular matrix regulates Sertoli cell differentiation, testicular cord formation, and germ cell development *in vitro*. *The Journal of Cell Biology* **101** 1511–1522.

**Hafez E** (2000) Anatomy of male reproduction. *Reproduction in Farm Animals, 7th Edition*.

**Hakovirta H, Yan W, Kaleva M, Zhang F, Vänttinen K, Morris PL, Söder M, Parvinen M and Toppari J** (1999) Function of stem cell factor as a survival factor of spermatogonia and localization of messenger ribonucleic acid in the rat seminiferous epithelium. *Endocrinology* **140** 1492–1498.

**van den Ham R, van Pelt AM, De Miguel MP, van Kooten PJ, Walther N and van Dissel-Emiliani FM** (1997) Immunomagnetic Isolation of Fetal Rat Gonocytes. *American Journal of Reproductive Immunology* **38** 39–45.

**Hammes A, Guo JK, Lutsch G, Leheste JR, Landrock D, Ziegler U, Gubler MC and Schedl A** (2001) Two splice variants of the Wilms' tumor 1 gene have distinct functions during sex determination and nephron formation. *Cell* **106** 319–329.

**Hamra FK, Chapman KM, Nguyen DM, Williams-Stephens AA, Hammer RE and Garbers DL** (2005) Self renewal, expansion, and transfection of rat spermatogonial stem cells in culture. *Proceedings of the National Academy of Sciences* **102** 17430–17435.

**Hamra FK, Chapman KM, Wu Z and Garbers DL** (2008) Isolating highly pure rat spermatogonial stem cells in culture. *Methods in Molecular Biology* **450** 163–179.

**Han IS, Sylvester SR, Kim KH, Schelling ME, Venkateswaran S, Blanckaert VD, McGuinness MP and Griswold MD** (1993) Basic fibroblast growth factor is a testicular germ cell product which may regulate Sertoli cell function. *Molecular Endocrinology* **7** 889–897.

**Han SY, Gupta MK, Uhm SJ and Lee HT** (2009) Isolation and *in vitro* culture of pig spermatogonial stem cell. *Asian-Australasian Journal of Animal Sciences* **22** 187–193.

**Haneji T, Maekawa M and Nishimune Y** (1983) *In vitro* differentiation of type a spermatogonia from mouse cryptorchid testes in serum-free media. *Biology of Reproduction* **28** 1217–1223.

**Haneji T, Koide SS, Tajima Y and Nishimune Y** (1991) Differential effects of epidermal growth factor on the differentiation of type A spermatogonia in adult mouse cryptorchid testes *in vitro*. *Journal of Endocrinology* **128** 383–388.

**Hara K, Kanai-Azuma M, Uemura M, Shitara H, Taya C, Yonekawa H, Kawakami H, Tsunekawa N, Kurohmaru M and Kanai Y** (2009) Evidence for crucial role of hindgut expansion in directing proper migration of primordial germ cells in mouse early embryogenesis. *Developmental Biology* **330** 427–439.

**Hasegawa H, Terada Y, Ugajin T, Yaegashi N and Sato K** (2010) A novel culture system for mouse spermatid maturation which produces elongating spermatids capable of inducing calcium oscillation during fertilization and embryonic development. *Journal of Assisted Reproduction & Genetics* **27** 565–570.

**Hasthorpe S** (2003) Clonogenic culture of normal spermatogonia: *In vitro* regulation of postnatal germ cell proliferation. *Biology of Reproduction* **68** 1354–1360.

**Hasthorpe S, Barbic S, Farmer PJ and Hutson JM** (1999) Neonatal mouse gonocyte proliferation assayed by an *in vitro* clonogenic method. *Journal of Reproduction & Fertility* **116** 335–344.

**Hasthorpe S, Barbic S, Farmer PJ and Hutson JM** (2000) Growth factor and somatic cell regulation of mouse gonocyte-derived colony formation *in vitro*. *Journal of Reproduction & Fertility* **119** 85–91.

**Hayashi K, de Sousa Lopes SMC and Surani MA** (2007) Germ cell specification in mice. *Science* **316** 394–396.

**Hayashi K, Ogushi S, Kurimoto K, Shimamoto S, Ohta H and Saitou M** (2012) Offspring from oocytes derived from *in vitro* primordial germ cell-like cells in mice. *Science* **338** 971–975.

**Haywood M, Spaliviero J, Jimemez M, King NJC, Handelsman DJ and Allan CM** (2003) Sertoli and germ cell development in hypogonadal ( *hpg* ) mice expressing transgenic follicle-stimulating hormone alone or in combination with testosterone. *Endocrinology* **144** 509–517.

**He J, Dong C, You R, Zhu Z, Lv L and Smith GW** (2009) Localization of epidermal growth factor (EGF) and its receptor (EGFR) during postnatal testis development in the alpaca (Lama pacos). *Animal Reproduction Science* **116** 155–161.

**He Y, Chen X, Zhu H and Wang D** (2015) Developments in techniques for the isolation, enrichment, main culture conditions and identification of spermatogonial stem cells. *Cytotechnology* **67** 921–930.

**Heidari B, Rahmati-Ahmadabadi M, Akhondi MM, Zarnani AH, Jeddi-Tehrani M, Shirazi A, Naderi MM and Behzadi B** (2012) Isolation, identification, and culture of goat spermatogonial stem cells using c-kit and PGP9.5 markers. *Journal of Assisted Reproduction & Genetics* **29** 1029–1038.

**Hermann BP and Orwig KE** (2011) Translating Spermatogonial Stem Cell Transplantation to the Clinic. In *Male Germline Stem Cells: Developmental & Regenerative Potential* (Eds Orwig K and Herman B), pp 227–253. Totowa, NJ: Humana Press.

**Hermann BP, Sukhwani M, Winkler F, Pascarella JN, Peters KA, Sheng Y, Valli H, Rodriguez M, Ezzelarab M, Dargo G *et al.*** (2012) Spermatogonial stem cell transplantation into rhesus testes regenerates spermatogenesis producing functional sperm. *Cell Stem Cell* **11** 715–726.

**Herrid M, Olejnik J, Jackson M, Suchowerska N, Stockwell S, Davey R, Hutton K, Hope S and Hill JR** (2009) Irradiation enhances the efficiency of testicular germ cell transplantation in sheep. *Biology of Reproduction* **81** 898–905.

**Hess R and Moore B** (1993) Histological Methods for Evaluation of the Testis. In *Methods in Reproductive Toxicology* (Eds Chapin RE and Heindel JJ), pp 52–85. San Diego, CA: Academic Press.

**Hill JR and Dobrinski I** (2006) Male germ cell transplantation in livestock. *Reproduction, Fertility & Development* **18** 13–18.

**Hill J, Brownlee A, Davey R, Herrid M, Hutton K, Vignarajan S and Dobrinski I** (2005) Initial results from male germ cell transfer between cattle breeds. *Reproduction, Fertility & Development* **17** 204.

**Hilscher B, Hilscher W, Bülthoff-Ohnolz B, Krämer U, Birke A, Pelzer H and Gauss G** (1974) Kinetics of gametogenesis.Comparative histological and autoradiographic studies of oocytes and transitional prospermatogonia during oogenesis and prespermatogenesis. *Cell & Tissue Research* **154** 443–470.

**Hilton DJ and Gough NM** (1991) Leukemia Inhibitory Factor: A biological perspective. *Journal of Cellular Biochemistry* **46** 21–26.

**Hinton RB, Alfieri CM, Witt SA, Glascock BJ, Khoury PR, Benson DW and Yutzey KE** (2008) Mouse heart valve structure and function: Echocardiographic and morphometric analyses from the fetus through the aged adult. *American Journal of Physiology. Heart & Circulatory Physiology* **294** H2480-8.

**Hirai K, Sasaki H, Yamamoto H, Sakamoto H, Kubota Y, Kakizoe T, Terada M and Ochiya T** (2004) HST-1/FGF-4 protects male germ cells from apoptosis under heat-stress condition. *Experimental Cell Research* **294** 77–85.

**Hiramatsu R, Matoba S, Kanai-Azuma M, Tsunekawa N, Katoh-Fukui Y, Kurohmaru M, Morohashi KI, Wilhelm D, Koopman P and Kanai Y** (2009) A critical time window of Sry action in gonadal sex determination in mice. *Development* **136** 129–138.

**Hochereau-de Reviers MT, Perreau C, Pisselet C, Locatelli A and Bosc M** (1995) Ontogenesis of somatic and germ cells in sheep fetal testis. *Journal of Reproduction & Fertility* **103** 41–46.

**Hoei-Hansen CE, Almstrup K, Nielsen JE, Brask Sonne S, Graem N, Skakkebaek NE, Leffers H and Rajpert-De Meyts E** (2005) Stem cell pluripotency factor NANOG is expressed in human fetal gonocytes, testicular carcinoma in situ and germ cell tumours. *Histopathology* **47** 48–56.

**Hofmann MC, Hess RA, Goldberg E and Millán JL** (1994) Immortalized germ cells undergo meiosis *in vitro*. *Proceedings of the National Academy of Sciences of the United States of America* **91** 5533–5537.

**Hofmann MC, Braydich-Stolle L and Dym M** (2005) Isolation of male germ-line stem cells; influence of GDNF. *Developmental Biology* **279** 114–124.

**Hogg K and Western PS** (2015) Differentiation of fetal male germline and gonadal progenitor cells is disrupted in organ cultures containing knockout serum replacement. *Stem Cells and Development* **24** 2899–2911.

**Honaramooz A** (2012) Cryopreservation of Testicular Tissue. In *Current Frontiers in Cryobiology*. Ed I Katkov. Rijeka, Croatia.

**Honaramooz A** (2014) Potential and Challenges of Testis Tissue Xenografting from Diverse Ruminant Species. In *Reproduction in Domestic Ruminants VII* (Eds Juengel JL, Miyamoto A, Price C, Reynolds LP, Smith MP and Webb R), pp 257–275. Leicestershire, England: Context Products Ltd.

**Honaramooz A and Yang Y** (2010) Recent advances in application of male germ cell transplantation in farm animals. *Veterinary Medicine International* **2011** 1–9.

**Honaramooz A, Snedaker A, Boiani M, Schöler H, Dobrinski I and Schlatt S** (2002a) Sperm from neonatal mammalian testes grafted in mice. *Nature* **418** 778–781.

**Honaramooz A, Megee SO and Dobrinski I** (2002b) Germ cell transplantation in pigs. *Biology of Reproduction* **66** 21–28.

**Honaramooz A, Behboodi E, Megee SO, Overton S a, Galantino-Homer H, Echelard Y and Dobrinski I** (2003a) Fertility and germline transmission of donor haplotype following germ cell transplantation in immunocompetent goats. *Biology of Reproduction* **69** 1260–1264.

**Honaramooz A, Behboodi E, Blash S, Megee SO and Dobrinski I** (2003b) Germ cell transplantation in goats. *Molecular Reproduction & Development* **64** 422–428.

**Honaramooz A, Li M-W, Penedo MCT, Meyers S and Dobrinski I** (2004) Accelerated maturation of primate testis by xenografting into mice. *Biology of Reproduction* **70** 1500–1503.

**Honaramooz A, Behboodi E, Hausler CL, Blash S, Ayres S, Azuma C, Echelard Y and Dobrinski I** (2005a) Depletion of endogenous germ cells in male pigs and goats in preparation for germ cell transplantation. *Journal of Andrology* **26** 698–705.

**Honaramooz A, Zeng W, Rathi R, Koster J, Ryder O and Dobrinski I** (2005b) Testis tissue xenografting to preserve germ cells from a cloned banteng calf. *Reproduction, Fertility & Development* **17** 247.

**Honaramooz A, Megee SO, Rathi R and Dobrinski I** (2007) Building a testis: Formation of functional testis tissue after transplantation of isolated porcine (*Sus scrofa*) testis cells. *Biology of Reproduction* **76** 43–47.

**Honaramooz A, Megee S, Zeng W, Destrempes MM, Overton S a, Luo J, Galantino-Homer H, Modelski M, Chen F, Blash S *et al.*** (2008) Adeno-associated virus (AAV)-mediated transduction of male germ line stem cells results in transgene transmission after germ cell transplantation. *The FASEB Journal* **22** 374–382.

**Honda S, Harada N, Ito S, Takagi Y and Maeda S** (1998) Disruption of sexual behavior in male aromatase-deficient mice lacking exons 1 and 2 of the cyp19 gene. *Biochemical & Biophysical Research Communications* **252** 445–449.

**Howroyd P, Hoyle-Thacker R, Lyght O, Williams D and Kleymenova E** (2005) Morphology of the fetal rat testis preserved in different fixatives. *Toxicologic Pathology* **33** 300–304.

**Hu J, Shima H and Nakagawa H** (1999) Glial cell line-derived neurotropic factor stimulates Sertoli cell proliferation in the early postnatal period of rat testis development. *Endocrinology* **140** 3416–3421.

**Hu Q, Guo W, Gao Y, Tang R and Li D** (2015) Molecular cloning and characterization of amh and dax1 genes and their expression during sex inversion in rice-field eel Monopterus albus. *Scientific Reports* **5** 16667.

**Huang HFS, Dyrenfurth I and Hembree WC** (1983) Endocrine changes associated with germ cell loss during vitamin a-induced recovery of spermatogenesis. *Endocrinology* **112** 1163–1171.

**Huang S, Sartini BL and Parks JE** (2008) Spermatogenesis in testis xenografts grafted from pre-pubertal Holstein bulls is re-established by stem cell or early spermatogonia. *Animal Reproduction Science* **103** 1–12.

**Huckins C** (1971) The spermatogonial stem cell population in adult rats. I. Their morphology, proliferation and maturation. *The Anatomical Record* **169** 533–557.

**Hughes PE and Varley MA** (1980) *Reproduction in the Pig*. London, Butterworth.

**Huleihel M and Lunenfeld E** (2004) Regulation of spermatogenesis by paracrine/autocrine testicular factors. *Asian Journal of Andrology* **6** 259–268.

**Huleihel M, Nourashrafeddin S and Plant TM** (2015) Application of three-dimensional culture systems to study mammalian spermatogenesis, with an emphasis on the rhesus monkey (*Macaca mulatta*). *Asian Journal of Andrology* **17** 972–980.

**Humes HD and Cieslinski DA** (1992) Interaction between growth factors and retinoic acid in the induction of kidney tubulogenesis in tissue culture. *Experimental Cell Research* **201** 8–15.

**Huminiecki L, Chan HY, Lui S, Poulsom R, Stamp G, Harris AL and Bicknell R** (2001) Vascular endothelial growth factor transgenic mice exhibit reduced male fertility and placental rejection. *Molecular Human Reproduction* **7** 255–264.

**Huppertz N, Tolba R and Grosse J** (2015) Micturition in Göttingen minipigs: First reference *in vivo* data for urological research and review of literature. *Laboratory Animals* **49** 336–344.

**Hurst M, Dalin AM and Rodriguez-Martinez H** (1991) Embryonic Development of the Porcine Indifferent Gonad and Testis. *Journal of Veterinary Medicine Series A* **38** 594–607.

**Ibtisham F, Wu J, Xiao M, An L, Banker Z, Nawab A, Zhao Y and Li G** (2017) Progress and future prospect of *in vitro* spermatogenesis. *Oncotarget* **8** 66709–66727.

**Illmensee K and Stevens LC** (1979) Teratomas and chimeras. *Scientific American* **240** 120–132.

**Ingram D and Legge K** (1970) The thermoregulatory behavior of young pigs in a natural environment. *Physiology & Behavior* **5** 981–987.

**Ishii K, Kanatsu-Shinohara M, Toyokuni S and Shinohara T** (2012) FGF2 mediates mouse spermatogonial stem cell self-renewal via upregulation of Etv5 and Bcl6b through MAP2K1 activation. *Development* **139** 1734–1743.

**Ito M, Hiramatsu H, Kobayashi K, Suzue K, Kawahata M, Hioki K, Ueyama Y, Koyanagi Y, Sugamura K, Tsuji K *et al.*** (2002) NOD/SCID/gamma(c)(null) mouse: An excellent recipient mouse model for engraftment of human cells. *Blood* **100** 3175–3182.

**Iwase R, Kasai K and Tada N** (1994) Direct injection of foreign DNA into mouse testis as a possible alternative of sperm-mediated gene transfer. *Animal Biotechnology* **5** 19–31.

**Izadyar F, Den Ouden K, Creemers LB, Posthuma G, Parvinen M and De Rooij DG** (2003a) Proliferation and differentiation of bovine type A spermatogonia during long-term culture. *Biology of Reproduction* **68** 272–281.

**Izadyar F, Den Ouden K, Stout TAE, Stout J, Coret J, Lankveld DPK, Spoormakers TJP, Colenbrander B, Oldenbroek JK, Van der Ploeg KD *et al.*** (2003b) Autologous and homologous transplantation of bovine spermatogonial stem cells. *Reproduction* **126** 765–774.

**Jafarnejad A, Aminafshar M, Zandi M, Sanjabi MR and Emamjomeh Kashan N** (2018) Optimization of *in vitro* culture and transfection condition of bovine primary spermatogonial stem cells. *South African Journal of Animal Science* **48** 108.

**Jahnukainen K, Ehmcke J, Hergenrother SD and Schlatt S** (2007) Effect of cold storage and cryopreservation of immature non-human primate testicular tissue on spermatogonial stem cell potential in xenografts. *Human Reproduction* **22** 1060–1067.

**Jaillard C, Chatelain PG and Saez JM** (1987) *In vitro* regulation of pig sertoli cell growth and function: Effects of fibroblast growth factor and somatomedin-C. *Biology of Reproduction* **37** 665–674.

**Jameson SA, Lin Y-T and Capel B** (2012) Testis development requires the repression of Wnt4 by Fgf signaling. *Developmental Biology* **370** 24–32.

**Jenab S and Morris PL** (1998) Testicular leukemia inhibitory factor (LIF) and LIF Receptor mediate phosphorylation of signal transducers and activators of transcription (STAT)-3 and STAT-1 and induce c-*fos* transcription and activator protein-1 activation in rat Sertoli but not germ cells. *Endocrinology* **139** 1883–1890.

**Jeong D, McLean DJ and Griswold MD** (2003) Long-term culture and transplantation of murine testicular germ cells. *Journal of Andrology* **24** 661–669.

**Jiang FX** (2001) Male germ cell transplantation: Promise and problems. *Reproduction, Fertility & Development* **13** 609–6014.

**Jiang FX and Short R V** (1995) Male germ cell transplantation in rats: Apparent synchronization of spermatogenesis between host and donor seminiferous epithelia. *International Journal of Andrology* **18** 326–330.

**Jiang FX and Short R V** (1998) Different fate of primordial germ cells and gonocytes following transplantation. *Acta Pathologica, Microbiologica, et Immunologica Scandinavica* **106** 58-63.

**Jiang X, Skibba M, Zhang C, Tan Y, Xin Y and Qu Y** (2013) The roles of fibroblast growth factors in the testicular development and tumor. *Journal of Diabetes Research* **2013** 489095.

**Joerg H, Janett F, Schlatt S, Mueller S, Graphodatskaya D, Suwattana D, Asai M and Stranzinger G** (2003) Germ cell transplantation in an azoospermic klinefelter bull. *Biology of Reproduction* **69** 1940–1944.

**Joffre BYM and Roche A** (1988) Follicle-stimulating hormone induces hyperpolarization of immature. 481–499.

**Josso N** (1992) Anti-Müllerian hormone and Sertoli cell function. *Hormone Research* **38** 72–76.

**Jost A, Vigier B, Prepin J and Perchellet JP** (1973) Studies on Sex Differentiation in Mammals. In *Proceedings of the 1972 Laurentian Hormone Conference*, pp 1–41. Elsevier.

**Kanatsu-Shinohara M and Shinohara T** (2013) Spermatogonial Stem Cell Self-Renewal and Development. *Annual Review of Cell & Developmental Biology* **29** 163–187.

**Kanatsu-Shinohara M, Ogonuki N, Inoue K, Miki H, Ogura A, Toyokuni S and Shinohara T** (2003) Long-Term proliferation in culture and germline transmission of mouse male germline stem cells. *Biology of Reproduction* **69** 612–616.

**Kanatsu-Shinohara M, Toyokuni S and Shinohara T** (2004a) CD9 Is a surface marker on mouse and rat male germline stem cells. *Biology of Reproduction* **70** 70–75.

**Kanatsu-Shinohara M, Inoue K, Lee J, Yoshimoto M, Ogonuki N, Miki H, Baba S, Kato T, Kazuki Y, Toyokuni S *et al.*** (2004b) Generation of Pluripotent stem cells from neonatal mouse testis. *Cell* **119** 1001–1012.

**Kanatsu-Shinohara M, Ogonuki N, Iwano T, Lee J, Kazuki Y, Inoue K, Miki H, Takehashi M, Toyokuni S, Shinkai Y *et al.*** (2005) Genetic and epigenetic properties of mouse male germline stem cells during long-term culture. *Development* **132** 4155–4163.

**Kanatsu-Shinohara M, Inoue K, Ogonuki N, Miki H, Yoshida S, Toyokuni S, Lee J, Ogura A and Shinohara T** (2007) Leukemia inhibitory factor enhances formation of germ cell colonies in neonatal mouse testis culture. *Biology of Reproduction* **76** 55–62.

**Kanatsu-Shinohara M, Muneto T, Lee J, Takenaka M, Chuma S, Nakatsuji N, Horiuchi T and Shinohara T** (2008a) Long-term culture of male germline stem cells from hamster testes. *Biology of Reproduction* **78** 611–617.

**Kanatsu-Shinohara M, Lee J, Inoue K, Ogonuki N, Miki H, Toyokuni S, Ikawa M, Nakamura T, Ogura A and Shinohara T** (2008b) Pluripotency of a single spermatogonial stem cell in mice. *Biology of Reproduction* **78** 681–687.

**Kanatsu-Shinohara M, Inoue K, Ogonuki N, Morimoto H, Ogura A and Shinohara T** (2011) Serum- and feeder-free culture of mouse germline stem cells. *Biology of Reproduction* **84** 97–105.

**Kanatsu-Shinohara M, Inoue K, Takashima S, Takehashi M, Ogonuki N, Morimoto H, Nagasawa T, Ogura A and Shinohara T** (2012) Reconstitution of mouse spermatogonial stem cell niches in culture. *Cell Stem Cell* **11** 567–578.

**Kanatsu-Shinohara M, Ogonuki N, Matoba S, Morimoto H, Ogura A and Shinohara T** (2014) Improved serum-and feeder-free culture of mouse germline stem cells. *Biology of Reproduction* **9188** 1–11.

**Kaneko H, Kikuchi K, Nakai M, Tanihara F, Noguchi J, Noguchi M, Ito J and Kashiwazaki N** (2012) Normal reproductive development of offspring derived by intracytoplasmic injection of porcine sperm grown in host mice. *Theriogenology* **78** 898–906.

**Kaproth MT, Lee DR and Parks JE** (2002) Transplantation of testicular explants from prepubertal bulls to nude mice and ex situ production of haploid gametes over a 20-week period. ASAS-ADSA Joint Ann Mtg 2002; 302.

**Kassab M, Abd-Elmaksoud A and Ali MA** (2007) Localization of the epidermal growth factor (EGF) and epidermal growth factor receptor (EGFR) in the bovine testis. *Journal of Molecular Histology* **38** 207–214.

**Kawasaki T, Imura F, Nakada A, Kubota H, Sakamaki K, Abe SI and Takamune K** (2006) Functional demonstration of the ability of a primary spermatogonium as a stem cell by tracing a single cell destiny in *Xenopus laevis*. *Development Growth & Differentiation* **48** 525–535.

**Kawasaki T, Saito K, Shinya M, Olsen LC and Sakai N** (2010) Regeneration of Spermatogenesis and Production of Functional Sperm by Grafting of Testicular Cell Aggregates in Zebrafish (Danio rerio). *Biology of Reproduction* **83** 533–539.

**Kayalioglu G, Altay B, Uyaroglu FG, Bademkiran F, Uludag B and Ertekin C** (2008) Morphology and innervation of the human cremaster muscle in relation to its function. *The Anatomical Record: Advances in Integrative Anatomy & Evolutionary Biology* **291** 790–796.

**Keefer C.** (2004) Production of bioproducts through the use of transgenic animal models. *Animal Reproduction Science* **82**–**83** 5–12.

**Kent Hamra F, Schultz N, Chapman KM, Grellhesl DM, Cronkhite JT, Hammer RE and Garbers DL** (2004) Defining the spermatogonial stem cell. *Developmental Biology* **269** 393–410.

**Kerr JB, Maddocks S and Sharpe RM** (1992) Testosterone and FSH have independent, synergistic and stage-dependent effects upon spermatogenesis in the rat testis. *Cell & Tissue Research* **268** 179–189.

**Khajavi N, Akbari M, Abdolsamadi HR, Abolhassani F, Dehpour AR, Koruji M and Habibi Roudkenar M** (2014) Role of somatic testicular cells during mouse spermatogenesis in three-dimensional collagen gel culture system. *Cell Journal* **16** 79–90.

**Kierszenbaum AL** (2005) Epigenetic reprogramming in germ cells and preimplantation embryos. In *Encyclopedia of Genetics, Genomics, Proteomics and Bioinformatics* (Eds Dunn MJ, Jorde LB, Little PFR and Subramaniam S), pp 1–5.Chichester: John Wiley & Sons, Ltd.

**Kim S and Izpisua Belmonte JC** (2011) Pluripotency of male germline stem cells. *Molecules and Cells* **32** 113–121.

**Kim Y, Kobayashi A, Sekido R, DiNapoli L, Brennan J, Chaboissier MCC, Poulat F, Behringer RR, Lovell-Badge R and Capel B** (2006a) Fgf9 and Wnt4 act as antagonistic signals to regulate mammalian sex determination. *PLoS Biology* **4** 1000–1009.

**Kim Y, Selvaraj V, Dobrinski I, Lee H, McEntee MC and Travis AJ** (2006b) Recipient Preparation and mixed germ cell isolation for spermatogonial stem cell transplantation in domestic cats. *Journal of Andrology* **27** 248–256.

**Kim Y, Selvaraj V, Pukazhenthi B and Travis AJ** (2007) Effect of donor age on success of spermatogenesis in feline testis xenografts. *Reproduction, Fertility & Development* **19** 869–876.

**Kim BGBJ, Cho CM, Lee YA, Kim BGBJ, Kim KJ, Kim YH, Min KS, Kim CG and Ryu BY** (2010a) Enrichment of testicular gonocytes and genetic modification using lentiviral transduction in pigs. *Biology of Reproduction* **82** 1162–1169.

**Kim K, Doi A, Wen B, Ng K, Zhao R, Cahan P, Kim J, Aryee MJ, Ji H, Ehrlich LIR *et al.*** (2010b) Epigenetic memory in induced pluripotent stem cells. *Nature* **467** 285–290.

**Kim KJ, Cho CM, Kim BGJ, Lee YA, Kim BGJ, Kim YH, Kim CG, Schmidt JA and Ryu BY** (2014) Lentiviral modification of enriched populations of bovine male gonocytes. *Journal of Animal Science* **92** 106–118.

**Kim Y, Rim YA, Yi H, Park N, Park SH and Ju JH** (2016) The generation of human induced pluripotent stem cells from blood cells: An efficient protocol using serial plating of reprogrammed cells by centrifugation. *Stem Cells International* **2016** 1–9.

**King GJ** (1993) *Reproduction in Domesticated Animals*. Elsevier Science, Amsterdam; New York.

**Kita K, Watanabe T, Ohsaka K, Hayashi H, Kubota Y, Nagashima Y, Aoki I, Taniguchi H, Noce T, Inoue K *et al.*** (2007) Production of functional spermatids from mouse germline stem cells in ectopically reconstituted seminiferous tubules. *Biology of Reproduction* **76** 211–217.

**Klonisch T, Fowler PA and Hombach-Klonisch S** (2004) Molecular and genetic regulation of testis descent and external genitalia development. *Developmental Biology* **270** 1–18.

**Ko K, Tapia N, Wu G, Kim JB, Bravo MJA, Sasse P, Glaser T, Ruau D, Han DW, Greber B *et al.*** (2009) Induction of pluripotency in adult unipotent germline stem cells. *Cell Stem Cell* **5** 87–96.

**Koopman P, Gubbay J, Vivian N, Goodfellow P and Lovell-Badge R** (1991) Male development of chromosomally female mice transgenic for Sry. *Nature* **351** 117–121.

**Korach KS** (1994) Insights from the study of animals lacking functional estrogen receptor. *Science*, **266** 1524–1527.

**Korn ED, Carlier MF and Pantaloni D** (1987) Actin polymerization and ATP hydrolysis. *Science* **238** 638–644.

**Korpelainen EI, Karkkainen MJ, Tenhunen A, Lakso M, Rauvala H, Vierula M, Parvinen M and Alitalo K** (1998) Overexpression of VEGF in testis and epididymis causes infertility in transgenic mice: Evidence for nonendothelial targets for VEGF. *The Journal of Cell Biology* **143** 1705–1712.

**Koshimizu U, Taga T, Watanabe M, Saito M, Shirayoshi Y, Kishimoto T and Nakatsuji N** (1996) Functional requirement of gp130-mediated signaling for growth and survival of mouse primordial germ cells *in vitro* and derivation of embryonic germ (EG) cells. *Development* **122** 1235–1242.

**Kossack N, Meneses J, Shefi S, Nguyen HN, Chavez S, Nicholas C, Gromoll J, Turek PJ and Reijo-Pera RA** (2009) Isolation and characterization of pluripotent human spermatogonial stem cell-derived cells. *Stem Cells* **27** 138–149.

**Koyama S and Kamimura S** (1998) Lowered sperm motility in subordinate social status of mice. *Physiology & Behavior* **65** 665–669.

**de Kretser DM, Huidobro C, Southwick GJ and Temple-Smith PD** (1998) The role of the epididymis in human infertility. *Journal of Reproduction & Fertility. Supplement* **53** 271–275.

**Kubota H and Brinster RL** (2006) Technology insight: *In vitro* culture of spermatogonial stem cells and their potential therapeutic uses. *Nature Clinical Practice. Endocrinology & Metabolism* **2** 99–108.

**Kubota H, Avarbock MR and Brinster RL** (2003) Spermatogonial stem cells share some, but not all, phenotypic and functional characteristics with other stem cells. *Proceedings of the National Academy of Sciences* **100** 6487–6492.

**Kubota H, Avarbock MR and Brinster RL** (2004a) Culture conditions and single growth factors affect fate determination of mouse spermatogonial stem cells. *Biology of Reproduction* **71** 722–731.

**Kubota H, Avarbock MR and Brinster RL** (2004b) Growth factors essential for self-renewal and expansion of mouse spermatogonial stem cells. *Proceedings of the National Academy of Sciences of the United States of America* **101** 16489–16494.

**Kubota H, Wu X, Goodyear SM, Avarbock MR and Brinster RL** (2011) Glial cell line-derived neurotrophic factor and endothelial cells promote self-renewal of rabbit germ cells with spermatogonial stem cell properties. *The FASEB Journal* **25** 2604–2614.

**Kuijk EW, Colenbrander B and Roelen BAJ** (2009) The effects of growth factors on *in vitro*-cultured porcine testicular cells. *Reproduction* **138** 721–731.

**Kunchala SR, Suzuki T and Murayama A** (2000) Photoisomerization of retinoic acid and its influence on regulation of human keratinocyte growth and differentiation. *Indian Journal of Biochemistry & Biophysics* **37** 71–76.

**Kurosawa H** (2007) Methods for inducing embryoid body formation: *In vitr*o differentiation system of embryonic stem cells. *Journal of Bioscience & Bioengineering* **103** 389–398.

**Kuzmuk KN and Schook LB** (2011) Pigs as a Model for Biomedical Sciences. In *The Genetics of the Pig* (Eds MF Rothschild and A Ruvinsky), pp 426–444.Wallingford: CABI.

**Labosky PA, Barlow DP and Hogan BL** (1994) Mouse embryonic germ (EG) cell lines: Transmission through the germline and differences in the methylation imprint of insulin-like growth factor 2 receptor (Igf2r) gene compared with embryonic stem (ES) cell lines. *Development* **120** 3197–3204.

**Lamb DJ** (1993) Growth factors and testicular development. *The Journal of Urology* **150** 583–592.

**Larsen HPE, Thorup J, Skovgaard LT, Cortes D and Byskov AG** (2002) Long-term cultures of testicular biopsies from boys with cryptorchidism: Effect of FSH and LH on the number of germ cells. *Human Reproduction* **17** 383–389.

**Laslett AL, McFarlane JR and Risbridger GP** (1997) Developmental response by Leydig cells to acidic and basic fibroblast growth factor. *The Journal of Steroid Biochemistry & Molecular Biology* **60** 171–179.

**Latham N and Mason G** (2004) From house mouse to mouse house: The behavioural biology of free-living Mus musculus and its implications in the laboratory. *Applied Animal Behaviour Science* **86** 261–289.

**Lauffenburger DA and Horwitz AF** (1996) Cell migration: A physically integrated molecular process. *Cell* **84** 359–369.

**Lee JH, Gye MC, Choi KW, Hong JY, Lee YB, Park DW, Lee SJ and Min CK** (2007a) *In vitro* differentiation of germ cells from nonobstructive azoospermic patients using three-dimensional culture in a collagen gel matrix. *Fertility & Sterility* **87** 824–833.

**Lee J, Kanatsu-Shinohara M, Inoue K, Ogonuki N, Miki H, Toyokuni S, Kimura T, Nakano T, Ogura A and Shinohara T** (2007b) Akt mediates self-renewal division of mouse spermatogonial stem cells. *Development* **134** 1853–1859.

**Lee WY, Park HJ, Lee R, Lee KH, Kim YH, Ryu BY, Kim NH, Kim JH, Kim JH, Moon SH *et al.*** (2013) Establishment and *in vitro* culture of porcine spermatogonial germ cells in low temperature culture conditions. *Stem Cell Research* **11** 1234–1249.

**Leeson TS and Cookson FB** (1974) The mammalian testicular capsule and its muscle elements. *Journal of Morphology* **144** 237–253.

**Lehmann R** (2012) Germline stem cells: Origin and destiny. *Cell Stem Cell* **10** 729–739.

**Levine E, Cupp AS, Miyashiro L and Skinner MK** (2000) Role of transforming growth factor-alpha and the epidermal growth factor receptor in embryonic rat testis development. *Biology of Reproduction* **62** 477–490.

**Li H, Papadopoulos V, Vidic B, Dym M and Culty M** (1997) Regulation of rat testis gonocyte proliferation by platelet-derived growth factor and estradiol: Identification of signaling mechanisms involved. *Endocrinology* **138** 1289–1298.

**Li N, Wang T and Han D** (2012) Structural, cellular and molecular aspects of immune privilege in the testis. *Frontiers in Immunology* **3** 152.

**Li Y, Zheng M and Chris Lau YF** (2014) The sex-determining factors SRY and SOX9 regulate similar target genes and promote testis cord formation during testicular differentiation. *Cell Reports* **8** 723–733.

**Lin Y and Page DC** (2005) Dazl deficiency leads to embryonic arrest of germ cell development in XY C57BL/6 mice. *Developmental Biology* **288** 309–316.

**Lin LF, Doherty DH, Lile JD, Bektesh S and Collins F** (1993) GDNF: A glial cell line-derived neurotrophic factor for midbrain dopaminergic neurons. *Science* **260** 1130–1132.

**Liu ZC and Chang TMS** (2010) Artificial cell microencapsulated stem cells in regenerative medicine, tissue engineering and cell therapy. *Advances in Experimental Medicine & Biology* **670** 68–79.

**Liu X and Yang Y** (2004) Effect of VEGF on the angiogenesis in male reproduction system. *Zhonghua Nan Ke Xue: National Journal of Andrology* **10** 49–51.

**Liu A, Flores C, Kinkead T, Carboni AA, Menon M and Seethalakshmi L** (1994) Effects of sialoadenectomy and epidermal growth factor on testicular function of sexually mature male mice. *The Journal of Urology* **152** 554–561.

**Liu WC, Huang Y, Liao YM and Li C** (2012) Testes asymmetry of Chinese endemic frog (*Rana omeimontis*) in relation to body condition and age. *North-Western Journal of Zoology* **8** 390–393.

**Livera G, Rouiller-Fabre V, Durand P and Habert R** (2000a) Multiple effects of retinoids on the development of Sertoli, germ, and Leydig cells of fetal and neonatal rat testis in culture. *Biology of Reproduction* **62** 1303–1314.

**Livera G, Rouiller-Fabre V, Valla J and Habert R** (2000b) Effects of retinoids on the meiosis in the fetal rat ovary in culture. *Molecular & Cellular Endocrinology* **165** 225–231.

**Livera G, Rouiller-Fabre V and Habert R** (2001) Retinoid receptors involved in the effects of retinoic acid on rat testis development. *Biology of Reproduction* **64** 1307–1314.

**Livera G, Rouiller-Fabre V, Pairault C, Levacher C and Habert R** (2002) Regulation and perturbation of testicular functions by vitamin A. *Reproduction* **124** 173–180.

**Llames S, García-Pérez E, Meana Á, Larcher F and del Río M** (2015) Feeder layer cell actions and applications. *Tissue Engineering. Part B, Reviews* **21** 345–353.

**Lo KC, Brugh VM, Parker M and Lamb DJ** (2005) Isolation and enrichment of murine spermatogonial stem cells using Rhodamine 123 mitochondrial dye. *Biology of Reproduction* **72** 767–771.

**Lohse L, Uttenthal A, Enøe C and Nielsen J** (2010) A study on the applicability of implantable microchip transponders for body temperature measurements in pigs. *Acta Veterinaria Scandinavica* **52** 29.

**Van Loo PLP, Van Zutphen LFM and Baumans V** (2003) Male management: Coping with aggression problems in male laboratory mice. *Laboratory Animals* **37** 300–313.

**Loveland KL and Schlatt S** (1997) Stem cell factor and c-kit in the mammalian testis: Lessons originating from mother nature's gene knockouts. *The Journal of Endocrinology* **153** 337–344.

**Lowry WE, Richter L, Yachechko R, Pyle AD, Tchieu J, Sridharan R, Clark AT and Plath K** (2008) Generation of human induced pluripotent stem cells from dermal fibroblasts. *Proceedings of the National Academy of Sciences of the United States of America* **105** 2883–2888.

**Lubahn DB, Moyer JS, Golding TS, Couse JF, Korach KS and Smithies O** (1993) Alteration of reproductive function but not prenatal sexual development after insertional disruption of the mouse estrogen receptor gene. *Proceedings of the National Academy of Sciences of the United States of America* **90** 11162–11166.

**Lund AW, Bush JA, Plopper GE and Stegemann JP** (2008) Osteogenic differentiation of mesenchymal stem cells in defined protein beads. *Journal of Biomedical Materials Research - Part B Applied Biomaterials* **87** 213–221.

**Luo J, Megee S, Rathi R and Dobrinski I** (2006) Protein gene product 9.5 is a spermatogonia-specific marker in the pig testis: Application to enrichment and culture of porcine spermatogonia. *Molecular Reproduction & Development* **73** 1531–1540.

**Machida T, Yonezawa Y and Noumura T** (1981) Age-associated changes in plasma testosterone levels in male mice and their relation to social dominance or subordinance. *Hormones & Behavior* **15** 238–245.

**Maekawa M, Kamimura K and Nagano T** (1996) Peritubular myoid cells in the testis: Their structure and function. *Archives of Histology & Cytology* **59** 1–13.

**Majumdar SS, Tsuruta J, Griswold MD and Bartke A** (1995) Isolation and culture of Sertoli cells from the testes of adult Siberian hamsters: Analysis of proteins synthesized and secreted by Sertoli cells cultured from hamsters raised in a long or a short photoperiod. *Biology of Reproduction* **52** 658–666.

**Mancini M, Vergara E, Salvatore G, Greco A, Troncone G, Affuso A, Liuzzi R, Salerno P, Di Santolo MS, Santoro M *et al.*** (2009) Morphological ultrasound microimaging of thyroid in living mice. *Endocrinology* **150** 4810–4815.

**Mankidy R, Ranjan B, Honaramooz A and Giesy JP** (2014) Effects of novel brominated flame retardants on steroidogenesis in primary porcine testicular cells. *Toxicology Letters* **224** 141–146.

**Manku G, Wang Y, Merkbaoui V, Boisvert A, Ye X, Blonder J and Culty M** (2015) Role of retinoic acid and platelet-derived growth factor receptor cross talk in the regulation of neonatal gonocyte and embryonal carcinoma cell differentiation. *Endocrinology* **156** 346–359.

**Manning HC, Merchant NB, Foutch a C, Virostko JM, Wyatt SK, Shah C, McKinley ET, Xie J, Mutic NJ, Washington MK *et al.*** (2008) Molecular imaging of therapeutic response to epidermal growth factor receptor blockade in colorectal cancer. *Clinical Cancer Research* **14** 7413–7422.

**Mannino G, Abdolrahimzadeh B, Calafiore S, Anselmi G, Mannino C and Lambiase A** (2016) A review of the role of ultrasound biomicroscopy in glaucoma associated with rare diseases of the anterior segment. *Clinical Ophthalmology* **10** 1453–1459.

**Mark M, Ghyselinck NB and Chambon P** (2009) Function of retinoic acid receptors during embryonic development. *Nuclear Receptor Signaling* **7** e002.

**Marret C and Durand P** (2000) Culture of porcine spermatogonia: Effects of purification of the germ cells, extracellular matrix and fetal calf serum on their survival and multiplication. *Reproduction, Nutrition, Development* **40** 305–319.

**Martineau J, Nordqvist K, Tilmann C, Lovell-Badge R and Capel B** (1997) Male-specific cell migration into the developing gonad. *Current Biology* **7** 958–968.

**Marziali G, Lazzaro D and Sorrentino V** (1993) Binding of germ cells to mutant Sld Sertoli cells is defective and is rescued by expression of the transmembrane form of the c-kit ligand. *Developmental Biology* **157** 182–190.

**Mather JP, Attie KM, Woodruff TK, Rice GC and Phillips DM** (1990) Activin stimulates spermatogonial proliferation in germ-sertoli cell cocultures from immature rat testis. *Endocrinology* **127** 3206–3214.

**Matsui Y, Toksoz D, Nishikawa S, Nishikawa S-I, Williams D, Zsebo K and Hogan BLM** (1991) Effect of Steel factor and leukaemia inhibitory factor on murine primordial germ cells in culture. *Nature* **353** 750–752.

**Matsui Y, Zsebo K and Hogan BL** (1992) Derivation of pluripotential embryonic stem cells from murine primordial germ cells in culture. *Cell* **70** 841–847.

**Matsui Y, Takehara A, Tokitake Y, Ikeda M, Obara Y, Morita-Fujimura Y, Kimura T and Nakano T** (2014) The majority of early primordial germ cells acquire pluripotency by AKT activation. *Development* **141** 4457–4467.

**Matte R and Sasaki M** (1971) Autoradiographic evidence of human male germ-cell differentiation *in vitro*. *Cytologia* **36** 298–303.

**Matthiesson KL, Stanton PG, O'Donnell L, Meachem SJ, Amory JK, Berger R, Bremner WJ and McLachlan RI** (2005) Effects of testosterone and levonorgestrel combined with a 5α-reductase inhibitor or gonadotropin-releasing hormone antagonist on spermatogenesis and intratesticular steroid levels in normal men. *The Journal of Clinical Endocrinology & Metabolism* **90** 5647–5655.

**Mauduit C, Hamamah S and Benahmed M** (1999) Stem cell factor/c-kit system in spermatogenesis. *Human Reproduction* **5** 535–545.

**McGuinness MP and Orth JM** (1992) Reinitiation of gonocyte mitosis and movement of gonocytes to the basement membrane in testes of newborn rats *in vivo* and *in vitro*. *The Anatomical Record* **233** 527–537.

**McIver SC, Stanger SJ, Santarelli DM, Roman SD, Nixon B and McLaughlin EA** (2012) A unique combination of male germ cell miRNAs coordinates gonocyte differentiation. *PloS One* **7** e35553.

**McLachlan RI, Wreford NG, de Kretser DM and Robertson DM** (1995) The effects of recombinant follicle-stimulating hormone on the restoration of spermatogenesis in the gonadotropin-releasing hormone-immunized adult rat. *Endocrinology* **136** 4035–4043.

**McLaren A** (2001) Mammalian germ cells: birth, sex, and immortality. *Cell Structure & Function* **26** 119–122.

**McLaren A** (2003) Primordial germ cells in the mouse. *Developmental Biology* **262** 1–15.

**McLaren A and Southee D** (1997) Entry of mouse embryonic germ cells into meiosis. *Developmental Biology* **187** 107–113.

**McLaren A, Mittwoch U and Josso N** (1995) Germ cells and germ cell sex. *Philosophical Transactions of the Royal Society B: Biological Sciences* **350** 229–233.

**McLean DJ, Friel PJ, Johnston DS and Griswold MD** (2003) Characterization of spermatogonial stem cell maturation and differentiation in neonatal mice. *Biology of Reproduction* **69** 2085–2091.

**McMillan M, Andronicos N, Davey R, Stockwell S, Hinch G and Schmoelzl S** (2014) Claudin-8 expression in Sertoli cells and putative spermatogonial stem cells in the bovine testis. *Reproduction, Fertility & Development* **26** 633–644.

**Meachem SJ, Mclachlan RI, Stanton PG, Robertson DM and Wreford NG** (1999) FSH immunoneutralization acutely impairs spermatogonial development in normal adult rats. *Journal of Andrology* **20** 756–62..

**Meachem SJ, Nieschlag E and Simoni M** (2001) Inhibin B in male reproduction: Pathophysiology and clinical relevance. *European Journal of Endocrinology* **145** 561–571.

**Meachem SJ, Ruwanpura SM, Ziolkowski J, Ague JM, Skinner MK and Loveland KL** (2005) Developmentally distinct *in vivo* effects of FSH on proliferation and apoptosis during testis maturation. *The Journal of Endocrinology* **186** 429–446.

**Meng X, Lindahl M, Hyvönen ME, Parvinen M, de Rooij DG, Hess MW, Raatikainen-Ahokas A, Sainio K, Rauvala H, Lakso M *et al.*** (2000) Regulation of cell fate decision of undifferentiated spermatogonia by GDNF. *Science* **287** 1489–1493.

**Merchant-Larios H and Moreno-Mendoza N** (1998) Mesonephric stromal cells differentiate into Leydig cells in the mouse fetal testis. *Experimental Cell Research* **244** 230–238.

**Miething A** Multinucleated spermatocytes in the aging human testis: Formation, morphology, and degenerative fate. *Andrologia* **25** 317–323.

**Miething A** (1995) Multinuclearity of germ cells in the senescent human testis originates from a process of cell-cell fusion. *Journal of Submicroscopic Cytology & Pathology* **27** 105–113.

**De Miguel MP, de Boer-Brouwer M, Paniagua R, van den Hurk R, de Rooij DG and van Dissel-Emiliani FM** (1996) Leukemia inhibitory factor and ciliary neurotropic factor promote the survival of Sertoli cells and gonocytes in coculture system. *Endocrinology* **137** 1885–1893.

**Mikkola M, Sironen A, Kopp C, Taponen J, Sukura A, Vilkki J, Katila T and Andersson M** (2006) Transplantation of normal boar testicular cells resulted in complete focal spermatogenesis in a boar affected by the immotile short-tail sperm defect. *Reproduction in Domestic Animals* **41** 124–128.

**Miller SC, Bowman BM and Rowland HG** (1983) Structure, cytochemistry, endocytic activity, and immunoglobulin (Fc) receptors of rat testicular interstitial-tissue macrophages. *American Journal of Anatomy* **168** 1–13.

**Mircea CN, Lujan ME, Jaiswal RS, Singh J, Adams GP and Pierson RA** (2009) Ovarian imaging in the mouse using ultrasound biomicroscopy (UBM): A validation study. *Reproduction, Fertility & Development* **21** 579–586.

**Molyneaux KA, Stallock J, Schaible K and Wylie C** (2001) Time-lapse analysis of living mouse germ cell migration. *Developmental Biology* **240** 488–498.

**Moniot B, Declosmenil F, Barrionuevo F, Scherer G, Aritake K, Malki S, Marzi L, Cohen-Solal A, Georg I, Klattig J *et al.*** (2009) The PGD2 pathway, independently of FGF9, amplifies SOX9 activity in Sertoli cells during male sexual differentiation. *Development* **136** 1813–1821.

**Moore A and Morris ID** (1993) Paracrine effects via the epidermal growth factor receptor in the rodent testis may be mediated by non-Leydig interstitial cells. *Journal of Endocrinology* **136** 439–446.

**Moraveji SF, Attari F, Shahverdi A, Sepehri H, Farrokhi A, Hassani SN, Fonoudi H, Aghdami N and Baharvand H** (2012) Inhibition of glycogen synthase kinase-3 promotes efficient derivation of pluripotent stem cells from neonatal mouse testis. *Human Reproduction* **27** 2312–2324.

**Morrison-Graham K and Takahashi Y** (1993) Steel factor and c-Kit receptor: From mutants to a growth factor system. *BioEssays* **15** 77–83.

**Morse HC** (2007) Building a Better Mouse: One hundred years of genetics and biology. In *The Mouse in Biomedical Research* (Eds Fox J, Barthold S, Davisson M, Newcomer C, Quimby F and Smith A), pp 1–11. Cambridge, MA: Academic Press USA

**Mota PC, Ehmcke J, Westernströer B, Gassei K, Ramalho-Santos J and Schlatt S** (2012) Effects of different storage protocols on cat testis tissue potential for xenografting and recovery of spermatogenesis. *Theriogenology* **77** 299–310.

**Motro B, van der Kooy D, Rossant J, Reith A and Bernstein A** (1991) Contiguous patterns of c-kit and steel expression: Analysis of mutations at the W and Sl loci. *Development* **113** 1207–1221.

**Movahedin M, Ajeen A, Ghorbanzadeh N, Tiraihi T, Valojerdi MR and Kazemnejad A** (2004) *In vitro* maturation of fresh and frozen-thawed mouse round spermatids. *Andrologia* **36** 269–276.

**Mullaney BP and Skinner MK** (1992) Basic fibroblast growth factor (bFGF) gene expression and protein production during pubertal development of the seminiferous tubule: Follicle-stimulating hormone-induced Sertoli cell bFGF expression. *Endocrinology* **131** 2928–2934.

**Murua A, Portero A, Orive G, Hernández RM, de Castro M and Pedraz JL** (2008) Cell microencapsulation technology: Towards clinical application. *Journal of Controlled Release* **132** 76–83.

**Nagano M, Avarbock MR, Leonida EB, Brinster CJ and Brinster RL** (1998) Culture of mouse spermatogonial stem cells. *Tissue & Cell* **30** 389–397.

**Nagano M, Avarbock MR and Brinster RL** (1999) Pattern and kinetics of mouse donor spermatogonial stem cell colonization in recipient testes. *Biology of Reproduction* **60** 1429–1436.

**Nagano R, Tabata S, Nakanishi Y, Ohsako S, Kurohmaru M and Hayashi Y** (2000) Reproliferation and relocation of mouse male germ cells (gonocytes) during prespermatogenesis. *The Anatomical Record* **258** 210–220.

**Nagano M, McCarrey JR and Brinster RL** (2001) Primate spermatogonial stem cells colonize mouse testes. *Biology of Reproduction* **64** 1409–1416.

**Nagano M, Patrizio P and Brinster RL** (2002) Long-term survival of human spermatogonial stem cells in mouse testes. *Fertility & Sterility* **78** 1225–1233.

**Nagano M, Ryu BY, Brinster CJ, Avarbock MR and Brinster RL** (2003) Maintenance of mouse male germ line stem cells *in vitro*. *Biology of Reproduction* **68** 2207–2214.

**Nakagawa T, Nabeshima Y and Yoshida S** (2007) Functional identification of the actual and potential stem cell compartments in mouse spermatogenesis. *Developmental Cell* **12** 195–206.

**Nakai M, Kaneko H, Somfai T, Maedomari N, Ozawa M, Noguchi J, Ito J, Kashiwazaki N and Kikuchi K** (2010) Production of viable piglets for the first time using sperm derived from ectopic testicular xenografts. *Reproduction* **139** 331–335.

**Nakamura M, Namiki M, Okuyama A, Matsui T, Doi Y, Takeyama M, Fujioka H, Nishimune Y, Matsumoto K and Sonoda T** (1987) Temperature sensitivity of human spermatogonia and spermatocytes *in vitro*. *Archives of Andrology* **19** 127–132.

**Nakazumi H, Sasano H, Maehara I and Orikasa S** (1996) Transforming growth factor-alpha, epidermal growth factor, and epidermal growth factor receptor in human testis obtained from biopsy and castration: Immunohistochemical study. *The Tohoku Journal of Experimental Medicine* **178** 381–388.

**Nalbandian A, Dettin L, Dym M and Ravindranath N** (2003) Expression of vascular endothelial growth factor receptors during male germ cell differentiation in the mouse. *Biology of Reproduction* **69** 985–994.

**Napoli JL** (2012) Physiological insights into all-trans-retinoic acid biosynthesis. *Biochimica et Biophysica Acta (BBA) - Molecular & Cell Biology of Lipids* **1821** 152–167.

**Nasiri Z, Hosseini SM, Hajian M, Abedi P, Bahadorani M, Baharvand H and Nasr-Esfahani MH** (2012) Effects of different feeder layers on short-term culture of prepubertal bovine testicular germ cells In-vitro. *Theriogenology* **77** 1519–1528.

**Naughton CK, Jain S, Strickland AM, Gupta A and Milbrandt J** (2006) Glial cell-line derived neurotrophic factor-mediated RET signaling regulates spermatogonial stem cell fate. *Biology of Reproduction* **74** 314–321.

**Neufeld G, Cohen T, Gengrinovitch S and Poltorak Z** (1999) Vascular endothelial growth factor (VEGF) and its receptors. *The FASEB Journal* **13** 9–22.

**Newton SC, Blaschuk OW and Millette CF** (1993) N-cadherin mediates sertoli cell-spermatogenic cell adhesion. *Developmental Dynamics* **197** 1–13.

**Nicodemus G and Bryant S** (2008) Cell encapsulation in biodegradable hydrogels for tissue engineering applications. *Tissue Engineering Part B: Reviews* **14** 149–165.

**Niemann H and Kues WA** (2007) Transgenic farm animals: An update. *Reproduction, Fertility & Development* **19** 762–770.

**Niu Z, Wu S, Wu C, Li N, Zhu H, Liu W, Hua J, Niu Z, Wu S, Wu C *et al.*** (2016) Multipotent male germline stem cells (mGSCs) from neonate porcine testis. *Brazilian Archives of Biology and Technology* **59** e16150449.

**O'Shaughnessy PJ, Baker PJ and Johnston H** (2006) The foetal Leydig cell - differentiation, function and regulation. *International Journal of Andrology* **29** 90–95.

**O'Shaughnessy PJ, Morris ID, Huhtaniemi I, Baker PJ and Abel MH** (2009) Role of androgen and gonadotrophins in the development and function of the Sertoli cells and Leydig cells: data from mutant and genetically modified mice. *Molecular & Cellular Endocrinology* **306** 2–8.

**O'Shaughnessy PJ, Monteiro A and Abel M** (2012) Testicular development in mice lacking receptors for follicle stimulating hormone and androgen. *PLoS ONE* **7** e35136.

**Oatley JM and Brinster RL** (2008) Regulation of spermatogonial stem cell self-renewal in mammals. *Annual Review of Cell & Developmental Biology* **24** 263–286.

**Oatley JM and Brinster RL** (2012) The germline stem cell niche unit in mammalian testes. *Physiological Reviews* **92** 577–595.

**Oatley JM, de Avila DM, McLean DJ, Griswold MD and Reeves JJ** (2002) Transplantation of bovine germinal cells into mouse testes. *Journal of Animal Science* **80** 1925–1931.

**Oatley JM, de Avila DM, Reeves JJ and McLean DJ** (2004) Spermatogenesis and germ cell transgene expression in xenografted bovine testicular tissue. *Biology of Reproduction* **71** 494–501.

**Oatley JM, Reeves JJ and McLean DJ** (2005) Establishment of spermatogenesis in neonatal bovine testicular tissue following ectopic xenografting varies with donor age. *Biology of Reproduction* **72** 358–364.

**Oatley JM, Avarbock MR, Telaranta AI, Fearon DT and Brinster RL** (2006) Identifying genes important for spermatogonial stem cell self-renewal and survival. *Proceedings of the National Academy of Sciences* **103** 9524–9529.

**Oatley JM, Avarbock MR and Brinster RL** (2007) Glial cell line-derived neurotrophic factor regulation of genes essential for self-renewal of mouse spermatogonial stem cells is dependent on Src family kinase signaling. *Journal of Biological Chemistry* **282** 25842–25851.

**Oatley JM, Oatley MJ, Avarbock MR, Tobias JW and Brinster RL** (2009) Colony stimulating factor 1 is an extrinsic stimulator of mouse spermatogonial stem cell self-renewal. *Development* **136** 1191–1199.

**Oatley MJ, Kaucher AV, Racicot KE and Oatley JM** (2011) Inhibitor of DNA binding 4 is expressed selectively by single spermatogonia in the male germline and regulates the self-renewal of spermatogonial stem cells in mice. *Biology of Reproduction* **85** 347–356.

**Ogawa T, Dobrinski I and Brinster RL** (1999) Recipient preparation is critical for spermatogonial transplantation in the rat. *Tissue and Cell* **31** 461–472.

**Ogawa T, Dobrinski I, Avarbock MR and Brinster RL** (2000) Transplantation of male germ line stem cells restores fertility in infertilemice. *Nature Medicine* **6** 29–34.

**Ogawa T, Ohmura M, Yumura Y, Sawada H and Kubota Y** (2003) Expansion of murine spermatogonial stem cells through serial transplantation. *Biology of Reproduction* **68** 316–322.

**Ogawa T, Ohmura M, Tamura Y, Kita K, Ohbo K, Suda T and Kubota Y** (2004) Derivation and morphological characterization of mouse spermatogonial stem cell lines. *Archives of Histology & Cytology* **67** 297–306.

**Ohbo K, Yoshida S, Ohmura M, Ohneda O, Ogawa T, Tsuchiya H, Kuwana T, Kehler J, Abe K, Schöler HR *et al.*** (2003) Identification and characterization of stem cells in prepubertal spermatogenesis in mice. *Developmental Biology* **258** 209–225.

**Ohinata Y, Payer B, O'Carroll D, Ancelin K, Ono Y, Sano M, Barton SC, Obukhanych T, Nussenzweig M, Tarakhovsky A *et al.*** (2005) Blimp1 is a critical determinant of the germ cell lineage in mice. *Nature* **436** 207–213.

**Ohmura M, Yoshida S, Ide Y, Nagamatsu G, Suda T and Ohbo K** (2004) Spatial analysis of germ stem cell development in Oct-4/EGFP transgenic mice. *Archives of Histology & Cytology* **67** 285–296.

**Ohta H, Wakayama T and Nishimune Y** (2004) Commitment of fetal male germ cells to spermatogonial stem cells during mouse embryonic development. *Biology of Reproduction* **70** 1286–1291.

**Olaso R and Habert R** (2000) Genetic and cellular analysis of male germ cell development. *Journal of Andrology* **21** 497–511.

**Olie RA, Looijenga LH, Dekker MC, de Jong FH, van Dissel-Emiliani FM, de Rooij DG, van der Holt B and Oosterhuis JW** (1995) Heterogeneity in the *in vitro* survival and proliferation of human seminoma cells. *British Journal of Cancer* **71** 13–17.

**Orth JM and Boehm R** (1990) Functional coupling of neonatal rat Sertoli cells and gonocytes in coculture. *Endocrinology* **127** 2812–2820.

**Orth JM and Jester WF** (1995) NCAM mediates adhesion between gonocytes and sertoli cells in cocultures from testes of neonatal rats. *Journal of Andrology* **16** 389–399.

**Orth JMJM and McGuinness MPMP** (1991) Neonatal gonocytes co-cultured with Sertoli cells on a laminin-containing matrix resume mitosis and elongate. *Endocrinology* **129** 1119–1121.

**Orth JM, Qiu J, Jester WF and Pilder S** (1997) Expression of the c-kit gene is critical for migration of neonatal rat gonocytes *in vitro*. *Biology of Reproduction* **57** 676–683.

**Orth JM, Jester WF, Li LH and Laslett AL** (2000) Gonocyte-Sertoli cell interactions during development of the neonatal rodent testis. *Current Topics in Developmental Biology* **50** 103–124.

**Orwig KE and Schlatt S** (2005) Cryopreservation and transplantation of spermatogonia and testicular tissue for preservation of male fertility. *Journal of the National Cancer Institute Monographs* **2005** 51–56.

**Orwig KE, Ryu BY, Avarbock MR and Brinster RL** (2002a) Male germ-line stem cell potential is predicted by morphology of cells in neonatal rat testes. *Proceedings of the National Academy of Sciences of the United States of America* **99** 11706–11711.

**Orwig KE, Avarbock MR and Brinster RL** (2002b) Retrovirus-mediated modification of male germline stem cells in rats. *Biology of Reproduction* **67** 874–879.

**Orwig KE, Shinohara T, Avarbock MR and Brinster RL** (2002c) Functional analysis of stem cells in the adult rat testis. *Biology of Reproduction* **66** 944–949.

**Ozisik G, Achermann JC, Meeks JJ and Jameson JL** (2003) SF1 in the Development of the Adrenal Gland and Gonads. *Hormone Research in Paediatrics* **59** 94–98.

**Pacchiarini T, Olague E, Sarasquete C and Cabrita E** (2014) Busulfan administration produces sublethal effects on somatic tissues and inhibits gametogenesis in Senegalese sole juveniles. *Histology & Histopathology* **29** 619–628.

**Panepinto LM** (1996) Miniature Swine Breeds used Worldwide in Research. In *Advances in Swine in Biomedical Research*, pp 681–691. Boston, MA: Springer US.

**Paris MCJ and Schlatt S** (2007) Ovarian and testicular tissue xenografting: Its potential for germline preservation of companion animals, non-domestic and endangered species. *Reproduction, Fertility & Development* **19** 771–782.

**Paris MCJ, Snow M, Cox SL and Shaw JM** (2004) Xenotransplantation: A tool for reproductive biology and animal conservation? *Theriogenology* **61** 277–291.

**Park SY and Jameson JL** (2005) Minireview: Transcriptional regulation of gonadal development and differentiation. *Endocrinology* **146** 1035–1042.

**Park JH, Kim SJ, Oh EJ, Moon SY, Roh S Il, Kim CG and Yoon HS** (2003) Establishment and maintenance of human embryonic stem cells on STO, a permanently growing cell line. *Biology of Reproduction* **69** 2007–2014.

**Park IH, Arora N, Huo H, Maherali N, Ahfeldt T, Shimamura A, Lensch MW, Cowan C, Hochedlinger K and Daley GQ** (2008) Disease-specific induced pluripotent stem cells. *Cell* **134** 877–886.

**Park IS, Kim SH, Kim YH, Kim IH and Kim SH** (2009) A collagen/smooth muscle cell-incorporated elastic scaffold for tissue-engineered vascular grafts. *Journal of Biomaterials Science. Polymer Edition* **20** 1645–1660.

**Parvari S, Abbasi M, Abbasi N, Malek VG, Amidi F, Aval FS, Roudkenar MH and Izadyar F** (2015) Stem cell isolation by a morphology-based selection method in postnatal mouse ovary. *Archives of Medical Science* **11** 670–678.

**Patni P, Mohanty SK and Singh R** (2017) Embryonic Development of the Testis. In *Male Infertility: Understanding, Causes and Treatment*, pp 13–24. Singapore: Springer Singapore.

**Pelletier RM and Byers SW** (1992) The blood-testis barrier and Sertoli cell junctions: Structural considerations. *Microscopy Research & Technique* **20** 3–33.

**van Pelt AM and de Rooij DG** (1990) Synchronization of the seminiferous epithelium after vitamin A replacement in vitamin A-deficient mice. *Biology of Reproduction* **43** 363–367.

**van Pelt AM, Morena AR, van Dissel-Emiliani FM, Boitani C, Gaemers IC, de Rooij DG and Stefanini M** (1996) Isolation of the synchronized A spermatogonia from adult vitamin A-deficient rat testes. *Biology of Reproduction* **55** 439–444.

**van Pelt AMM and de Rooij DG** (1991) Retinoic acid is able to reinitiate spermatogenesis in vitamin A-deficient rats and high replicate doses support the full development of spermatogenic cells. *Endocrinology* **128** 697–704.

**Pereira LA, Tanaka H, Nagata Y, Sawada K, Mori H, Chimelli LM and Nishimune Y** (1998) Characterization and expression of a stage specific antigen by monoclonal antibody TRA 54 in testicular germ cells. *International Journal of Andrology* **21** 34–40.

**Perlman RL** (2016) Mouse models of human disease: An evolutionary perspective. *Evolution, Medicine & Public Health* **2016** 170–176.

**Perrett RM, Turnpenny L, Eckert JJ, O'Shea M, Sonne SB, Cameron IT, Wilson DI, Meyts ER-D and Hanley NA** (2008) The early human germ cell lineage does not express SOX2 during *in vivo* development or upon *in vitro* culture. *Biology of Reproduction* **78** 852–858.

**Pesce M, Farrace MG, Piacentini M, Dolci S, De Felici M, DeChiara TM and Yancopoulous GD** (1993) Stem cell factor and leukemia inhibitory factor promote primordial germ cell survival by suppressing programmed cell death (apoptosis). *Development* **118** 1089–1094.

**Piquet-Pellorce C, Dorval-Coiffec I, Pham MD and Jégou B** (2000) Leukemia inhibitory factor expression and regulation within the testis. *Endocrinology* **141** 1136–1141.

**Piravar Z, Jeddi-Tehrani M, Sadeghi MR, Mohazzab A, Eidi A and Akhondi MM** (2013) *In vitro* culture of human testicular stem cells on feeder-free condition. *Journal of Reproduction and Infertility* **14** 17–22.

**Poels J, van Langendonckt A, Dehoux JP, Donnez J and Wyns C** (2012) Vitrification of non-human primate immature testicular tissue allows maintenance of proliferating spermatogonial cells after xenografting to recipient mice. *Theriogenology* **77** 1008–1013.

**Poels J, van Langendonckt A, Many MC, Wese FX and Wyns C** (2013) Vitrification preserves proliferation capacity in human spermatogonia. *Human Reproduction* **28** 578–589.

**Poels J, Abou-Ghannam G, Herman S, Van Langendonckt A, Wese FX and Wyns C** (2014) In search of better spermatogonial preservation by supplementation of cryopreserved human immature testicular tissue xenografts with n-acetylcysteine and testosterone. *Frontiers in Surgery* **1** 47.

**Popsueva A, Poteryaev D, Arighi E, Meng X, Angers-Loustau A, Kaplan D, Saarma M and Sariola H** (2003) GDNF promotes tubulogenesis of GFRα1-expressing MDCK cells by Src-mediated phosphorylation of Met receptor tyrosine kinase. *The Journal of Cell Biology* **161** 119–129.

**Povlsen CO, Skakkebaek NE, Rygaard J and Jensen G** (1974) Heterotransplantation of human foetal organs to the mouse mutant nude. *Nature* **248** 247–249.

**Pratt SA, Scully NF and Shur BD** (1993) Cell Surface β1,4 galactosyltransferase on primary spermatocytes facilitates their initial adhesion to sertoli cells *in vitro*. *Biology of Reproduction* **49** 470–482.

**Print CG and Loveland KL** (2000) Germ cell suicide: New insights into apoptosis during spermatogenesis. *BioEssays* **22** 423–430.

**Rabinovici J and Jaffe RB** (1990) Development and regulation of growth and differentiated function in human and subhuman primate fetal gonads. *Endocrine Reviews* **11** 532–557.

**Radhakrishnan B, Oke BO, Papadopoulos V, DiAugustine RP and Suarez-Quian CA** (1992) Characterization of epidermal growth factor in mouse testis. *Endocrinology* **131** 3091–3099.

**Rajpert-De Meyts E** (2006) Developmental model for the pathogenesis of testicular carcinoma in situ: Genetic and environmental aspects. *Human Reproduction* **12** 303–323.

**Rajpert-De Meyts E, Hanstein R, Jørgensen N, Graem N, Vogt PH and Skakkebaek NE** (2004) Developmental expression of POU5F1 (OCT-3/4) in normal and dysgenetic human gonads. *Human Reproduction* **19** 1338–1344.

**El Ramy R, Verot A, Mazaud S, Odet F, Magre S and Le Magueresse-Battistoni B** (2005) Fibroblast growth factor (FGF) 2 and FGF9 mediate mesenchymal-epithelial interactions of peritubular and Sertoli cells in the rat testis. *The Journal of Endocrinology* **187** 135–147.

**Rastegar T, Habibi Roudkenar M, Parvari S and Baazm M** (2015) The interaction between Sertoli cells and luekemia inhibitory factor on the propagation and differentiation of spermatogonial stem cells *in vitro*. *Iranian Journal of Reproductive Medicine* **13** 679–686.

**Rathi R, Honaramooz A, Zeng W, Schlatt S and Dobrinski I** (2005) Germ cell fate and seminiferous tubule development in bovine testis xenografts. *Reproduction* **130** 923–929.

**Rathi R, Honaramooz A, Zeng W, Turner R and Dobrinski I** (2006) Germ cell development in equine testis tissue xenografted into mice. *Reproduction* **131** 1091–1098.

**Rathi R, Zeng W, Megee S, Conley A, Meyers S and Dobrinski I** (2008) Maturation of testicular tissue from infant monkeys after xenografting into mice. *Endocrinology* **149** 5288–5296.

**Reddy N, Mahla RS, Thathi R, Suman SK, Jose J and Goel S** (2012) Gonadal status of male recipient mice influences germ cell development in immature buffalo testis tissue xenograft. *Reproduction* **143** 59–69.

**Reding SC, Stepnoski AL, Cloninger EW and Oatley JM** (2010) THY1 is a conserved marker of undifferentiated spermatogonia in the pre-pubertal bull testis. *Reproduction* **139** 893–903.

**Reijo R, Alagappan RK, Patrizio P and Page DC** (1996) Severe oligozoospermia resulting from deletions of azoospermia factor gene on Y chromosome. *Lancet* **347** 1290–1293.

**Reijo RA, Dorfman DM, Slee R, Renshaw AA, Loughlin KR, Cooke H and Page DC** (2000) DAZ family proteins exist throughout male germ cell development and transit from nucleus to cytoplasm at meiosis in humans and mice. *Biology of Reproduction* **63** 1490–1496.

**Resnick JL, Bixler LS, Cheng L and Donovan PJ** (1992) Long-term proliferation of mouse primordial germ cells in culture. *Nature* **359** 550–551.

**Riboldi M, Rubio C, Pellicer A, Gil-Salom M and Simón C** (2012) *In vitro* production of haploid cells after coculture of CD49f+ with Sertoli cells from testicular sperm extraction in nonobstructive azoospermic patients. *Fertility & Sterility* **98** 580–590.

**Richards AJ, Enders GC and Resnick JL** (1999) Differentiation of murine premigratory primordial germ cells in culture. *Biology of Reproduction* **61** 1146–1151.

**Robertson KM, O'Donnell L, Jones ME, Meachem SJ, Boon WC, Fisher CR, Graves KH, McLachlan RI and Simpson ER** (1999) Impairment of spermatogenesis in mice lacking a functional aromatase (cyp 19) gene. *Proceedings of the National Academy of Sciences of the United States of America* **96** 7986–7991.

**Rodriguez-Sosa JR and Dobrinski I** (2009) Recent developments in testis tissue xenografting. *Reproduction* **138** 187–194.

**Rodriguez-Sosa JR, Silvertown J, Foster R, Medin J and Hahnel A** (2009) Transduction and transplantation of spermatogonia into the testis of ram lambs through the extra-testicular rete. *Reproduction in Domestic Animals* **44** 612–620.

**Rodriguez-Sosa JR, Rathi R, Wang Z and Dobrinski I** (2011) Development of bovine fetal testis tissue after ectopic xenografting in mice. *Journal of Andrology* **32** 271–281.

**Rodriguez I, Ody C, Araki K, Garcia I and Vassalli P** (1997) An early and massive wave of germinal cell apoptosis is required for the development of functional spermatogenesis. *The EMBO Journal* **16** 2262–2270.

**Romero Y, Vuandaba M, Suarez P, Grey C, Calvel P, Conne B, Pearce D, de Massy B, Hummler E and Nef S** (2012) The Glucocorticoid-Induced Leucine Zipper (GILZ) is essential for spermatogonial survival and spermatogenesis. *Sexual Development* **6** 169–177.

**de Rooij DG** (1998) Stem cells in the testis. *International Journal of Experimental Pathology* **79** 67–80.

**de Rooij DG, Okabe M and Nishimune Y** (1999) Arrest of spermatogonial differentiation in jsd/jsd, Sl17H/Sl17H, and cryptorchid mice. *Biology of Reproduction* **61** 842–847.

**de Rooij DG** (2001a) Proliferation and differentiation of spermatogonial stem cells. *Reproduction* **121** 347–354.

**de Rooij DG** (2001b) Review proliferation and differentiation of spermatogonial stem cells. *Reproduction* **121** 347–354.

**de Rooij DG** (2009) The spermatogonial stem cell niche. *Microscopy Research & Technique* **72** 580–585.

**de Rooij DG and Russell LD** (2000) All you wanted to know about spermatogonia but were afraid to ask. *Journal of Andrology* **6512** 776–798.

**Roosen-Runge EC and Leik J** (1968) Gonocyte degeneration in the postnatal male rat. *American Journal of Anatomy* **122** 275–299.

**Rosenfeld CS, Ganjam VK, Taylor JA, Yuan X, Stiehr JR, Hardy MP and Lubahn DB** (1998) Transcription and translation of estrogen receptor-β in the male reproductive tract of estrogen receptor-α knock-out and wild-type mice. *Endocrinology* **139** 2982–2987.

**Rosselot C, Kierszenbaum AL, Rivkin E and Tres LL** (2003) Chronological gene expression of ADAMs during testicular development: Prespermatogonia (gonocytes) express fertilin beta (ADAM2). *Developmental Dynamics* **227** 458–467.

**Rudolfsson SH, Wikström P, Jonsson A, Collin O and Bergh A** (2004) Hormonal regulation and functional role of vascular endothelial growth factor a in the rat testis. *Biology of Reproduction* **77** 340–347.

**Russell LD** (1980) Sertoli-germ cell interrelations: A review. *Gamete Research* **3** 179–202.

**Russell LD** (1990) *Histological and Histopathological Evaluation of the Testis*. Cache River Press.

**Russell LD, Ettlin RA, Hikim APS and Clegg ED** (1993) Histological and histopathological evaluation of the testis. *International Journal of Andrology* **16** 83–83.

**Ruwanpura SM, McLachlan RI, Matthiesson KL and Meachem SJ** (2007) Gonadotrophins regulate germ cell survival, not proliferation, in normal adult men. *Human Reproduction* **23** 403–411.

**Ryu BY, Kubota H, Avarbock MR and Brinster RL** (2005) Conservation of spermatogonial stem cell self-renewal signaling between mouse and rat. *Proceedings of the National Academy of Sciences* **102** 14302–14307.

**Sabour D and Schöler HR** (2012) Reprogramming and the mammalian germline: The Weismann barrier revisited. *Current Opinion in Cell Biology* **24** 716–723.

**Sadri-Ardekani H, Mizrak SC, van Daalen SKM, Korver CM, Roepers-Gajadien HL, Koruji M, Hovingh S, de Reijke TM, de la Rosette JJMCH, van der Veen F *et al.*** (2009) Propagation of human spermatogonial stem cells *in vitro*. *The Journal of the American Medical Association* **302** 2127.

**van Saen D, Goossens E, Bourgain C, Ferster A and Tournaye H** (2011) Meiotic activity in orthotopic xenografts derived from human postpubertal testicular tissue. *Human Reproduction* **26** 282–293.

**Saga Y** (2008) Mouse germ cell development during embryogenesis. *Current Opinion in Genetics & Development* **18** 337–341.

**Sahare M, Otomo A, Komatsu K, Minami N, Yamada M and Imai H** (2015) The role of signaling pathways on proliferation and self-renewal of cultured bovine primitive germ cells. *Reproductive Medicine & Biology* **14** 17–25.

**Sahare M, Kim SM, Otomo A, Komatsu K, Minami N, Yamada M and Imai H** (2016) Factors supporting long-term culture of bovine male germ cells. *Reproduction, Fertility & Development* **28** 2039–2050.

**Saito K, O'Donnell L, McLachlan RI and Robertson DM** (2000) Spermiation failure is a major contributor to early spermatogenic suppression caused by hormone withdrawal in adult rats. *Endocrinology* **141** 2779–2785.

**Saitou M** (2009) Germ cell specification in mice. *Current Opinion in Genetics & Development* **19** 386–395.

**Saitou M and Yamaji M** (2012) Primordial germ cells in mice. *Cold Spring Harbor Perspectives in Biology* **4** a008375.

**Samarut E and Rochette-Egly C** (2012) Nuclear retinoic acid receptors: Conductors of the retinoic acid symphony during development. *Molecular & Cellular Endocrinology* **348** 348–360.

**Sato Y, Nozawa S, Yoshiike M, Arai M, Sasaki C and Iwamoto T** (2010) Xenografting of testicular tissue from an infant human donor results in accelerated testicular maturation. *Human Reproduction* **25** 1113–1122.

**Sato T, Katagiri K, Gohbara A, Inoue K, Ogonuki N, Ogura A, Kubota Y and Ogawa T** (2011a) *In vitro* production of functional sperm in cultured neonatal mouse testes. *Nature* **471** 504–507.

**Sato T, Katagiri K, Yokonishi T, Kubota Y, Inoue K, Ogonuki N, Matoba S, Ogura A and Ogawa T** (2011b) *In vitro* production of fertile sperm from murine spermatogonial stem cell lines. *Nature Communications* **2** 472.

**Sato T, Yokonishi T, Komeya M, Katagiri K, Kubota Y, Matoba S, Ogonuki N, Ogura A, Yoshida S and Ogawa T** (2012) Testis tissue explantation cures spermatogenic failure in c-Kit ligand mutant mice. *Proceedings of the National Academy of Sciences of the United States of America* **109** 16934–16938.

**Sato T, Katagiri K, Kojima K, Komeya M, Yao M and Ogawa T** (2015) *In vitro* spermatogenesis in explanted adult mouse testis tissues. *PLOS ONE* **10** e0130171.

**Schlatt S, Kim SS and Gosden R** (2002a) Spermatogenesis and steroidogenesis in mouse, hamster and monkey testicular tissue after cryopreservation and heterotopic grafting to castrated hosts. *Reproduction* **124** 339–346.

**Schlatt S, Honaramooz A, Boiani M, Schöler HR and Dobrinski I** (2002b) Progeny from sperm obtained after ectopic grafting of neonatal mouse testes. *Biology of Reproduction* **68** 2331–2335.

**Schlatt S, Honaramooz A, Ehmcke J, Goebell PJ, Rübben H, Dhir R, Dobrinski I and Patrizio P** (2006) Limited survival of adult human testicular tissue as ectopic xenograft. *Human Reproduction* **21** 384–389.

**Schlatt S, Gassei K, Westernströer B and Ehmcke J** (2010) Modulating testicular mass in xenografting: A model to explore testis development and endocrine function. *Endocrinology* **151** 4018–4023.

**Schmahl J, Eicher EM, Washburn LL and Capel B** (2000) Sry induces cell proliferation in the mouse gonad. *Development* **127** 65–73.

**Schmidt JA, de Avila JM and McLean DJ** (2006a) Grafting period and donor age affect the potential for spermatogenesis in bovine ectopic testis xenografts. *Biology of Reproduction* **75** 160–166.

**Schmidt JA, de Avila JM and McLean DJ** (2006b) Effect of vascular endothelial growth factor and testis tissue culture on spermatogenesis in bovine ectopic testis tissue xenografts. *Biology of Reproduction* **75** 167–175.

**Schmidt JA, deAvila JM de and McLean DJ** (2007) Analysis of gene expression in bovine testis tissue prior to ectopic testis tissue xenografting and during the grafting period. *Biology of Reproduction* **76** 1071–1080.

**Schneider EL and Fowlkes BJ** (1976) Measurement of DNA content and cell volume in senescent human fibroblasts utilizing flow multiparameter single cell analysis. *Experimental Cell Research* **98** 298–302.

**Schneider EL and Mitsui Y** (1976) The relationship between *in vitro* cellular aging and *in vivo* human age. *Proceedings of the National Academy of Sciences of the United States of America* **73** 3584–3588.

**Schnell SA, Staines WA and Wessendorf MW** (1999) Reduction of lipofuscin-like autofluorescence in fluorescently labeled tissue. *Journal of Histochemistry & Cytochemistry* **47** 719–730.

**Schöne M, Männicke N, Somerson JS, Marquaß B, Henkelmann R, Aigner T, Raum K and Schulz RM** (2016) 3D ultrasound biomicroscopy for assessment of cartilage repair tissue: Volumetric characterisation and correlation to established classification systems. *European Cells & Materials* **31** 119–135.

**Schrader M, Heicappell R, Müller M, Straub B and Miller K** (2001) Impact of chemotherapy on male fertility. *Oncology Research & Treatment* **24** 326–330.

**Schrans-Stassen BHGJ, van de Kant HJG, de Rooij DG and van Pelt AMM** (1999) Differential expression of c-kit in mouse undifferentiated and differentiating type A Spermatogonia. *Endocrinology* **140** 5894–5900.

**Schulze C** (1984) Sertoli Cells and Leydig Cells in Man. *Advances in Anatomy, Embryology & Cell Biology* **88** 1–104.

**Seandel M, James D, Shmelkov S V, Falciatori I, Kim J, Chavala S, Scherr DS, Zhang F, Torres R, Gale NW *et al.*** (2007) Generation of functional multipotent adult stem cells from GPR125+ germline progenitors. *Nature* **449** 346–350.

**Sekido R, Bar I, Narváez V, Penny G and Lovell-Badge R** (2004) SOX9 is up-regulated by the transient expression of SRY specifically in Sertoli cell precursors. *Developmental Biology* **274** 271–279.

**Seok J, Warren HS, Cuenca AG, Mindrinos MN, Baker H V, Xu W, Richards DR, McDonald-Smith GP, Gao H, Hennessy L *et al.*** (2013) Genomic responses in mouse models poorly mimic human inflammatory diseases. *Proceedings of the National Academy of Sciences of the United States of America* **110** 3507–3512.

**Setchell BP** (1990) The testis and tissue transplantation: Historical aspects. *Journal of Reproductive Immunology* **18** 1–8.

**Setchell B, Maddocks S and Brooks DE** (1994) Anatomy, vasculature, innervation, and fluids of the male reproductive tract. In *The Physiology of Reproduction* (Eds Knobil and Neill JD), pp 1063–1175. Raven Press, New York.

**Shalaby F, Rossant J, Yamaguchi TP, Gertsenstein M, Wu XF, Breitman ML and Schuh AC** (1995) Failure of blood-island formation and vasculogenesis in Flk-1-deficient mice. *Nature* **376** 62–66.

**Shen MM, Skoda RC, Cardiff RD, Campos-Torres J, Leder P and Ornitz DM** (1994) Expression of LIF in transgenic mice results in altered thymic epithelium and apparent interconversion of thymic and lymph node morphologies. *The EMBO Journal* **13** 1375–85.

**Shen ZP, Brayman AA, Chen L and Miao CH** (2008) Ultrasound with microbubbles enhances gene expression of plasmid DNA in the liver via intraportal delivery. *Gene Therapy* **15** 1147–1155.

**Shinohara T, Avarbock MR and Brinster RL** (1999) Beta1- and alpha6-integrin are surface markers on mouse spermatogonial stem cells. *Proceedings of the National Academy of Sciences of the United States of America* **96** 5504–5509.

**Shinohara T, Avarbock MR and Brinster RL** (2000a) Functional analysis of spermatogonial stem cells in steel and cryptorchid infertile mouse models. *Developmental Biology* **220** 401–411.

**Shinohara T, Orwig KE, Avarbock MR and Brinster RL** (2000b) Spermatogonial stem cell enrichment by multiparameter selection of mouse testis cells. *Proceedings of the National Academy of Sciences of the United States of America* **97** 8346–8351.

**Shinohara T, Orwig KE, Avarbock MR and Brinster RL** (2001) Remodeling of the postnatal mouse testis is accompanied by dramatic changes in stem cell number and niche accessibility. *Proceedings of the National Academy of Sciences* **98** 6186–6191.

**Shinohara T, Inoue K, Ogonuki N, Kanatsu-Shinohara M, Miki H, Nakata K, Kurome M, Nagashima H, Toyokuni S, Kogishi K *et al.*** (2002) Birth of offspring following transplantation of cryopreserved immature testicular pieces and *in-vitro* microinsemination. *Human Reproduction* **17** 3039–3045.

**Shweiki D, Itin A, Soffer D and Keshet E** (1992) Vascular endothelial growth factor induced by hypoxia may mediate hypoxia-initiated angiogenesis. *Nature* **359** 843–845.

**Simon L, Ekman GC, Tyagi G, Hess RA, Murphy KM and Cooke PS** (2007) Common and distinct factors regulate expression of mRNA for ETV5 and GDNF, Sertoli cell proteins essential for spermatogonial stem cell maintenance. *Experimental Cell Research* **313** 3090–3099.

**Simon L, Hess RA and Cooke PS** (2010) Spermatogonial stem cells, *in vivo* transdifferentiation and human regenerative medicine. *Expert Opinion on Biological Therapy* **10** 519–530.

**Simorangkir DR, Ramaswamy S, Marshall GR, Pohl CR and Plant TM** (2009) A selective monotropic elevation of FSH, but not that of LH, amplifies the proliferation and differentiation of spermatogonia in the adult rhesus monkey (Macaca mulatta). *Human Reproduction* **24** 1584–1595.

**Sinclair AH, Berta P, Palmer MS, Hawkins JR, Griffiths BL, Smith MJ, Foster JW, Frischauf AM, Lovell-Badge R and Goodfellow PN** (1990) A gene from the human sex-determining region encodes a protein with homology to a conserved DNA-binding motif. *Nature* **346** 240–244.

**Singh J, O'Neill C and Handelsman DJ** (1995) Induction of spermatogenesis by androgens in gonadotropin-deficient (hpg) mice. *Endocrinology* **136** 5311–5321.

**Siu MKY and Cheng CY** (2004a) Dynamic cross-talk between cells and the extracellular matrix in the testis. *BioEssays* **26** 978–992.

**Siu MKY and Cheng CY** (2004b) Interactions of proteases, protease inhibitors, and the β1 Integrin/Laminin γ3 protein complex in the regulation of ectoplasmic specialization dynamics in the rat testis. *Biology of Reproduction* **70** 945–964.

**Skakkebaek NE, Jensen G, Povlsen CO and Rygaard J** (1974) Heterotransplantation of human foetal testicular and ovarian tissue to the mouse mutant nude. A preliminary study. *Acta Obstetricia et Gynecologica Scandinavica. Supplement* **29** 73–75.

**Skakkebaek NE, Berthelsen JG, Giwercman A and Müller J** (1987) Carcinoma-in-situ of the testis: Possible origin from gonocytes and precursor of all types of germ cell tumours except spermatocytoma. *International Journal of Andrology* **10** 19–28.

**Skinner MK, McLachlan RI and Bremner WJ** (1989) Stimulation of Sertoli cell inhibin secretion by the testicular paracrine factor PModS. *Molecular & Cellular Endocrinology* **66** 239–249.

**Smith AG, Heath JK, Donaldson DD, Wong GG, Moreau J, Stahl M and Rogers D** (1988) Inhibition of pluripotential embryonic stem cell differentiation by purified polypeptides. *Nature* **336** 688–690.

**Snedaker AK, Honaramooz A and Dobrinski I** (2004) A game of cat and mouse: Xenografting of testis tissue from domestic kittens results in complete cat spermatogenesis in a mouse host. *Journal of Andrology* **25** 926–930.

**Söder O** (2007) Sexual dimorphism of gonadal development. *Best Practice and Research Clinical Endocrinology & Metabolism* **21** 381–391.

**Sordoillet C, Chauvin MA, de Peretti E, Morera AM and Benahmed M** (1991) Epidermal growth factor directly stimulates steroidogenesis in primary cultures of porcine Leydig cells: actions and sites of action. *Endocrinology* **128** 2160–2168.

**Sordoillet C, Savona C, Chauvin MA, de Peretti E, Feige JJ, Morera AM and Benahmed M** (1992) Basic fibroblast growth factor enhances testosterone secretion in cultured porcine Leydig cells: Site(s) of action. *Molecular & Cellular Endocrinology* **89** 163–171.

**Sousa M, Cremades N, Alves C, Silva J and Barros A** (2002) Developmental potential of human spermatogenic cells co-cultured with Sertoli cells. *Human Reproduction***17** 161–172.

**Spiller CM, Wilhelm D and Koopman P** (2010) Retinoblastoma 1 protein modulates XY Germ cell entry into G1/G0 arrest during fetal development in mice. *Biology of Reproduction* **82** 433–443.

**Sprengel R, Braun T, Nikolics K, Segaloff DL and Seeburg PH** (1990) The testicular receptor for follicle stimulating hormone: Structure and functional expression of cloned cDNA. *Molecular Endocrinology* **4** 525–530.

**Springer ML, Sievers RE, Viswanathan MN, Yee MS, Foster E, Grossman W and Yeghiazarians Y** (2005) Closed-chest cell injections into mouse myocardium guided by high-resolution echocardiography. *American Journal of Physiology. Heart and Circulatory Physiology* **289** H1307–H1314.

**Spurney CF, Lo CW and Leatherbury L** (2006) Fetal mouse imaging using echocardiography: A review of current technology. *Echocardiograph* **23** 891–899.

**Stevens LC** (1984) Spontaneous and experimentally induced testicular teratomas in mice. *Cell Differentiation* **15** 69–74.

**Stewart CL, Gadi I and Bhatt H** (1994) Stem cells from primordial germ cells can reenter the germ line. *Developmental Biology* **161** 626–628.

**Stockwell S, Herrid M, Davey R, Brownlee A, Hutton K and Hill JR** (2009) Microsatellite detection of donor-derived sperm DNA following germ cell transplantation in cattle. *Reproduction, Fertility & Development* **21** 462–468.

**Stubbs SC, Hargreave TB and Habib FK** (1990) Localization and characterization of epidermal growth factor receptors on human testicular tissue by biochemical and immunohistochemical techniques. *The Journal of Endocrinology* **125** 485–492.

**Stukenborg JB, Wistuba J, Luetjens CM, Elhija MA, Huleihel M, Lunenfeld E, Gromoll J, Nieschlag E and Schlatt S** (2008) Coculture of spermatogonia with somatic cells in a novel three-dimensional soft-agar-culture-system. *Journal of Andrology* **29** 312–329.

**Suarez-Quain CA and Niklinski W** (1990) Immunocytochemical localization of the epidermal growth factor receptor in mouse testis. *Biology of Reproduction* **43** 1087–1097.

**Suarez-Quian CA, Oke BO and Radhakrishnan B** (1994) Relationship between submandibular gland epidermal growth factor and spermatogenesis in C3H mice. *Tissue & Cell* **26** 285–298.

**Sun X, Meyers EN, Lewandoski M and Martin GR** (1999) Targeted disruption of Fgf8 causes failure of cell migration in the gastrulating mouse embryo. *Genes & Development* **13** 1834–1846.

**Suzuki S and Sato K** (2003) The fertilising ability of spermatogenic cells derived from cultured mouse immature testicular tissue. *Zygote* **11** 307–316.

**Suzuki H, Sada A, Yoshida S and Saga Y** (2009) The heterogeneity of spermatogonia is revealed by their topology and expression of marker proteins including the germ cell-specific proteins Nanos2 and Nanos3. *Developmental Biology* **336** 222–231.

**Svingen T and Koopman P** (2013) Building the mammalian testis: Origins, differentiation, and assembly of the component cell populations. *Genes & Development* **27** 2409–2426.

**Swindle MM, Makin A, Herron AJ, Clubb FJ and Frazier KS** (2012) Swine as models in biomedical research and toxicology testing. *Veterinary Pathology* **49** 344–356.

**Tadokoro Y, Yomogida K, Ohta H, Tohda A and Nishimune Y** (2002) Homeostatic regulation of germinal stem cell proliferation by the GDNF/FSH pathway. *Mechanisms of Development* **113** 29–39.

**Takahashi K and Yamanaka S** (2006) Induction of pluripotent stem cells from mouse embryonic and adult fibroblast cultures by defined factors. *Cell* **126** 663–676.

**Takahashi K, Tanabe K, Ohnuki M, Narita M, Ichisaka T, Tomoda K and Yamanaka S** (2007) Induction of pluripotent stem cells from adult human fibroblasts by defined factors. *Cell* **131** 861–872.

**Takashima Y, Guo G, Loos R, Nichols J, Ficz G, Krueger F, Oxley D, Santos F, Clarke J, Mansfield W *et al.*** (2014) Resetting transcription factor control circuitry toward ground-state pluripotency in human. *Cell* **158** 1254–1269.

**Takeuchi Y, Yoshizaki G and Takeuchi T** (2003) Generation of live fry from intraperitoneally transplanted primordial germ cells in rainbow trout. *Biology of Reproduction* **69** 1142–1149.

**Tam PP and Snow MH** (1981) Proliferation and migration of primordial germ cells during compensatory growth in mouse embryos. *Journal of Embryology & Experimental Morphology* **64** 133–147.

**Tanaka SS and Nishinakamura R** (2014) Regulation of male sex determination: Genital ridge formation and Sry activation in mice. *Cellular & Molecular Life Sciences* **71** 4781–4802.

**Tanaka T, Kanatsu-Shinohara M, Hirose M, Ogura A and Shinohara T** (2015) Pluripotent cell derivation from male germline cells by suppression of Dmrt1 and Trp53. *Journal of Reproduction & Development* **61** 473–484.

**Tang DD and Gerlach BD** (2017) The roles and regulation of the actin cytoskeleton, intermediate filaments and microtubules in smooth muscle cell migration. *Respiratory Research* **18** 54.

**Taub M, Wang Y, Szczesny TM and Kleinman HK** (1990) Epidermal growth factor or transforming growth factor alpha is required for kidney tubulogenesis in matrigel cultures in serum-free medium. *Proceedings of the National Academy of Sciences of the United States of America* **87** 4002–4006.

**Tegelenbosch RA and de Rooij DG** (1993) A quantitative study of spermatogonial multiplication and stem cell renewal in the C3H/101 F1 hybrid mouse. *Mutation Research* **290** 193–200.

**Tesarik J, Greco E, Rienzi L, Ubaldi F, Guido M, Cohen-Bacrie P and Mendoza C** (1998) Differentiation of spermatogenic cells during in-vitro culture of testicular biopsy samples from patients with obstructive azoospermia: Effect of recombinant follicle stimulating hormone. *Human Reproduction* **13** 2772–2781.

**Tesarik J, Bahceci M, Özcan C, Greco E and Mendoza C** (1999) Restoration of fertility by *in-vitro* spermatogenesis. *The Lancet* **353** 555–556.

**Theodosiou M, Laudet V and Schubert M** (2010) From carrot to clinic: An overview of the retinoic acid signaling pathway. *Cellular & Molecular Life Sciences* **67** 1423–1445.

**Thomson JA, Itskovitz-Eldor J, Shapiro SS, Waknitz MA, Swiergiel JJ, Marshall VS and Jones JM** (1998) Embryonic stem cell lines derived from human blastocysts. *Science* **282** 1145–1147.

**Thuillier R, Wang Y and Culty M** (2003) Prenatal exposure to estrogenic compounds alters the expression pattern of platelet-derived growth factor receptors α and β in neonatal rat testis: Identification of gonocytes as targets of estrogen exposure. *Biology of Reproduction* **68** 867–880.

**Tilgner K, Atkinson SP, Golebiewska A, Stojković M, Lako M and Armstrong L** (2008) Isolation of primordial germ cells from differentiating human embryonic stem cells. *Stem Cells* **26** 3075–3085.

**Tiptanavattana N, Radtanakatikanon A, Hyttel P, Holm H, Buranapraditkun S, Setthawong P, Techakumphu M and Tharasanit T** (2015) Determination phase at transition of gonocytes to spermatogonial stem cells improves establishment efficiency of spermatogonial stem cells in domestic cats. *Journal of Reproduction & Development* **61** 581–588.

**Toda K, Okada T, Takeda K, Akira S, Saibara T, Shiraishi M, Onishi S and Shizuta Y** (2001) Oestrogen at the neonatal stage is critical for the reproductive ability of male mice as revealed by supplementation with 17-oestradiol to aromatase gene (Cyp19) knockout mice. *Journal of Endocrinology* **168** 455–463.

**Tong MH, Mitchell D, Evanoff R and Griswold MD** (2011) Expression of Mirlet7 family microRNAs in response to retinoic acid-induced spermatogonial differentiation in mice. *Biology of Reproduction* **85** 189–197.

**Töyräs J, Laasanen MS, Saarakkala S, Lammi MJ, Rieppo J, Kurkijärvi J, Lappalainen R and Jurvelin JS** (2003) Speed of sound in normal and degenerated bovine articular cartilage. *Ultrasound in Medicine & Biology* **29** 447–454.

**Trautmann E, Guerquin MJ, Duquenne C, Lahaye JB, Habert R and Livera G** (2008) Retinoic acid prevents germ cell mitotic arrest in mouse fetal testes. *Cell Cycle* **7** 656–664.

**Trefil P, Micáková A, Mucksová J, Hejnar J, Poplstein M, Bakst MR, Kalina J and Brillard JP** (2006) Restoration of spermatogenesis and male fertility by transplantation of dispersed testicular cells in the chicken. *Biology of Reproduction* **75** 575–581.

**Trefil P, Bakst MR, Yan H, Hejnar J, Kalina J and Mucksová J** (2010) Restoration of spermatogenesis after transplantation of c-Kit positive testicular cells in the fowl. *Theriogenology* **74** 1670–1676.

**Tsutsumi O, Kurachi H and Oka T** (1986) A physiological role of epidermal growth factor in male reproductive function. *Science* **233** 975–977.

**Tu J, Fan L, Tao K, Zhu W, Li J and Lu G** (2007) Stem cell factor affects fate determination of human gonocytes *in vitro*. *Reproduction* **134** 757–765.

**Tumbleson ME and Schook LB** (1996) *Advances in Swine in Biomedical Research : Volume 2*. Boston, MA: Springer US.

**Turner RM, Rathi R, Honaramooz A, Zeng W and Dobrinski I** (2010) Xenografting restores spermatogenesis to cryptorchid testicular tissue but does not rescue the phenotype of idiopathic testicular degeneration in the horse ( *Equus caballus* ). *Reproduction, Fertility & Development* **22** 673-683.

**Tzouanas SN, Ekenseair AK, Kasper FK and Mikos AG** (2014) Mesenchymal stem cell and gelatin microparticle encapsulation in thermally and chemically gelling injectable hydrogels for tissue engineering. *Journal of Biomedical Materials Research - Part A* **102** 1222–1230.

**Unni SK, Modi DN, Pathak SG, Dhabalia J V and Bhartiya D** (2009) Stage-specific localization and expression of c-kit in the adult human testis. *The Journal of Histochemistry & Cytochemistry* **57** 861–869.

**Valli H, Sukhwani M, Dovey SL, Peters KA, Donohue J, Castro CA, Chu T, Marshall GR and Orwig KE** (2014) Fluorescence- and magnetic-activated cell sorting strategies to isolate and enrich human spermatogonial stem cells. *Fertility & Sterility* **102** 566–580.

**Valve E, Penttilä TL, Paranko J and Härkönen P** (1997) FGF-8 is expressed during specific phases of rodent oocyte and spermatogonium development. *Biochemical & Biophysical Research Communications* **232** 173–177.

**Vergouwen RP, Jacobs SG, Huiskamp R, Davids JA and de Rooij DG** (1991) Proliferative activity of gonocytes, Sertoli cells and interstitial cells during testicular development in mice. *Journal of Reproduction & Fertility* **93** 233–243.

**Vergouwen RP, Huiskamp R, Bas RJ, Roepers-Gajadien HL, Davids JA and de Rooij DG** (1993) Postnatal development of testicular cell populations in mice. *Journal of Reproduction & Fertility* **99** 479–485.

**Vernet N, Dennefeld C, Rochette-Egly C, Oulad-Abdelghani M, Chambon P, Ghyselinck NB and Mark M** (2006) Retinoic acid metabolism and signaling pathways in the adult and developing mouse testis. *Endocrinology* **147** 96–110.

**Vidal VPI, Chaboissier M-C, de Rooij DG and Schedl A** (2001) Sox9 induces testis development in XX transgenic mice. *Nature Genetics* **28** 216–217.

**Vigier M, Weiss M, Perrard MH, Godet M and Durand P** (2004) The effects of FSH and of testosterone on the completion of meiosis and the very early steps of spermiogenesis of the rat: An *in vitro* study. *Journal of Molecular Endocrinology* **33** 729–742.

**Viglietto G, Dolci S, Bruni P, Baldassarre G, Chiariotti L, Melillo RM, Salvatore G, Chiappetta G, Sferratore F, Fusco A *et al.*** (2000) Glial cell line-derived neutrotrophic factor and neurturin can act as paracrine growth factors stimulating DNA synthesis of Ret-expressing spermatogonia. *International Journal of Oncology* **16** 689–694.

**Vigueras-Villaseñor RM, Moreno-Mendoza NA, Reyes-Torres G, Molina-Ortiz D, León MC and Rojas-Castañeda JC** (2006) The effect of estrogen on testicular gonocyte maturation. *Reproductive Toxicology* **22** 513–520.

**Wahab-Wahlgren A, Martinelle N, Holst M, Jahnukainen K, Parvinen M and Söder O** (2003) EGF stimulates rat spermatogonial DNA synthesis in seminiferous tubule segments *in vitro*. *Molecular & Cellular Endocrinology* **201** 39–46.

**Walczak-Jedrzejowska R, Kula K, Oszukowska E, Marchlewska K, Kula W and Slowikowska-Hilczer J** (2011) Testosterone and oestradiol in concert protect seminiferous tubule maturation against inhibition by GnRH-antagonist. *International Journal of Andrology* **34** e378–e385.

**Wang Y and Culty M** (2007) Identification and distribution of a novel platelet-derived growth factor receptor β Variant: Effect of retinoic acid and involvement in cell differentiation. *Endocrinology* **148** 2233–2250.

**Wang JL, Swartz-Basile DA, Rubin DC and Levin MS** (1997) Retinoic acid stimulates early cellular proliferation in the adapting remnant rat small intestine after partial resection. *The Journal of Nutrition* **127** 1297–1303.

**Wang Y, Thuillier R and Culty M** (2004) Prenatal estrogen exposure differentially affects estrogen receptor-associated proteins in rat testis gonocytes. *Biology of Reproduction* **71** 1652–1664.

**Wang J, Cao H, Xue X, Fan C, Fang F, Zhou J, Zhang Y and Zhang X** (2014) Effect of vitamin C on growth of caprine spermatogonial stem cells *in vitro*. *Theriogenology* **81** 545–555.

**Wang X, Chen T, Zhang Y, Li B, Xu Q and Song C** (2015) Isolation and culture of pig spermatogonial stem cells and their *in vitro* differentiation into neuron-like cells and adipocytes. *International Journal of Molecular Sciences* **16** 26333–26346.

**Wang H, Xiang J, Zhang W, Li J, Wei Q, Zhong L, Ouyang H and Han J** (2016a) Induction of germ cell-like cells from porcine induced pluripotent stem cells. *Scientific Reports* **6** 27256.

**Wang S, Wang X, Ma L, Lin X, Zhang D, Li Z, Wu Y, Zheng C, Feng X, Liao S *et al.*** (2016b) Retinoic acid is sufficient for the *in vitro* induction of mouse spermatocytes. *Stem Cell Reports* **7** 80–94.

**Watanabe T, Hayashi H, Kita K, Kubota Y and Ogawa T** (2009) Ectopic porcine spermatogenesis in murine subcutis: Tissue grafting versus cell-injection methods. *Asian Journal of Andrology* **11** 317–323.

**Waterston RH, Lindblad-Toh K, Birney E, Rogers J, Abril JF, Agarwal P, Agarwala R, Ainscough R, Alexandersson M, An P *et al.*** (2002) Initial sequencing and comparative analysis of the mouse genome. *Nature* **420** 520–562.

**van der Wee K and Hofmann MC** (1999) An *in vitro* tubule assay identifies hgf as a morphogen for the formation of seminiferous tubules in the postnatal mouse testis. *Experimental Cell Research* **252** 175–185.

**Weinbauer GF, Luetjens CM, Simoni M and Nieschlag E** (2010) Physiology of testicular function. In *Andrology: Male Reproductive Health and Dysfunction*, pp 11–59. Berlin, Heidelberg: Springer Berlin Heidelberg.

**Welsh M, Saunders PTK, Atanassova N, Sharpe RM and Smith LB** (2009) Androgen action *via* testicular peritubular myoid cells is essential for male fertility. *The FASEB Journal* **23** 4218–4230.

**Wernig M, Meissner A, Foreman R, Brambrink T, Ku M, Hochedlinger K, Bernstein BE and Jaenisch R** (2007) *In vitro* reprogramming of fibroblasts into a pluripotent ES-cell-like state. *Nature* **448** 318–324.

**Western PS, Miles DC, van den Bergen JA, Burton M and Sinclair AH** (2008) Dynamic regulation of mitotic arrest in fetal male germ cells. *Stem Cells* **26** 339–347.

**White JC, Highland M, Kaiser M and Clagett-Dame M** (2000) Vitamin A deficiency results in the dose-dependent acquisition of anterior character and shortening of the caudal hindbrain of the rat embryo. *Developmental Biology* **220** 263–284.

**Wilhelm D and Englert C** (2002) The Wilms tumor suppressor WT1 regulates early gonad development by activation of Sf1. *Genes & Development* **16** 1839–1851.

**Wilhelm D, Martinson F, Bradford S, Wilson MJ, Combes AN, Beverdam A, Bowles J, Mizusaki H and Koopman P** (2005) Sertoli cell differentiation is induced both cell-autonomously and through prostaglandin signaling during mammalian sex determination. *Developmental Biology* **287** 111–124.

**Willerton L, Smith RA, Russell D and Mackay S** (2004) Effects of FGF9 on embryonic Sertoli cell proliferation and testicular cord formation in the mouse. *The International Journal of Developmental Biology* **48** 637–643.

**Wing TY and Christensen AK** (1982) Morphometric studies on rat seminiferous tubules. *The American Journal of Anatomy* **165** 13–25.

**Wreford NG, Rajendra Kumar T, Matzuk MM and de Kretser DM** (2001) Analysis of the testicular phenotype of the follicle-stimulating hormone beta-subunit knockout and the activin type II receptor knockout mice by stereological analysis. *Endocrinology* **142** 2916–2920.

**Wu Z, Templeman JL, Smith RA and Mackay S** (2005) Effects of glial cell line-derived neurotrophic factor on isolated developing mouse Sertoli cells *in vitro*. *Journal of Anatomy* **206** 175–184.

**Wu X, Schmidt JA, Avarbock MR, Tobias JW, Carlson CA, Kolon TF, Ginsberg JP and Brinster RL** (2009) Prepubertal human spermatogonia and mouse gonocytes share conserved gene expression of germline stem cell regulatory molecules. *Proceedings of the National Academy of Sciences* **106** 21672–21677.

**Wu X, Goodyear SM, Tobias JW, Avarbock MR and Brinster RL** (2011) Spermatogonial stem cell self-renewal requires ETV5-mediated downstream activation of Brachyury in mice. *Biology of Reproduction* **85** 1114–1123.

**Wu J, Song W, Zhu H, Niu Z, Mu H, Lei A, Yang C, Peng S, Li X, Li G *et al.*** (2013) Enrichment and characterization of Thy1-positive male germline stem cells (mGSCs) from dairy goat (*Capra hircus*) testis using magnetic microbeads. *Theriogenology* **80** 1052–1060.

**Würbel H** (2001) Ideal homes? Housing effects on rodent brain and behaviour. *Trends in Neurosciences* **24** 207–211.

**Wylie C** (1999) Germ cells. *Cell* **96** 165–174.

**Wyns C, Curaba M, Martinez-Madrid B, Van Langendonckt A, François-Xavier W and Donnez J** (2007) Spermatogonial survival after cryopreservation and short-term orthotopic immature human cryptorchid testicular tissue grafting to immunodeficient mice. *Human Reproduction* **22** 1603–1611.

**Wyns C, Van Langendonckt A, Wese FX, Donnez J and Curaba M** (2008) Long-term spermatogonial survival in cryopreserved and xenografted immature human testicular tissue. *Human Reproduction* **23** 2402–2414.

**Wyns C, Curaba M, Petit S, Vanabelle B, Laurent P, Wese JFX and Donnez J** (2011) Management of fertility preservation in prepubertal patients: 5 years' experience at the Catholic University of Louvain. *Human Reproduction* **26** 737–747.

**Xia Y, Prawirasatya M, Heng BC, Boey F and Venkatraman SS** (2011) Seeding density matters: Extensive intercellular contact masks the surface dependence of endothelial cell-biomaterial interactions. *Journal of Materials Science: Materials in Medicine* **22** 389–396.

**Xie B, Qin Z, Huang B, Xie T, Yao H, Wei Y, Yang X, Shi D and Jiang H** (2010) *In vitro* culture and differentiation of buffalo (Bubalus bubalis) spermatogonia. *Reproduction in Domestic Animals* **45** 275–282.

**Yabuta Y, Kurimoto K, Ohinata Y, Seki Y and Saitou M** (2006) Gene expression dynamics during germline specification in mice identified by quantitative single-cell gene expression profiling. *Biology of Reproduction* **75** 705–716.

**Yamaguchi S, Kimura H, Tada M, Nakatsuji N and Tada T** (2005) Nanog expression in mouse germ cell development. *Gene Expression Patterns* **5** 639–646.

**Yamamoto H, Ochiya T, Tamamushi S, Toriyama-Baba H, Takahama Y, Hirai K, Sasaki H, Sakamoto H, Saito I, Iwamoto T *et al.*** (2002) HST-1/FGF-4 gene activation induces spermatogenesis and prevents adriamycin-induced testicular toxicity. *Oncogene* **21** 899–908.

**Yamanaka S and Blau HM** (2010) Nuclear reprogramming to a pluripotent state by three approaches. *Nature* **465** 704–712.

**Yan YC, Sun YP, Zhang ML and Koide SS** (1998) Testis epidermal growth factor and spermatogenesis. *Archives of Andrology* **40** 133–146.

**Yan W, Suominen J and Toppari J** (2000a) Stem cell factor protects germ cells from apoptosis *in vitro*. *Journal of Cell Science* **113** 161–168.

**Yan W, Kero J, Huhtaniemi I and Toppari J** (2000b) Stem cell factor functions as a survival factor for mature leydig cells and a growth factor for precursor leydig cells after ethylene dimethane sulfonate treatment: Implication of a role of the stem cell factor/c-Kit system in Leydig cell development. *Developmental Biology* **227** 169–182.

**Yang Y and Han C** (2010) GDNF stimulates the proliferation of cultured mouse immature Sertoli cells via its receptor subunit NCAM and ERK1/2 signaling pathway. *BMC Cell Biology* **11** 78.

**Yang Y and Honaramooz A** (2010) Effects of medium and hypothermic temperatures on preservation of isolated porcine testis cells. *Reproduction, Fertility & Development* **22** 523–532.

**Yang Y and Honaramooz A** (2011) Efficient purification of neonatal porcine gonocytes with Nycodenz and differential plating. *Reproduction, Fertility & Development* **23** 496–505.

**Yang Y and Honaramooz A** (2012) Characterization and quenching of autofluorescence in piglet testis tissue and cells. *Anatomy Research International* **2012** 1–10.

**Yang Y, Yarahmadi M and Honaramooz A** (2010) Development of novel strategies for the isolation of piglet testis cells with a high proportion of gonocytes. *Reproduction, Fertility & Development* **22** 1057–1065.

**Yang J, Dungrawala H, Hua H, Manukyan A, Abraham L, Lane W, Mead H, Wright J and Schneider BL** (2011) Cell size and growth rate are major determinants of replicative lifespan. *Cell Cycle* **10** 144–155.

**Yano H, Readhead C, Nakashima M, Ren SG and Melmed S** (1998) Pituitary-directed leukemia inhibitory factor transgene causes Cushing's Syndrome: Neuro-immune-endocrine modulation of pituitary development. *Molecular Endocrinology* **12** 1708–1720.

**Yao HHC, DiNapoli L and Capel B** (2003) Meiotic germ cells antagonize mesonephric cell migration and testis cord formation in mouse gonads. *Development* **130** 5895–5902.

**Yefimova MG, Messaddeq N, Harnois T, Meunier AC, Clarhaut J, Noblanc A, Weickert J-L, Cantereau A, Philippe M, Bourmeyster N *et al.*** (2013) A chimerical phagocytosis model reveals the recruitment by Sertoli cells of autophagy for the degradation of ingested illegitimate substrates. *Autophagy* **9** 653–666.

**Ying Y, Liu XM, Marble A, Lawson KA and Zhao GQ** (2000) Requirement of *Bmp8b* for the generation of primordial germ cells in the mouse. *Molecular Endocrinology* **14** 1053–1063.

**Yokonishi T, Sato T, Komeya M, Katagiri K, Kubota Y, Nakabayashi K, Hata K, Inoue K, Ogonuki N, Ogura A *et al.*** (2014) Offspring production with sperm grown *in vitro* from cryopreserved testis tissues. *Nature Communications* **5** 4320.

**Yomogida K, Yagura Y, Tadokoro Y and Nishimune Y** (2003) Dramatic expansion of germinal stem cells by ectopically expressed human glial cell line-derived neurotrophic factor in mouse sertoli cells. *Biology of Reproduction* **69** 1303–1307.

**Yoshida S** (2006) The first round of mouse spermatogenesis is a distinctive program that lacks the self-renewing spermatogonia stage. *Development* **133** 1495–1505.

**Yoshinaga K, Nishikawa S, Ogawa M, Hayashi S, Kunisada T, Fujimoto T and Nishikawa S** (1991) Role of c-kit in mouse spermatogenesis: Identification of spermatogonia as a specific site of c-kit expression and function. *Development* **113** 689–699.

**Yoshizaki G and Lee S** (2018) Production of live fish derived from frozen germ cells via germ cell transplantation. *Stem Cell Research* **29** 103–110.

**Yu ZH** (1998) Asymmetrical testicular weights in mammals, birds, reptiles and amphibia. *International Journal of Andrology* **21** 53–55.

**Yu X, Sidhu JS, Hong S and Faustman EM** Essential role of extracellular matrix (ECM) overlay in establishing the functional integrity of primary neonatal rat Sertoli cell/gonocyte co-cultures: An improved *in vitro* model for assessment of male reproductive toxicity.*Toxicological Sciences* **84** 378–393.

**Yu J, Cai ZM, Wan HJ, Zhang FT, Ye J, Fang JZ, Gui YT and Ye JX** (2006) Development of neonatal mouse and fetal human testicular tissue as ectopic grafts in immunodeficient mice. *Asian Journal of Andrology* **8** 393–403.

**Yu J, Vodyanik MA, Smuga-Otto K, Antosiewicz-Bourget J, Frane JL, Tian S, Nie J, Jonsdottir GA, Ruotti V, Stewart R *et al.*** (2007) Induced pluripotent stem cell lines derived from human somatic cells. *Science* **318** 1917–1920.

**Yu X, Hong S, Moreira EG and Faustman EM** (2009) Improving *in vitro* Sertoli cell/gonocyte co-culture model for assessing male reproductive toxicity: Lessons learned from comparisons of cytotoxicity versus genomic responses to phthalates. *Toxicology & Applied Pharmacology* **239** 325–336.

**Zadrag-Tecza R, Kwolek-Mirek M, Bartosz G and Bilinski T** (2009) Cell volume as a factor limiting the replicative lifespan of the yeast *Saccharomyces cerevisiae*. *Biogerontology* **10** 481–488.

**Zeng W, Avelar GF, Rathi R, Franca LR and Dobrinski I** (2006) The length of the spermatogenic cycle is conserved in porcine and ovine testis xenografts. *Journal of Andrology* **27** 527–533.

**Zeng W, Snedaker AK, Megee S, Rathi R, Chen F, Honaramooz A and Dobrinski I** (2009) Preservation and transplantation of porcine testis tissue. *Reproduction, Fertility & Development* **21** 489–497.

**Zeng W, Tang L, Bondareva A, Honaramooz A, Tanco V, Dores C, Megee S, Modelski M, Rodriguez-Sosa JR, Paczkowski M *et al.*** (2013) Viral transduction of male germline stem cells results in transgene transmission after germ cell transplantation in pigs. *Biology of Reproduction* **88** 27.

**Zhang ML, Chang Yan Y, Sun YP and Koide SS** (1997) Identification and expression of epidermal growth factor gene in mouse testis. *Cell Research* **7** 51–59.

**Zhang Z, Renfree MB and Short RV** (2003) Successful Intra- and interspecific male germ cell transplantation in the rat. *Biology of Reproduction* **68** 961–967.

**Zhang Z, Hill J, Holland M, Kurihara Y and Loveland KL** (2008) Bovine sertoli cells colonize and form tubules in murine hosts following transplantation and grafting procedures. *Journal of Andrology* **29** 418–430.

**Zhao GQ, Deng K, Labosky PA, Liaw L and Hogan BL** (1996) The gene encoding bone morphogenetic protein 8B is required for the initiation and maintenance of spermatogenesis in the mouse. *Genes & Development* **10** 1657–1669.

**Zheng Y, Tian X, Zhang Y, Qin J, An J and Zeng W** (2013) *In vitro* propagation of male germline stem cells from piglets. *Journal of Assisted Reproduction & Genetics* **30** 945–952.

**Zheng Y, He Y, An J, Qin J, Wang Y, Zhang Y, Tian X and Zeng W** (2014a) THY1 is a surface marker of porcine gonocytes. *Reproduction, Fertility & Development* **26** 533.

**Zheng Y, Zhang Y, Qu R, He Y, Tian X and Zeng W** (2014b) Spermatogonial stem cells from domestic animals: Progress and prospects. *Reproduction* **147** R65–R74.

**Zhou Q, Nie R, Li Y, Friel P, Mitchell D, Hess RA, Small C and Griswold MD** (2008) Expression of stimulated by retinoic acid gene 8 (Stra8) in spermatogenic cells induced by retinoic acid: An *in vivo* study in vitamin A-sufficient postnatal murine testes. *Biology of Reproduction* **79** 35–42.

**Zirkin BR, Awoniyi C, Griswold MD, Russel LD and Sharpeh R** (1994) Is FSH Required for Adult Spermatogenesis? *Journal of Andrology* **15** 273–276.

**Zogbi C, Tesser RB, Encinas G, Miraglia SM and Stumpp T** (2012) Gonocyte development in rats: Proliferation, distribution and death revisited. *Histochemistry & Cell Biology* **138** 305–322.

# APPENDIX A

## SUPPLEMENTARY VIDEOS

**Video 1** Organization of neonatal porcine testis cells in prolonged culture at 0–24 h (00:04s), 25–48 h (00:09s), 17–120 h (00:15s), D7 (00:20s), D14 d (00:27s), D21 (00.33s) and D28 (00:39s) (time-lapse:15 fps). Images were taken every 1 hr for 24 hr from day 0 to day 3, every 2 hr for 24 hr from day 4 to day 7 and finally every 1 hr for 24 hr at days 14, 24 and 28.

**Video 2** Cytoplasmic projections and amoeboid-like movement of gonocytes at 1-wk (a) in the media (00:04s) and (b) on top of somatic cell monolayer (00:12s). The images were taken every 2.5 sec for 30 sec (time-lapse: 1 fps) and 5 min for gonocytes (time lapse: 4 fps) floating in the media and on the somatic monolayer, respectively.

**Video 3** The stages in the formation of embryoid body-like colony (EBLC) formation. The images were taken every 2.5 sec for 5 min (time-lapse: 4 fps). (a) Gonocytes first settled on the somatic cell monolayer either singles or paired (00:04s). (b) Continuous migration of gonocytes towards each other results in the formation of morula-like (grape-like) colonies (00:11s). (c) The morula-like colonies increased in size over time (00:18s). (d) The EBCL formed after ~14 d of culture (00:24s). Cytoplasmic fusions of adjacent gonocytes seemed to transform the morula-like colonies into an embryoid body-like colony (00:34s). (e-f) Continued fusion of migrating gonocytes increased the mass of the EBLC (00:44s). (g) Note the presence of extensive cytoplasmic projections possessed by EBLC which seemed to assist with its movement, and further attachment of migrating gonocytes (00:56s). (h) Higher magnification of active movement of cytoplasmic projections of EBLC (01:06).

# APPENDIX B

## A PRELIMINARY STUDY OF HISTOMORPHOMETRY AND IMMUNOHISTOCHEMICAL EXPRESSION PATTERNS OF FACTORS ASSOCIATED WITH TESTIS DEVELOPMENT IN PORCINE TESTIS

**Background:** This study was conducted as part of this PhD research, but due to the preliminary nature of its results, it was not included as a separate chapter. The main objective of this study was to gain insight into the histomorphometry and expression patterns of various factors associated with testis development.

**Methodology:** Testis tissue samples of prenatal (82 dpc, *n*=3), neonatal (1, 2, 3, and 4 wk of age, *n*=5/age), prepubertal (9 and 14 wk of age, *n*=5/age), and sexually mature (*n*=4) Yorkshire-cross pigs were subjected to hematoxylin and eosin (H&E) staining and immunohistochemistry. Expression patterns of five factors that were deemed potentially associated with the testis tissue development were examined using horseradish peroxidase (HRP) immunoassay. These factors included sex determining region Y (SRY), SRY-box 9 (SOX9), fibroblast growth factor 9 (FGF9), prostaglandin D2 synthase (PGD2), and anti-Müllerian hormone (AMH).

**Results:** The histomorphometric and immunohistochemistry finding are presented in Appendix B.1 through B.4. The immunohistochemistry results remain inconclusive due to inconsistencies we observed among the samples. The major issue was the presence of background staining, which is a common challenge when working with testis tissue. Preliminary results of the localization of the examined factors are summarized in Appendix B.4. These observations need to be further validated after optimization of staining protocols.

**APPENDIX B.1**

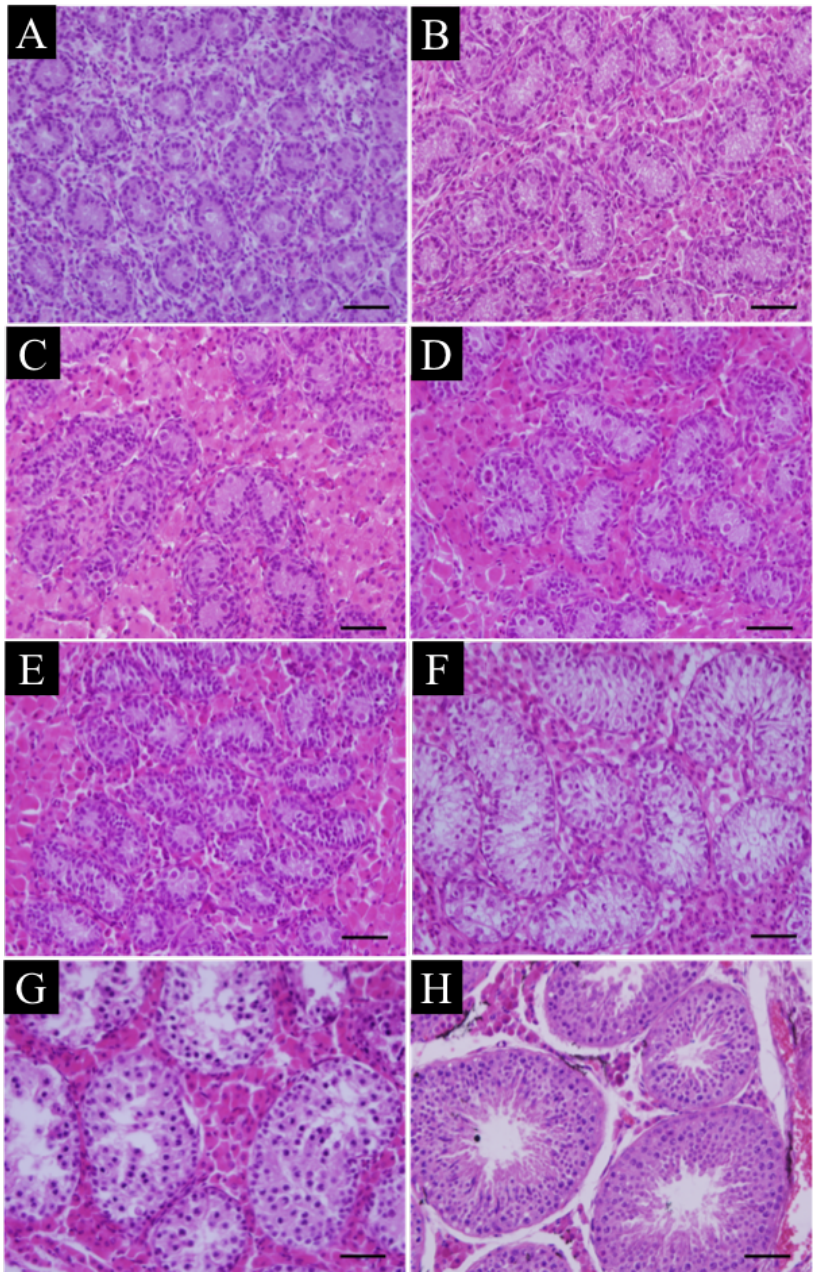


Representative histological photomicrographs of cross-sections of the testis tissue of pigs at different developmental stages. (A) 82 days of fetal age, (B) 1 wk of age, (C) 2 wk of age, (D) 3 wk of age, (E) 4 wk of age, (F) 9 wk of age, (G) 14 wk of age, and (H) mature pig. H&E staining (scale bar = 50 μm).

**APPENDIX B.2**

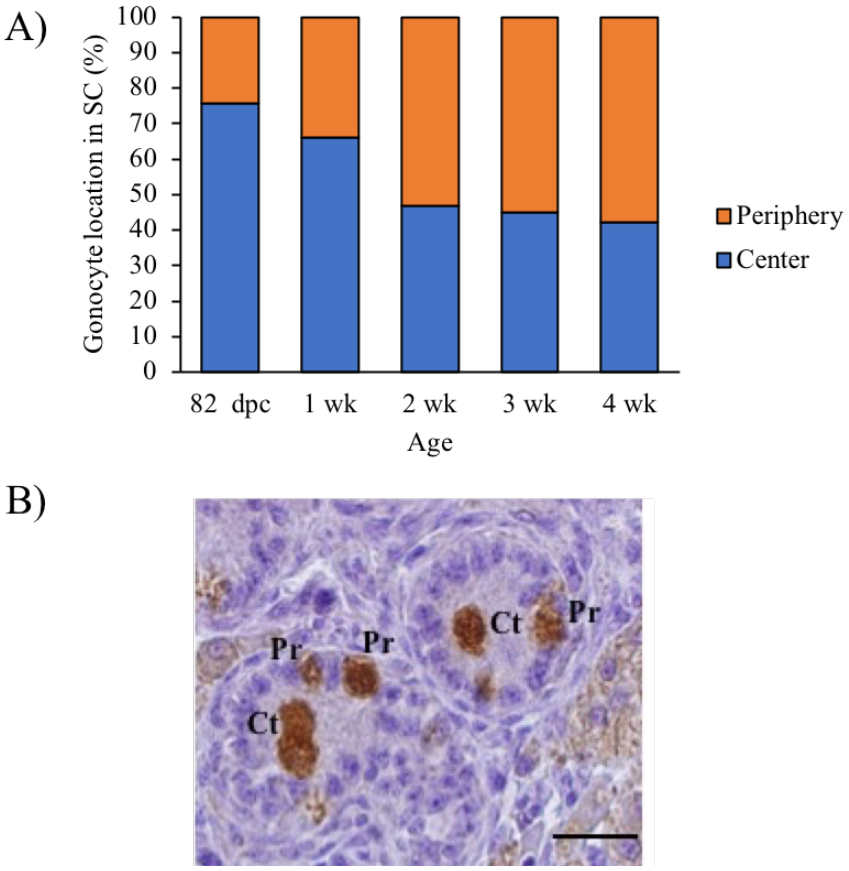


The distribution of gonocytes in prenatal (82 dpc) and neonatal (1, 2, 3, and 4 wk of age) testis tissue of pigs. (A) A stacked graph demonstrating the proportion (%) of gonocytes residing at the center (**Ct**) and the periphery (**Pr**) of the seminiferous cords. (B) Identification of gonocytes using PGP 9.5 immunohistochemistry (1:1000 dilution). (Scale bar = 20 μm.

## APPENDIX B.3

Histomorphometric analysis of the somatic and germ cells in the porcine testis tissues of different ages.

| Variable | | Pig Age | | | | | | | |
|---|---|---|---|---|---|---|---|---|---|
| | | Prenatal (82 dpc) *n*=3 | Neonatal | | | | Prepubertal | | Mature *n*=4 |
| | | | 1 wk *n*=5 | 2 wk *n*=5 | 3 wk *n*=5 | 4 wk *n*=5 | 9 wk *n*=5 | 14 wk *n*=5 | |
| Number of SC or ST/mm$^2$ | | 214.13 ± 3.8$^{a}$ | 88.48 ± 2.4$^{b}$ | 87.27 ± 1.9$^{bc}$ | 83.92 ± 1.7$^{bc}$ | 79.90 ± 0.8$^{c}$ | 57.78 ± 2.0$^{d}$ | 32.98 ± 0.9$^{e}$ | 12.45 ± 0.5$^{f}$ |
| SC or ST area (%) | | 32.75 ± 1.4$^{a}$ | 34.78 ± 0.6$^{ab}$ | 35.44 ± 0.9$^{ab}$ | 35.54 ± 0.9$^{ab}$ | 39.78 ± 0.5$^{b}$ | 48.61 ± 1.0$^{c}$ | 49.11 ± 2.0$^{c}$ | 67.86 ± 1.4$^{d}$ |
| Diameter of SC or ST (µm) | | 34.56 ± 0.4$^{a}$ | 39.10 ±0.3$^{b}$ | 39.86 ± 0.3$^{b}$ | 42.85 ± 0.3$^{bc}$ | 46.84 ± 0.4$^{c}$ | 70.65 ± 0.5$^{d}$ | 90.03 ± 1.0$^{e}$ | 210.30 ± 2.2$^{f}$ |
| Diameter of ST lumen (µm) ** | | - | - | - | - | - | - | 22 36 ± 0.6$^{a}$ | 91.74 ± 1.7$^{b}$ |
| Gonocytes | Center (%) | 75.67 ± 2.2$^{a,x}$ | 66.04 ± 2.6$^{b,x}$ | 46.73 ± 1.6$^{c}$ | 44.92 ± 1.2$^{c,x}$ | 42.15 ± 1.1$^{c,x}$ | - | - | - |
| | Periphery (%) | 24.33$^{a,y}$ | 33.96$^{b,y}$ | 53.27$^{c}$ | 55.08$^{c,y}$ | 57.85$^{c,y}$ | - | - | - |
| | Number/1,000 SC | 190 ± 6.3$^{a}$ | 132.6 ± 5.9$^{b}$ | 102.8 ± 3.3$^{c}$ | 86.8 ± 3.4$^{c}$ | 49.8 ± 4$^{d}$ | | | |
| Most advanced germ cell stage | | Gonocytes | Spermatogonia | Spermatogonia | Spermatogonia | Spermatogonia | Spermatogonia | Secondary spermatocytes | Sperm |

SC = Seminiferous cords; ST = Seminiferous tubules.
Data are mean ± SEM.
One way ANOVA (or independent-samples t-test **) was used for statistical analyses, and $P<0.05$ was considered as significant.
$^{abcdef/xy}$ Within each row/column, data with different superscripts differ significantly ($P < 0.05$).

## APPENDIX B.4

Summary of localization of different factors associated with testis development in the porcine testis tissue of different ages.

| Factor | Pig Age | | | | | | | |
|---|---|---|---|---|---|---|---|---|
| | Prenatal (82 dpc) *n*=3 | Neonatal | | | Prepubertal | | | Mature *n*=4 |
| | | 1wk *n*=5 | 2 wk *n*=5 | 3 wk *n*=5 | 4 wk *n*=5 | 9 wk *n*=5 | 14 wk *n*=5 | |
| SRY | + /SC,GC | + /SC,GC | +/ SC,GC | +/ SC,GC | - | - | - | - |
| SOX9 | +/SC,GC,LC | +/ SC,GC, LC | + /SC,GC | +/ SC,GC, LC | + /SC,GC, LC | +/SC,GC,LC | +/ SC,GC,LC | +/SC,GC,LC |
| FGF9 | +/SC,GC | +/SC,GC | +/SC,GC | +/SC,GC | +/SC,GC | +/LC | +/LC | +/LC |
| PGD2 | +/ SC | +/SC | +/ SC | +/ SC | +/SC | +/SC | +/LC | +/LC |
| AMH | +/SC | +/SC | +/SC | +/SC | +/SC | +/SC | +/SC | - |

The examined factors included the sex determining region Y (*SRY*); SRY-box 9 (*SOX9*); fibroblast growth factor 9 (*FGF9*); prostaglandin D2 synthase (*PGD2*); and anti-Müllerian hormone (*AMH*).
The immunohistochemistry was performed using the OneStep polymer HRPO (only horseradish peroxidase) staining system.
The expression of these factors was evaluated qualitatively, and recorded as presence (+) or absence (-).
The cellular localization were recorded as Sertoli cells (SC), germ cells (GC), or Leydig cells (LC).